

ISSN 0973-8916

Current Trends in Biotechnology and Pharmacy

Volume 13

Issue 3

July 2019



www.abap.co.in

Current Trends in Biotechnology and Pharmacy

ISSN 0973-8916 (Print), 2230-7303 (Online)

Editors

Prof.K.R.S. Sambasiva Rao, India
krssrao@abap.co.in

Prof. Karnam S. Murthy, USA
skarnam@vcu.edu

Editorial Board

Prof. Anil Kumar, India
Prof. P.Appa Rao, India
Prof. Bhaskara R.Jasti, USA
Prof. Chellu S. Chetty, USA
Dr. S.J.S. Flora, India
Prof. H.M. Heise, Germany
Prof. Jian-Jiang Zhong, China
Prof. Kanyaratt Supaibulwatana, Thailand
Prof. Jamila K. Adam, South Africa
Prof. P.Kondaiah, India
Prof. Madhavan P.N. Nair, USA
Prof. Mohammed Alzoghaibi, Saudi Arabia
Prof. Milan Franek, Czech Republic
Prof. Nelson Duran, Brazil
Prof. Mulchand S. Patel, USA
Dr. R.K. Patel, India
Prof. G.Raja Rami Reddy, India
Dr. Ramanjulu Sunkar, USA
Prof. B.J. Rao, India
Prof. Roman R. Ganta, USA
Prof. Sham S. Kakar, USA
Dr. N.Sreenivasulu, Germany
Prof.Sung Soo Kim, Korea
Prof. N. Udupa, India

Dr.P. Ananda Kumar, India
Prof. Aswani Kumar, India
Prof. Carola Severi, Italy
Prof. K.P.R. Chowdary, India
Dr. Govinder S. Flora, USA
Prof. Huangxian Ju, China
Dr. K.S.Jagannatha Rao, Panama
Prof.Juergen Backhaus, Germany
Prof. P.B.Kavi Kishor, India
Prof. M.Krishnan, India
Prof. M.Lakshmi Narasu, India
Prof.Mahendra Rai, India
Prof.T.V.Narayana, India
Dr. Prasada Rao S.Kodavanti, USA
Dr. C.N.Ramchand, India
Prof. P.Reddanna, India
Dr. Samuel J.K. Abraham, Japan
Dr. Shaji T. George, USA
Prof. Sehamuddin Galadari, UAE
Prof. B.Srinivasulu, India
Prof. B. Suresh, India
Prof. Swami Mruthinti, USA
Prof. Urmila Kodavanti, USA

Assistant Editors

Dr.Giridhar Mudduluru, Germany

Prof. Mohamed Ahmed El-Nabarawi, Egypt

Dr. Sridhar Kilaru, UK

Prof. Chitta Suresh Kumar, India

www.abap.co.in

ISSN 0973-8916

Current Trends in Biotechnology and Pharmacy

(An International Scientific Journal)

Volume 13

Issue 3

July 2019



www.abap.co.in

Indexed in Chemical Abstracts, EMBASE, ProQuest, Academic SearchTM, DOAJ, CAB Abstracts, Index Copernicus, Ulrich's Periodicals Directory, Open J-Gate Pharmoinfonet.in Indianjournals.com and Indian Science Abstracts.

Association of Biotechnology and Pharmacy (Regn. No. 28 OF 2007)

The *Association of Biotechnology and Pharmacy (ABAP)* was established for promoting the science of Biotechnology and Pharmacy. The objective of the Association is to advance and disseminate the knowledge and information in the areas of Biotechnology and Pharmacy by organising annual scientific meetings, seminars and symposia.

Members

The persons involved in research, teaching and work can become members of Association by paying membership fees to Association.

The members of the Association are allowed to write the title **MABAP** (Member of the Association of Biotechnology and Pharmacy) with their names.

Fellows

Every year, the Association will award Fellowships to the limited number of members of the Association with a distinguished academic and scientific career to be as Fellows of the Association during annual convention. The fellows can write the title **FABAP** (Fellow of the Association of Biotechnology and Pharmacy) with their names.

Membership details

(Membership and Journal)		India	SAARC	Others
Individuals	– 1 year	Rs. 600	Rs. 1000	\$100
	LifeMember	Rs. 4000	Rs. 6000	\$500
Institutions (Journal only)	– 1 year	Rs. 1500	Rs. 2000	\$200
	Life member	Rs.10000	Rs.12000	\$1200

Individuals can pay in two instalments, however the membership certificate will be issued on payment of full amount. All the members and Fellows will receive a copy of the journal free.

Association of Biotechnology and Pharmacy
(Regn. No. 28 OF 2007)
#5-69-64; 6/19, Brodipet
Guntur – 522 002, Andhra Pradesh, India

Current Trends in Biotechnology and Pharmacy

ISSN 0973-8916

Volume 13 (3)	CONTENTS	July 2019
Research Papers		
Development and Validation of Rapid, Sensitive and In-expensive Protein G-based Point of Care Diagnostic Assay for Serodiagnosis of Paratuberculosis at Resource-Limited Areas <i>Rudrama Devi Punati, Prudhvi Chand Mallepaddi, Revathi Poonati, Mukta Jain, Soumendra Nath Maity, Jagdip Singh Sohal, Sudhakar Podha, Kavi Kishor PB and Rathnagiri Polavarapu</i>		232-242
Design, Synthesis, Cytotoxicity Evaluation, and Molecular Docking Studies of 1,3,4 Oxadiazole substituted 1,4-Naphthoquinone Derivatives <i>Mousumi Besan, Manoj K. Gautam, Sushant K. Shrivastava</i>		243-258
Characterization of a Cohort of Patients with Arterial Thrombosis from the Georgian Adjarian Population <i>Sopio Garakanidze, Elísio Costa, Elsa Bronze-Rocha, Alice Santos-Silva, Giorgi Nikolaishvili, Irina Nakashidze, Nona Kakauridze, Salome Glonti, Rusudan Khukhunaishvili, Marina Koridze, Sarfraz Ahmad</i>		259-269
Development and Validation of Point of Care Diagnostics for the Rapid Detection of Multiple Species of <i>Leptospira</i> at Resource-Limited Areas <i>Revathi Poonati, Prudhvi Chand Mallepaddi, Rudrama Devi Punati, Soumendra Nath Maity, Anusha Alamuri, Srihari Manchikalapudi, Krishna Satya Alapati, Kavi Kishor PB and Rathnagiri Polavarapu</i>		270-282
Development of 1, 4-Naphthoquinones as Potential Epidermal Growth Factor Receptor Inhibitors For The Treatment of Cancer <i>Mousumi Besan, Manoj K. Gautam and Sushant K. Shrivastava</i>		283-308
Screening of ACC-deaminase and antifungal metabolites producing fluorescent pseudomonads isolated from rhizosphere soil of groundnut <i>Nirmala Jyothi Lukkani and Dr. EC. Surendranatha Reddy</i>		309-316
<i>In-Silico</i> Analysis and Identification of functional Single Nucleotide Polymorphism (SNPs) of the DISC1 gene <i>Neema Tufchi, Kumud Pant, Syed Mohsin Waheed, Devvret</i>		317-324
Molecular Characterization of a Biopolymer Producing Bacterium Isolated from Sewage Sample <i>A. Ranganadha Reddy, S. Krupanidhi, T.C.Venkateswarulu, R. Bharat Kumar, P. Sudhakar, K. Vidya Prabhakar</i>		325-335
Image Capturing of Major Plant Pathogens Using Smart Mobile Phone Camera <i>Kondal Reddy Gaddam, Venkateswarlu Vadapally, Santosh Singh, Shyam Haibatpure, Kartik Maheshwari, Varunbhai Priyam Mehta, Madhan Mohan Kolluru</i>		336-345
Insilico Studies of Ras Protein in Cancer <i>A. Ranganadha Reddy, S. Krupanidhi, P. Sudhakar</i>		346-349
Review Papers		
Application of Medicinal Plants in Management of Endogenous Bioactive Molecules as Potential Biomarkers for Cardiovascular Disease and Disorders <i>Jitendra Gupta, Reena Gupta, Varun Kalra, Nitin Wahi</i>		350-365
News Item		

Information to Authors

The *Current Trends in Biotechnology and Pharmacy* is an official international journal of *Association of Biotechnology and Pharmacy*. It is a peer reviewed quarterly journal dedicated to publish high quality original research articles in biotechnology and pharmacy. The journal will accept contributions from all areas of biotechnology and pharmacy including plant, animal, industrial, microbial, medical, pharmaceutical and analytical biotechnologies, immunology, proteomics, genomics, metabolomics, bioinformatics and different areas in pharmacy such as, pharmaceuticals, pharmacology, pharmaceutical chemistry, pharma analysis and pharmacognosy. In addition to the original research papers, review articles in the above mentioned fields will also be considered.

Call for papers

The Association is inviting original research or review papers and short communications in any of the above mentioned research areas for publication in *Current Trends in Biotechnology and Pharmacy*. The manuscripts should be concise, typed in double space in a general format containing a title page with a short running title and the names and addresses of the authors for correspondence followed by Abstract (350 words), 3 – 5 key words, Introduction, Materials and Methods, Results and Discussion, Conclusion, References, followed by the tables, figures and graphs on separate sheets. For quoting references in the text one has to follow the numbering of references in parentheses and full references with appropriate numbers at the end of the text in the same order. References have to be cited in the format below.

Mahavadi, S., Rao, R.S.S.K. and Murthy, K.S. (2007). Cross-regulation of VAPC2 receptor internalization by m2 receptors via c-Src-mediated phosphorylation of GRK2. *Regulatory Peptides*, 139: 109-114.

Lehninger, A.L., Nelson, D.L. and Cox, M.M. (2004). *Lehninger Principles of Biochemistry*, (4th edition), W.H. Freeman & Co., New York, USA, pp. 73-111.

Authors have to submit the figures, graphs and tables of the related research paper/article in Adobe Photoshop of the latest version for good illumination and alignment.

Authors can submit their papers and articles either to the editor or any of the editorial board members for onward transmission to the editorial office. Members of the editorial board are authorized to accept papers and can recommend for publication after the peer reviewing process. The email address of editorial board members are available in website www.abap.in. For submission of the articles directly, the authors are advised to submit by email to krssrao@abap.co.in or krssrao@yahoo.com.

Authors are solely responsible for the data, presentation and conclusions made in their articles/research papers. It is the responsibility of the advertisers for the statements made in the advertisements. No part of the journal can be reproduced without the permission of the editorial office.

Development and Validation of Rapid, Sensitive and Inexpensive Protein G-based Point of Care Diagnostic Assay for Serodiagnosis of Paratuberculosis at Resource-Limited Areas

Rudrama Devi Punati^{1,2,3}, Prudhvi Chand Mallepaddi^{1,2,3}, Revathi Poonati^{1,2,3}, Mukta Jain⁵, Soumendranath Maity^{2,3}, Jagdip Singh Sohal⁵, Sudhakar Podha¹, Kavi Kishor PB^{*,1,2,3} and Rathnagiri Polavarapu^{1,2,3,4}

¹Department of Biotechnology, Acharya Nagarjuna University, Guntur 522 510, Andhra Pradesh, India

²Department of Clinical Microbiology, Genomix Molecular Diagnostics Pvt. Ltd., Hyderabad 500 072, India

³Department of Veterinary Microbiology, GenomixCARL Pvt.Ltd., Pulivendula, Kadapa 516 390, Andhra Pradesh, India

⁴Genomix Biotech Inc, 2620 Braithwood Road, Atlanta, GA 30345, USA

⁵AMITY Center for Mycobacterial Division, AMITY University, Jaipur 302 001, Rajasthan, India

*For Correspondence - pbkavi@yahoo.com

Running title –

Abstract

Paratuberculosis is caused by *Mycobacterium avium* subspecies *paratuberculosis* (MAP). It affects domestic cattle, ruminant livestock species with emerging zoonotic concerns and also causes human Crohn's disease. It is a chronic granulomatous enteritis and results in huge economic loss to domestic dairy cattle and ruminant industry. Further, there is mounting evidence on the zoonotic role of MAP in human Crohn's disease. MAP is not killed by pasteurization, therefore, milk and milk products are major sources of infection for humans. The disease affects cattle and small ruminant industries, thus impacting farmer's economy. Control of the disease is hampered by the lack of rapid and accurate diagnostic tests. Therefore, it is urgently needed to develop affordable as well as high performing diagnostic tools. So, the present study was aimed to develop a simple, inexpensive, rapid and robust point of care (POC) lateral flow diagnostic test kit for serodiagnosis of paratuberculosis infection in bovine cattle and in small ruminant livestock species. We developed a rapid, pen-side lateral flow antibody (Ab)

diagnostic test kit for onsite screening of paratuberculosis. The rapid kit detects infection in 20 minutes and can be used directly by a farmer without the requirement of an expert or equipment. We evaluated 2,502 samples using lateral flow assay (LFA) which included 243 reference sera and 2,259 field samples. The results suggest that the sensitivity and the specificity of LFA were 91.01% and 98.94% respectively in comparison with the gold standard culture, polymerase chain reaction (PCR) and delayed-type hypersensitivity (DTH) methods. Thus, LFA aids to detect the MAP specific antibodies (Ab) in the collected samples at POC resource-limited areas and help the bovine and small ruminant livestock healthcare systems. This assay is well suited for the early diagnosis of MAP in less equipped laboratories and in resource-limited POC settings suitable for the Indian environment.

Key Words: *Mycobacterium avium* subspecies *paratuberculosis*, lateral flow assay, point of care diagnosis, delayed-type hypersensitivity, resource-limited areas.

Introduction

Mycobacterium avium subspecies *paratuberculosis* (MAP) is the causative agent of chronic enteric granulomatous inflammation in animals known as paratuberculosis or Johne's disease (1,2,3). The disease is one of the most wide spread bacterial diseases and capable of infecting varied livestock species in developed and in developing countries (4,5,6). It is considered as one of the most serious diseases affecting many domestic and wild animals including dairy cattle, sheep and other ruminants. The Office International des Epizooties (OIE) considers paratuberculosis as a disease of major global threat and categorizes it as a list B transmissible disease (7). It is prevalent in domestic animals worldwide and has a significant impact on the global economy. The disease has an endemic distribution globally in reducing the production of food in both developed as well as in developing countries. The infections with MAP often leads to chronic granulomatous enteritis with clinical signs of diarrhoea, weight loss, decreased milk production and mortality. Under natural conditions, the disease is spread by ingestion of MAP from the contaminated environment (8). The MAP has the potential to cause public health implications also, as the cells of these organisms have the ability to survive pasteurization and transmission via raw milk, meat and even contact with animals (9,10,11). Economic losses to the dairy cattle industry occur due to decreased yield of milk production, weight loss in young calves, and reduction in the slaughter value. This prompts to take action for early culling and trade restriction. On an average, the economic loss caused by bovine paratuberculosis has been estimated to be higher than those for other bovine diseases such as bovine viral diarrhoea, enzootic bovine leukosis and neosporosis (12).

In this century, MAP is considered as a major pathogen of domestic animals as well as humans (2,3,13,14). In domestic livestock, in spite of high prevalence and endemic nature of the MAP, the impact of the disease has neither been realized nor estimated at the national level. This

is primarily due to the dearth of indigenous tests as well as kits. Control of paratuberculosis has proven to be experimentally very difficult primarily due to the nature of MAP infections (2). The animal population becomes infected at an early age by ingesting MAP organisms shed in the feces or from the milk of the older or parental animals. In India, limited studies (15,16) were carried on the variable incidence (2-18%) in domestic livestock (2). The domestic animals may either receive infection from infected parents through semen, in-utero, milk or colostrums (17) or pick up infection from contaminated environment soon after birth. Existing diagnostic kits for the detection of paratuberculosis are based on the detection of MAP in the feces by culture or by PCR assay. The cultivation of MAP organisms from feces and tissue samples is time consuming and may require sophisticated lab, equipment, and trained professionals (18,19). Further, these tests especially the fecal cultures and PCR tests are incapable of detecting prepatent MAP infections. The fecal culture test is very slow, time consuming and requires 5 to 16 weeks for cultivation and its sensitivity level estimated to be approximately 38% (2,6). PCR is a molecular diagnostic test for the detection of MAP infection from feces, blood and tissue samples with sensitivity comparable with bacterial culture (20,21). But, PCR also entails sophisticated lab, trained technicians and variability in the sensitivity levels. Further, PCR cannot be performed at field conditions where the laboratory testing facilities are not available.

Because of the above limitations, there is an urgent need to develop a rapid, sensitive, simple, easy to use and inexpensive POC lateral flow diagnostic test kits for the detection of MAP infection in the cattle and in small ruminants at resource-limited areas. In recent years, the usage of lateral flow diagnostics is increasing due to its simple, easy to handle, less expensive nature, without standard protocols and expertise or any special equipment to perform the assay at on-site. In the present study, an immunochromatographic detection method was used for identifying

MAP in the collected samples. It requires only a few drops of whole blood and sample diluent. The interpretation of the assay can be visually read by the formation of colored lines at control and test positions. The developed protein G-based LFA kit can detect MAP specific antibodies in humans and in animal species such as cows, buffaloes, sheep and goats at POC resource-limited areas.

Materials and Methods

Study site and sampling information: The complete kit development and validation process was carried out at the Genomix Molecular Diagnostics Pvt. Ltd., Hyderabad, during January 2017 till December 2018. A total of 2,502 animal samples, 60 OIE reference (30 positive and 30 negative) from the Division of Infectious Diseases and Microbiology, the Huck Institutes of the Life Sciences, the Pennsylvania State University, PA, USA, and 183 (89 positive and 94 negative) control samples confirmed for MAP by fecal culture and PCR assays were procured from AMITY Center for Mycobacterial Division, AMITY University, Jaipur, India. Out of 89 positive samples, 29 are from heavy shedders (>50 colony forming units (CFU/slant), 23 from moderate shedders (10-50 CFU/slant) and 37 from low shedders (<10 CFU/slant). The remaining 2,259 field samples were analyzed at on-site by LFA and compared with DTH as the field standard method for detecting MAP. The field samples were collected from 10 different farms in southern parts of India.

Sample collection and processing: Approximately 5 ml of whole blood samples were collected from jugular vein of animal in a lithium-heparin coated BD vacutainer tubes (REF 367820) for serological studies with the consent of farm owners under the supervision of local veterinarians. The collected samples were stored at -20°C until further use.

Skin test (DTH): The DTH is the animal skin test method performed by following the established OIE referenced protocol (22). Briefly, 0.1 ml of johnin purified protein derivative (PPD) (3000 IU/dose, MAP MTCC19698 from IVRI, Izatnagar) was

injected to each animal intradermally with the help of a veterinarian. If the inoculation part of the animal skin thickness increases more than 3 mm after 72 h of injection, then the animal is considered as positive to DTH test.

Antigen preparation: The MAP strain was grown on a specific Harold egg yolk medium with 0.0002% (weight/volume) mycobactin J supplement and the culture was harvested as per the OIE recommended protocol (22). The antigen preparation was slightly modified as described by Speer et al. (23). Ten ml of sterile phosphate buffered saline (PBS) with pH 7.2 was added to the well grown MAP culture (>100 CFU) slants. Bacterial cells were dissolved in PBS and pelleted by centrifugation at 10,000 x g for 10 min at 4°C temperature. The pellet was washed two times with sterile PBS. The washed pellet was resuspended with PBS and sonicated with 55% amplitude for 30 min with 30 sec intervals. The clear antigen was separated by centrifugation at 12,000 x g for 15 min and stored at -20°C until further use. The complete cultural process and the antigen preparation process were carried out at the Amity University, Jaipur, India as per the institutional biosafety handling procedures. Purified antigen was used in the preparation of lateral flow diagnostic test kits for the detection of MAP in the bovine as well as small ruminant livestock species at resource-limited settings.

Development of protein G-based lateral flow assay (LFA): Due to its robustness and simplicity, the assay is highly suitable for application under field conditions (24). The purified antigen was impregnated on nitrocellulose membrane (MDI membrane technologies, India) test (T) position at a concentration of 1 mg/ml using BioDotQuant-2000 Biojet apparatus (Bio Dot Inc., USA). The biotinylated BSA (Genomix Biotech. Inc., USA) was immobilized to the control position at a concentration of 1 mg/ml parallel to the test position. The colloidal gold nano particles with 40 nm size (Arista Biologicals Inc., USA) were conjugated with protein G along with streptavidin (Genomix Biotech, Inc. USA) by using well

established protocol and dispensed on to a conjugate matrix (MDI membrane technologies, India). XYZ-Biojet dispensing apparatus (BioDot Inc., USA) was used at a concentration of 2 μ l per each centimeter length. All the components of the LFA sheets were assembled on a 300 mm length x 60 mm width plastic adhesive backing sheets consisting of a nitrocellulose membrane with control and test lines at the middle. One end of the nitrocellulose membrane was flanked by a sample pad followed by conjugation matrix and the other end fixed with absorption pad. The assembled components were cut in to 4.2 mm width and 60 mm long strips using strips cutter instrument Model-M70 (MDI technologies, India). The strips were placed in a plastic device followed by pressing and the final cassette was sealed in an aluminum foil pouch with a desiccant in a dehumidified room to increase the longevity of the developed LFA product.

Analysis of the LFA: The developed LFA kits were analyzed by the visual observation of the dark purple colored bands on control and test line positions of the nitrocellulose membrane. Around 5 μ l volumes of collected samples were used at sample well "S" position followed by the addition of two drops of sample diluent buffer as shown in the figure 1. As a result of capillary action of nitrocellulose membrane, the sample moves from sample pad to the end of absorption pad resulting in the appearance of colored bands at "C and T" positions indicating that the test is positive for MAP. The absence of colored line at test position indicates that the sample is negative for MAP infection.

Statistical analysis: LFA was evaluated with reference samples obtained from OIE reference laboratory and AMITY University, Jaipur, India. The collected samples were tested with the lateral flow test devices. The overall statistical analysis of the developed assays was evaluated and the test results tabulated in terms of the sensitivity, specificity, positive predictive value (PPV), negative predictive value (NPV) and efficiency. MedCalc's diagnostic test evaluation statistical analysis software was used to calculate the sensitivity, specificity, PPV, NPV and efficiency of individual assays. The 'p' value was calculated with Chi-square statistical analysis online software.

Field studies: Protein G-based lateral flow diagnostic assay for detection of MAP were tested for the field applicability by collecting the whole blood samples randomly from 2,259 apparently healthy cattle from 10 different farms in southern parts of India. All the 2,259 field samples were analyzed at on-site by LFA in comparison with DTH as the field standard method for detection of MAP infection.

Results and Discussion

The purified MAP specific antigen was used in the preparation of lateral flow diagnostic test kits. The colloidal gold conjugated protein G acts as a detector and the test line was coated with purified antigen. The samples containing paratuberculosis specific antibodies bound to the protein G colloidal gold conjugate were captured at test position. The disease specific captured antibodies were visualized as purple coloured

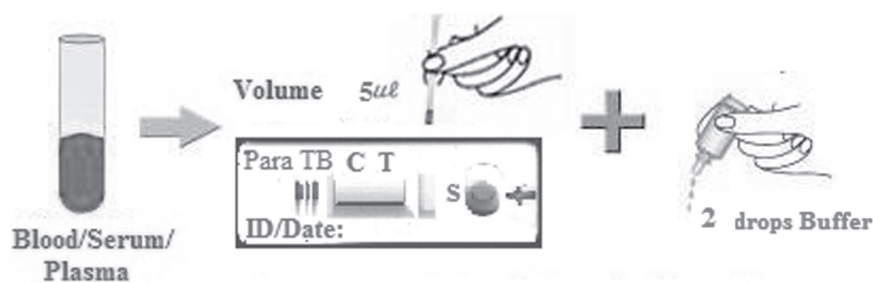


Fig. 1. Diagrammatic representation of paratuberculosis lateral flow assay test procedure

bands at test position. Absence of a colour band at the test position indicated absence of antibodies against paratuberculosis in the test sample. Such a sample is considered as negative. The LFA kit developed in the present study was tested with positive and negative samples and shown in the fig. 2.

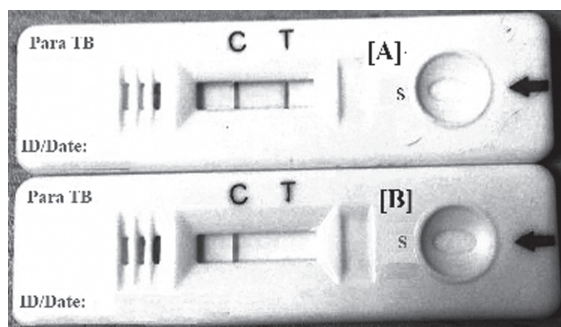


Fig. 2. Paratuberculosis lateral flow kit tested with (A) positive and (N) negative samples

Validation of LFA with reference samples: LFA, developed in the present study was validated for the sensitivity, specificity, positive predictive value, negative predictive value and efficiency by using the collected reference samples. A total of 243 reference sera samples were used in the validation

part collected from the reference laboratories. Out of that, 183 samples were procured from AMITY Center for Mycobacterial Division and the remaining 60 from OIE reference laboratory. All the reference samples were confirmed by culture, PCR assay and DTH. Out of 183 samples from AMITY, 89 samples were found positive and 94 negative for MAP by fecal culture and PCR assay. Out of 89 reference positive samples obtained from AMITY, 8 showed false negative results. Out of 94 negative samples, one showed false positive by LFA. On the other hand, DTH assay displayed 32 false negative and 12 false positive results. The complete assay comparison data and the sample information is shown in Table 1.

Statistical data and the comparative analysis of all the diagnostic methods for the detection of paratuberculosis are shown in Table 2. The LFA was validated with 60 OIE reference samples (positive = 30, negative = 30). Out of 30 positive samples, 3 exhibited false negative and out of 30 negative, 1 sample showed false positive results with LFA. The overall statistical analysis of the assays was evaluated in terms of sensitivity, specificity, positive predictive value (PPV), negative predictive value (NPV) and efficiency (Table 2).

Table 1. Comparison of different diagnostic assays for the detection of paratuberculosis with reference samples

S. No	Assays	Sample volume	Total no. of samples		TP	TN	FP	FN
			Positive	Negative				
1	Culture	100 µl	89	94	89	94	0	0
2	PCR	2.0 µl	89	94	89	94	0	0
3	DTH	1.0 ml	69	114	57	82	12	32
4	Lateral flow assay	5.0 µl	82	101	81	93	1	8

*Note: TP- True positive (reactive), TN- true negative (non-reactive), FP- false positive, FN- false negative

Table 2. Evaluation of the diagnostic assays in comparison of its parameters with reference samples

Assay	Sensitivity	Specificity	Results (95% CI)		NPV	Efficiency
			PPV			
Culture	100 (95.79) [0.18]	100 (103.89) [0.15]	100 (102.54) [0.06]	100 (97.95) [0.04]	100 (99.84) [0.00]	
PCR	100 (95.79) [0.18]	100 (103.89) [0.15]	100 (102.54) [0.06]	100 (97.95) [0.04]	100 (99.84) [0.00]	
DTH	64.04 (72.61) [1.02]	87.23 (78.75)[0.87]	82.61 (77.72) [0.24]	71.93 (74.25) [0.14]	75.96 (75.68) [0.01]	
LFA	91.01 (90.81) [0.00]	98.94 (98.48) [0.00]	98.78 (97.20) [0.01]	92.08(92.86) [0.01]	95.80 (94.65) [0.00]	

* Values are represented in terms of positivity; values in parenthesis represent 95% confidential interval.

The developed LFA showed 91.01% sensitivity and 98.94% specificity. In contrast, the field standard DTH assay showed 64.04% sensitivity and 87.23% specificity in comparison with standard culture, PCR and LFA methods. The positive likelihood ratio and negative likelihood ratio of LFA was 85.55% and 0.09%, whereas the DTH assay showed 5.02% and 0.41% respectively. The remaining PPV, NPV and efficiency data for all these assays differed with the standard values (Table 2). The Chi-Square statistical value is 3.605, and P value 0.994301. P value is significant at <0.05. The comparative diagnostic parameters and statistical analysis data proved that the protein

G-based LFA is more sensitive and specific when compared to the field standard DTH method for the detection of paratuberculosis.

Field-based analysis

The collected field samples were used to validate the protein G-based lateral flow diagnostic assay for the detection of MAP and to check the field applicability. The field samples collected from different livestock species was used to screen the LFA in comparison with the field standard DTH method. Overall, 2,259 field samples were collected on-site, including cows (n = 597), buffaloes (n = 682), sheep (n = 581), and goats (n

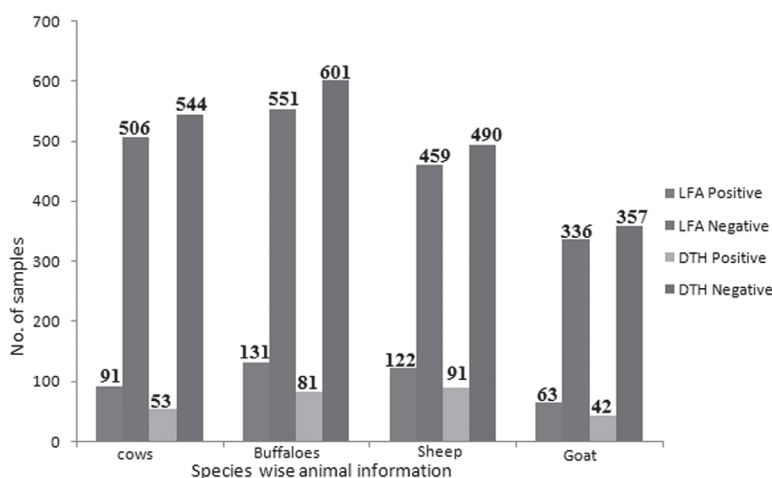


Fig. 3. The data represent species-wise positive and negative results using LFA and DTH at the field level

= 399). Out of 2,259 samples, 407 animals showed positive and 1,852 negative by LFA. The species-wise positivity of LFA was 91 in cows, 131 in buffaloes, 122 in sheep, 63 in goat samples when tested on-site. Contrarily, the DTH method showed 267 positive and 1,992 animal samples as negative. The species-wise positivity of DTH method was 53 in cows, 81 in buffaloes, 91 in sheep, and 42 in goat samples in the field level detection. Over all, the prevalence of paratuberculosis appeared as 18.02% by the LFA in the field animals.

MAP is an intracellular, highly potent, slow growing pathogenic bacterium with chronic progressive infection in a wide range of domestic animals. Paratuberculosis has been reported in all Indian domestic ruminants since 1930s and considered as a problem more in the organized farm animals than the animals reared in villages and under semi-intensive system. It is distributed all over the world and now has gained potential importance as an emerging global zoonotic agent causing inflammatory bowel disease or Crohn's disease in humans (25,26,27). MAP is also detected in the water bodies, pasture land, dams (28,29,30), in raw and pasteurized milk and milk powder (17,31). MAP infects animals during the early stages of life mostly at neonatal stages. The infected animals move from silent phase to sub-clinical and later on to clinical and advanced stages with very strong shedding of MAP bacilli organism. Thus, shedding of bacilli by infected organisms spreads the disease to other susceptible animals and humans. Also, each of four stages of the disease requires a different and specific diagnostic method. The control of paratuberculosis infection has been very severely hampered due to the lack of proper and stage specific diagnostic test kits to diagnose early and sub-clinical stages of MAP infection (32). Gold standard methods are regularly employed for the detection of MAP bacilli. Over and above, different types of standard detection tests used for the diagnosis of paratuberculosis infection include fecal culture, biochemical and molecular based PCR assays. These methods have many

disadvantages and require prolonged incubation time for culture, expensive instrumentation, and experienced microbiologists. Besides, the available methods are cumbersome and time taking. Further, variability in the sensitivity levels is very high, and could not be performed at field conditions or remote areas where the laboratory testing facilities are not available. The most common test employed for the detection of MAP infection is ELISA-based on the disease specific antibodies present in the collected serum and milk samples. Though existing serological methods are inexpensive and able to handle huge number of samples at a time, ELISA has low sensitivity in detecting MAP during the early stages of infection. In addition, the cross-reactivity of the antigenic epitopes shared with other species of *Mycobacterium*, *Corynebacterium* and *Nocardia* also decrease its sensitivity and specificity (33,34,35). Existing literature suggests that the type of MAP strain used for the preparation of diagnostics may also influence the sensitivity and specificity of the test (35). Moreover, majority of the commercially available kits are being imported to India and comprise disease specific antigens obtained from foreign strains of MAP. This may be one of the reasons for decreased sensitivity and specificity of the existing diagnostic tests.

Present study explains the development and validation of a rapid, sensitive and inexpensive POC diagnostics for the early stage detection of MAP infection in humans as well as in animal populations. Keeping in mind the major drawbacks in the existing diagnostic techniques and significance of the disease mentioned, our attention focused on the development of improved sero-diagnostics using secretory protein antigens obtained from an indigenous strain having 83.3% prevalence in India. The secretory proteins were found as more effective antigenic/immunogenic and can be used as antigen candidates for the development of highly sensitive diagnostics for the MAP disease control and its management. A total of 2,502 samples were used for the validation of LFA. Our results confirmed that the developed assays are highly specific and sensitive, rendering them useful for on-site diagnosis of

paratuberculosis. There are no indigenous lateral flow commercially available kits for the detection of paratuberculosis infection. The lateral flow kit developed in the present study is the first indigenous kit that can be recommended for on-site detection of paratuberculosis. The results obtained in the present study are in agreement with those obtained by Shin et al. (35). Their results revealed that the secretory proteins can be used as solid phase and for better sero-diagnostic antigens over protoplasmic antigens. It appears that the immunogenic secretory proteins of indigenous strains have more potent diagnostic value than the imported commercial tests in diagnosis of MAP infection. Shin et al. (35) for the first time studied the significance of MAP secreted proteins/antigens collected at stationary growth phase in diagnosis. They noticed a great degree of sensitivity and specificity (74 and 99% respectively) while detecting early and subclinical infections by ELISA assay. They opined that the use of MAP secreted antigens increased the sensitivity by 25% over the commercial kits in low shedders. Rouhollah et al. (36) also investigated the sensitivity and specificity of proteins using cattle sera which were 86 and 99% respectively with indirect ELISA. Our findings showed that the usage of secretory proteins isolated from Indian strain reacted more specifically with antibodies obtained from samples of MAP infected animals (goat, sheep and cattle) and humans when compared with the results obtained by other methodologies. This indicates greater (98.94%) specificity of LFA as a field-based kit and superior over DTH method. This also points out that LFA should be used in place of imported commercial kits for the detection of paratuberculosis. Our results also show that secreted proteins of indigenous strain of MAP are the ideal choice for developing new diagnostic assays for detection of MAP infection. Imported commercial kits may not be of any use for Indian conditions due to their low sensitivity.

The lateral flow diagnostic test kits developed in the present study are simple, easy, and convenient to use, inexpensive, reproducible

and reliable. In addition, LFA, does not require any lengthy protocol, specific expertise, special equipment to perform the assay and at the same time can be used at field or at resource-limited areas. Instead of using species specific anti-immunoglobulin IgG gold conjugated components for different animal species, LFA developed with protein G-based kit can be used to detect MAP specific antibodies in humans and animal species such as cows, buffaloes, sheep and goats. The LFA kit can detect large number of animal populations and serves as a guide to identify the infected animals and helps in implementing the disease control, eradication programs and in preventive measures. The results proved that the LFA developed in the present study for the detection of paratuberculosis is an ideal kit for use at on-site where the laboratory facilities to perform confirmatory assays are not available. The diagnostic kit developed in the present study is the first indigenous, lateral flow-based kit and can be used at primary healthcare centers and hence it is recommended to veterinarians for epidemiological studies. It is also suitable as a diagnostic tool for the detection of paratuberculosis in cattle and in small ruminants under resource-limited conditions for POC diagnosis.

Conclusions

LFA developed in the present study is a simple, inexpensive, reliable, user-friendly, effective, POC serodiagnostic assay for the detection of MAP infection at resource-limited areas. It requires no sophisticated equipment and highly trained professionals. The lateral flow results are interpretable by the naked eye within 10 to 20 min of addition of the sample. So, the present study proves that the newly established LFA is highly stable, sensitive, specific and hence recommended to veterinarians for epidemiological studies and for detecting paratuberculosis infection. The kit is suitable for detecting MAP in Indian domestic cattle, small ruminant live stock species and in human populations under resource-limited field settings.

Acknowledgements

Authors are grateful and acknowledge the help rendered by Dr. Vivek Kapur, Associate Director for Strategic Initiatives, The Huck Institutes of the Life Sciences, Pennsylvania State University, USA for providing the reference samples. The work was financially supported by the Department of Biotechnology, Government of India, New Delhi, India, under the CRS project entitled "Shielding the livestock from paratuberculosis using point of care diagnostics (PoCD) (Sanction Order Number: BIRAC/BT/CRS0226/CRS-11/17). The authors gratefully acknowledge the financial support provided by DBT, New Delhi.

Conflict of interests

The authors declare that they have no conflict of interest.

Ethical clearance

The study was approved by the organizational animal ethical committee. All applicable institutional guidelines for the care and use of animals were followed.

References

1. Chiodini, R.J., Van Kruiningen, H.J. and Merkal, R.S. (1984). Ruminant paratuberculosis (Johne's disease): The current status and future prospects. *Cornell Vet.* 74:218-262.
2. Tripathi, B.N., Munjal, S.K. and Paliwal, O.P. (2002). An overview of paratuberculosis (Johne's disease) in animals. *Indian J. Vet. Pathol.* 26:1-10.
3. Sweeney, R.W., Collins, M.T., Koets, A.P., McGuirk, S.M. and Roussel, A.J. (2012). Paratuberculosis (Johne's disease) in cattle and other susceptible species. *J. Vet. Internal Med.* 26:1239-1250.
4. Ayele, W.Y., Machackova, M. and Pavlik, I. (2001). The transmission and impact of paratuberculosis infection in domestic and wild ruminants. *Vet. Med. Czech.* 46:205-224.
5. Hruska, K. (2004). Research on paratuberculosis: Analysis of publications 1994-2004. *Vet. Med. Czech.* 49:271-282.
6. Barad, D.B., Chandel, B.S., Dadawala, A.T., Chauhan H.C., Kher, H.S., Shroff, S., Bhagat, A.G., Singh, S.V., Singh P.K., Singh, A.V., Sohal, J.S., Gupta, S., Chaubey, K.K., Chakraborty, S., Tiwari, R., Deb R. and Dhama, K. (2014). Incidence of *Mycobacterium Avium* Subspecies paratuberculosis in Mehsani and Surti Goats of Indian Origin using Multiple Diagnostic Tests. *J. Biological Sci.* 14:124-133.
7. OIE. (2001). Paratuberculosis (Johne's disease). In: *Manual of Diagnostic Tests and Vaccines for Terrestrial Animals*. Ch. 2.1.11. World Organization for Animal Health, Paris, France.
8. Bhutediya, J.M., Dandapat, P., Chakrabarty, A., Das, R., Nanda, P.K., Bandyopadhyay, S. and Biswas, T.K. (2017). Prevalence of paratuberculosis in organized and unorganized dairy cattle herds in West Bengal, India, *Veterinary World.* 10(6):574-579.
9. Chiodini, R.J. and Hermon-Taylor, J. (1993). The thermal resistance of *Mycobacterium paratuberculosis* in raw milk under conditions simulating pasteurization. *J. Vet. Diagn. Invest.* 5:629.
9. Alluwaimi, A.M. (2007). The etiology of *Mycobacterium avium* subspecies *paratuberculosis* in Crohn's disease. *Saudi Med. J.* 28:1479-1484.
10. Eltholth, M.M., Marsh, V.R., Van Winden, S. and Guitian, F.J. (2009). Contamination of food products with *Mycobacterium avium paratuberculosis*: A systematic review. *Appl. Microbiol.* 107:1061-1071.
11. Chi, J., Van Leeuwen, J.A., Weersink, A. and Keefe, G.P. (2002) Direct production losses and treatment costs from bovine viral diarrhoea virus, bovine leukosis virus,

- Mycobacterium avium* subspecies *paratuberculosis*, and *Neospora caninum*. *Prev. Vet. Med.* 55:137-153.
12. Manning, E.J.B. and Collins, M.T. (2001). *Mycobacterium avium* subsp. *paratuberculosis*: Pathogen, pathogenesis and diagnosis. *Rev. Sci. Tech.* 20:133-150.
 13. Momotani, E. (2012). Epidemiological situation and control strategies for paratuberculosis in Japan. *Jpn. J. Vet. Res.* 60:19-29.
 14. Pande, P.G. (1940). Paratuberculosis (Johne's disease) of cattle in Assam. Its incidence and epizootiology. *Ind. J. Vet. Sci.* 10:40-46.
 15. Singh, S.V., Singh, A.V., Singh, P.K., Sohal, J.S. and Singh, N.P. (2007). Evaluation of an indigenous ELISA for diagnosis of Johne's disease and its comparison with commercial kits. *Ind. J. Microbiol.* 47:251-258.
 16. Shankar, H., Singh, S.V., Singh, P.K., Singh, A.V., Sohal J.S. and Greenstein, R.J. (2010). Presence, characterization and genotype profiles of *Mycobacterium avium* subspecies *paratuberculosis* from unpasteurized individual and pooled milk, commercial pasteurized milk and milk products in India by culture, PCR and PCR-REA methods. *Int. J. Infect. Dis.* 14:121-126.
 17. Cocito, C., Gilot, P., Coene, M., De Kesel, M., Poupart, P. and Vannuffel, P. (1994). Paratuberculosis. *J. Clin. Microbiol. Rev.* 7:328-345.
 18. Sockett, D.C., Carr D.J. and Collins, M.T. (1992). Evaluation of conventional and radiometric fecal culture and a commercial DNA probe for diagnosis of *Mycobacterium paratuberculosis* infections in cattle. *Canad. J. Vet. Res.* 56:148-153.
 19. Singh, A.V., Singh, S.V., Singh, P.K. and Sohal, J. S. (2010). Is *Mycobacterium avium* subsp. *paratuberculosis*, the cause of Johne's disease in animals, a good candidate for Crohn's disease in man? *Ind. J. Gastroenterol.* 29(2):53-58.
 20. Dhama, K., Mahesh, M., Tiwari, R., Singh, D.S., Deepak K., Singh, S.V. and Pradeep M.S. (2011). Tuberculosis in birds: Insights into the *Mycobacterium avium* infections. *Veterin. Med. Internat.* Article ID 712369, 14.
 21. OIE. (2014). Paratuberculosis. In manual of tests and vaccines for terrestrial animals. Johne's disease. Ch.2.1.11. World Organization for Animal Health, Paris, France.
 22. Speer, C.A., Scott, M.C., John, P. B., Waters, R.W., Yasuyuki, M., Whitlock, R.H., and Shigetoshi, E. (2006). A novel enzyme-linked immunosorbent assay for diagnosis of *Mycobacterium avium* subsp. *paratuberculosis* infections (Johne's disease) in Cattle. *Clinical Vaccine Immunol.* 13(5):535-540.
 23. Stewart, L.D., Nuria, T., Paul, M., Argudo J.M., Ruramayi, N., Neil, R., Delahay J.R., Roland, A., Ian Montgomery, W. and Irene R.G. (2017). Development of a novel immuno chromatographic lateral flow assay specific for *Mycobacterium bovis* cells and its application in combination with immuno magnetic separation to test badger faeces. *BMC Veterinary Res.* 13:131.
 24. Greenstein, R.J. (2003). Is Crohn's disease caused by a *Mycobacterium*? Comparisons with leprosy, tuberculosis and Johne's disease. *The Lancet Infectious Dis.* 3:507-514.
 25. Sechi, L.A. and Dow, C.T. (2015). *Mycobacterium avium* sp. *paratuberculosis* Zoonosis-The Hundred Year War-Beyond Crohn's Disease. *Front. Immunol.* 6:96.
 26. Davis, W.C., Kuenstner, J.T., and Singh, S.V. (2017). Resolution of Crohn's (Johne's) disease with antibiotics: what are the next

- steps? Expert Rev. Gastroenterol. Hepatol, 11(5):393-396.
27. Pickup, R.W., Rhodes, G., Arnott, S., Sidi-Boumedine, K., Bull, T.J., Weightman, A., Hurley, M. and Hermon-Taylor, J. (2005). *Mycobacterium avium* subsp. *paratuberculosis* in the catchment area and water of the River Taff in South Wales, United Kingdom, and its potential relationship to clustering of Crohn's disease cases in the city of Cardiff. Applied Environ. Microbiol. 71:2130-2139.
 28. Singh, S.V., Tiwari, A., Singh, A.V., Singh, P.K., Singh, B., Kumar, A., Gururaj, K., Gupta, S. and Kumar, N. (2012). Contamination of natural resources (soil and river water) with *Mycobacterium avium* subspecies *paratuberculosis* in three districts of Uttar Pradesh: a pilot study. Haryana Veterinar. 51:1-5.
 29. Rhodes, L., Harwood, T., Smith, K., Argyle, P. and Munday, R. (2014). Production of ciguatoxin and maitotoxin by strains of *Gambierdiscus australes*, *G. pacificus* and *G. polynesiensis* (Dinophyceae) isolated from Rarotonga, Cook Islands. Harmful Algae 39:185-190.
 30. Acharya, K.R., Dhand, N.K., Whittington, R.J. and Plain, K.M. (2017). Detection of *Mycobacterium avium* subspecies *paratuberculosis* in powdered infant formula using IS900 quantitative PCR and liquid culture media. Int. J. Food Microbiol. 257:1-9.
 31. Barrington, G.M., Gay, J.M., Eriks, I.S., Davis, W.C., Evermann, J.F., Emerson, C. and Bradway, D.S. (2003). Temporal patterns of diagnostic results in serial samples from cattle with advanced paratuberculosis infections. J. Veterin. Diagnostic Invest. 15(2):195-200.
 32. Collins, M.T. (1996). Diagnosis of paratuberculosis. Veterinary Clinics of North America: Food Animal Practice 12(2):357-371.
 33. Kumar, V., Bhatia, A.K., and Singh, S.V. (2006). Evaluation of efficacy of the species specific antigens in the diagnosis of ovine and caprine Paratuberculosis using plate ELISA. J. Immunol. Immunopathol. 8(1):48-53.
 34. Gupta, S., Singh, S.V. and Bhatia, A.K. (2016). Immuno-reactivity pattern of secretory proteins of *Mycobacterium avium* subspecies *paratuberculosis* vaccine strain 'S 5' with potential for diagnosis of Johne's disease in early infection. Ind. J. Biotechnol. 15(3):306-312.
 35. Shin, S.J., Cho, D. and Collins, M.T. (2008). Diagnosis of bovine paratuberculosis by a novel enzyme linked immunosorbent assay based on early secreted antigens of *Mycobacterium avium* subsp. *paratuberculosis*. Clin. Vaccine Immunol. 15(8):1277-1281.
 36. Rouhollah, K., Ali, M., Nader, M., Keyvan, T., Shamseddin, G., Farzaneh, F. and Shojaat, D.P. (2016). Development and optimization of a high sensitive and specific ELISA system for rapid detection of paratuberculosis in cattle. Int. J. Adv. Biotechnol. Res. 7(1):1-9.

Design, Synthesis, Cytotoxicity Evaluation, and Molecular Docking Studies of 1,3,4 Oxadiazole substituted 1,4-Naphthoquinone Derivatives

Mousumi Besan¹, Manoj K. Gautam², Sushant K. Shrivastava^{1*}

¹Department of Pharmaceutical Engineering and Technology, Indian Institute of Technology (Banaras Hindu University), Varanasi-221005, India.

²University Institute of Pharmaceutical Sciences, Panjab University, Chandigarh, 160014, India.

*For Correspondence - skshrivastava.phe@itbhu.ac.in

Abstract

In this manuscript we have designed and synthesized 1,4-Naphthoquinone analogs substituted with 1,3,4 Oxadiazolenucleus. The synthesized compound (M1- M14) were characterized using the different analytical technique ¹H NMR, ¹³C NMR, FTIR, Mass spectroscopy, melting point, elemental analysis and further subjected for the evaluation of their anticancer activity using MCF-7, Hela and HepG2 cancer cell lines. The compound M-5 was found to exhibit most potent cytotoxicity against cancer cell lines i.e. HeLa (IC₅₀ = 10.76 ± 0.11 μM), MCF-7 (IC₅₀ = 9.30 ± 0.14 μM) and HepG2 (IC₅₀ = 11.93 ± 0.38 μM). Compound M-5 has also shown potent tyrosine kinase inhibitory activity with IC₅₀ = 1.53 ± 0.05 μM. Moreover, molecular docking has exposed that compound M-5 has strong binding affinity to the active site of tyrosine kinase. These results give promising beginning stages to assist in the improvement of novel and powerful anticancer agents.

Keywords: Molecular Docking, Cytotoxicity Evaluation, 1,3,4 Oxadiazole, Tyrosine Kinase Inhibition

Introduction

Cancer is one of foremost ailments in which cells grow abnormally and can occur in all the living cells at every stage of human life. Cancer has become the second cause of mortality in the

world. The invasiveness of cancer and its metastatic behavior makes it unpredictable for treatment (1). By identifying the biological pathway which is participating to cancer progression by sophisticated biological tools will help in eradication of cancer. Using tobacco is the greatest risk factor for cancer mortality worldwide causing an estimated 22% of cancer deaths per annum. 22% of mouth and oropharynx cancers in men are attributable to alcohol (2). Almost 22% of cancer deaths in the developing world, 6% in industrialized countries are due to infectious agents and polluted air, water, and soil having carcinogenic chemicals accounts for 1–4% of all cancers. 3–14% of all lung cancers are caused by residential exposure to radon gas from soil and building materials, which makes it the second cause of lung cancer after tobacco smoke. Ultraviolet (UV) radiation, in particular solar radiation, is carcinogenic to humans, causing all major types of skin cancer, which includes basal cell carcinoma, squamous cell carcinoma, and melanoma (3). Breast cancer is the most frequently diagnosed cancer in female and the leading cause of cancer death, accounting for 23% of the total cancer cases and 14% of the cancer deaths (4). The therapeutic approach of cancer includes chemotherapy, radiotherapy, surgery, immunotherapy, monoclonal antibody therapy, hormonal therapy, targeted therapy, and angiogenesis inhibition. Existing anticancer drugs associated with the resistance, cytotoxicity, and

genotoxicity are the reasons that undoubtedly warrant the search for newer anticancer agents.

Tyrosine kinases can be involved in any of several steps of cancer development and progression. It can play major etiologic roles in the initiation of malignancy. Alternatively, contribution of tyrosine kinases to the uncontrolled proliferation of cancer cells, tumor progression, and development of metastatic disease, without directly initiating the cancer process is a matter of concern. All of them possess an extracellular ligand-binding domain, typically glycosylated, which conveys ligand specificity. The tyrosine kinase domain is part of the cytoplasmic domain of the receptor (5). Ligand binding induces activation of the intracellular tyrosine kinase domain, leading to receptor dimerization. The conformational change as a result from ligand binding and receptor dimerization leads to interactions between adjacent cytoplasmic domains and activation of the tyrosine kinase. When EGF binds with its receptor, it causes dimerization of the epidermal growth factor receptor (EGFR) and finally activation of tyrosine kinase (6). Moreover, EGFR is over expressed in a variety of tumor (cancers) i.e. brain cancer, pancreatic cancer, lung cancer and neck cancer (7). The controlling of EGFR has been esteemed as a vital methodology for the improvement of cancer therapy. Thus, EGFR is an alluring focus for the finding of novel anticancer agents.

The various quinone scaffolds has been reported for the treatment of cancer. Especially, 1, 4-naphthoquinones are lively quinone derivatives that are broadly utilized in pharmaceuticals(8). 1, 4-naphthoquinone derivatives has been accounted to be utilized as anticancer agents (9). It is having two ketone chromophore which is essential for the biological activities from their capacity to accept the electrons. Structure-activity relationship (SAR) exposed that cytotoxicity potency of 1,4-naphthoquinone is firmly connected with their electron accepting ability (10), which offers lead to reactive oxygen species generation(ROS) promoting DNA destruction and ultimately cell death.

Designing considerations

Quinone ring play a key role in most preclinically tested and clinically investigated anticancer agents such as mitomycin-C, daunorubicin, doxorubicin, idarubicin, epirubicin, aclarubicin, mitoxantrone (anthraquinone), atovaquone, binaphthoquinones, and b-lapachone which are commonly used for the treatment of solid and hematologic neoplasms(11). The cytotoxic mechanisms of action of these compounds mainly include the formation of semiquinone radicals and quinone redox cycling ensuing in the initiation and propagation of intracellular free oxygen radical chain reactions.

Additionally, the 1, 4-naphthoquinone pharmacophore exhibits anticancer activity and has been the focus of various studies. Compounds like plumbagin, mitomycin and shikonin having 1, 4-naphthoquinone moiety which are used in the development of potent anticancer drugs (12). On the other hand, these compounds exhibit high levels of cytotoxicity and significant side effects, making their application as anticancer drugs in the clinical setup to be challenging.

2-Methyl-1,4-naphthoquinone, which is both a redox-cycling and an alkylating quinone, was shown to lead to the activation of the extracellular signal-regulated kinase (ERK) 1 and ERK 2, which are well known for their prominent role in the regulation of cellular proliferation. The activation of ERK was blocked by inhibitors of the direct upstream kinases of ERK 1/2, MAPK/ERK kinase (MEK) 1, and MEK 2 and by inhibitors of the epidermal growth factor receptor (EGFR) tyrosine kinase, leading to the hypothesis that ligand-independent activation of the EGFR by 2-methyl-1,4-naphthoquinone was responsible for the above-described effects (13). The most interesting is the synthesis of compounds with antitumor activity as selective inhibitors of biological targets, epidermal growth factor receptor (EGFR). Thus, 1, 4-naphthoquinone moiety is regarded as a privileged framework in medicinal chemistry.

Besides, the quinone derivatives, recently, the oxadiazole chemistry has been developed extensively and is still developing. Most of the

drugs are used clinically, which comprise oxadiazole moiety in association with various heterocyclic rings. Oxadiazoles are an important type of oxygen and nitrogen containing aromatic heterocyclic compounds, which possess desirable electronic and charge-transport properties and the various functional groups are easily introduced into the structurally rigid oxadiazole ring. These characteristics resulted in the extensive potential applications of oxadiazole based derivatives in the field of medicinal chemistry.

The biological prospects of oxadiazoles as anticancer (14), antitubercular (15), anticonvulsant (16), antimicrobial (17), anti-HIV (18), anti-inflammatory (19) etc., has inspired us to go further on with the investigation of this moiety. Focussing on the antitumor activity only, the characteristics of the oxadiazole template make this molecular subunit a useful and well-positioned system in the rational design of drugs.

Considering the reported literature, it is clear that fervent desire and pervasive drug designing will be necessary to make new anticancer agent, hence we hypothesized that the development of hybrid molecules through the

combination of different pharmacophore i.e., 1,4-naphthoquinone and 1,3,4-oxadiazole moiety in one frame may lead to compounds with improved anticancer profiles. Thus, we believed that the designing of a molecule with 1,4-naphthoquinone moiety as a molecular scaffold by using strategies like linking with oxadiazole moiety and by using carbon chain length as a linker will ensemble for better anticancer activity. Based on hybrid pharmacophore approach, the 1,4-naphthoquinone moiety was tethered to substituted 1,3,4-oxadiazole nucleus with the aim of developing ligands having ability to inhibit tyrosine kinase and serve as anticancer agent (Fig 1).

Material and Methods

Instrumentation and Chemicals: The chemical reagents were obtained from various commercially accessible suppliers, HiMedia Laboratories Pvt. Ltd., Mumbai, India, Sigma Aldrich (India). Silica gel 60-F₂₅₄ plates, thin-layer chromatography (TLC) were used to monitor the progress of the reaction. The obtained product was recrystallized to get pure products using suitable solvents. The melting point of compounds was recorded using Veego melting point apparatus. PerkinElmer spectrum (Ver 10.03.08) utilized for the FTIR data collection.

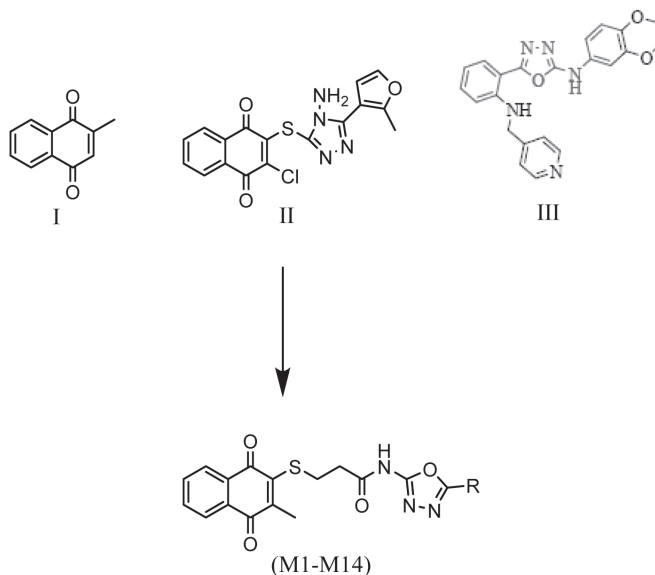


Fig. 1. Designing strategy for the target compounds

1,3,4-Oxadiazoles as anticytotoxic agents

¹³CNMR and ¹HNMR spectra of synthesized compounds were collected with the help of Bruker Advance II 400 NMR spectrometer. The chemical shifts (δ) represented as parts per million (ppm). Elemental analysis was done with the help of Thermo Scientific and Mass spectroscopy was performed through Waters Q-TOF MICROMASS (ESI-MS).

Chemistry

General procedure for the synthesis of 3-((3-methyl-1, 4-dioxo-1,4-dihydro naphthalen-2-yl) thio) propanoic acid (3): Compound 3 was obtained by condensation of 2-methylnaphthalene-1,4-dione (1) (0.516 g, 3 mmol) with 3-mercaptopropionic acid (2) (0.360 g, 3 mmol) in absolute ethanol (50 ml) and the reaction mixture was refluxed for 3-5 h. The obtained crude product was recrystallized from methanol (9, 20).

3-((3-methyl-1, 4-dioxo-1, 4-dihydro naphthalen-2-yl) thio) propanoic acid (3): Obtained as solid in 65 % yield; mp: 112-114 °C. IR (KBr, ν cm⁻¹) 3458, 3061, 2938, 1720, 1667, 1514, 1431, and 883 cm⁻¹. ¹H NMR (CDCl₃): δ 9.47 (s, 1H, COOH), 8.23 (m, 2H, ArH), 7.70 (m, 2H, ArH), 3.47 (t, 2H, SCH₂, J = 6.60 Hz), 2.70 (t, 2H, CH₂C=O, J = 6.60 Hz).

General procedure for the synthesis of compounds (M1-M14): All the titled compounds (M1-M14) was prepared by dissolving compound-3 in dry dichloromethane (DCM) and an equimolar quantity of thionyl chloride was added gradually. The reaction mixture was stirred for 3-5 hrs for the formation of acid chloride product. Further different substituted oxadiazoles in equimolar ratio was added, followed by addition of acid chloride and the reaction mixture was stirred for 9-10 hrs. (9) When the reaction was completed, sodium bicarbonate solution was used to wash the organic layer, evaporated and the final products were purified with the help of column chromatography. The spectral data of the synthesized compound has been shown in table no 6.

N-(5-methyl-1,3,4-oxadiazol-2-yl)-3-((3-methyl-1, 4-dioxo-1,4-dihydro naphthalen-2-yl)thio)propanamide (M-1): Obtained as white solid in 58 % yield; mp: 220-222 °C; IR (KBr, ν cm⁻¹) 3356, 3076, 2989, 1673, 1634, 1466, 1297 and 763 cm⁻¹. ¹HNMR (CDCl₃, 400 MHz, δ): 9.48 (s, 1H, -NH), 8.18 (m, 4H, ArH), 2.98 (t, 2H, J = 5.64 Hz, -SCH₂), 2.85 (t, 2H, J = 5.48 Hz, -COCH₂), 2.77 (s, 3H, CH₃), 2.19 (s, 3H, CH₃). ¹³CNMR (CDCl₃, 100 MHz, δ): 185.73 (C=O), 178.54 (C=O), 170.21 (C=O), 152.84 (ArC_q), 151.50 (ArC_q), 139.45 (ArC_q), 137.50 (ArC_q), 133.84 (ArC_q), 132.40 (2 \times ArC), 130.93 (ArC), 127.90 (ArC), 128.93 (ArC), 34.04 (S-CH₂), 30.31 (COCH₂), 15.11 (CH₃), 8.96 (CH₃). MS: m/z 357.08; Anal. Calcd. C₁₇H₁₅N₃O₄S: C 54.32, H 3.73, N 28.79. Found: C 54.83, H 3.12, N 28.83.

N-(5-ethyl-1,3,4-oxadiazol-2-yl)-3-((3-methyl-1, 4-dioxo-1,4-dihydro naphthalen-2-yl)thio)propanamide (M-2): Obtained as brown solid in 63 % yield; mp: 209-211 °C; IR (KBr, ν cm⁻¹) 3395, 3105, 2950, 1686, 16474, 1467, 1189 and 757 cm⁻¹. ¹HNMR (CDCl₃, 400 MHz, δ): 9.54 (s, 1H, -NH), 8.19 (m, 2H, ArH), 7.74 (m, 2H, ArH) 3.18 (t, 2H, J = 5.48 Hz, -SCH₂), 2.85 (t, 2H, J = 5.52 Hz, -COCH₂), 2.77 (s, 3H, CH₃), 2.57 (q, 2H, J = 6.80 Hz, CH₂), 1.29 (t, 3H, J = 6.76 Hz, CH₃). ¹³CNMR (CDCl₃, 100 MHz, δ): 185.72 (C=O), 178.83 (C=O), 170.79 (C=O), 155.28 (ArC_q), 154.17 (ArC_q), 139.45 (ArC_q), 137.50 (ArC_q), 133.83 (ArC), 132.39 (2 \times ArC_q), 130.80 (ArC_q), 128.83 (ArC), 127.89 (ArC), 34.36 (CH₂C=O), 30.20 (S-CH₂), 18.78 (CH₂), 15.97 (CH₃), 7.14 (CH₃). MS: m/z 371.12; Anal. Calcd. for C₁₈H₁₇N₃O₄S: C, 58.21, H 4.61, N 11.31. Found: C 58.93, H 4.24, N 11.39.

3-((3-methyl-1,4-dioxo-1,4-dihydro naphthalen-2-yl)thio)-N-(5-propyl-1,3,4-oxadiazol-2-yl)propanamide (M-3): Obtained as a white crystalline solid in 52 % yield; mp: 183-185 °C; IR (KBr, ν cm⁻¹) 3366, 2995, 1703, 1658, 1449, 1245 and 765 cm⁻¹. ¹HNMR (CDCl₃, 400 MHz, δ): 9.54 (s, 1H, -NH), 8.19 (m, 2H, ArH), 7.75 (m, 2H, ArH) 3.20 (t, 2H, J = 5.52 Hz, -SCH₂), 2.86 (t, 2H, J = 5.52 Hz, -COCH₂), 2.78 (s, 3H, CH₃), 2.67 (t,

2H, $J = 8.04$ Hz, CH_2), 1.68 (m, 2H, CH_3), 1.02 (t, 3H, $J = 6.64$ Hz, CH_3). ^{13}C NMR ($CDCl_3$, 100 MHz, δ): 185.86 (C=O), 178.77 (C=O), 170.57 (C=O), 156.77 (ArC_q), 155.50 (ArC_q), 139.44 (ArC_q), 137.82 (ArC), 133.58 (ArC), 132.40 ($2 \times ArC_q$), 130.38 (ArC_q), 128.04 (ArC), 127.90 (ArC_q), 34.68 ($CH_2C=O$), 30.97 (S- CH_2), 27.51, (CH_2), 18.78 (CH_2), 17.14 (CH_3) 15.32 (CH_3). MS: m/z : 385.09; Anal. Calcd. for $C_{19}H_{19}N_3O_4S$: C59.21, H4.97, N25.83. Found: C59.64, H5.12, N25.43.

3-((3-methyl-1,4-dioxo-1,4-dihydronaphthalen-2-yl)thio)-N-(5-phenyl-1,3,4-oxadiazol-2-yl)propanamide (M-4): Obtained as yellow solid in 46 % yield; mp: 146-148 °C; IR (KBr, ν cm^{-1}) 3354, 30137, 2952, 1671, 1644, 1446, 1193 and 721 cm^{-1} . 1H NMR ($CDCl_3$, 400 MHz, δ): 9.79 (s, 1H, -NH), 8.20 (dd, 1H, $J_m = 1.52$ Hz, $J_o = 7.52$ Hz, ArH), 8.14 (dd, 1H, $J_m = 1.52$ Hz, $J_o = 7.52$ Hz, ArH), 7.73 (m, 1H ArH), 7.70 (m, 2H, ArH) 7.63 (m, 1H, ArH), 7.45 (m, 3H, ArH) 3.16 (t, 2H, $J = 5.60$ Hz, - SCH_2), 2.86 (t, 2H, $J = 5.64$ Hz, - $COCH_2$), 2.63 (s, 3H, CH_3). ^{13}C NMR ($CDCl_3$, 100 MHz, δ): 185.13 (C=O), 178.04 (C=O), 170.31 (C=O), 155.80 (ArC_q), 154.90 (ArC_q), 139.23 (ArC_q), 137.79 (ArC), 133.51 (ArC), 132.04 ($2 \times ArC_q$), 130.31 (ArC_q), 129.04 ($2 \times ArC$), 128.13 (ArC_q), 127.02 ($2 \times ArC$), 127.52 ($2 \times ArC$), 126.61 (ArC_q), 34.19 ($CH_2C=O$), 30.12 (S- CH_2), 15.86 (CH_3). MS: m/z 419.16; Anal. Calcd. for $C_{22}H_{17}N_3O_4S$: C, 63.02, H 4.09, N 10.02. Found: C 63.43, H 4.34, N 10.25.

N-(5-(4-methoxyphenyl)-1,3,4-oxadiazol-2-yl)-3-((3-methyl-1,4-dioxo-1,4-dihydronaphthalen-2-yl)thio)propanamide (M-5): Obtained as brown solid in 49 % yield; mp: 215-217 °C; IR (KBr, ν cm^{-1}) 3329, 3178, 2941, 1684, 1633, 1486, 1281 and 778 cm^{-1} . 1H NMR ($CDCl_3$, 400 MHz, δ): 9.45 (s, 1H, -NH), 8.20 (m, 2H, ArH), 7.74 (m, 2H, ArH), 7.61 (d, 2H $J = 7.44$ Hz, ArH), 7.06 (d, 2H, $J = 7.44$ Hz, ArH) 3.78 (s, 3H, - OCH_3), 3.07 (t, 2H, $J = 5.88$ Hz, - SCH_2), 2.90 (t, 2H, $J = 5.84$ Hz, - $COCH_2$), 2.66 (s, 3H, CH_3). ^{13}C NMR ($CDCl_3$, 100 MHz, δ): 185.15 (C=O), 178.21 (C=O), 170.21 (C=O), 162.15 (ArC_q), 155.62 (ArC_q), 154.93 (ArC_q), 139.25 (ArC_q), 137.86 (ArC), 133.77 (ArC), 132.77 ($2 \times ArC_q$), 130.26 (ArC_q), 128.41 (ArC), 127.21

(ArC), 127.89 ($2 \times ArC$), 121.54 (ArC_q) 113.87 ($2 \times ArC$), 56.03 (OCH_3), 34.73 ($CH_2C=O$), 30.80 (S- CH_2), 15.18 (CH_3). MS: m/z 449.06; Anal. Calcd. for $C_{23}H_{19}N_3O_5S$: C61.46, H 4.26, N 9.35. Found: C 61.29, H 4.15, N 9.96.

N-(5-(2-methoxyphenyl)-1,3,4-oxadiazol-2-yl)-3-((3-methyl-1,4-dioxo-1,4-dihydronaphthalen-2-yl)thio)propanamide (M-6): Obtained as brownish solid in 62% yield; mp: 230-232 °C; IR (KBr, ν cm^{-1}) 3342, 3077, 2940, 1685, 1650, 1487, 1255 and 720 cm^{-1} . 1H NMR ($CDCl_3$, 400 MHz, δ): 9.67 (s, 1H, -NH), 8.08 (dd, 1H, $J_m = 1.52$, $J_o = 7.48$ Hz, Hz, ArH), 8.03 (dd, 1H, $J_m = 1.52$ Hz, $J = 7.40$ Hz, ArH), 7.77 (td, 1H, $J_m = 1.52$ Hz, $J_o = 7.52$ Hz, ArH), 7.56 (m, 2H, ArH), 7.35 (td, 1H, $J_m = 1.44$ Hz, $J_o = 7.45$ Hz, ArH), 7.12 (m, 2H, ArH), 3.80 (s, 3H, OCH_3), 3.29 (t, 2H, $J = 5.20$ Hz, - SCH_2), 2.89 (t, 2H, $J = 5.16$ Hz, - $COCH_3$), 2.56 (s, 3H, - CH_3). ^{13}C NMR ($CDCl_3$, 100 MHz, δ): 186.31 (C=O), 178.40 (C=O), 170.30 (C=O), 158.40 (ArC_q), 155.87 (ArC_q), 143.56 (ArC_q), 139.47 (ArC_q), 137.31 (ArC), 133.05 (ArC), 132.16 (ArC_q), 131.09 (ArC), 131.08 (ArC), 130.58 (ArC_q), 128.57 (ArC), 127.89 (ArC), 120.54 (ArC_q), 118.87 (ArC_q), 115.30 (ArC), 56.03 (OCH_3), 34.36 ($CH_2C=O$), 30.37 (S- CH_2), 15.73 (CH_3). MS: m/z 449.13; Anal. Calcd. for $C_{23}H_{19}N_3O_5S$: C 61.46, H 4.26, N 9.35. Found: C 61.12, H 4.76, N 9.27.

N-(5-(3-methoxyphenyl)-1,3,4-oxadiazol-2-yl)-3-((3-methyl-1,4-dioxo-1,4-dihydronaphthalen-2-yl)thio)propanamide (M-7): Obtained as white solid in 58 % yield; mp: 205-207 °C; IR (KBr, ν cm^{-1}) 3370, 2979, 1699, 1640, 1401, 1212 and 743 cm^{-1} . 1H NMR ($CDCl_3$, 400 MHz, δ): 9.54 (s, 1H, -NH), 8.18 (m, 2H, ArH), 7.76 (m, 2H, ArH), 7.47 (t, 1H, $J = 7.48$ Hz, ArH), 7.27 (m, 2H, ArH), 7.12 (m, 1H, ArH), 6.92 (m, 1H, ArH), 3.79 (s, 3H, - OCH_3), 3.01 (t, 2H, $J = 5.88$ Hz, - SCH_2), 2.86 (t, 2H, $J = 5.80$ Hz, - $COCH_2$), 2.63 (s, 3H, CH_3). ^{13}C NMR ($CDCl_3$, 100 MHz, δ): 185.96 (C=O), 178.28 (C=O), 170.36 (C=O), 161.17 (ArC_q), 155.11 (ArC_q), 153.42 (ArC_q), 139.06 (ArC_q), 137.94 (ArC_q), 133.36 (ArC), 132.84 (ArC_q), 130.53 (ArC), 128.54 (ArC), 128.00 (ArC), 127.82 (ArC), 125.25 (ArC_q), 120.51 (ArC), 117.36 (ArC),

114.11(ArC), 115.30 (ArC), 56.03 (OCH₃), 34.12(CH₂C=O), 30.82 (S-CH₂), 15.52 (CH₃).MS: *m/z* 449.02; Anal. Calcd. for C₂₃H₁₉N₃O₅S: C 61.46, H 4.26, N 9.35. Found: C 61.63, H 4.81, N 9.30.

***N*-(5-(2,4-dimethoxyphenyl)-1,3,4-oxadiazol-2-yl)-3-((3-methyl-1,4-dioxo-1,4-dihydronaphthalen-2-yl)thio)propanamide (M-8)**: Obtained as white solid in 49 % yield; mp: 221-223 °C; IR (KBr, ν cm⁻¹) 3399, 3002, 1706, 1649, 1433, 1261 and 727 cm⁻¹. ¹HNMR (CDCl₃, 400 MHz, δ): 9.64 (s, 1H, -NH), 8.13 (m, 2H, ArH), 7.79 (m, 2H, ArH), 7.53 (m, 1H, ArH), 6.74 (m, 2H, ArH), 3.80 (s, 6H, OCH₂), 3.30 (t, 2H, *J* = 5.28 Hz, -SCH₂), 2.86 (t, 2H, *J* = 5.28 Hz, -COCH₂), 2.42 (s, 3H, CH₃). ¹³CNMR (CDCl₃, 100 MHz, δ): 185.91 (C=O), 178.73 (C=O), 170.56 (C=O), 161.96 (ArC_q), 159.32 (ArC_q), 155.88 (ArC_q), 143.32, (ArC_q), 139.60 (ArC_q), 137.53 (ArC_q), 133.49 (ArC), 132.55 (2 × ArC), 130.47 (ArC_q), 130.42 (ArC), 128.43 (ArC), 127.90 (ArC), 116.17 (ArC_q), 107.96 (ArC), 101.25 (ArC), 56.78 (OCH₃), 56.03 (OCH₃), 34.93(CH₂C=O), 30.31 (S-CH₂), 15.62 (CH₃).MS: *m/z* 479.88; Anal. Calcd. for C₂₄H₂₁N₃O₆S: C 60.12, H 4.41, N 8.76. Found: C 60.23, H 4.33, N 8.69.

***N*-(5-(4-chlorophenyl)-1,3,4-oxadiazol-2-yl)-3-((3-methyl-1,4-dioxo-1,4-dihydronaphthalen-2-yl)thio)propanamide (M-9)**: Obtained as brownish solid in 62 % yield; mp: 181-183 °C; IR (KBr, ν cm⁻¹) 3363, 2956, 1681, 1643, 1441, 1268, 750 cm⁻¹. ¹HNMR (CDCl₃, 400 MHz, δ): 9.70 (s, 1H, -NH), 8.19 (m, 2H, ArH), 7.74 (m, 2H, ArH), 7.48 (q, 4H, *J* = 7.52 Hz, ArH), 3.17 (t, 2H, *J* = 8.16 Hz, SCH₂), 2.78 (t, 2H, *J* = 8.20 Hz, -COCH₂), 2.70 (s, 3H, CH₃). ¹³CNMR (CDCl₃, 100 MHz, δ): 185.55 (C=O), 178.46 (C=O), 170.55 (C=O), 155.14 (ArC_q), 154.55 (ArC_q), 139.50 (ArC_q), 137.84 (ArC_q), 137.74 (C-Cl) 133.64 (ArC), 132.22 (2 × ArC_q), 130.49 (ArC_q), 129.25 (2 × ArC), 128.85 (ArC_q), 128.61 (ArC), 128.59 (2 × ArC), 127.71 (ArC), 34.02(CH₂C=O), 30.30 (S-CH₂), 15.22 (CH₃).MS: *m/z* 453.17 (M⁺ + 1), 455.17 (M⁺ + 2); Anal. Calcd. for C₂₂H₁₆ClN₃O₄S: C 58.21, H 3.55, N 9.26. Found: C 58.31, H 3.48, N 9.20.

***N*-(5-(2-chlorophenyl)-1,3,4-oxadiazol-2-yl)-3-((3-methyl-1,4-dioxo-1,4-dihydronaphthalen-2-yl)thio)propanamide (M-10)**: Obtained as white solid in 64 % yield; mp 178-180 °C; IR (KBr, ν cm⁻¹) 3340, 2931, 1695, 1651, 1411, 1192, 718 cm⁻¹. ¹HNMR (CDCl₃, 400 MHz, δ): 9.73 (s, 1H, -NH), 8.22 (m, 2H, ArH), 7.73 (m, 2H, ArH), 7.60 (m, 1H, ArH), 7.43 (m, 1H, ArH), 7.33 (m, 2H, ArH), 3.16 (t, 2H, *J* = 8.20 Hz, SCH₂), 2.78 (t, 2H, *J* = 8.16 Hz, -COCH₂), 2.74 (s, 3H, CH₃). ¹³CNMR (CDCl₃, 100 MHz, δ): 185.93 (C=O), 178.27 (C=O), 170.18 (C=O), 155.60 (ArC_q), 142.35 (ArC_q), 139.96 (ArC_q), 137.12 (ArC_q), 134.28 (C-Cl) 133.17 (ArC), 132.11 (2 × ArC_q), 131.94 (ArC), 131.06 (ArC), 130.36 (ArC_q), 128.84 (ArC), 127.56 (ArC), 127.60 (ArC_q), 127.00 (ArC), 126.54 (ArC), 34.92(CH₂C=O), 30.25 (S-CH₂), 15.61 (CH₃).MS: *m/z* 453.12 (M⁺ + 1), 455.12 (M⁺ + 2); Anal. Calcd. for C₂₂H₁₆ClN₃O₄S: C 58.21, H 3.55, N 9.26. Found: C 58.28, H 3.49, N 9.30.

***N*-(5-(2,3-dichlorophenyl)-1,3,4-oxadiazol-2-yl)-3-((3-methyl-1,4-dioxo-1,4-dihydronaphthalen-2-yl)thio)propanamide (M-11)**: Obtained as yellow solid in 57 % yield; mp; 191-193 °C; IR (KBr, ν cm⁻¹) 3332, 3076, 2940 1686, 1634, 1486, 1281, 777 cm⁻¹. ¹HNMR (CDCl₃, 400 MHz, δ): 9.87 (s, 1H, -NH), 8.25 (m, 2H, ArH), 7.78 (m, 2H, ArH), 7.37 (m, 2H, ArH), 7.24 (m, 1H, ArH), 3.11 (t, 2H, *J* = 8.00 Hz, SCH₂), 2.82 (t, 2H, *J* = 7.92 Hz, -COCH₂), 2.65 (s, 3H, -CH₃). ¹³CNMR (CDCl₃, 100 MHz, δ): 185.30 (C=O), 178.67 (C=O), 170.65 (C=O), 155.26 (ArC_q), 141.87 (ArC_q), 139.21 (ArC_q), 137.39 (ArC_q), 135.95 (C-Cl) 134.91 (C-Cl) 133.37 (ArC), 132.76 (2 × ArC_q), 131.27 (ArC), 130.36 (ArC_q), 128.67 (ArC), 128.64 (ArC), 128.11 (ArC_q), 127.67 (ArC), 124.03 (ArC), 34.32(CH₂C=O), 30.53 (S-CH₂), 15.08 (CH₃).MS: *m/z* 488.958 (M⁺ + 1), 490.98 (M⁺ + 2); 490.95; Anal. Calcd. for C₂₂H₁₅Cl₂N₃O₄S: C 51.56, H 2.42, N 18.72. Found: C 51.86, H 2.37, N 18.23.

3-((3-methyl-1,4-dioxo-1,4-dihydronaphthalen-2-yl)thio)-*N*-(5-(*p*-tolyl)-1,3,4-oxadiazol-2-yl)propanamide (M-12): Obtained as white solid in 56 % yield; mp: 157-159 °C; IR (KBr, ν cm⁻¹) 3372, 2971, 1698, 1654, 1461, 1258, 771 cm⁻¹. ¹HNMR (CDCl₃, 400 MHz, δ): 9.79 (s, 1H, -NH),

8.16 (m, 2H, ArH), 7.71 (td, 1H, $J_m = 1.40$ Hz, $J_o = 7.48$ Hz, ArH), 7.55 (m, 3H, ArH), 7.32 (d, 2H, $J = 5.64$ Hz, ArH), 3.17 (t, 2H, $J = 5.64$ Hz, SCH₂), 2.87 (t, 2H, $J = 5.64$ Hz, -COCH₂), 2.63 (s, 3H, -CH₃), 2.36 (s, 3H, CH₃). ¹³CNMR (CDCl₃, 100 MHz, δ): 185.61 (C=O), 178.80 (C=O), 170.00 (C=O), 155.38 (ArC_q), 154.36 (ArC_q), 140.51 (ArC_q), 139.64 (ArC_q), 137.07 (ArC_q), 133.67 (ArC), 132.33 (2 × (ArC_q), 130.28 (ArC_q), 129.08 (2 × ArC), 128.16 (ArC), 127.33 (ArC), 126.83 (2 × ArC), 125.39 (ArC_q), 40.91 (ArC), 34.80 (CH₂C=O), 30.57 (S-CH₂), 15.21 (CH₃). MS: m/z 433.04; Anal. Calcd. for C₂₃H₁₉N₃O₄S: C 63.73, H 4.42, N 9.69. Found: C 63.42, H 4.47, N 9.74.

***N*-(5-(2,5-dimethylphenyl)-1,3,4-oxadiazol-2-yl)-3-((3-methyl-1,4-dioxo-1,4-dihydronaphthalen-2-yl)thio)propanamide (M-13)**: Obtained as creamy solid in 63 % yield; mp: 236-238 °C; IR (KBr, ν cm⁻¹) 3325, 3048, 2912, 1694, 1648, 1423, 1226 and 702 cm⁻¹. ¹H NMR (CDCl₃, 400 MHz, δ): 9.59 (s, 1H, -NH), 8.18 (m, 2H, ArH), 7.73 (m, 2H, ArH), 7.47 (d, 1H, $J = 1.40$ Hz, ArH), 7.18 (m, 2H, ArH), 3.07 (t, 2H, $J = 5.92$ Hz, -SCH₂), 2.90 (t, 2H, $J = 5.88$ Hz, -COCH₂), 2.66 (s, 3H, -SCH₃), 2.43 (s, 3H, CH₃), 2.32 (s, 3H, CH₃). ¹³CNMR (CDCl₃, 100 MHz, δ): 185.80 (C=O), 178.54 (C=O), 170.86 (C=O), 155.79 (ArC_q), 148.28 (ArC_q), 139.45 (ArC_q), 137.98 (ArC_q), 137.38 (ArC_q), 136.49 (ArC_q), 133.82 (2 × ArC), 132.41 (2 × ArC), 130.58 (ArC), 130.57 (ArC_q), 128.75 (ArC), 128.55 (ArC_q), 128.53 (ArC), 127.84 (ArC), 34.09 (CH₂C=O), 30.65 (S-CH₂), 121.19 (CH₃), 121.23 (CH₃), 15.98 (CH₃). MS: m/z 447.14; Anal. Calcd. for C₂₄H₂₁N₃O₄S: C 64.41, H 4.73, N 9.39. Found: C 64.53, H 4.64, N 9.33.

***N*-(5-(4-hydroxy-3-methylphenyl)-1,3,4-oxadiazol-2-yl)-3-((3-methyl-1,4-dioxo-1,4-dihydronaphthalen-2-yl)thio)propanamide (M-14)**: Obtained as yellow solid in 51 % yield; mp: 213-215 °C; IR (KBr, ν cm⁻¹) 3321, 3109, 2984, 1701, 1667, 1443, 1282, 740 cm⁻¹. ¹H NMR (CDCl₃, 400 MHz, δ): 9.45 (s, 1H, -NH), 8.18 (m, 3H, ArH), 7.74 (m, 2H, ArH), 7.28 (m, 2H, ArH), 6.85 (d, 1H $J = 7.44$ Hz, ArH), 3.14 (m, 2H, SCH₂), 2.83 (t, 2H, $J = 5.60$ Hz, COCH₂), 2.71 (s, 3H, -CH₃), 2.32 (t,

3H, $J = 5.60$ Hz, -CH₃). ¹³CNMR (CDCl₃, 100 MHz, δ): 185.42 (C=O), 178.74 (C=O), 170.01 (C=O), 157.42 (ArC_q), 155.23 (ArC_q), 154.21 (ArC_q), 139.10 (ArC_q), 137.27 (ArC_q), 133.38 (ArC), 132.19 (2 × (ArC_q), 130.20 (ArC_q), 128.76 (ArC), 127.98 (ArC), 127.08 (ArC), 126.67 (ArC), 125.56 (ArC_q), 117.51 (ArC_q), 112.97 (ArC), 34.25 (CH₂C=O), 30.58 (S-CH₂), 16.01 (CH₃), 15.29 (CH₃). MS: m/z 449.93; Anal. Calcd. for C₂₃H₁₉N₃O₅S: C 61.46, H 4.26, N 9.35. Found: C 61.86, H 4.23, N 9.38.

Cell culture: Cancer cell lines MCF-7, Hela and HeGP 2 were purchased from the National Center for Cell Sciences (NCCS) Pune. Dulbecco's modified Eagle medium (DMEM) supplemented with 1% penicillin-streptomycin (Gibco), 10% (v/v) heat-inactivated FBS and 10% fetal bovine serum (Gibco) was used to culture the procured cancer cell lines. Further, this media was maintained at 37 °C in a humidity controlled incubator containing 5% carbon dioxide (21).

In vitro cytotoxicity (MTT assay): *In vitro* anticancer activity (cytotoxicity) was investigated by means of MTT assay. The cancer cell lines were spread in 96-well cell culture plate (5 × 10³ cells/well) and were allowed to stand in a humidified atmosphere (5% CO₂) overnight at 37°C. Various concentrations (10, 20, 30, 40 and 50 μ M) of synthesized compounds were added after 24 h of incubation. Further cells were incubated for another 24 h. The phosphate buffer solution was utilized for washing the cells in well, subsequently plate was incubated at 37 °C after adding 20 μ L MTT staining solution (0.005 % w/w in phosphate buffer) to each well. For dissolving the formazan crystals, in each well 100 μ L of dimethyl sulfoxide (DMSO) was added, and the absorbance of the resulting solution was observed at 570 nm using microtiter plate reader (22) The IC₅₀ was computed by employing graph Pad Prism Version 5.

Tyrosine kinase inhibitory activity: The kinase activity was evaluated with enzyme-linked immunosorbent assay (ELISA). The assays were

performed in 96-well microtiter plates that had been coated overnight with 2.0 μg of a polyGlu-Tyr peptide (4:1) (Sigma P-0275) in 0.1 mL of PBS per well. The purified kinases were diluted in kinase assay buffer (100 mM HEPES pH 7.5, 100 mM NaCl, and 0.1 mM sodium orthovanadate) and added to all test wells at 5 ng of GST fusion protein per 0.05 mL volume buffer. Test compounds were diluted in DMSO and added to test wells (0.025 mL/well). The kinase reaction was initiated by the addition of 0.025 mL of 40 μM ATP/40 mM MnCl_2 , and plates were shaken for 10 min before stopping the reactions with the addition of 0.025 mL of 0.5 M EDTA. The final ATP concentration was 10 μM , which is twice the experimentally determined K_m value for ATP. Negative control wells received MnCl_2 alone without ATP. The plates were washed three times with 10 mM Tris pH 7.4, 150 mM NaCl, and 0.05% Tween-20 (TBST). Rabbit polyclonal anti-phosphotyrosine antiserum was added to the wells at a 1:10000 dilution in TBST for 1 h. The plates were then washed three times with TBST. Goat anti-rabbit antiserum conjugated with horseradish peroxidase was then added to all wells (Biosource Cat. No. ALI0404; 1:10000 dilution in TBST) for 1 h. The plates were washed three times with TBST, and the peroxidase reaction was detected with the addition of 2,2'-azino-bis(3-ethylbenzothiazoline-6-sulfonic acid) (ABTS) (Sigma A1888). Plate was read using a multiwell spectrophotometer at 492 nm. The inhibitory rate (%) was calculated with the formula: $[1 - (\text{treated groups} / \text{control groups})] \times 100\%$. IC_{50} values were calculated from the inhibitory curves.

Molecular Docking: Epidermal growth factor receptor (EGFR), (PDB: 2GS6) was obtained from the Protein Data Bank (PDB). Molecular docking was performed with the help of VLifeMDS (version 15.2). All the synthesized compounds (M1-M14) were docked using an irreversible inhibitor of EGFR protein as a covalent docking module. First of all the protein was prepared and refined by excluding water molecules from the complex protein structure followed by the addition of hydrogen atoms as well as deleting the cofactor and ligand. The structure of compounds (2D) was

drawn with the help of ChemBioDraw ultra 12.0, and then these structures were subjected to conversion from 2D to 3D followed by refinement and energy minimization (Merck Molecular Force Field) method. The analytical gradient and lowest energy conformations were selected for further studies.

Statistical analysis: The statistical analysis was run using Sigma Plot (version 11.1) by applying a one-way analysis of variance (ANOVA), followed by Tukey's multiple comparison tests. Statistical significance was considered at $p < 0.05$.

Result and Discussion

Chemistry: The pathway for the synthesis of compounds (M1-M14) has been depicted in Scheme 1. The key intermediate 3-((3-methyl-1,4-dioxo-1,4-dihydronaphthalen-2-yl)thio)propanoic acid (**3**) was synthesized according to the reported method(9) summarized in the proceeding text. Compounds (M1-M14) were synthesized by naphthalene-1,4-dione (**1**) with 4-mercapto propanoic acid (**2**) to form compound 3-((3-methyl-1,4-dioxo-1,4-dihydronaphthalen-2-yl)thio)propanoic acid (**3**) which in turn were converted to final compounds (M1-M14) by reaction with thionyl chloride and substituted 1,3,4-oxadiazoles.

The structures of the synthesized compounds were established using spectral techniques (IR, ^1H NMR and ^{13}C NMR). The presence of the carboxylic acid functionality in all the synthesized compounds was confirmed by the disappearance of -OH band at 3358.31 cm^{-1} in the IR spectra and appearance of a characteristic peak of the amide carbonyl group between 1680 cm^{-1} to 1630 cm^{-1} . The presence of C-O-C function of the oxadiazole ring showed absorption in the range of $1150\text{--}1298\text{ cm}^{-1}$. In the proton NMR spectra of all the compounds, the disappearance of characteristic broad singlet of the hydroxyl proton at $\delta 9.78\text{ ppm}$ confirmed the substitution at the hydroxyl group. The aromatic protons resonated in the range of $\delta 8.21$ to 5.64 ppm in the proton NMR spectra. In the ^{13}C NMR spectrum, carbonyl carbon of naphthalene ring

was observed at $\delta \approx 186.0$ ppm and 175.0 whereas carbon of aliphatic carbonyl of the target compounds appeared at $\delta \approx 170.0$ ppm. Signals of ^{13}C NMR spectrum further confirmed the synthesis of the targeted compounds as all the aromatic carbons appeared in the range of δ 162.00-101.00 ppm. However the methylene carbon peak emerged at δ 34.15-54.36 ppm. The physicochemical data of the synthesized compounds has been listed in the **Table 1**.

Pharmacological Evaluation

In vitro Cytotoxic activity: The cytotoxic effects of all newly synthesized compounds (M1-M14) were subjected to assess *in vitro* anticancer potency using various cancer cell lines, MCF-7, (breast carcinoma), HepG2 (liver carcinoma) and cervical carcinoma (Hela) using imatinib as standard. *In vitro* cytotoxicity results suggested that the cytotoxicity were dose-dependent. Almost

all the compound showed anticancer activity in dose-dependent manner. Cell viability decreased or cytotoxicity increases with increase in the concentration of compound. The synthesized compounds exposed that the cytotoxicity were found to be poor to strong comparatively to the reference drug (imatinib) (Table 2). The compounds **M-5** and **M-13** exhibited intense anticancer activity on HeLa cell line. Especially, **M-5** and **M-13** exhibited stronger activity than Imatinib. Two compounds (**M-5**, **M-9**) against MCF-7 cell line demonstrated great antineoplastic action. The compounds **M-12** exposed good cytotoxic with HepG2 cell lines. Moreover, the remaining synthesized compounds showed moderate cytotoxic action. Thus, the compound **M-5** and **M-13** revealed as a most potent anticancer agent against MCF-7, HepG2 and HeLa cell lines when compared to standard drug imatinib.

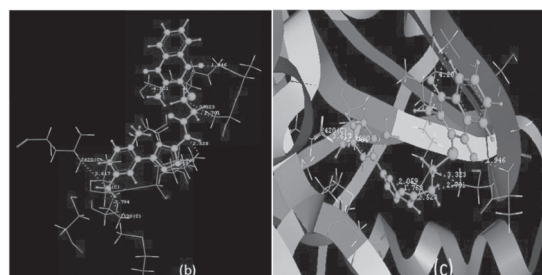
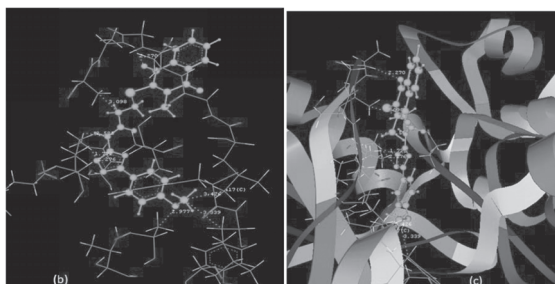
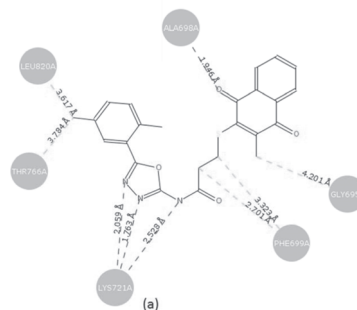
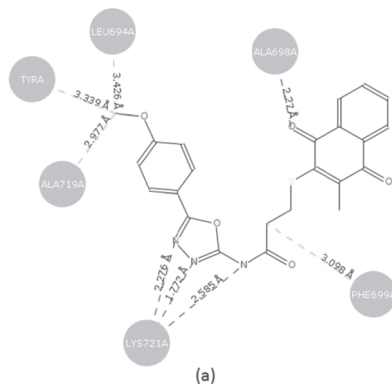


Fig. 2. (a) 2D Hydrogen Bonding Interaction, (b) 3D Binding orientation, (c) Ribbon form showing the binding orientation of the compounds M-5 into the active side of 2GS6.

Hydrophobic Interactions

Fig. 3. (a) 2D Hydrogen Bonding Interaction, (b) 3D Binding orientation, (c) Ribbon form showing the binding orientation of the compounds M-13 into the active side of 2GS6.

Hydrophobic Interactions
 Hydrogen Bonding

In-vitro Enzymatic assay (EGFR kinases inhibition): After *in-vitro* cytotoxicity screening of the synthesised compound against the MCF-7, Hela and HepG-2 cell lines, were subjected to assess EGFR kinases inhibition with the help ELISA kit of tyrosine kinase using imatinib as standard drug. Evidently, the majority of compounds indicated pronounced tyrosine kinase inhibition. Table 3 summarized the inhibition IC_{50} values of all the synthesized compounds. Compound M-5 have most potent inhibition ($IC_{50} = 1.53 \pm 0.05 \mu\text{M}$), approximately three times more than standard drug Imatinib ($IC_{50} = 3.54 \pm 0.11 \mu\text{M}$). Thus, compound M-5 is a optimistic kinase inhibitor.

Molecular docking : Molecular docking has been applied to design these compounds. It is the collection of electronic and steric features which is essential to build considerable supramolecular interactions with a specific

biological target that block or activate the biological activity.

In the present manuscript, docking study was carried out on the epidermal growth factor receptor (EGFR). Docking studies suggested that the privileged protein-ligand binding of synthesized compounds with key amino acid of the protein. Methionine residues (MET 793), cytosine (CYS797) and tyrosine (TYR253) are the key residues of the protein-ligand binding (23). These amino acid residues play a key role in the formation of a bridge within EGFR. Moreover, docking assessment of (M1-M14) on EGFR demonstrated a considerable binding communication of the synthesized compound on the peripheral site and catalytic site of amino acid. All the compounds have been found to possess a good binding affinity with the EGFR and afforded high dock score from -50.71 to -67.04. Amongst all the docked ligand, compound M-5 has shown a high binding affinity for EGFR with a highest

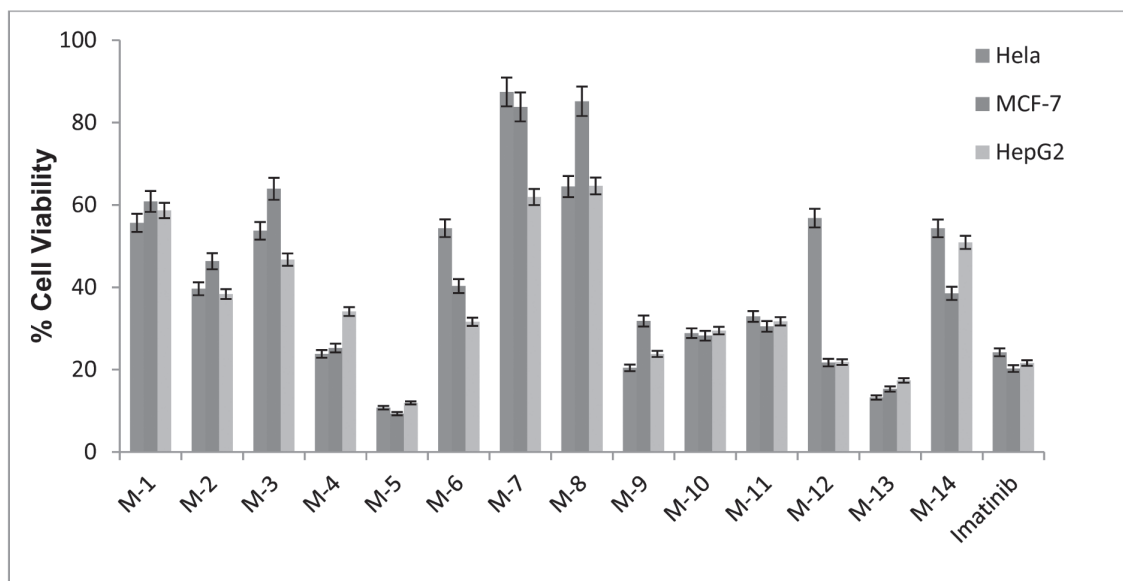


Fig. 4. In-vitro cell viability of compounds. The differences in the percentage of cell viability of compounds M-5 and M-13, are statistically significant ($P = <0.05$ ($n=3$)).

dock score (67.04). Table 4 described molecular docking score of all the synthesized compounds. The 2D/3D and binding pocket representation of the ligand-receptor interactions of the most active compounds MB-5 and MB-13 displayed in the figure 2a-c and figure 3a-c. Grip values docked pose of the fitted ligands were visualized extending deep into the active site pocket and showing several interactions such as Vander Waal's, hydrophobic contacts, hydrogen bonds and δ - δ stacking interactions with the key residues of the active site catalytic site as well as peripheral site. The high score of compound MB-5 attributed to its strong hydrogen bonds between amino acid residue ALA698 to the oxygen of ring naphthoquinone ring along with distance 2.22 Å and nitrogen of oxadiazole ring as well as nitrogen of amide with LYS 721 along with distance 2.276, 1.772 and 2.585 Å respectively. Compound M-13 formed hydrogen bond with ALA698 amino residue of oxygen of naphthoquinone ring with distance 1.946 and and nitrogen of oxadiazole ring as well as nitrogen of amide with LYS 721 amino residue with distance 2.059 Å, 1.763 Å and

2.528 Å. The hydrophobic interactions also involved in both compounds. The compound M-5 with amino acid residues LEU694, TYRA, ALA719 and PHE 699 with the distance distanced 3.426 Å, 3.339 Å, 2.977 Å and 3.098 Å respectively. However, the compound M-13 have been formed hydrophobic interactions with LEU820, THR766, PHE699 and GLY 695 along with distance 3.617 Å, 3.784 Å, 2.701 Å, 3.323 Å, and 4.201 Å of same amino acid.

Therefore, compounds 1,4-naphthoquinone derivatives with 1,3,4-oxadiazole substitutions formed considerable interactions with essential amino acid residues and revealed association of the docking studies with anticancer activity of the compounds.

Drug likeliness: Compound MB-5 was evaluated for drug –likeness characteristics using the QikProp module of Schrodinger software and the result was found to be comparable with standard drug imatinib (table-5). The predicted QPlogKhsa values affirm their strong binding with plasma protein. The outcome of Lipinski's rule of five

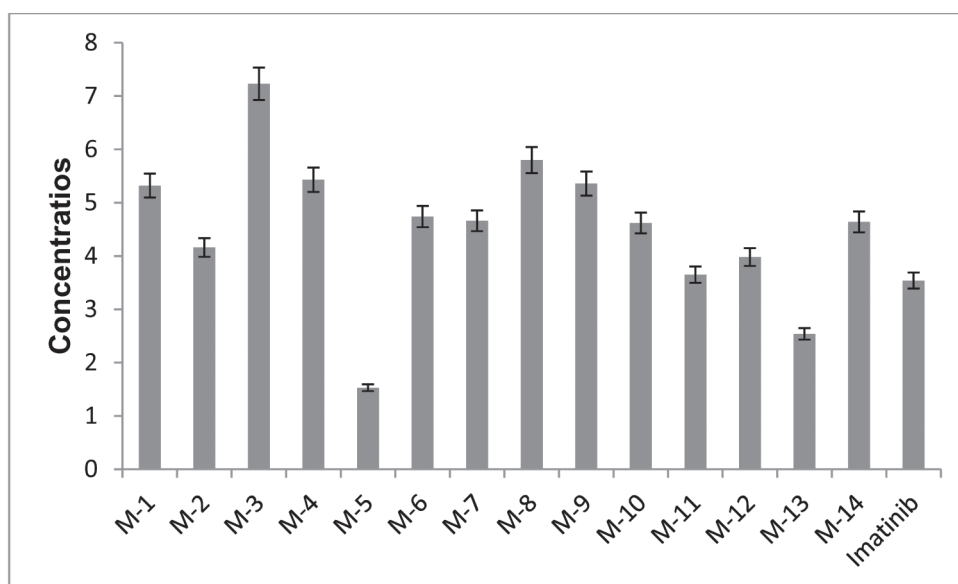


Fig. 5. Enzyme inhibitory activity of protein tyrosine kinase of compounds. The differences in the inhibitory activity of compounds M-5 and M-13, are statistically significant ($P = <0.05$ ($n=3$)).

(molwt < 500, QPlogPo/w < 5, donorHB- 0 to 6.0, acceptorHB- 2.0 to 20) along with the other predicted parameters (SASA 300 to 1000, QPlogBB -3.0 to 1.2, QPlogPo/w -2.0 to 6.5) reflected that compound MB-5 elicited “drug like” characteristics.

Conclusion

In conclusion, we have successfully synthesized a series of 1,3,4- oxadiazole substituted 1,4-naphthoquinone derivatives. The compounds were evaluated for their cytotoxic effect using MCF-7, Hela, and HepG-2 cancer cell lines. Almost all the synthesized derivatives possess considerable anticancer activity. Compound **M-5** revealed utmost powerful anticancer agent. Furthermore, on the enzyme inhibition assay, compound **M-5** showed the good

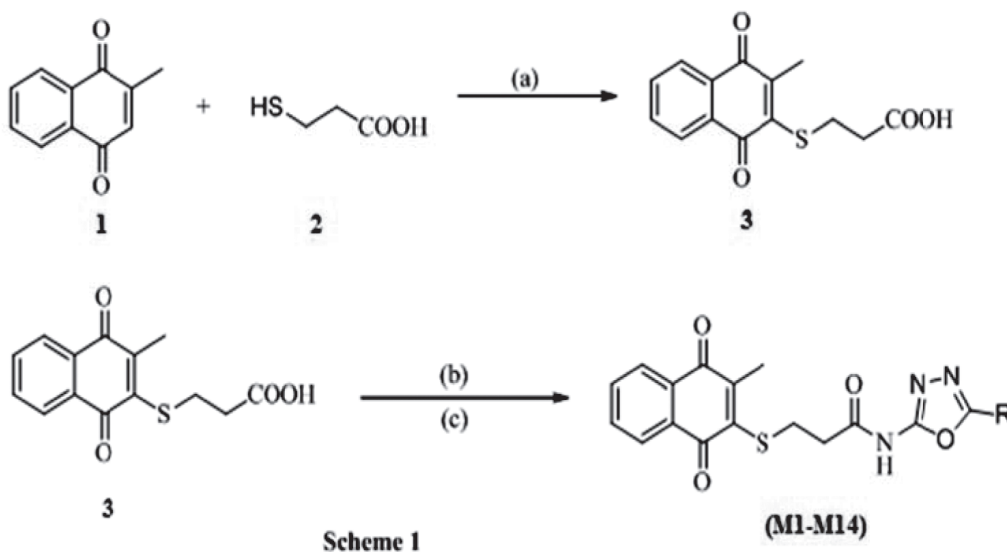
promising inhibitory activity with $IC_{50} = 1.53 \pm 0.12 \mu\text{M}$. Molecular docking study revealed the strong binding capability with the active sites of enzymes. Therefore, these findings suggested that the rational design of 1,3,4- oxadiazole substituted 1,4-naphthoquinones as a hopeful potential anticancer agent for auxiliary expansion in cancer therapy.

Acknowledgement

The authors gratefully acknowledge IIT-BHU for the funding of this work. The authors also acknowledge to Panjab University, Chandigarh and NIPER Mohali, Panjab to provide spectral and cell line facilities.

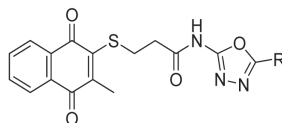
Conflict of Interest

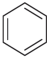
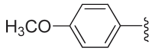
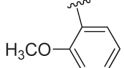
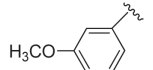
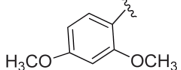
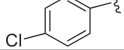
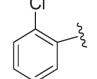
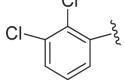
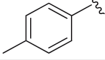
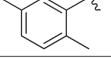
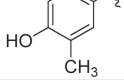
The authors declare that they have no competing interests with whomsoever.



Scheme 1. Synthesis of target compounds. Reagents and conditions: (a) absolute ethanol, reflux, 3-5 h. (b) dry DCM, thionyl chloride, r.t, 3-5 h. (c) dry DCM, substituted 1,3,4- oxadiazoles, stirring, 9-10 h.

Table1. Chemical structure of various 1,3,4- oxadiazole substituted 1,4-naphthoquinone derivatives



Compounds	R	MW	MF	LogP	mp (°C)	Appearance	% Yield	Solubility
M1	CH ₃	357.38	C ₁₇ H ₁₅ N ₃ O ₄ S	0.77	220-222	White	58	Methanol
M2	CH ₂ CH ₃	371.41	C ₁₈ H ₁₇ N ₃ O ₄ S	1.34	209-211	Brown	63	Methanol
M3	CH ₂ CH ₂ CH ₃	385.44	C ₁₉ H ₁₉ N ₃ O ₄ S	1.76	183-185	White	52	Chloroform
M4		419.45	C ₂₂ H ₁₇ N ₃ O ₄ S	2.15	146-148	Yellow	46	Methanol
M5		449.48	C ₂₃ H ₁₉ N ₃ O ₅ S	2.03	215-217	Brown	49	Chloroform
M6		449.48	C ₂₃ H ₁₉ N ₃ O ₅ S	2.03	230-232	Brown	62	Ethanol
M7		449.48	C ₂₃ H ₁₉ N ₃ O ₅ S	2.03	205-207	White	58	Methanol
M8		479.51	C ₂₄ H ₂₁ N ₃ O ₆ S	1.9	221-223	White	49	Chloroform
M9		453.90	C ₂₂ H ₁₆ ClN ₃ O ₄ S	2.71	181-183	Brown	62	Chloroform
M10		453.90	C ₂₂ H ₁₆ ClN ₃ O ₄ S	2.71	178-180	White	64	Ethanol
M11		488.34	C ₂₂ H ₁₅ Cl ₂ N ₃ O ₄ S	3.27	191-193	Yellow	57	Ethanol
M12		433.48	C ₂₃ H ₁₉ N ₃ O ₄ S	2.64	157-159	White	56	Chloroform
M13		447.51	C ₂₄ H ₂₁ N ₃ O ₄ S	3.13	236-238	Creamy	63	Chloroform
M14		449.48	C ₂₃ H ₁₉ N ₃ O ₅ S	2.25	213-215	Yellow	51	Methanol

*MW is molecular weight; mp is melting point; MF is molecular formula;

Table 2. IC₅₀ of the tested compounds against Hela, MCF-7 and HepG-2 cell lines.

Compounds	Hela cell	MCF-7 cell	HepG2 cell
	IC ₅₀ (μ M) \pm SEM	IC ₅₀ (μ M) \pm SEM	IC ₅₀ (μ M) \pm SEM
MB-1	55.65 \pm 1.32	60.83 \pm 0.88	58.64 \pm 0.74
MB-2	39.64 \pm 0.09	46.34 \pm 0.63	38.34 \pm 1.84
MB-3	53.73 \pm 0.84	63.92 \pm 1.15	46.72 \pm 0.73
MB-4	23.82 \pm 0.66	28.24 \pm 0.85	34.12 \pm 0.92
MB-5	10.76 \pm 0.11	9.30 \pm 0.14	11.93 \pm 0.83
MB-6	54.34 \pm 0.98	40.30 \pm 0.82	31.62 \pm 0.45
MB-7	87.44 \pm 0.45	83.80 \pm 0.39	61.93 \pm 0.68
MB-8	64.47 \pm 1.85	85.16 \pm 0.54	64.63 \pm 0.87
MB-9	20.44 \pm 0.85	26.82 \pm 0.83	23.80 \pm 0.67
MB-10	28.85 \pm 0.71	28.25 \pm 0.53	29.48 \pm 0.25
MB-11	32.93 \pm 0.86	30.51 \pm 0.89	31.73 \pm 0.92
MB-12	56.79 \pm 0.71	21.73 \pm 0.18	21.82 \pm 0.54
MB-13	13.23 \pm 0.27	15.30 \pm 0.42	17.39 \pm 0.87
MB-14	54.32 \pm 0.68	38.53 \pm 0.85	50.90 \pm 0.26
Imatinib	21.38 \pm 0.76	23.16 \pm 0.30	24.48 \pm 0.71

IC₅₀: Compounds concentration required to inhibit the cell viability, SEM = standard error mean; each value is the mean of three values.

References

- Kim, J.W., Galanzha, E. I., Zaharoff, D. A., Griffin, R. J., & Zharov, V. P. (2013). Nanotheranostics of circulating tumor cells, infections and other pathological features in vivo. *Mole Pharm*, 10(3): 813-830.
- John, H., Lada, K., Anthony, A., Nancy, B., Susan, M., Chang, R et al., (2018). *Clinical Cancer Advances: Annual Report on Progress Against Cancer From the American Society of Clinical Oncology*, 33(7): 786-811.
- Ahsan, M. J., Sharma, J., Singh, M., Jadav, S. S., & Yasmin, S. (2014). Synthesis and anticancer activity of N-aryl-5-substituted-1, 3, 4-oxadiazol-2-amine analogues. *BioMed research international*, 2014:1-9.
- Jemal, A., Bray, F., Center, M. M., Ferlay, J., Ward, E., & Forman, D. (2011). Global cancer statistics. *CA: a cancer journal for clinicians*, 61(2): 69-90.
- Paul, M. K., & Mukhopadhyay, A. K. (2004). Tyrosine kinase—role and significance in cancer. *International journal of medical sciences*, 1(2): 101–115.
- Kolibaba, K. S. and Druker, B. J. (1997). Protein tyrosine kinases and cancer. *BiochimBiophysActa*, 1333 (3): F217-248.
- Wee P, Wang Z. (2017). Epidermal growth factor receptor cell proliferation signaling pathways. *Cancers*, 9(5):52-61.

Table 3. Enzyme inhibitory activity of protein tyrosine kinase of synthesized compounds.

Compounds	Tyrosine kinase inhibitory activity IC ₅₀ (μM) ± SEM
MB-1	5.32 ± 0.15
MB-2	4.16 ± 0.13
MB-3	7.23 ± 0.16
MB-4	5.43 ± 0.10
MB-5	1.53 ± 0.05
MB-6	4.74 ± 0.12
MB-7	4.66 ± 0.11
MB-8	5.80 ± 0.16
MB-9	5.36 ± 0.15
MB-10	4.62 ± 0.19
MB-11	3.65 ± 0.12
MB-12	3.98 ± 0.12
MB-13	2.54 ± 0.10
MB-14	4.64 ± 0.13
Imatinib	3.54 ± 0.11

Table 4. Docking scores of compounds

Compound No	D-Score
MB-1	- 50.71
MB-2	- 58.37
MB-3	- 58.36
MB-4	- 59.75
MB-5	- 67.04
MB-6	- 59.89
MB-7	- 65.87
MB-8	- 56.20
MB-9	- 57.07
MB-10	- 56.77
MB-11	- 60.16
MB-12	- 54.67
MB-13	- 63.34
MB-14	- 63.34
Imatinib	- 62.92

IC₅₀: Compound concentration required to inhibit the enzyme activity by 50%, SEM = Standard error mean; each value is the mean of three values.

Table 5. QikProp analysis of compound M-5

Compound	Mol Wt ^a	Donor HB ^b	Acceptor HB ^c	SASA ^d BB ^e	QPlog	QPlogPo/w ^f	QPPMDCK ^g	QPlogKhsa ^h
M-5	449.48	1	10.25	770.612	-1.917	2.626	133.245	-0.091
Imatinib	493.61	2	10.5	923.694	-0.661	3.7	31.749	0.634

^aMolWt - molecular weight of the molecule (130-725).

^bDonor HB -number of hydrogen bonds(0.0 - 6.0).

^cAcceptorHB- number of hydrogen bonds(2.0 - 20.0).

^dSASA- Total solvent accessible surface area in square angstroms using a probe with 1.4Å^o radius(300-1000).

^eQPlogBB - predicted brain/blood partition coefficient(-3.0 - 1.2).

^fQPlogPo/w - this gives the predicted octanol/water partition coefficient(-2.0 - 6.5).

^gQPPMDCK- predicted MDCK cell permeability in nm/s using the affix scale(< 25 is considered

- Fry, D. W., Bridges, A. J., Denny, W. A., Doherty, A., Greis, K. D., Hicks, J. L., Hook, K. E., Keller, P. R., Leopold, W. R. and Loo, J. A. (1998). Specific, irreversible inactivation of the epidermal growth factor receptor and erbB2, by a new class of tyrosine kinase inhibitor. Proceedings of the National Academy of Sciences, 95 (20): 12022-12027.
- Tandon, V. K., Singh, R. V. and Yadav, D. B. (2004). Synthesis and evaluation of novel 1,4-naphthoquinone derivatives as antiviral, antifungal and anticancer agents. Bioorg Med Chem Lett, 14 (11): 2901-2904.

10. Prachayasittikul, V., Pingaew, R., Worachartcheewan, A., Nantasenamat, C., Prachayasittikul, S. and Ruchirawat, S. (2014). Synthesis, anticancer activity and QSAR study of 1,4-naphthoquinone derivatives. *Eur J Med Chem*, 84: 247-263.
11. Emadi, A., Ross, A. E., Cowan, K. M., Fortenberry, Y. M. and Vuica-Ross, M. (2010). A chemical genetic screen for modulators of asymmetrical 2, 22 -dimeric naphthoquinones cytotoxicity in yeast. *PloS one*, 5 (5): 10846.
12. Wang, Y., Luo, Y H., Piao, X J., Shen, G N., Meng, L Q., Zhang, Y., Wang, J R., Li, J. Q., Wang, H., Xu, W T., Liu, Y., Zhang, T., Wang, S N., Sun, H N., Han, Y H., Jin, M. H., Zang, Y Q., Zhang, D J. and Jin, C H. (2019). Novel 1,4naphthoquinone derivatives induce reactive oxygen species mediated apoptosis in liver cancer cells. *Mol Med Rep*, 19 (3): 1654-1664.
13. Abdelmohsen, K., Gerber, P. A., von Montfort, C., Sies, H., & Klotz, L. O. (2003). Epidermal growth factor receptor is a common mediator of quinone-induced signaling leading to phosphorylation of connexin-43 role of glutathione and tyrosine phosphatases. *Journal of Biological Chemistry*, 278(40), 38360-38367.
14. Salahuddin S M, Majumdar A, Ahsan M.J. (2014). Synthesis, characterization and anticancer evaluation of 2-(Naphthalen-1-ylmethyl/Naphthalen-2-yloxymethyl)-1-[5-(substitutedphenyl)-[1,3,4]oxadiazol-2-ylmethyl]-1H-benzimidazole. *Arab. J. Chem*, 7: 418-424.
15. Makane VB, Krishna V S, Krishna E V, Shukla M, Mahizhaveni B, Misra S, Chopra S, Sriram D, AzgerDusthacker V N, Rode H B. (2019). Novel 1,3,4-oxadiazoles as antitubercular agents with limited activity against drug-resistant tuberculosis. *Future Med Chem*, 11(6):499-510.
16. Rajak, H., Thakur, B. S., Singh, A., Raghuvanshi, K., Sah, A. K., Veerasamy, R., Sharma, P. C., Pawar, R. S. and Kharya, M. D. (2013). Novel limonene and citral based 2, 5-disubstituted-1, 3, 4-oxadiazoles: a natural product coupled approach to semicarbazones for antiepileptic activity. *Bioorg Med Chem Lett*, 23 (3): 864-868.
17. Bakht, M. A., Yar, M. S., Abdel-Hamid, S. G., Al Qasoumi, S. I. and Samad, A. (2010). Molecular properties prediction, synthesis and antimicrobial activity of some newer oxadiazole derivatives. *Eur J Med Chem*, 45 (12): 5862-5869.
18. Khan, M. U., Akhtar, T., Al-Masoudi, N. A., Stoeckli-Evans, H. and Hameed, S. (2012). Synthesis, crystal structure and anti-HIV activity of 2-adamantyl/adamantylmethyl-5-aryl-1,3,4-oxadiazoles. *Med Chem*, 8 (6): 1190-1197.
19. Ramaprasad G.C., Kalluraya B, Kumar S, Mallaya S. (2013). Synthesis of new oxadiazole derivatives as anti-inflammatory, analgesic, and antimicrobial agents. *Med. Chem. Res*, 22: 5381-5389.
20. Chen, C, Yi-Zhong Liu, P.Y., a Kak-Shan Shiab, K. S., Yi, T. H. (2002). Synthesis and Anticancer Evaluation of Vitamin K3 Analogues, *Bioorg Med Chem Lett*, (12), 2729–2732.
21. Liu, C., Liu, D., Bai, F., Zhang, J. and Zhang, N. (2010). In vitro and in vivo studies of lipid-based nanocarriers for oral N3-o-toluyfl-fluorouracil delivery. *Drug Deliv*, 17 (5): 352-363.
22. Hemaiswarya S, Doble M. (2013). Combination of phenylpropanoids with 5-fluorouracil as anti-cancer agents against human cervical cancer (HeLa) cell line. *Phytomedicine*, 20:151-158.
23. Srivastava JK, Pillai GG, Bhat HR, Verma A, Singh UP. (2017). Design and discovery of novel monastrol-1, 3, 5-triazines as potent anti-breast cancer agent via attenuating epidermal growth factor receptor tyrosine kinase. *Scientific reports*, 7:5851-5869.

Characterization of a Cohort of Patients with Arterial Thrombosis from the Georgian Adjarian Population

Sopio Garakanidze¹, Elísio Costa², Elsa Bronze-Rocha², Alice Santos-Silva², Giorgi Nikolaishvili³, Irina Nakashidze^{1,3}, Nona Kakauridze⁵, Salome Glonti⁴, Rusudan Khukhunaishvili¹, Marina Koridze^{1*}, Sarfraz Ahmad^{6*}

¹Department of Biology, Faculty of Natural Sciences & Health Care, Batumi Shota Rustaveli State University, Batumi, Georgia;

²Research Unit on Applied Molecular Biosciences (UCIBIO), Rede de Química e Tecnologia (REQUIMTE), Faculty of Pharmacy, University of Porto, Porto, Portugal;

³Department of Clinical Medicine, Faculty of Natural Sciences & Health Care, Batumi Shota Rustaveli State University, Batumi, Georgia;

⁴Department of Public Health and Evidence-Based Medicine, Faculty of Natural Sciences & Health Care, Batumi Shota Rustaveli State University, Batumi, Georgia.

⁵Department of Internal Medicine, Faculty of Medicine, Tbilisi State Medical University, Tbilisi, Georgia;

⁶Dept. of Gynecologic Oncology, AdventHealth Cancer Institute, Orlando, FL 32804, USA

*For Correspondence – koridzemarina@gmail.com, sarfraz.ahmad@AdventHealth.com

Abstract

Cardiovascular disorders (CVD) broadly include coronary heart disease, stroke, congenital heart disease, peripheral artery disease, deep vein thrombosis, and other less common conditions. The risk factors for arterial thrombosis are usually divided into those that are modifiable and non-modifiable. Herein, we aimed to characterize a cohort of arterial thrombosis patients from the Georgian Adjarian population.

In this study, 89 arterial thrombosis patients (male=71.3%, female=28.7%) were enrolled. Patients' mean age was 66.3±12.1 years. Troponin levels from the venous blood from patients and computed tomography (CT) assessments were used for myocardial infarction (MI) and ischemic stroke diagnosis. The venous blood from arterial thrombosis patients were used for polymerase chain reaction (PCR). PCR was performed to determine the presence of three genetic markers of thrombosis risk, viz., factor V Leiden (FVL) G1691A, prothrombin (PT) G20210A, and methylenetetrahydrofolate reductase (MTHFR) C677T polymorphisms.

In all, 83% of cases were diagnosed with MI and 13% with ischemic stroke. Also, 22.5% of the patients had diabetes, 73% hypertension, 49.3% had a family history of thrombosis, 34.8% consumed alcohol regularly (all males), and 63.4% of cases were smokers. The frequency of the FVL allele polymorphism in our cohort was 2.25%, which corresponded to a heterozygous frequency of 4.5%. The frequency of heterozygosity for the PT G20210A polymorphism was 2.25%; while the frequency of the MTHFR C677T allele polymorphism was 31.46%, which corresponded to heterozygous and homozygous stage frequencies of 51.7% and 5.6%, respectively.

In conclusion, we described the first cohort of arterial thrombosis patients in the Georgian Adjarian population, and the description of the clinical and molecular characteristics of patients with arterial thrombosis thus obtained may be useful to researchers, healthcare professionals, and policy makers while making decisions regarding the prevention, treatment, and follow-up of such patients.

Key Words: Arterial thrombosis, Myocardial infarction, Ischemic stroke, FVL G1691A, PT G20210A, MTHFR (C677T), gene polymorphisms

Introduction

Cardiovascular disorders (CVD) include coronary heart disease, stroke, congenital heart disease (CHD), peripheral artery disease (PAD), deep vein thrombosis (DVT), and other less common conditions (1). CVD accounts for nearly 801,000 deaths per year in the United States (U.S.), and about 2,200 Americans die of CVD each day, an average of one death every 40 seconds. About 92.1 million American adults are living with some form of CVD or the after-effects of a stroke. Direct and indirect costs of CVD and stroke are estimated to the total of more than U.S. \$316 billion per year, including both health expenditures and lost productivity (2). CVD is also the leading cause of mortality in Europe, where it causes just over 1.8 million deaths each year, and around 800,000 deaths in men and one-million deaths in women. In the year 2015, there were just under 11.3 million new cases of CVD in Europe. According to the European Cardiovascular Disease Statistics, the number of new CVD cases in Georgia was 29,007 (men) and 33,509 (women) during the year 2015 (3). CVD is still one of the leading causes of death worldwide. Impaired endothelial function, followed by inflammation of the vessel wall, leads to atherosclerotic lesion formation that causes myocardial infarction (MI) and stroke (4). Heart attacks and strokes are mainly caused by a blockage that prevents blood from flowing to the heart or the brain. The most common reason for CVD build-up of fatty deposits on the inner walls of the blood vessels that supply blood to the heart or the brain. This makes the blood vessels narrower and less flexible (5).

CVD accounts for nearly 801,000 deaths a year in the United States (U.S.), and about 2,200 Americans die of CVD each day, an average of one death every 40 seconds. About 92.1 million American adults are living with some form of CVD or the after-effects of a stroke. Direct and indirect costs of CVD and stroke are estimated to the total

of more than U.S. \$316 billion per year, including both health expenditures and lost productivity (4). CVD is also the leading cause of mortality in Europe, where it causes just over 1.8 million deaths each year, and around 800,000 deaths in men and one-million deaths in women. In the year 2015, there were just under 11.3 million new cases of CVD in Europe. According to the European Cardiovascular Disease Statistics, the number of new CVD cases in Georgia was 29,007 (men) and 33,509 (women) during the year 2015 (5).

Risk factors for arterial thrombosis are usually divided into two categories, viz., a) non-modifiable (e.g., age, gender, ethnicity, low birth weight, inherited diseases), and b) modifiable (e.g., hypertension, diabetes, heart diseases, smoking, alcohol abuse, use of oral contraceptives, hormone treatment in post-menopausal women, and PAD, etc.) (6).

It should be noted that C677T MTHFR, FVL G1691A, and PT G20210A, polymorphisms have some contribution to predisposition towards CVD. Several peer-reviewed studies have reported the association between C677T MTHFR polymorphism and arterial thrombosis (7,8). Our previous study suggested that C677T MTHFR polymorphism might be tending the risk of arterial thrombosis in the Georgian population (9). It should be noted that FVL and FII G20210A and the susceptibility of arterial thrombosis remain unclear. According to our previous studies, FVL could be associated with arterial thrombosis; however the PTG20210A polymorphism seems not to be associated with arterial thrombosis in the Georgian population (10).

There is a lack of information about arterial thrombosis in Georgia, including the genetic and clinical characterization of patients and its association with the hereditary risk factors. For this reason, in this study, we sought to characterize a cohort of patients with arterial thrombosis from the Georgian Adjarian population.

Material and Methods

Subjects: In this study, 89 patients with arterial thrombosis (males=71.3%, females=28.7%) were

enrolled, and the mean age of these patients was 66.3 ± 12.1 years. Troponin measurements and computed tomography (CT) assessments were used for the MI and ischemic stroke diagnosis of the patients.

Venous blood samples were collected at the Heart Disease Department and Medical Ward of Batumi Hospital, Government of Autonomous Republic of Adjara, Georgia, and processed at the Faculty of Pharmacy, University of Porto, Portugal. All the study subjects gave their written informed consent to participate in this study, and the Ethics Committee approved this study from the "Unimed Adjara" (Adjara, Georgia, Ltd.).

DNA Extraction: The genomic DNA was extracted from dried blood spots on Whatman filter papers according to the manufacturer's instructions provided with the KAPA Express Extract Kit (KAPA Biosystems, Wilmington, MA, USA). The DNA samples thus obtained were stored at -20°C until further use.

Polymerase Chain Reaction: The polymerase chain reactions (PCR) were performed in order to determine the polymorphisms of the methylenetetrahydrofolate reductase (MTHFR) C677T gene as previously described (11). To discriminate the single base changes between the normal (N) and mutated (M) alleles, two reverse (R) primers (normal: 5'-AAGGAGA AGGTGT CTGCGGGCGC-3' and mutated: 5'-AAGGAGA AGGTGTCTGCGGGCGT-3') were used, and these were paired with a common forward (F) primer (5'-AAGATCCCGGGGACGATGGGG-3'). The PCR reaction was performed with an initial denaturation of 95°C for 3 min, followed by 39 cycles of 95°C for 30 sec; 67°C (annealing temperature) for 30 sec, and 72°C for 1 min; a final extension at 72°C for 5 min was also performed. The amplification products were analyzed by electrophoresis on a 2% agarose gel and visualized with ethidium bromide. For FVL F: 5'-TGTTATCACTGG TGCTTAA-3', R-N: 5'-CAGATCCCTGGACAGACG -3', R-M: 5'-CAGATCCCTGGACAGACA-3', For PTG20210A F: 5'-TCTAGAAACAGTTGCCTGGC-

3', R-N: 5'-CACTGGGAGCATTGAGGATC-3', R-M: 5'-CACTGGGAGCATTGAGGATT-3'. The PCR reactions were performed with an initial denaturation of 95°C for 3 min, followed by 39 and 36 cycles of 95°C for 30 sec for FVL and PT G20210A, respectively; annealing temperatures of 58°C and 56°C for FV Leiden and PT G20210A, respectively, for 30 sec; 72°C for 1 min for both polymorphisms; and a final extension at 72°C for 5 min.

Statistical Analysis: Statistical analyses were performed using the Statistical Package for Social Sciences (SPSS) version 21.0 for Windows (SPSS Inc., Armonk, NY, USA). The values of all continuous variables are presented as a mean \pm standard deviation (SD). Depending on the type of distribution, parametric or non-parametric, for the comparisons between the groups, we used Student's t-test or the Mann-Whitney test, respectively. The association between the categorical variables was analyzed using the test χ^2 or Fischer's exact test. Differences between the groups were considered statistically significant at $p < 0.05$.

Results

We evaluated the data on 89 patients with arterial thrombosis, and a summary of the results thus obtained are provided in Table 1. The mean age of patients was 66.3 ± 12.1 years, with significant differences in the diagnosis age by gender (males = 60.9 ± 12.1 years, and females = 73.7 ± 10.2 years; $p < 0.001$) [Fig. 1A]).

Most of the patients were diagnosed with myocardial infarction (83%), while 13% of the cases had ischemic strokes. Significant differences were found between the age of diagnosis of MI and ischemic stroke patients (62.6 ± 12.9 vs. 71.5 ± 11.7 years; $p = 0.013$) (Table 1; Fig. 1B). Moreover, we found differences in the distribution of the MI and ischemic stroke patients with respect to gender (Table 1). Notably, 12 patients (11 males and 1 female) with an MI experienced recurrent-MI episodes. These recurrent episodes occurred at a median of 4.6 ± 4.6 years after the first episode.

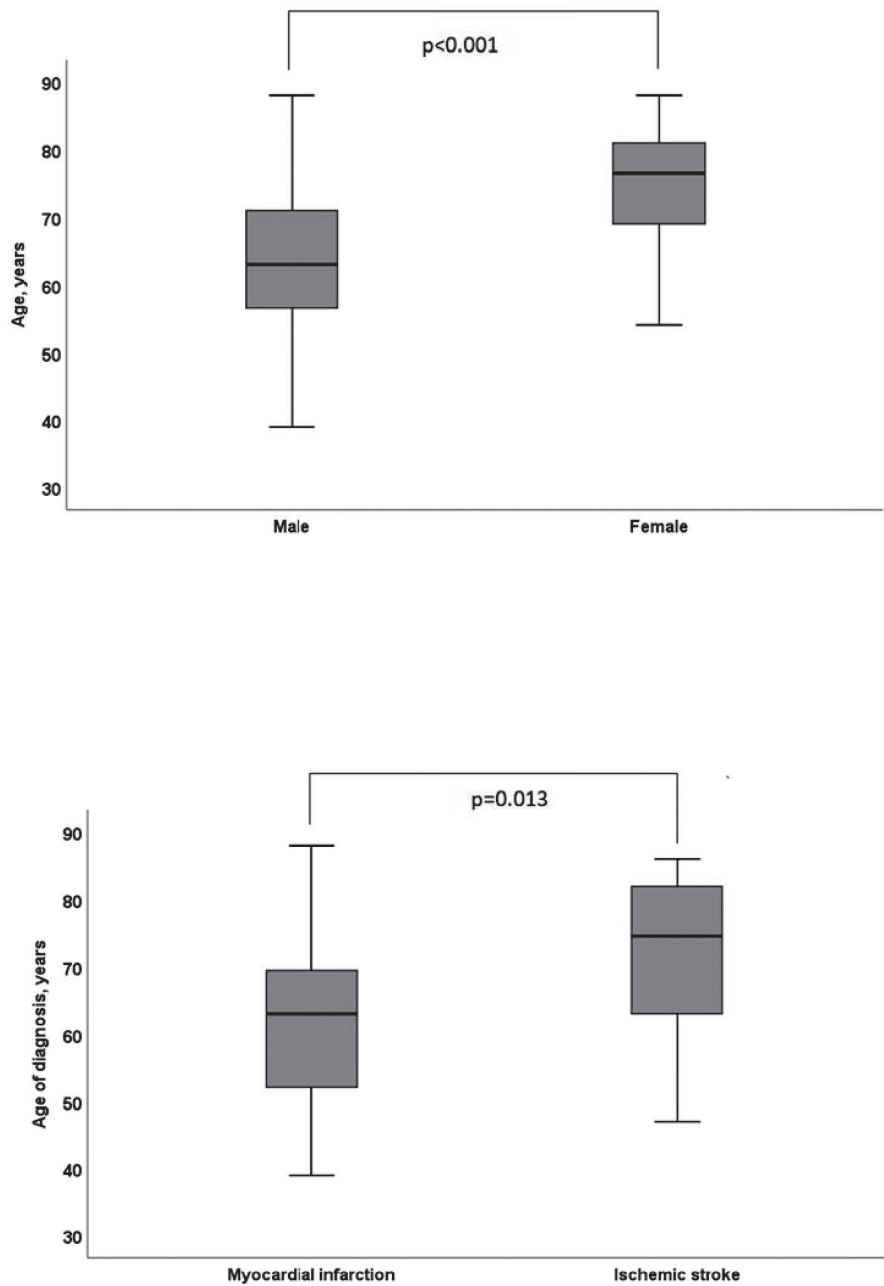


Fig. 1. (A) Comparison of age for the diagnosis of arterial thrombosis between the genders. **(B)** Comparison of age for the diagnosis for myocardial infarction and ischemic stroke (n = 89; p = 0.013).

Table 1. Distribution of various cardiovascular and lifestyle risk factor in patients with arterial thrombosis from the Georgian Adjarian population with emphasis on the comparison of myocardial infarction and ischemic stroke (N = 89).

Risk Factors	n (%)	n (%)	Total	p-Value
Gender	Myocardial Infarction	Ischemic Stroke		
Male	57 (79.2)	7 (41.2)	64	0.005
Female	15 (20.8)	10 (58.8)	25	
Diabetes				
Yes	17 (23.6)	3 (17.6)	20	0.423
No	55 (76.4)	14 (82.4)	69	
Hypertension				
Yes	54 (75.0)	11 (64.7)	65	0.283
No	18 (25.0)	6 (35.3)	24	
Consume Alcohol (n=66)*				
Yes	21 (37.5)	2 (20.0)	23	0.474
No	35 (62.5)	8 (80.0)	43	
Smokers (n=71)*				
Yes	37 (60.7)	8 (80.0)	45	0.209
No	24 (39.3)	2 (20.0)	26	
Family History of Thrombosis (n=69)*				
Yes	32 (50.8)	2 (33.3)	34	0.673
No	31 (49.2)	4 (66.7)	35	

* Out of a total 89 cases from the entire study cohort, only these number of cases responded for the parameters analyzed.

The diagnosis of diabetes was confirmed in 22.5% (20/89) of the cases in our study cohort. However, no significant difference was found in the diabetic status of myocardial infarction and ischemic stroke patients (Table 1). While 73% of patients (n=65) had hypertension, there was also no significant differences in the proportion of such patients between the MI and ischemic stroke groups (Table 1).

Despite all outspelling is correct efforts, we were able to obtain the alcohol consumption information for only 66 patients, with 34.8% (n=23) consuming alcohol regularly, and interestingly enough all of whom were male subjects. No significant difference was found in the number of that drinking alcohol between the MI and ischemic stroke patient groups (Table 1).

Likewise, we were able to get the tobacco use information from only 71 patients and found that 63.4% (n=45) of the subjects were smokers; however, there was no statistical difference in the proportion of the smoker-patients between the MI and ischemic stroke groups [Table 1]. Of the 69 patients with available records, 49.3% (n=34) had a family history of thrombosis. No significant difference was observed in the family history of thrombosis between the MI and ischemic stroke patients (Table 1).

The frequency of FVL allele polymorphism in this cohort was determined to be 2.25%, which corresponded to a heterozygous stage frequency of 2.25% (Table 2); homozygosity for FVL was not found. The frequency of heterozygosity for the PTG20210A polymorphism was 2.25%, which corresponded to an estimated allelic frequency of 1.12% [Table 2]. While the frequency of the MTHFR C677T allele polymorphism was 31.46%, which corresponded to heterozygous and homozygous frequencies of 51.7% and 5.6%, respectively. When patients were stratified according to the MI and ischemic stroke status, no significant difference was observed in the prevalence of FVL, PTG20210A, and MTHFR C677T polymorphisms. Also, no significant difference was found in the recurrent-MI group of the patients (Table 2).

Discussion

CVD is the leading global cause of death that accounts for more than 17.3 million deaths per year in 2013, a number that is expected to grow to more than 23.6 million by the year 2030 (2). Arterial disorders are associated with risk factors such as age, gender, inherited diseases, hypertension, diabetes, heart disease, smoking, and alcohol abuse, etc. (6).

The most important risk factor for thrombosis (both arterial and venous) is the prevalence of thrombosis that increases with the age in an exponential way, in both women and men, mainly due to the increasing prevalence of atherosclerosis (12). The mean age of arterial thrombosis diagnosis in our Georgian Adjarian cohort was 66.3 ± 12.1 years, which is comparable to other studies reported in the peer-reviewed literature (12-16).

Generally, CVD develops 7-10 years later among women than in men; but is still the leading cause of death in women over the age of 65 years (17). Indeed, significant differences were found by gender in our study cohort, the mean age for the diagnosis of arterial thrombosis among males was 60.9 ± 12.1 years, while for females it was 73.7 ± 10.2 years. Our observations are consistent with the previous reports that the incidence of arterial thrombosis varied according to both gender and age (18-20).

Diabetes is considered one of the most critical risk factors for arterial thrombosis, mainly because diabetic patients also have an increased risk of endothelial dysfunction and atherosclerosis (17,18), which are the primary contributory causes of blood vessel damage. Type 2 diabetes has been associated with an increased level of coagulation factors in circulating blood. Insulin resistance is characterized by a prothrombotic state, which can accelerate the development of CVD (23). The prevalence of diabetes in the European Union (EU) on average (5.1%) is higher than that in Europe as a whole (3.8%). The prevalence of diabetes was reported to be 2.2% in Georgia during the year 2014 (3), which is lower than in our study and could be related to a higher prevalence of diabetes

a
t
t
v
a
v
f
f

Table 2. Genotype and allelic frequencies of polymorphisms FVL, PT G20210A and C677T of MTHFR in patient cohort.

Patients	FVL Polymorphism				PT G20210A Polymorphism				C677T MTHFR Polymorphism							
	n	Genotype Frequencies	p-Value	Allele frequencies	Genotype Frequencies	p-Value	Allele Frequencies	Genotype Frequencies	p-Value	Allele Frequencies						
		G/G n (%)	G/A n (%)	A/A n (%)		G/G n (%)	G/A n (%)	A/A n (%)		G (%)	A (%)	C/C n (%)	C/T n (%)	T/T n (%)	C (%)	T (%)
All	89	85 (95.5)	4 (4.5)	0	-	97.75	2.25		-	98.8	1.12	38 (42.7)	46 (51.7)	5 (5.6)	68.54	31.46
Myocardial Infarction	73	69 (94.5)	4 (5.5)	0	-	97.26	2.74		-	98.6	1.37	30 (41.1)	40 (54.8)	3 (4.1)	70.55	29.45
Recurrent Myocardial Infarction	11	10 (90.9)	1 (9.1)	0	>0.05*	95.45	4.55		-	100	0	5 (45.5)	5 (45.5)	1 (9)	72.73	27.27
Ischemic Stroke	16	16 (100)	0	0	-	100	0	0	-	100	0	7 (43.75)	7 (43.75)	2 (12.5)	71.87	28.13

* p-Value vs. Myocardial infarction patient.

Abbreviations: FVL = Factor V Leiden; PT = Prothrombin; MTHFR = Methyltetrahydrofolate Reductase.

study findings, 22.5% of the patients were diabetic (20/89); According to our studies, no significant difference was found in diabetes prevalence between the MI and ischemic stroke patients. [Table 1].

Hypertension is also an important risk factor for thrombosis in relation to MI and ischemic stroke. Globally, the prevalence of hypertension is variable in different populations, ranging from 3% to 70% (26). Men with hypertension have an increased risk of stroke, MI, and mortality from coronary heart disease compared with non-hypertensive men of a similar age group (27). Both the systolic and diastolic hypertension increases the risk of arterial thrombosis. Almost 40% of the patients with ischemic heart disease have a history of hypertension, and those with hypertension have a high mortality rate after the MI (28). Hypertension was found in 73% of the patients in our study cohort. Based on our findings, it is presumed that there is positive correlation between hypertension and arterial thrombosis.

It is widely recognized that both stroke and MI are complex diseases, which are impacted by the genetic and environmental factors. Researchers/clinicians should consider both genetic and environmental conditions while studying the family history of thrombosis in order to make the right decisions/conclusions for managing the patients optimally (29). The same approach is also essential in preventing the disease; as individuals in families with a history of these conditions may be more motivated to change their lifestyle if they understand that they have potentially increased risk (s) for future disease (30). In our study cohort, almost half of the patients (49.3%) had a family history of thrombosis. Moreover, we observed that 50.8% of the patients with MI and 33.3% of the patients with ischemic stroke had a family history of thrombosis. Thus, our study suggests that no significant difference in the prevalence was found between the MI and ischemic stroke patients (Table 1).

Tobacco smoking is an important modifiable risk factor for some of the diseases and the most

common cause of premature death in Europe. Among men, the prevalence of smoking was generally highest in Eastern European and former Soviet Union states. Indeed, all four European countries where more than 50% of men smoked were the former Soviet Union states [i.e., Georgia (51%), Moldova (51%), Latvia (52%), and Russia (55%)]. By contrast, in the Western and Northern Europe, the smoking rate among the males was generally less than 30%. The opposite pattern was noted for women, as the smoking prevalence rates were very low in the former Soviet Union countries [Azerbaijan (<0.1%), Turkmenistan (0.5%), Uzbekistan (0.9%), Armenia (1.3%), Kyrgyzstan (0.7%)], low in the Eastern and Central European countries [Ukraine (5.7%), Albania (6.2%)], but higher in the Northern, Western and Southern European countries [UK (17%), France (25%), Greece (26%)].

While moderate habitual alcohol consumption is associated with a relatively lower risk of cardiovascular events, heavy episodic (binge) drinking results in a relatively higher cardiovascular risk (31). Among the causal effects, high alcohol consumption is known to increase the risk of CVD by raising blood pressure and the levels of triglycerides. For the year 2014, the average recorded level of alcohol consumption in Europe was 8.6 liters per person per year. The average for the EU was almost 20% higher than that for Europe as a whole, at 10.2 liters per person per year (5). A study of the Japanese men and women has shown that heavy alcohol consumption is associated with an increased mortality rate from stroke and CVD in men, with increased mortality from coronary heart disease for women (32). The European CVD statistics show that in Georgia, 51.1% of males and 4% of females were smokers in the year 2010, and alcohol consumption was 6.1 liters per capita for the year 2014 (3). In our study cohort, 63.4% of patients were found to be smokers, and 34.8% were alcohol users [Table 1]. Thus, the smoker patients have more risk for arterial thrombosis.

In conclusion, we described the first cohort of patients with arterial thrombosis from the

Georgian Adjarian population. Data shows that 83% of the cases were diagnosed with MI and 13% with ischemic stroke. Also, 22.5% of the patients had diabetes, 73% hypertension, 49.3% had a family history of thrombosis, 34.8% consumed alcohol regularly (all males), and 63.4% of cases were smokers. The frequency of the FVL allele polymorphism was 2.25%, which corresponded to a heterozygous frequency of 4.5%. The frequency of heterozygosity for the PT G20210A polymorphism was 2.25%; while the frequency of the MTHFR C677T allele polymorphism was 31.46%, which corresponded to heterozygous and homozygous stage frequencies of 51.7% and 5.6%, respectively. This description of clinical and molecular characteristics of patients with arterial thrombosis may be useful in future for researchers, healthcare professionals, and policymakers, in making informed decisions regarding the prevention, treatment, and follow-up of these patients.

Funding

This research work received financial support from the European Union (FEDER funds POCI/01/0145/FEDER/007728) and the National Funds (FCT/MEC, Fundação para a Ciência e Tecnologia and Ministério da Educação e Ciência, Portugal) under the Partnership Agreement PT2020 UID/MULTI/04378/2013.

Declaration of Conflicting of Interests

The authors declare that there is no conflict of interest associated with this research manuscript.

References

1. Nason, E. (2007). An overview of cardiovascular disease and research Santa Monica. CA: RAND Corporation. https://www.rand.org/pubs/working_papers/WR467.html. Accessed April 22, 2019.
2. Benjamin, E.J., Blaha, M.J., Chiuve, S.E., Cushman, M., Das, S.R., Deo, R., de Ferranti, S.D., Floyd, J, Fornage, M, Gillespie, C, Isasi, C.R., Jiménez, M.C., Jordan, L.C, Judd, S.E., Lackland, D., Lichtman, J.H., Lisabeth, L., Liu S., Longenecker, C.T., Mackey, R.H., Matsushita, K., Mozaffarian, D., Mussolino, M.E., Nasir, K., Neumar, R.W., Palaniappan, L., Pandey, D.K., Thiagarajan, R.R., Reeves, M.J., Ritchey, M., Rodriguez, C.J., Roth, G.A., Rosamond, W.D., Sasson, C., Towfighi, A., Tsao, C.W., Turner, M.B., Virani, S.S., Voeks, J.H., Willey, J.Z., Wilkins, J.T, Wu, JH, Alger, H.M, Wong, S.S, and Muntner P.(2017). Heart disease and stroke statistics - 2017 update: A report from the American Heart Association. *Circulation*, 135(10):e146-e603.doi: 10.1161/CIR.0000000000000485.
3. Wilkins, E., Wilson, L., Wickramasinghe, K., Bhatnagar, P., Leal, J., Luengo-Fernandez, R., Burns, R., Rayner, M. and Townsend N (2017). *European Cardiovascular Disease Statistics*. Brussels Belgium: European Heart Network
4. Dimmeler, S.(2011). Cardiovascular disease review series. *EMBO Molecular Medicine*, 3(12):697.doi: 10.1002/emmm.201100182.
5. World Health Organization. *Avoiding heart attacks and strokes; don't be a victim protect yourself*. Geneva, Switzerland: WHO Press, 2005.
6. Arboix, A. (2015). Cardiovascular risk factors for acute stroke: Risk profiles in the different subtypes of ischemic stroke. *World Journal of Clinical Cases*, 3(5):418-29.doi: 10.12998/wjcc.v3.i5.418.
7. Huh, H.J., Chi H.S., Shim E.H., Jang S. and Park C.J. (2006). Gene—nutrition interactions in coronary artery disease: correlation between the MTHFR C677T polymorphism and folate and homocysteine status in a Korean population. *Thrombosis Research*, 117(5):501-6.
8. Wang, Y., Xu, X., Huo, Y., Liu, D., Cui, Y., Liu, Z., Zhao, Z., Xu, X., Liu, L., Li, X. and Jiang, S. (2015). Predicting hyperhomocysteinemia by methylenetetrahydrofolate reductase C677T polymorphism in Chinese patients with

- hypertension. *Clinical and Applied Thrombosis/Hemostasis*, 21(7):661-666.
9. Garakanidze S., Costa E., Bronze-Rocha E., Santos-Silva A., Nikolaishvili G., Nakashidze I., Kakauridze N., Glonti S., Khukhunaishvili R., Koridze M. and Ahmad S. (2018). Methylenetetrahydrofolate reductase gene polymorphism (C677T) as a risk factor for arterial thrombosis in Georgian patients. *Clinical and Applied Thrombosis/Hemostasis*, 24(7):1061-1066. doi: 10.1177/1076029618757345.
 10. Garakanidze, S., Costa, E., Bronze-Rocha, E., Santos-Silva, A., Nikolaishvili, G., Glonti, S., Kakauridze, N. And Koridze, M. (2017). Factor V Leiden G1691A and prothrombin G20210A polymorphism in Georgian arterial thrombosis patients. *International Journal of Advanced Research*, 5(7):1171-1175.
 11. Angelini, A., Di Febbo, C., Rullo, A., Di Ilio, C., Cuccurullo, F. and Porreca, E. (2002). New method for the extraction of DNA from white blood cells for the detection of common genetic variants associated with thrombophilia. *Pathophysiology of Haemostasis and Thrombosis*, 32:180–183. doi: 10.1159/000070424.
 12. Lowe, G.D. (2004). Venous and arterial thrombosis: Epidemiology and risk factors at various ages. *Maturitas*, 47(4):259-63. doi:10.1016/j.maturitas.2003.12.009.
 13. Kaarisalo, M.M., Immonen-Räihä, P., Marttila, R.J., Salomaa, V., Kaarsalo, E., Salmi, K., Sarti, C., Sivenius, J., Torppa, J. and Tuomilehto, J. (1997). Atrial fibrillation and stroke: Mortality and causes of death after the first acute ischemic stroke. *Stroke*, 28(2):311-5.
 14. Jánosi, A., Ofner, P., Forster, T., Édes, I., Tóth, K., Merkely, B. (2014). Clinical characteristics, hospital care, and prognosis of patients with ST elevation myocardial infarction: Hungarian Myocardial Infarction Registry. *European Heart Journal Supplements*, 16:A12–A15. doi.org/10.1093/eurheartj/sut004.
 15. Kvakkestad, K.M., Sandvik, L., Andersen, G.Ø., Sunde, K., Halvorsen, S. (2018). Long-term survival in patients with acute myocardial infarction and out of the hospital cardiac arrest: A prospective cohort study. *Resuscitation*, 122:41–47. doi.org/10.1016/j.resuscitation.2017.11.047.
 16. Mohseni, J., Kazemi, T., Maleki, M.H., Beydokhti, H.A. (2017). Systematic review on the prevalence of acute myocardial infarction in Iran. *Heart Views*, 18(4):125–132. doi: 10.4103/HEARTVIEWS.HEARTVIEWS_71_17.
 17. Maas, A.H.E.M., Appelman, Y.E.A. (2010). Gender differences in coronary heart disease. *Netherlands Heart Journal*, 18(12): 598–602. doi.org/10.1007/s12471-010-0841-y.
 18. Qiu, H., Depre, C., Vatner, S.F. and ; Vatner, D.E. (2007). Sex differences in myocardial infarction and rupture. *Journal of Molecular Cellular Cardiology*, 43(5):532–534. doi:10.1016/j.yjmcc.2007.08.006.
 19. Ahmadi, A., Khaledifar, A., Sajjadi, H. and, Soori, H. (2014). Relationship between risk factors and in-hospital mortality due to myocardial infarction by educational level: A national prospective study in Iran. *International Journal Equity for Health*, 13:116. doi: 10.1186/s12939-014-0116-0.
 20. Yang, H.Y., Huang, J.H., Hsu, C.Y., and Chen, Y.J. (2012). Gender differences and the trend in the acute myocardial infarction: A 10-year nationwide population-based analysis. *Scientific World Journal*, [184075]. doi:10.1100/2012/184075.
 21. Roberts, J.D., Oudit, G.Y. and Fitchett, D.H. (2009). Acute coronary thrombosis in a patient with diabetes and severe hyperglycemia. *Canadian Journal of*

- Cardiology. 25(6):e217–e219.doi:10.1016/s0828-282x(09)70113-8.
22. Al-Nozha, M.M., Ismail, H.M., A.I. and Nozha, O.M. (2016). Coronary artery disease and diabetes mellitus. *Journal of Taibah University Medical Science* 11(4):330-338.doi.org/10.1016/j.jtumed.2016.03.005.
 23. Schneider, D.J.(2005). Abnormalities of coagulation, platelet function, and fibrinolysis associated with syndromes of insulin resistance. *Coronary Artery Disease*,16(8) :473-6.Doi:10.1097/00019501-200512000-00003.
 24. Wannamethee, S.G., Shaper, A.G., Whincup, P.H., Lennon, L. and Sattar, N. (2011). Impact of diabetes on cardiovascular disease risk and all-cause mortality in older men: Influence of age at onset, diabetes duration, and established and novel risk factors. *Archives of Internal Medicine*, 171(5):404-10.doi:10.1001/archinternmed.2011.2.
 25. Cho, E., Rimm, E.B., Stampfer, M.J., Willett, W.C. and Hu, F.B. (2002). The impact of diabetes mellitus and prior myocardial infarction on mortality from all causes and from coronary heart disease in men. *Journal of American College of Cardiology*, 40(5):954-60.doi.org/10.1016/S0735-1097(02)02044-2.
 26. Hasan, Z.N., Hussein, M.Q.; and Haji, G.F. (2011). Hypertension as a risk factor: Is it different in ischemic stroke and acute myocardial infarction comparative cross-sectional study?. *International Journal of Hypertensions*, 2011:701029. doi: 10.4061/2011/701029.
 27. Almgren, T., Persson, B., Wilhelmsen, L., Rosengren, A. and Andersson, O.K. (2005). Stroke and coronary heart disease in treated hypertension: A prospective cohort study over three decades. *Journal of Internal Medicine*, 257(6):496-502.doi.org/10.1111/j.1365-2796.2005.01497.x.
 28. Dunn, F.G. (1983). Hypertension and myocardial infarction. *Journal of American College of Cardiology*, 1(2):528-32.doi.org/10.1016/S0735-1097(83)80084-9.
 29. Kennedy, R.E., Howard, G., Go, R.C., Rothwell, P.M., Tiwari, H.K., Feng, R., McClure, L.A., Prineas, R.J., Banerjee, A. and Arnett D.K.(2012). Association between family risk of stroke and myocardial infarction with prevalent risk factors and coexisting diseases. *Stroke*, 43(4):974-9.doi: 10.1161/STROKEAHA.111.645044.
 30. Berentzen, N.E., Wijga, A.H., van Rossem, L., Koppelman, G.H., van Nieuwenhuizen, B., Gehring, U., Spijkerman, A.M and Smit H.A. (2016). Family history of myocardial infarction, stroke and diabetes and cardiometabolic markers in children. *Diabetologia*, 59(8):1666-74. doi.org/10.1007/s00125-016-3988-2.
 31. Mostofsky, E., van der Bom J.G., Mukamal, K.J., Mostofsky, E., van der Bom J.G., Mukamal, K.J., Maclure, M., Tofler, G.H., Muller, J.E. and Mittleman, M.A. Risk of myocardial infarction immediately after alcohol consumption. *Epidemiology*. 2015 Mar;26(2):143-50. doi: 10.1097/EDE.0000000000000227.
 32. Ikehara, S., Iso, H., Toyoshima, H., Date, C, Yamamoto, A, Kikuchi, S, Kondo, T, Watanabe, Y, Koizumi, A, Wada, Y, Inaba, Y, Tamakoshi, A and Japan Collaborative Cohort Study Group. (2008). Alcohol consumption and mortality from stroke and coronary heart disease among Japanese men and women: The Japan collaborative cohort study. *Stroke*, 39(11):2936-42.doi: 10.1161/STROKEAHA.108.520288.

Development and Validation of Point of Care Diagnostics for the Rapid Detection of Multiple Species of *Leptospira* at Resource-Limited Areas

Revathi Poonati^{1,2,3}, Prudhvi Chand Mallepaddi^{1,2,3}, Rudrama Devi Punati^{1,2,3},
Soumendra Nath Maity^{2,3},
Anusha Alamuri², Srihari Manchikalapudi^{2,3}, Krishna Satya Alapati¹, Kavi Kishor PB^{*1,2,3}
and Rathnagiri Polavarapu^{*1,2,3,4}

¹Department of Biotechnology, Acharya Nagarjuna University, Guntur 522 510, Andhra Pradesh, India

²Department of Clinical Microbiology, Genomix Molecular Diagnostics Pvt. Ltd, Hyderabad 500 072, India

³Department of Veterinary Microbiology, GenomixCARL Pvt. Ltd, Pulivendula, Kadapa 516 390, Andhra Pradesh, India

⁴Genomix Biotech Inc, 2620 Braithwood Road, Atlanta, GA 30345, USA

*For Correspondence - pbkavi@yahoo.com, giri@genomixbiotech.com

Abstract

Leptospirosis is a life threatening, emerging, infectious zoonotic disease of humans and livestock all over the world. The diagnosis of this disease is frequently ineffective. Conventional methods of diagnosis, gold standard bacterial culture and microscopic agglutination test (MAT) are being used. These tests are time-consuming and the test for the disease can be positive more than 2 weeks after the onset of the disease. Present study was taken up to circumvent the problems and disadvantages in the methods/ protocols being used currently in leptospirosis diagnosis. This study aimed to develop a point of care lateral flow (LFA) and indirect ELISA assays to detect disease-specific antibodies in the whole blood/serum/plasma for the rapid diagnosis of acute infection. The *Leptospira* specific lipopolysaccharide (LPS) was used in combination with recombinant multi-epitope membrane protein as an antigen candidate for the detection of disease specific antibodies. The developed lateral flow (LFA) and indirect ELISA assays were compared with gold standard MAT and commercial ELISA kit. The MAT confirmed standard reference

sera were used for validation of developed assays. A total of 223 positive and 115 non-positive samples for leptospirosis were used in the present validation. Indirect ELISA assay developed in the present study showed higher sensitivity and specificity of 98.65% and 100% respectively. In contrast, the sensitivity and specificity of the commercial ELISA and LFA were 96.41%, 97.39%, 87.44% and 98.26% respectively. The results obtained proved that LFA and indirect ELISA assays were more effective than the conventional methods for the diagnosis of acute leptospirosis, especially within the onset and useful for the point of care diagnosis at resource-limited areas.

Key Words: Microscopic agglutination test (MAT), lateral flow assay (LFA), point of care (POC) diagnosis, iELISA, leptospirosis and lipopolysaccharide (LPS)

Introduction

Leptospirosis is a neglected, tropical, zoonotic disease of global concern, caused by pathogenic spirochetes of the genus *Leptospira*

of which more than 250 serovars have been recognized (1). The health impacts of *Leptospirosis* in humans have been predominantly attributed to acute infections and early complications such as pulmonary haemorrhage and renal failure (2). Rodents and domestic mammals such as cattle, pigs and dogs serve as the major reservoir hosts but *Leptospire*s have been isolated from virtually all mammalian species. The infected animals may excrete *Leptospire*s intermittently or regularly for months or years or even for their lifetime. Vaccinated animals may still shed infectious organisms in the urine. The burden of this disease in recent years is estimated to be 1.03 million human cases and 58,900 deaths worldwide in each year (3, 4). The incidence of the disease is up to 1,945 cases per 100,000 populations in Futuna (a Polynesian island) during a multi-year outbreak (5). In India, carrier animals include rats, pigs, cattle, bandicoots and dogs. The predominant serovars in India are *Copenhageni*, *Autumnalis*, *Pyrogenes*, *Grippotyphosa*, *Canicola*, *Australis*, *Javanica*, *Sejroe*, *Louisiana* and *Pomona* (6). The disease is contagious and known to affect human beings, domestic animals and wildlife (7, 8). In humans, the clinical manifestations of leptospirosis are too generalized, non-specific and difficult to differentiate from other prevalent and endemic infectious diseases with similar symptoms, especially, those co-infected with dengue virus in endemic areas (9,10,11,12). Due to under recognition of disease and lack of suitable diagnostic tools for the rapid detection of leptospirosis, the incidence, its prevalence and the burden of the disease are still unclear.

The differential diagnosis of leptospirosis disease is challenging not only due to the lack of defined clinical presentations but also because of limitations in screening tests. The gold standard method for the detection of leptospirosis is the microscopic agglutination test that detects the disease specific agglutinating antibodies in an indirect signature of infection (7). However, this MAT is inadequate for rapid detection and identification of the disease. Since MAT assay

can give false negative results during the stage of acute infection of the leptospirosis (due to the low MAT titers obtained during acute infection), it may lead to false diagnosis of the infection. The outer membrane of *Leptospira* bacteria contains a variety of trans-membrane outer proteins and lipopolysaccharide (LPS). LPS is also present in most of the other Gram negative bacteria and can act as antigenic candidates (13). Differences in the highly immunogenic LPS structure account for the numerous serovars of *Leptospira* (7). Highly conserved domains like *LipL32*, *LipL41*, *LigA*, *LigB*, *LipL48*, *KWG*, *fliE*, *flhB*, *lenA-F*, *leuA*, *cimA*, *gyrB*, *ImpL63* and *OmpL1* are common among pathogenic serovars of *Leptospira interrogans*. With the identification of disease specific antigens, these domains are being increasingly used in diagnostics. This is because the results are comparable to MAT. *LipL32* (14,15,16,17), *LipL41* and *Omp1* (18), iron-regulated hemin binding protein HbpA (19), *Lip21* (20) and *LigB* have been shown as antigen candidates with diagnostic potential. In recent years, the usage of point of care (POC) diagnostics is increasing for field deployed conditions because of its simplicity, easy to use and cost effective nature. Moreover, for testing these lateral flow diagnostic kits at field, experts or technical persons, equipment and lab facilities are not needed. This field-based, simplified, lateral flow technique requires whole blood, serum or plasma as a test sample and can be added to the sample pad for detection. Leptospirosis poses a serious occupational hazard to humans involved in animal husbandry since it occurs mostly in humans who come in contact with soil and water contaminated with *Leptospira* or urine of rodents, dogs, cattle and pigs. The major challenge for the serological diagnosis for leptospirosis is to find a specific antigen that can allow a broad spectrum of detection of antibodies directed against the wide variety of serovars. Hence, there is a need for the development of a simple, rapid, inexpensive, POC diagnostic test for early and species specific diagnosis of leptospirosis infection at resource-limited areas.

We therefore described the development and validation of a novel POC lateral flow and indirect ELISA diagnostic assays for early detection of pathogenic leptospirosis in combination with disease specific recombinant multi-epitope protein and purified LPS obtained from *Leptospira*. In this study, 19 different serovars were used as antigen candidates to improve the detection levels, sensitivity and specificity of the developed assays. The study is aimed at detecting antibodies specific for leptospirosis caused by different species. Such a diagnostic kit helps in the identification of immunoglobulin G class against the leptospirosis in both humans and livestock. Instead of using anti-immunoglobulin detection reagent for each species, the protein G detection system can do the same function for all the animal species and humans. The present study describes the development and validation of LFA and indirect ELISA for rapid detection of leptospirosis in diverse livestock at resource-limited point of care areas.

Materials and Methods

Study site and sample collection: The overall development and the validation of leptospirosis POC diagnostics were carried out at the Genomix Molecular Diagnostics Pvt. Ltd., Hyderabad, India for nearly four years from January 2015 till January 2019. The culture process of live organisms was handled and processed in accordance to guidelines laid down by the institutional biosafety committee. A total of 882 individual human and animal whole blood samples were collected from the referral veterinary polyclinics and research centers and organized dairy farms from Andhra Pradesh and Telangana states. In that, a total of 338 MAT confirmed samples [positives (n = 223) and negatives (n = 115)] were obtained from Translational Research Platform for Veterinary Biologicals (TRPVB), TANUVAS, Chennai, Tamil nadu, India. The remaining 544 samples were collected from the field that includes 237 from bovine species, 123 from dogs, 69 from humans and 115 from sheep and goats. Approximately 2 ml volume of whole blood was collected from jugular vein of the animal in lithium - heparin

coated BD vacutainer tubes (REF 367820) for serological studies with the consent of the farm owners and the farmers under the supervision of veterinarian.

Microscopic agglutination test: The microscopic agglutination test is the gold standard conventional method for the detection of *Leptospira species*. In MAT, the viable cells of *Hardjo* antigen grown in Ellinghausen-McCullough-Johnson-Harris medium (EMJH) for 2-3 days at 30°C until the formation of turbidity (21). The content was further diluted to approximately 2×10^8 bacteria per ml in phosphate buffer saline with pH 7.2. The sera were titrated in two-fold dilutions from 1:64 to 1:80, 192 with the end point defined as the dilution at which half of the cells of *Leptospira* present were agglutinated. Finally, the sera which did not react at 1:64 dilutions were considered as pure negative samples.

Reference strains growth and harvesting: The live reference strains of leptospirosis were obtained from the regional medical research centre (RMRC), Port Blair, Andaman and Nicobar Islands, India. The list of reference strains that were used in this study were *L. interrogans* (*Australis* strain *Ballico*, *Bangkinang* strain *Bangkinang I*, *Canicola* strain *Hond Utrecht IV*, *Hebdomadis* strain *Hebdomadis*, *Hadjo* strain *Hadjo prajitno*, *Pyrogenes saline*, *Icterohaemorrhagiae* strain *RGA* (ATCC443642), *Djasiman* strain *Djasiman*, *copenhageni* strain *M20*, *Bataviae* strain *Swart and Pomona* strain *Pomona*), *L. borgpetersenii* (*Tarassovi* strain *Perepelicin* and *Javanica* strain *poi*), *L. biflexa* (*Andamana* strain *CH11*, *Patoc* strain *Patoc I*), *L. santarosai* (*Shermani* strain *1342K*, strain *LT64-68*), *L. kirschneri* (*Grippotyphosa* strain *Moskva V*), *L. fainei* (*Hustbridge* strain *BUT6*), and *L. noguchi* (*panama* strain *CZ214K*). All these strains of leptospirosis were grown at 29°C and maintained by regular sub culturing in Ellinghausen McCullough Johnson Harris (EMJH) medium fortified with 10% enrichment medium (Difco Laboratories, USA) followed by the institution biosafety manuals.

Antigen preparation: The lipopolysaccharide present in the outer membrane of *Leptospira* bacterial cells was used as an antigenic candidate. The LPS preparation was carried out by the protocol described by Gowri et al. (22) with minor modifications. Briefly, the LPS antigen was prepared from a well grown culture of *Leptospira* (100 ml) in EMJH medium. The culture was washed with phosphate buffered saline three times by centrifugation at 6000 x *g* to remove the medium residuals. The bacterial pellet was resuspended in bicarbonate buffer with pH 9.6 containing 0.5% formalin (v/v) to inactivate the live cells of *Leptospira*. Further, the inactivated bacterial cells were heated in a boiling water bath for 30 min and centrifuged at 10,000 x *g* for 30 min. Proteinase K was added to supernatant and passed through 5 kDa cut off tube. The content retained after passing through was considered as lipopolysaccharide (LPS). The LPS was collected and stored at -80°C for further use. The LPS antigens yielded a band size of approximately 15 to 18 kDa which were identified by SDS-PAGE followed by silver staining (23). The concentrated LPS were further used in the development of lateral flow and indirect ELISA POC diagnostic assays.

Cloning of multi-epitope recombinant genes:

The multi-epitope recombinant protein clone of leptospirosis was acquired from the TRPVB. Briefly, the gene sequence of multi-epitope recombinant protein of *Leptospira* was designed by assembling the conserved regions of 4 antigenic outer membrane proteins. Gene sequences of outer membrane proteins namely *LipI32*, *LipI21*, *LipI41* and *OmpL1* are collected from more than 35 serovars of 11 pathogenic *Leptospira* species from NCBI GenBank database. The conserved epitope sequences were assembled together with tetraglycyl linkers forming a 480 bp sequence coding for 160 amino acid peptide molecules. Constructed sequence contains 8 epitopes of 4 antigenic outer membrane proteins linked with tetraglycyl linkers. The protein sequence was also found to be antigenic using Kolaskar and Tongaonkar antigenicity based prediction of antigenic peptide tool available on

Immuno Medicine Group (<http://imed.med.ucm.es/Tools/antigenic.pl>). The whole construct was inserted into pET28a plasmid vector system and were ligated with T4 DNA ligase enzyme. The ligated vector was transformed in to *E. coli* BL21 cells for expression of targeted multi-epitope recombinant protein.

Expression and purification of multi-epitope recombinant protein:

The *E. coli* BL21 cells with desired vector was added in to 10 ml of LB broth with ampicillin and incubated overnight at 37°C. From overnight culture, 2 ml was added to 200 ml of LB broth with ampicillin and incubated at 37°C till it reached an optical density (OD) of 0.6 to 0.8 at A590 nm. Once the culture reached 0.6 OD, it was induced with 1 mM IPTG and incubated at 37°C for 6 hours. After induction, the culture was centrifuged at 8000 x *g* for 10 min and the pellet was collected. The pellet was used for protein purification. The pellets were resuspended in 10 ml of binding buffer (6M urea, 0.5N NaCl and 0.1M Tris with pH 8.0) and kept overnight at 4°C. After overnight incubation, the pellet suspension was subjected to sonication. The cycling conditions for sonicator included 15 seconds on and 30 seconds off at 55% amplitude and the process was repeated 10 times. After sonication, the cell lysate was centrifuged at 10,000 x *g* for 30 min at 4°C to pellet out the cell debris. The supernatant was collected, added to Ni-NTA column and allowed to bind for 45 min at room temperature. The column was washed with 10 ml of washing buffer (6M Urea, 0.5N NaCl, 0.1M Tris, 50 mM imidazole with pH 6.5) twice. Finally, the protein bound to the matrix was eluted with 5 ml of elution buffer (6M Urea, 0.5N NaCl, 0.1M Tris, 250 mM imidazole with pH 4.5). The purification resulted in high purity protein with a band size of approximately 35 kDa as identified by SDS-PAGE separation followed by Coomassie blue staining. Eluted fractions containing the protein were pooled and dialyzed against 1x phosphate buffer saline (137 mM NaCl, 10 mM Na₂HPO₄, 2.7 mM KCl with pH 7.4) overnight at 4°C with continues stirring. The protein concentrations were measured using the spectrophotometer (Model sp-8001,

Metertech Inc, Taiwan). The concentrated fractions were further used in the development of lateral flow and indirect ELISA assays.

Development of LFA: Concentrated and purified fractions of LPS and multi-epitope recombinant proteins were used in the development of LFA. Concentration of antigen was adjusted to 2 mg/ml by freeze drying the purified fractions. The development of lateral flow assay for the detection of *Leptospira* species was carried out by following the modified protocol of Smits et al. (24). The mixture of LPS and multi-epitope recombinant protein was used as antigen and the biotinylated BSA (Genomix Biotech, USA) coated on the nitrocellulose membrane at test (T) and control (C) line positions respectively as parallel lines using BioDotQuanti-2000 Bio jet apparatus (Bio Dot Inc, USA). The protein G conjugated to 40 nm size gold colloidal particles along with streptavidin (Genomix Biotech Inc, USA) was used at conjugate matrix. While one end of nitrocellulose membrane flanked by sample pad was followed by conjugation matrix, the other end by absorption pad. The membrane laminated was cut into 4.2 mm strips and placed into a plastic cassette. The test device was sealed into a foil pouch with sample collection dropper and with a desiccant. The sample diluent buffer (0.2% Tris, 2% casein, 1% Triton-X 100 with pH adjusted to 8.9) was used to test the samples. LFA was performed by the addition of 5 μ l of sample onto the sample well followed by the addition of two drops of sample diluent buffer. The results were visualized within 10 min after the addition of sample. The *Leptospira* disease specific IgG antibodies present in the test sample were bound to the test line, resulting in the formation of a purple colored line at test position, which indicated presence of the disease. The negative result was interpreted by the absence of colored line at test position. The colored line at control position indicated proper functioning of LFA test device.

Development of indirect ELISA assay: The mixture of purified fractions of multi-epitope recombinant protein and LPS were used in the

development of indirect ELISA assay. Each well of polystyrene microtitre NUNC plates (Thermo Fisher, India) was filled with 100 μ l of antigen. The concentration of antigen used per well was optimized and coated followed by overnight incubation at 4°C. After overnight incubation, the ELISA plates were washed with PBST (0.15M phosphate buffered saline with pH 7.2 and 0.05% Tween 20). The plates were blocked with 3% skimmed milk (HI-MEDIA), followed by incubation at room temperature for 1 h. Then washing with PBST was repeated four times followed by the addition of 100 μ l of test samples. The microstrips were shaken for 10 sec and incubated for 60 min at room temperature. After the process of incubation, the incubated plates were washed with 1x phosphate buffer saline with 0.05% Tween 20 (PBST) for four times. Then, 100 μ l of protein G HRP conjugate solution was added to each well of microtiter plate. After the addition of HRP conjugate solution, the plates were incubated at 37°C for 1 h. After successful incubation, the plates were washed four times with washing buffer (1x PBST). Then, 100 μ l of substrate solution (TMB substrate, Abcam, USA) was added into each well and stored in a dark place for 15 minutes. The color development was stopped by the addition of 100 μ l of stop solution (1N H₂SO₄) and the OD values were read at 450 nm in a hand-held ELISA reader. The OD values were documented for interpretation.

Cut-off value: The indirect ELISA cut off value which served as threshold between the actual positive and negative samples was derived by calculating the mean OD values obtained from 115 negative samples plus three times standard deviation (25). All these samples were negative by MAT at a dilution of 1:100 for all the serovars of *Leptospira*.

$$\text{Cut off} = X + 3 \text{ SD} \quad (X - \text{mean, SD} - \text{standard deviation})$$

Statistical analysis : The collected whole blood samples were tested with the lateral flow and ELISA test devices. Calculation of specificity, sensitivity, positive predictive (PPV), negative

predictive values (NPV) and efficiency were carried using statistical analysis software SPSS20.0 (26).

Field studies: The developed assays were tested for field applicability by collecting the whole blood samples randomly from the field. That included 237 samples from bovine species, 123 from dogs, 69 from humans and 115 from sheep and goats. The samples were stored at -20°C for further use. All these samples were used to validate the lateral flow and indirect ELISA assays at field settings.

Results

The purified fractions of lipopolysaccharide from 19 different serovars of *Leptospira* were characterized on SDS-PAGE followed by the silver staining method. The 5 different lots of purified LPS mixture from all the serovars were pooled into a single vial. The pooled 5 lots were run on a 12% SDS-PAGE gel to check the purity and to confirm the size of LPS. The LPS was observed at 10 to 18 kDa and immunogenic outer membrane proteins as smears at 42 kDa size as shown in Figure 1.

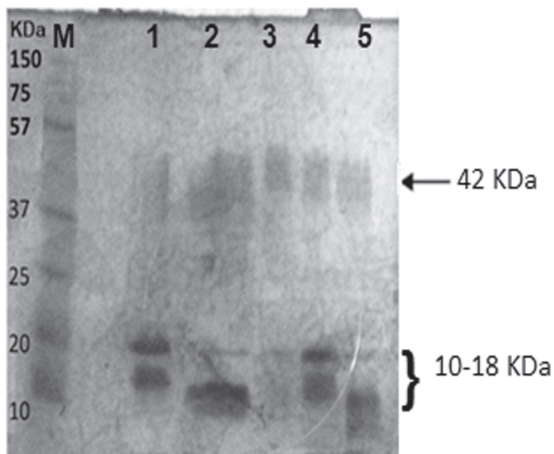


Fig. 1. Silver staining gel image of LPS mix was obtained from all the 19 *Leptospira* serovars. Lane M is Bio-Rad precision plus protein standard marker, lane 1 to 5 is the mix of five different lots of LPS. The LPS was observed with a band size from 10-18 kDa.

A total of 8 mg of *Leptospira* specific multi-epitope recombinant protein was obtained and its purity characterized by 12% SDS-PAGE gel electrophoresis. The gel was run with 10 µl of eluted protein fractions and was further stained with Coomassie brilliant blue (CBB) solution. After destaining, clear bands were observed (approximately 35 kDa) as shown in the figure 2. Thus, the recombinant protein purification process resulted in obtaining the high quality multi-epitope recombinant protein.

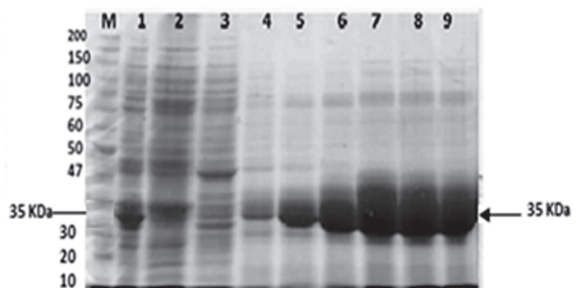


Fig. 2. The purified fractions of *Leptospira* multi-epitope recombinant protein. M- Protein standard marker, Lanes 1-9: load; pass through, wash and elutions from 1, 2, 3, 4, 5 and 6.

The confirmed lots of lipopolysaccharide and multi-epitope recombinant protein were used in the preparation of POC antibody based lateral flow and indirect ELISA diagnostics for the detection of leptospirosis serovars at resource-limited areas.

Statistical analysis: The characterized lipopolysaccharide and multi-epitope recombinant protein mixture was used as an antigen candidate for the development of protein G-based lateral flow and indirect ELISA assays. MAT confirmed samples (338) were used for the validation of four different assays such as LFA, indirect ELISA and compared with commercial ELISA and MAT as the standard method for the detection of leptospirosis as shown in the Table 1. MAT is the gold standard method for leptospirosis diagnosis which exhibited high accuracy in terms of sensitivity and specificity. The protein G-based indirect ELISA assay was found to be more

sensitive and specific whereas the LFA showed better sensitivity and specificity in detecting *Leptospira* specific antibodies compared to other serological assays at field level.

The overall statistical analysis of both LFA and indirect ELISA assays were validated with known control samples that are confirmed by microscopic agglutination test. The test results are tabulated for sensitivity, specificity, positive predictive value (PPV), negative predictive value (NPV) and efficiency. The microscopic agglutination test is the gold standard method for the detection of leptospirosis with high level of accuracy and compared with commercial ELISA kit for serological diagnostic methods. Protein G-based lateral flow and indirect ELISA assays showed 87.44% and 98.65% sensitivity and

98.26% and 100% specificity respectively as shown in the Table 2. The remaining positive and negative predictive values and efficiency of all these diagnostic assays differing with the standard values are shown in Table 2. The Chi-square statistic value is 1.7263 and the *p*-value is 0.999724 which is not significant at *p*<0.05.

Analysis of LFA with reference sera: The developed POC lateral flow test kits were validated with known 338 MAT (223 positive and 115 negative) confirmed reference sera obtained from TRPVB, Chennai. Out of 223 positive samples, 197 showed positive by LFA and the remaining displayed false negatives. Out of 115 negative samples, 2 exhibited reactivity with LFA. In all, LFA exhibited 87.44% sensitivity and 98.26% specificity (Tables 1 and 2). Thus, the *Leptospira*

Table 1. A comparative diagnostic evaluation data of four diagnostic assays for the detection of Leptospirosis

Note: Wb- whole blood, TP- True positive (Reactive), TN- True negative (Non-reactive), FP- False positive, FN- False negative.

S.No	Test type	Specimen Type	Total no. of samples (n=338)		TP	TN	FP	FN
			Positive	Negative				
1.	MAT	Serum	223	115	223	115	0	0
2.	Commercial ELISA	Serum/Plasma	219	119	215	112	3	8
3.	Indirect ELISA	Wb/Serum/Plasma	220	118	220	115	0	3
4.	Lateral flow	Wb/Serum/Plasma	197	141	195	113	2	28

Table 2. The statistical analysis of leptospirosis diagnostic assays and their comparison with different parameters. The Chi-square statistic is 1.7263. The P-value is 0.999724. The result is not significant at *P*< 0.05. Values are represented in terms of percentage; values in parenthesis represent 95% confidential intervals

Note: PPV- Positive predictive value, NPV- Negative predictive value

Assay	Sensitivity %	Specificity %	PPV	NPV	Efficiency
MAT	100%	100%	100%	100%	100%
Commercial ELISA	96.41%	97.39%	98.62%	93.33%	96.75%
Indirect ELISA	98.65%	100%	100%	97.46 %	99.11%
Lateral flow assay	87.44%	98.26%	99.98%	80.14%	91.12%



Fig. 3. Developed *Leptospira* lateral flow test kits showing positive and negative results. (a) Test negative, (b) Test positive

lateral flow test devices displayed positive and negative results which are shown in the figure 3.

Standardization of ELISA assay: To optimize the coating concentration, different concentrations of antigen starting from 10 $\mu\text{g}/\text{well}$ to 0.01 $\mu\text{g}/\text{well}$ at two-fold serial dilutions was used on a polysorb ELISA nunc plates. The optimum antigen concentration was checked with positive sera. The minimal antigen reactivity concentration has been found to be 160 ng per well. To optimize serum dilution, dilutions ranging from 1:50 to 1:400 were analyzed with 160 ng as antigen concentration. The maximum, minimal antigen reactivity concentration difference between both the human and animal positive and negative sera was observed at 1:100 dilutions. As the dilution increased, the OD difference between positive and negative sera narrowed down. It is inferred that a minimum of 1:100 dilution can be used as an optimal serum dilution. To optimize conjugate dilution, dilutions ranging from 1:5000 to 1:30000 of protein G horseradish peroxidase conjugate were analyzed with 160 ng as antigen concentration. Maximum OD difference with positive and negative sera was noticed at 1:10,000 dilutions.

Defining the cut off value: The mean OD of negative samples was screened using indirect ELISA assay. This was developed using the

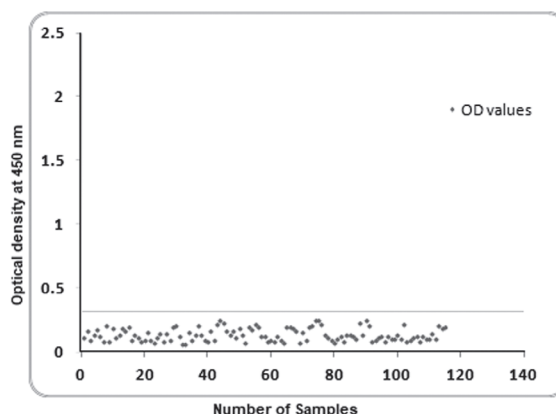


Fig. 4. Diagrammatic representation of optical density values for hundred and fifteen MAT negative samples for defining the negative cut off value. While X-axis shows the number of samples, Y-axis deals with the optical density of 115 negative samples at 450 nm.

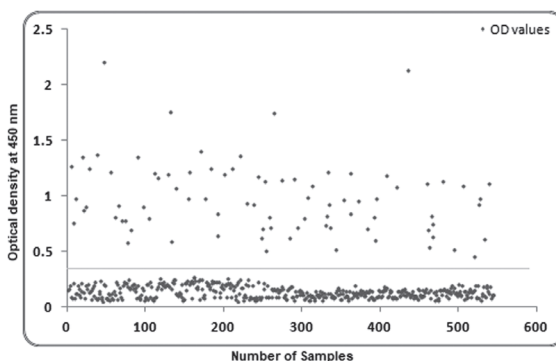


Fig. 5. Diagrammatic representation of optical density values for five hundred and forty four field samples for defining the positive and negative values. While the X-axis shows the number of samples, Y-axis deals with the optical density of five hundred and forty four field samples at 450 nm.

mixture of concentrated lipopolysaccharide from all the serovars of leptospirosis and a multi-epitope recombinant protein used as an antigenic candidate. The confirmed negative samples (115) obtained from TRPVB were used to examine the negativity using indirect ELISA assay. The mean

OD values of these 115 disease free samples were 0.138 and the standard deviation (SD) of these samples 0.053 (Figure 4). On an average, most of the negative samples tested displayed an OD value of 0.138. The mean OD value for the cut off control was 0.297 at 450 nm. So, the samples with an OD value below 0.3 at 450 nm were termed as negatives and more than 0.4 OD values as positives and in between 0.3 to 0.4 as equivocal.

Field sample analysis: For field level validation of the developed POC lateral flow and indirect ELISA assays, 544 multi species field samples were collected from the veterinary poly clinics and organized dairy farms. The samples included 237 from bovine, 123 from dogs, 69 from humans and 115 from sheep and goats. Out of 544 field samples, 83 were positive and the remaining 461 negative for leptospirosis when tested with indirect ELISA assay as shown in figure 5. A total of 67 samples were shown positive for leptospirosis and the remaining 477 negative from field samples by LFA. The overall percentage of positivity for all the field samples was 8.69%, 20.91%, 18.2% and 22.3% for human, bovine, dog, sheep and goat samples respectively as carried out by indirect ELISA. The sample positivity using LFA was 4.35% in humans, 17.3% in bovine, 11.85% in dogs and 17.3% in sheep and goats.

Discussion

Leptospirosis diagnosis based on antibody identification methods such as MAT has emerged as the most practical approach, but this test normally fails to detect the disease in the early acute phase (13). Often the disease is underdiagnosed, since the culture of *Leptospira* and seroconversion requires weeks to grow and maintain (21). Isolation of *Leptospira* from the clinical specimen is difficult because they are fastidious, slow growing, requires special growth culture media, time-consuming and laborious (27). Therefore, it is important for an early and definitive detection of leptospirosis among the animal species so that the clinician can start appropriate treatment as soon as possible and minimize the associated complications. Fewer studies have analyzed the presence of pathogenic *Leptospira*

in the dairy environment where humans regularly contact with contaminated water sources (28). Ever since the diagnosis of leptospirosis, MAT has been used as a gold standard method with high sensitivity and specificity. However, it does not represent perfect sensitivity due to the requirement of different live serovar existing in each local region. Since a better diagnostic technique is not available at present, and *Leptospira* species are widespread as pathogens having over 200 serovars, species or genus specific, simple, rapid and accurate diagnostic method is necessary (29). *Leptospira* lateral flow achieves the highest sensitivity during the third and fourth weeks of illness. The diagnosis of leptospirosis in dog veterinarians often dictates broad-spectrum antimicrobial agents to treat not only the possible *Leptospira* infection, but also for other potential infectious diseases considered as differential diagnosis. The potential of leptospirosis as well as other pathogens to develop resistance to antimicrobial agents cannot be over-emphasized. Reports exist on the *in vitro* antimicrobial susceptibilities of *Leptospira* spp. This is also a reason to develop a new diagnostic method to detect leptospirosis.

This study indicates that a protein-G based indirect ELISA and LFA using LPS *Leptospira* antigenic preparation made from commonly occurring pathogenic serovars is a specific, sensitive, and practical test for the detection of antibodies against leptospirosis in multiple species. The results of these immunoassays were expressed relative to those obtained with the internationally recognized MAT test. This analysis showed that recombinant multi-epitope protein and all serovars mixed antigen could detect IgG antibodies in all 338 specimens, classified as *L. interrogans serovars Icterohaemorrhagiae, Hebdomadis, Pomona, Canicola, Hadjo, Grippotyphosa, Australis* and *Autumnalis* in our previous work using MAT method and an MAT titer of >80. When the mixed protein was used as an antigen, the ELISA and LFA methods detected most of the sero groups, and overcame the restriction of the single sero group specificity of

single *Leptospira* protein antigens. The overall sensitivity of the ELISA and lateral flow assay thus was calculated to be 98.65% [95% confidence interval [CI], and 96.12% to 99.72%) and 87.14% (82.37% to 91.49%)]. The specificity of the ELISA and LFA were 100% (95% CI, 96.84% to 100.00%) and 98.26% (95% CI, 93.86% to 99.79%).

The developed POC LFA has the same advantages as compared to other standard tests. The LFA is a quick and easy to use in resource-limited settings. This assay does not require sophisticated instrument, refrigeration for storage and electricity to perform the diagnosis. All these characteristics make the assay ideal to perform in rural or resource-limited areas as well as in the field level study for the epidemiological survey. The result from lateral flow assay should be interpreted with respect to clinical diagnosis. The sero conversion for leptospirosis takes 5 to 7 days after the onset of the disease. Therefore, the sensitivity and negative predictive values for the leptospirosis LFA are low for specimens collected during the early stages of disease. Hence, it is mandatory to repeat the test, if the first specimens showed negative results and clinical diagnosis of leptospirosis results of both indirect ELISA and LFA are comparable with standard specimens confirmed by gold standard method. Our findings support the results obtained by Terpstra et al. (30), who indicated that the antigen could be prepared from different serovars and may contain serogroup and possibly type-specific fractions, apart from the broadly reactive genus-specific fraction or fractions. Thus, there is an urgent need for a diagnostic test that not only incorporates high degrees of sensitivity and specific for leptospirosis diagnosis but also covers diverse serovars. As the lateral-flow test is read by visual inspection for staining of the antigen line, reading of the test is subjective for samples giving a weak staining. A weak positive result may be due to cross-reactivity or may correlate with low or borderline titers in the IgM ELISA. Weak positive results by the lateral flow assay, like low or borderline in an ELISA, should be confirmed by testing second sample collected at a later stage to look for an increase in antibody level.

The indirect ELISA developed in this study exhibited 100% specificity relative to the MAT when human/animal sera with MAT titres of e¹⁰⁰ to different serovars were tested. The ELISA displayed a sensitivity of 98.65% relative to the MAT. Of the 223 MAT-positive sera tested, 3 showed negative results in the ELISA. In one of these studies, an indirect ELISA detected non-agglutinating antibodies in the sera of infected dogs during the initial stage of infection (12). Thus, it is possible that indirect ELISA detected *Leptospira* specific, non-agglutinating antibodies in the 7 sera that gave discrepant results in this study. On immunoblot, 5 of these 7 sera recognized some of the antigens visualized by the anti-*Pomona* rabbit serum and the positive canine serum (data not shown). The results indicate the presence of *Leptospira* specific, non-agglutinating antibodies in these sera. Thus, both LFA and indirect ELISA display better sensitivity and specificity compared with gold standard and existing commercial diagnostic kits. So, based on the above results the developed POC diagnostics are recommended for the detection of leptospirosis in multiple species at resource-limited areas.

Conclusion

The developed point of care lateral flow and ELISA diagnostic methods were sensitive and specific for the recombinant and all serovar mixed protein, which recognized IgG in the collected whole blood/serum samples. We consider that the recombinant multi-epitope protein mixed with LPS is preferable for the diagnosis of leptospirosis in the acute and convalescent phases to improve the sensitivity and specificity and high level accuracy in disease detection. Particularly, the developed protein G point of care lateral flow and indirect ELISA assays have high potential for early diagnosis of leptospirosis in multiple species without using species specific anti antibodies in the detection system. So, the LFA and indirect ELISA assays are recommended for point of care diagnosis of leptospirosis at field deployable resource-limited areas.

Conflict of interest : Authors declare that they have no conflict of interest.

Ethical clearance : All the experimental procedures were performed with the approval of the Institute Animal Ethics Committee, Genomix Molecular Diagnostics Pvt. Ltd, Hyderabad, India. All applicable institutional guidelines for the care and use of animals were followed with the consent of the animal owners under the supervision of the field veterinarian.

Acknowledgements

Authors are grateful to the Director of Regional Medical Research Centre (RMRC), Port Blair, Andaman and Nicobar Islands, India for their support and procuring the *Leptospira* serovars to execute this study. The project entitled "Developing rapid, sensitive, inexpensive point of care diagnostic kits for canine diseases" was funded and supported by the Ministry of Science and Technology, Department of Biotechnology, through the order No: 102/IFD/ SAN/5304/2017-2018, New Delhi and the authors are thankful to the Department of Biotechnology, New Delhi.

References

1. Adler, B., Lo, M., Seemann, T. and Murray, G.L. (2011). Pathogenesis of leptospirosis: the influence of genomics. *Vet. Microbiol*, 153: 73-81.
2. Goris, M.G., Kikken, V., Straetemans, M., Alba, S., Goeijenbier, M. and Van Gorp, E.C. (2013). Towards the burden of human leptospirosis: duration of acute illness and occurrence of post leptospirosis symptoms of patients in the Netherlands. *PLoS One*, 8(10): e76549.
3. Costa, F., Hagan, J.E., Calcagno, J., Kane, M., Torgerson, P. and Martinez, M.S. (2015). Global Morbidity and Mortality of Leptospirosis: A Systematic Review. *PLoS Negl. Trop. Dis.*, 9(9): e0003898.
4. Hartskeerl, R.A., Collares, P.M. and Ellis, W.A. (2011). Emergence, control and re-emerging leptospirosis: dynamics of infection in the changing world. *Clin. Microbiol. Infect.*, 17: 494-501.
5. Massenet, D., Yvon, J.F., Couteaux, C. and Goarant, C. (2015). An Unprecedented High Incidence of Leptospirosis in Futuna, South Pacific, 2004-2014, Evidenced by Retrospective Analysis of Surveillance Data. *PLoS One*, 10(11): e0142063.
6. Victoriano, A.F., Smythe, L.D., Gloriani, B.N., Cavinta, L.L., Kasai, T., Limpakarmjanarat, K., Ong, B.L., Gongal, G., Hall, J., Coulombe, C.A., Yanagihara, Y., Yoshida, S. and Adler, B. (2009). Leptospirosis in the Pacific region. *BMC Infect. Dis.*, 9:147.
7. Levett, P.N. (2001). Leptospirosis. *Clin Microbiol Rev*, 14(2): 296-326.
8. Vinetz, J.M. (2001). Leptospirosis. *Curr. Opin. Infect. Dis.*, 14(5):527-38.
9. Rele, M.C., Rasal, A., Deshpande, S.D., Koppikar, G.V. and Lahiri, K.R. (2001). Mixed infection due to *Leptospira* and Dengue in a patient with pyrexia. *Indian J. Med. Microbiol.*, 19(4): 206-207.
10. Libraty, D.H., Khin, M.S.A., Clinton, M.K., Robert, G.V., Mammen, M.P., Timothy, E.P., Wenjun, Li., David, V.W., Ananda, N.W., Siripen, K., Duane, H.R., Sharone, G., Ala, R.L. and Francis, E. (2007). A comparative study of leptospirosis and dengue in Thai children. *PLoS. Negl. Trop. Dis.*, 1: e111.
11. Hin, H.S., Ramalingam, R., Chunn, K.Y., Ahmad, N., Rahman, Ab. J. and Mohamed, M.S. (2012). Fatal co-infection-melioidosis and leptospirosis. *American Journal of Medicine and Hygiene*, 87: 737-740.
12. Wijesinghe, A., Gnanapragash, N., Ranasinghe, G. and Ragunathan, M.K. (2015). Fatal co-infection with Leptospirosis and dengue in a Sri Lankan male. *BMC Res. Notes.*, 8: 348.

13. Cullen, P.A., Cordwell, S.J., Bulach, D.M., Haake, D.A. and Adler, B. (2002). Global analysis of outer membrane proteins from *Leptospira interrogans* serovars Lai. *Infect. Immun.*, 70: 2311-2318.
14. Boonyod, D., Poovorawan, Y., Bhattarakosol, P. and Chirathaworn, C. (2005). LipL32, an outer membrane protein of *Leptospira*, as an antigen in a dipstick assay for diagnosis of leptospirosis. *Asian. Pac. J. Allergy. Immunol.*, 23(2-3): 133-141.
15. Bourhy, P., Collet, L., Clement, S., Huerre, M., Ave, P., Giry, C., Francois, P., Mathieu, P. (2010). Isolation and Characterization of New *Leptospira* Genotypes from Patients in Mayotte (Indian Ocean). *PLoS Negl. Trop. Dis.*, 4(6): e724.
16. Ye, C., Yan, W., Xiang, H., Hongxuan, He., Yang, M., Ijaz, M., Nicodemus, U., Ching-Lin, H., McDonough, P.L., McDonough, S.P., Hussni, M., Yang, Z. and Yung-Fu, C. (2014). Recombinant Antigens rLipL21, rLoa22, rLipL32 and rLigACon4-8 for Serological Diagnosis of Leptospirosis by Enzyme-Linked Immunosorbent Assays in Dogs. *PLoS ONE*, 9(12): e111367.
17. Tahiliani, P., Kumar, M.M., Chandu, D., Kumar, A., Nagaraj, C. and Nandi, D. (2005). Gel purified LipL32: a prospective antigen for detection of leptospirosis. *J. Postgrad. Med.*, 51(3): 164-168.
18. Natarajaseenivasan, K., Vijayachari, P., Sharma, S., Sugunan, A.P., Selvin, J. and Sehgal, S.C. (2008). Serodiagnosis of severe Leptospirosis: evaluation of ELISA based on the recombinant OmpL1 or LipL41 antigens of *Leptospira interrogans* serovar autumnalis. *Ann. Trop. Med. Parasitol.*, 102(8): 699-708.
19. Asuthkar, S., Sridhar, V., Johannes, S., Friedrich, A. and Manjula, S. (2007). Expression and Characterization of an Iron-Regulated Hemin-Binding Protein, HbpA, from *Leptospira interrogans* Serovar Lai. *Infection And Immunity*, 75 (9): 4582-4591.
20. Siju, J., Thomas, N., Thangapandian, E., Vijendra, S.P., Verma, R. and Srivastava, S.K. (2012). Evaluation and comparison of native and recombinant LipL21 protein based ELISA for the diagnosis of bovine leptospirosis. *J. Vet. Sci.* 13(1): 99-101.
21. Cerqueira, G. M. and Picardeau, M. A. (2009). Century of *Leptospira* strain typing. *Infect. Genet. Evol.*, 9: 760-768.
22. Gowri, P.C., Bhavani, K., Rathinam, S.R. and Muthukkaruppan, V.R. (2003). Identification and evaluation of LPS antigen for serodiagnosis of uveitis associated with Leptospirosis. *J Med Microbiol*, 52: 667-673.
23. Riazi, M., Abdul Rani, B., Fairuz, A. and Zainul, F.Z. (2010). A low molecular weight lipopolysaccharide antigen preparation reactive to acute leptospirosis heterologous sera. *Tropical Biomedicine*, 27(2): 241-253.
24. Smits, L.H., Eapen, C.K., Sheela, S.N., Mariamma, K., Gasem, M.H., Claude, Y., David, S., Bambang, P., Marc, V., Theresia, H.A. and George, C.G. (2001). Lateral Flow Assay for Rapid Serodiagnosis of Human Leptospirosis. *Clinical and diagnostic laboratory immunology, J. Clin. Microbiol*, 8(1): 166-169.
25. Marcelo, J.R., Robert, H., Marcelo, G. and Lallier, R. (2000). Development of an indirect enzyme linked immunosorbent assay for the detection of Leptospiral antibodies in dogs. *The Canadian Journal of Veterinary Research*, 64: 32-37.
26. Joseph, L.F. (2003). *Statistical methods for rates & proportions*. 3rd edition New Jersey, USA: John Wiley & Sons.
27. Katz, A.R. (2012). Quantitative Polymerase Chain Reaction: Filling the Gap for Early Leptospirosis Diagnosis. *Clinical Infectious Diseases*, 54(9): 1256-1258.

28. Mason, M.R., Encina, C., Sreevatsan, S. and Munoz-Zanzi, C. (2016). Distribution and Diversity of Pathogenic *Leptospira* Species in Peri-domestic Surface Waters from South Central Chile. *PLoS Negl. Trop. Dis.*, 10(8): e0004895.
29. Lee, J.W., Park, S., Kim, S.H., Christova, I., Jacob, P., Vanasco N.B., Kang, Y.M., Woo, Y.J., Kim, M.S., Kim, Y.J., Cho, M.K. and Kim, Y.W. (2016). Clinical Evaluation of Rapid Diagnostic Test Kit Using the Polysaccharide as a Genus-Specific Diagnostic Antigen for Leptospirosis in Korea, Bulgaria, and Argentina. *J Korean Med Sci.*, 31: 183-189.
30. Terpstra, J., Ligthart, S. and Schoone, J. (1980). Serodiagnosis of human leptospirosis by enzyme-linked-immunosorbent- assay (ELISA). *Zentralblatt für Bakteriologie. Mikrobiologie und Hygiene (Abteilung I, Originale A)*, 247: 400-405.

Development of 1, 4-Naphthoquinones as Potential Epidermal Growth Factor Receptor Inhibitors For The Treatment of Cancer

Mousumi Besan¹, Manoj K. Gautam² and Sushant K. Shrivastava^{1*}

¹Department of Pharmaceutical Engineering and Technology, Indian Institute of Technology (Banaras Hindu University), Varanasi-221005, India.

²University Institute of Pharmaceutical Sciences, Panjab University, Chandigarh-160014, India.

*For Correspondence - skshrivastava.phe@iitbhu.ac.in

Abstract

In this manuscript, we have designed, synthesized and characterized 1, 4-naphthoquinone derivatives. The synthesized compounds (MB1-MB19) were further subjected for evaluation of their anticancer activity using MCF-7, HeLa and HepG2 cancer cell lines. The compound **MB-9** was observed to be most active against these three cancer cell lines i.e. MCF-7 ($IC_{50} = 15.63 \pm 0.47 \mu\text{M}$), HeLa ($IC_{50} = 13.45 \pm 0.48 \mu\text{M}$), and HepG2 ($IC_{50} = 23.87 \pm 0.59 \mu\text{M}$). Compound **MB-9** has also shown potent tyrosine kinase inhibitory activity with $IC_{50} = 1.80 \pm 0.06 \mu\text{M}$. Moreover, molecular docking investigations revealed that compound MB-9 has strong binding affinity to the active site residues of tyrosine kinase. These outcomes give a promising beginning to assist in the improvement of novel and powerful anticancer agents.

Keywords: Molecular Docking, *In-vitro* cytotoxicity, 1, 4-Naphthoquinone, Tyrosine kinase, Epidermal growth factor receptor

INTRODUCTION

Cancer is a broad term which is described as the disease caused by the result of cellular changes and characterized by abnormal cellular growth, division without control and is able to invade other tissues. It is the fastest developing disease in the world. In developed nations, cancer

growth has turned into the main source of mortality and in developing nations; it is the second driving reason for death after cardiovascular diseases (1). It is predicted that the yearly number of new cancer patients would reach 21 million around the world by 2030(2, 3). It is reported that one in every six worldwide death cases happened because of various cancer. As indicated by American Cancer Society, there are about 4750 new malignant cases as well as 1670 death cases daily (4). Rapid improvement into the diagnostic area and advancement of novel cancer therapy, it is possible to identify a biological pathway which is participating in cancer progression by sophisticated biological tools (5). Tyrosine kinases play essential roles in initiating various signal transduction pathways inside the cell and are associated with differentiation, cellular proliferation and numerous monitoring mechanisms (6). They act to transfer a phosphate from ATP to tyrosine residues on specific cellular proteins. Despite the essential contribution of tyrosine kinases, they may contribute to the uncontrolled proliferation of cancer cells, tumor progression and development of the metastatic disease. Epidermal growth factor receptor is a type of tyrosine kinase receptor which is a transmembrane glycoprotein responsible for the migration, cell growth, proliferation, differentiation, and adhesion under typical physiological conditions.

Binding of EGFR to its cognate ligands leads to autophosphorylation of receptor tyrosine kinase and subsequent activation of signal transduction pathways that are involved in cellular proliferation, differentiation and survival. Moreover, EGFR is over expressed in a variety of tumour (cancers) i.e. brain cancer, pancreatic cancer, lung cancer and neck cancer (7). Thus, EGFR is an alluring focus for the finding of novel anticancer agents. It is a 170 kilodalton glycoprotein that consists of Single transmembrane domain, Intracellular tyrosine kinase domain and extracellular ligand binding domain. Although the receptor exists as an inactive monomer, dimerization takes place once it is activated by its ligands from the autophosphorylation of the intracellular tyrosine kinase (8-11). While the receptor occurs as a passive monomer, dimerization happens once it is initiated by its ligands, followed by autophosphorylation at intracellular tyrosine kinase domain (TKD) (12,13). In addition, the vast majority of the revealed inhibitors were planned by focusing on the kinase domain of EGFR. Thus, the controlling of EGFR has been esteemed as a vital methodology for the improvement of cancer therapy (14, 15). The various EGFR inhibitors have been reported in the last decade i.e. Gefitinib, erlotinib, lapatinib, neratinib, vandetanib, dacomitinib, osimertinib, cetuximab, panitumumab, necitumumab. Currently, US FDA approved Tagrisso (Osimertinib) as 1st line treatment for EGFR mutated non-small cell lung cancer. Beside this prolonged inhibition and high potency of EGFR functions has been reported for several reversible inhibitors (16). These drugs exhibit several side effects, such as papulopustular rash, diarrhoea, moderate alopecia, hypomagnesemia, hypokalemia, which limit their use. Therefore the ultimate goal is to develop novel anticancer agents that will impede EGFR function and help in decelerate tumor progression.

The various quinone scaffolds have been reported for the treatment of cancer. Especially, 1, 4-naphthoquinones are active quinone derivatives that are broadly utilized as crude materials in agrochemicals industries and

pharmaceuticals (17). A various cluster of bioactivities has been accounted for 1, 4-naphthoquinone derivatives to be utilized as antiviral (18-21), antiplatelet (22), anticancer (23), trypanocidal (22), antifungal (24) and antimicrobial (25). 1, 4-Naphthoquinone having two ketone chromophore which is essential for the biological activities from their capacity to accept the electrons. Structure-activity relationship (SAR) exposed that cytotoxicity potency of 1,4-naphthoquinone is firmly connected with their electron accepting ability (26), which offers ascend to responsive oxygen species generation prompting DNA destruction and cell death.

Designing considerations

Quinone moieties such as mitomycin-C and RH1 (27) (benzoquinone) (28), daunorubicin, doxorubicin, idarubicin, epirubicin, aclarubicin and mitoxantrone (anthraquinone) (29) and atovaquone (30), binaphthoquinones (31) and b-lapachone (32, 33) are the most preclinically tested and clinically investigated anticancer agents commonly used for the treatment of solid and hematologic neoplasms. The cytotoxic mechanisms of action of these compounds mainly include the formation of semiquinone radicals and quinone redox cycling ensuing in the initiation and propagation of intracellular free oxygen radical chain reactions.

In addition, the 1, 4-naphthoquinone pharmacophore exhibits anticancer activity and has been the focus of various studies. Among the 1, 4-naphthoquinone compounds, plumbagin, mitomycin and shikonin have been used in the development of potent anticancer drugs (34). On the other hand, these compounds exhibit high levels of cytotoxicity and significant side effects, making their application as anticancer drugs in the clinical setup to be challenging (35).

Menadione (2-methyl-1,4-naphthoquinone, vitamin K3), which is both a redox-cycling and an alkylating quinone, was shown to lead to the activation of the extracellular signal-regulated kinase (ERK) 1 and ERK 2, which are well known for their prominent role in the regulation of cellular proliferation. The activation of ERK was blocked

by inhibitors of the direct upstream kinases of ERK 1/2, MAPK/ERK kinase (MEK) 1, and MEK 2 and by inhibitors of the Epithelial growth factor receptor (EGFR) tyrosine kinase, leading to the hypothesis that ligand-independent activation of the EGFR by menadione was responsible for the above-described effects (36). The most interesting is the synthesis of compounds with antitumor activity as selective inhibitors of biological targets, Epidermal growth factor receptor (EGFR). Thus, 1,4-naphthoquinone moiety is regarded as a privileged framework in medicinal chemistry.

Besides, the quinone derivatives, the piperazine ring has emerged as a promising pharmacophore. Piperazine ring suggested a successful emergence of the pharmacophore. The piperazine scaffold has been regarded as a core and is frequently found in natural active substances across a variety of different therapeutic drugs (37). The synthetic flexibility of piperazine scaffold led to the synthesis of a variety of its substituted analogs. Slight modification to the substitution pattern on the piperazine nucleus facilitates a recognizable difference in the medicinal potential of the resultant molecules (38). Maintaining the balance between pharmacodynamic and pharmacokinetic profiles of drug-like molecules is an important factor in designing and developing new drugs. Thus, one of the goals in the drug discovery process is to design molecules with high affinity for its targets and appropriate physicochemical properties. Piperazine core has two primary nitrogen atoms which exert the improvement in pharmacokinetic features of drug candidates because of their appropriate pKa. For this purpose, the characteristics of the piperazine template make this molecular subunit a useful and well-positioned system in the rational design of drugs (39).

Considering the reported literature, in the design of new anticancer agent, the development of hybrid molecules through the combination of different pharmacophore i.e., 1,4-naphthoquinone and piperazine moiety in one frame may lead to compounds with improved anticancer profiles. Thus, we hypothesized that the designing of a

molecule with 1,4-naphthoquinone moiety as a molecular scaffold by using strategies like linking with piperazine and by using carbon chain length as a linker and for better anticancer activity. Based on hybrid pharmacophore approach, the 1,4-naphthoquinone moieties was tethered to substituted piperazine nucleus with the aim of developing ligands having the ability to inhibit tyrosine kinase and serve as an anticancer agent (Figure 1).

Material and Methods

Instrumentation and Chemicals : The chemical reagents were obtained from various commercially accessible suppliers like HiMedia Laboratories Pvt. Ltd., Mumbai, India, and Sigma Aldrich (India) Silica gel 60-F₂₅₄ plates, thin-layer chromatography (TLC) were used to monitor the progress of the reaction. The obtained products were recrystallized to get pure products using suitable solvents. The melting points of compounds were recorded using Veego melting points apparatus. PerkinElmer spectrum (Ver 10.03.08) was utilized for the FTIR data collection. ¹³CNMR and ¹HNMR spectra of synthesized compounds were collected with the help of Bruker Advance II 400 NMR spectrometer. The chemical shifts (δ) represented as parts per million (ppm).

Chemistry : General procedure for the synthesis of 3-((3-methyl-1,4-dioxo-1,4-dihydro naphthalene-2-yl) thio) propanoic acid (**3**).

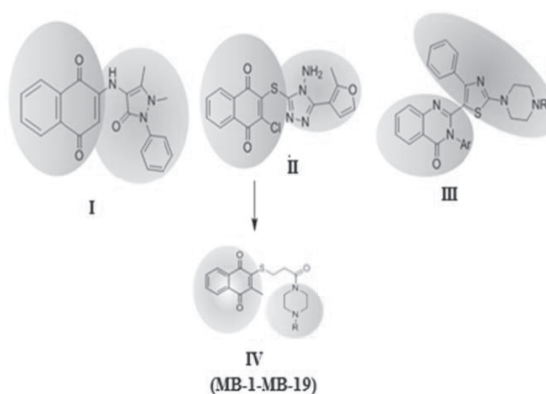


Figure 1: Designing strategy for the target compounds

Compound 3 was obtained by condensation of 2-Methylnaphthalene-1,4-dione (**1**) (0.516 g, 3 mmol) with 3-mercaptopropionic acid (**2**) (0.360 g, 3 mmol) in absolute ethanol (50 ml) and the reaction mixture was refluxed for 3-5 h that has given product of acid derivative and recrystallized from methanol. Yield: 0.455g, 54.95%, m.p.159-161 (Lit.161°C).

3-((3-methyl-1, 4-dioxo-1, 4-dihydro naphthalen-2-yl) thio) propanoic acid (3) : FTIR (KBr, ν cm^{-1}) : 3337.90 (O-H); 3110.83 (aromatic C-H stretch); 2953.84 (aliphatic C-H stretch); 1701.72 (C=O stretch); 1656.70 (C=O stretch); 1547.63 (C=C ring stretch); 1235.42 (C-O stretch); 744.40 cm^{-1} (C-H bend). $^1\text{H NMR}$ (CDCl_3): δ 9.47 (s, 1H, COOH), 8.23 (m, 2H, ArH), 7.70 (m, 2H, ArH), 3.47 (t, 2H, SCH_2 , $J = 6.60$ Hz), 2.70 (t, 2H, $\text{CH}_2\text{C}=\text{O}$, $J = 6.60$ Hz), 2.45 (s, 3H, CH_3).

General procedure for the synthesis of compounds (MB-1-MB-19) : All the titled compounds MB1-MB-19 was prepared by dissolving compound **3** in dry dichloromethane (DCM) and an equimolar amount of thionyl chloride was added gradually. The reaction mixture was stirred for 3-5 h for the formation of acid chloride product. Further different substituted piperazines in equimolar ratio were added in dry dichloromethane followed by addition of acid chloride then the reaction mixture was stirred for 9-10 hours to yield final compounds (**MB-1-MB-19**).

2-methyl-3-((3-oxo-3-(piperazin-1-yl) propyl) thio) naphthalene-1, 4-dione (MB-1) : Obtained as white solid in 58 % yield; mp 146-148 °C. FTIR (KBr, ν cm^{-1}): 3320.12 (N-H stretch); 3068.08 (aromatic C-H stretch); 2927.11 (aliphatic C-H stretch); 1735.77 (C=O stretch); 1689.24 (C=O stretch); 1624.70, 1505.83 (C=C ring stretch); 1415.08 (C-N stretch), 1268.44, 1215.39 (C-O stretch); 734.38 cm^{-1} (C-H bend). $^1\text{H NMR}$ (CDCl_3 , 400 MHz): δ 8.16 (m, 2H, ArH), 7.72 (m, 2H, ArH), 3.56 (t, 2H, $J = 4.12$ Hz, -N- CH_2), 3.33 (m, 4H, -N- CH_2 ; - SCH_2), 2.88 (m, 6H, $\text{NH}(\text{CH}_2)_2$; - CH_2CO), 2.77 (s, 3H, CH_3), 1.27 (s, 1H, -NH). $^{13}\text{C NMR}$ (CDCl_3 , 100 MHz): δ 185.73 (C=O), 178.54 (C=O),

171.15 (C=O), 139.11 (ArC_q), 137.48 ($2 \times \text{ArC}$), 133.84 (ArC_q), 132.95 ($2 \times \text{ArC}_q$), 130.94 (ArC), 128.10 (ArC), 46.84 ($2 \times \text{CH}_2$ piperazinyl), 44.92 ($2 \times \text{CH}_2$ piperazinyl) 35.73 (S- CH_2), 29.56 ($\text{CH}_2\text{C}=\text{O}$), 12.40 (CH_3). MS: m/z 344.86; Anal. Calcd. For $\text{C}_{18}\text{H}_{20}\text{N}_2\text{O}_3\text{S}$: C, 62.58; H, 5.65; N, 8.21. Found: C, 62.45; H, 5.95; N, 8.71.

2-methyl-3-((3-oxo-3-(4-phenylpiperazin-1-yl) propyl) thio) naphthalene-1, 4-dione (MB-2): Obtained as brown solid in 63 % yield; mp 200-202 °C. FTIR (KBr, ν cm^{-1}): 3068.08 (aromatic C-H stretch); 2916.47 (aliphatic C-H stretch); 1738.78 (C=O stretch); 1690.04 (C=O stretch); 1623.42 (C=C ring stretch); 1428.3 (C-N stretch), 1227.74 (C-O stretch); 750.23 cm^{-1} (C-H bend). $^1\text{H NMR}$ (CDCl_3 , 400 MHz): δ 8.25 (dd, 1H, $J_m = 1.44$ Hz, $J_o = 5.60$ Hz, ArH), 8.17 (dd, 1H, $J_m = 1.40$ Hz, $J_o = 5.80$ Hz ArH), 7.74 (m, 2H, ArH), 7.07 (t, 2H, $J = 5.88$ Hz, ArH), 6.62 (m, 3H, ArH), 3.79 (m, 4H, -N(CH_2) $_2$), 3.66 (m, 2H, N- CH_2), 3.46 (m, 2H, N- CH_2), 3.13 (t, 2H, $J = 4.36$ Hz, - SCH_2), 3.00 (t, 2H, $J = 4.40$ Hz, - CH_2CO), 2.76 (s, 3H, CH_3). $^{13}\text{C NMR}$ (CDCl_3 , 100 MHz): δ 185.73 (C=O), 178.54 (C=O), 171.40 (C=O), 150.96 (ArC_q), 139.68 (ArC_q), 137.51 ($2 \times \text{ArC}$), 133.84 (ArC), 132.92 ($2 \times \text{ArC}_q$), 130.94 (ArC_q), 129.35 ($2 \times \text{ArC}$), 128.15 (ArC), 120.31 (ArC), 116.77 ($2 \times \text{ArC}$), 49.17 ($2 \times \text{CH}_2$ piperazinyl), 44.84 ($2 \times \text{CH}_2$ piperazinyl), 35.73 (S- CH_2), 29.56 ($\text{CH}_2\text{C}=\text{O}$), 15.12 (CH_3). MS: m/z: 419.65; Anal. Calcd. for $\text{C}_{24}\text{H}_{24}\text{N}_2\text{O}_3\text{S}$: C, 68.32; H, 5.46; N, 6.39. Found: C, 68.42; H, 5.36; N, 6.34.

2-((3-(4-benzhydrylpiperazin-1-yl)-3-oxopropyl) thio)-3-methylnaphthalene-1, 4-dione (MB-3): Obtained as a yellow crystalline solid in 64 % yield; mp 195-197 °C. FTIR (KBr, ν cm^{-1}): 3384.66 (aromatic C-H stretch); 2943.91 (aliphatic C-H stretch); 1724.39 (C=O stretch); 1695.18 (C=O stretch); 1629.13, 1585.27 (C=C ring stretch); 1412.46 (C-N stretch), 1218.84 (C-O stretch); 733.20 cm^{-1} (C-H bend). $^1\text{H NMR}$ (CDCl_3 , 400 MHz): δ 8.04 (dd, 1H, $J_m = 1.40$ Hz, $J_o = 5.80$ Hz ArH), 8.00 (dd, 1H, $J_m = 1.40$ Hz, $J_o = 5.80$ Hz ArH), 7.69 (m, 2H, ArH), 7.27 (m, 10H, ArH), 3.52 (t, 2H, $J = 4.08$ Hz, -N- CH_2), 3.42 (t, 2H, $J = 4.08$ Hz, -N- CH_2), 3.34 (t, 2H, $J = 4.16$, - SCH_2), 2.96 (t, 2H, $J = 4.08$, -N- CH_2), 2.90 (t, 2H, $J = 4.08$, -N- CH_2),

2.64 (m, 5H, $-CH_2CO$; CH_3). ^{13}C NMR ($CDCl_3$, 100 MHz): δ 184.55 (C=O), 179.34 (C=O), 171.80 (C=O), 140.56 ($2 \times ArC_q$), 139.46 (ArC_q), 137.51 (ArC), 133.84 (ArC_q), 132.40 ($2 \times ArC$), 130.94 ($2 \times ArC_q$), 129.28 ($4 \times ArC$), 128.85 ($4 \times ArC$), 128.39 (ArC), 126.73 ($4 \times ArC$), 77.58 (CH), 50.80 ($2 \times CH_2$ piperazinyl), 44.55 ($2 \times CH_2$ piperazinyl), 35.73 (S- CH_2), 29.56 ($CH_2C=O$), 13.12 (CH_3). MS: m/z 510.55; Anal. Calcd. for $C_{31}H_{30}N_2O_3S$: C, 72.37; H, 5.10; N, 5.21. Found: C, 72.56; H, 5.21; N, 5.27.

2-((3-(4-benzylpiperazin-1-yl)-3-oxopropyl)thio)-3-methylnaphthalene-1, 4-dione (MB-4):

Obtained as brownish solid in 71 % yield; mp 161-163 °C; FTIR (KBr, ν cm^{-1}): 3035.42 (aromatic C-H stretch); 2925.02 (aliphatic C-H stretch); 1735.81 (C=O stretch); 1692.80 (C=O stretch); 1627.99 (C=C ring stretch); 1467.80 (C-N stretch), 1233.26 (C-O stretch); 736.29 cm^{-1} (C-H bend). 1H NMR ($CDCl_3$, 400 MHz): δ 8.18 (dd, 1H, $J_m = 1.41$ Hz, $J_o = 5.80$ Hz ArH), 8.05 (dd, 1H, $J_m = 1.40$ Hz, $J_o = 5.82$ Hz ArH), 7.75 (m, 2H, ArH), 7.25 (m, 5H, ArH), 3.62 (m, 4H, $-NH(CH_2)_2$), 3.44 (t, 2H, $J = 6.66$ Hz, $-N-CH_2-C$), 3.35 (t, 2H, $J = 4.24$ Hz, $-N-CH_2$), 2.88 (m, 4H, $-SCH_2$; $-CH_2CO$), 2.66 (t, 2H, $J = 4.24$ Hz, $N-CH_2$), 2.48 (s, 3H, CH_3). ^{13}C NMR ($CDCl_3$, 100 MHz): δ 186.55 (C=O), 178.54 (C=O), 177.95 (C=O), 139.46 (ArC_q), 138.39 (ArC_q), 137.17 (ArC), 133.84 (ArC), 132.38 ($2 \times ArC$), 130.33 ($2 \times ArC_q$), 128.93 ($2 \times ArC$), 127.90 ($2 \times ArC$), 127.90 (ArC), 126.55 (ArC), 63.66 (ArC_q), 51.15 ($2 \times CH_2$ piperazinyl) 44.25 ($2 \times CH_2$ piperazinyl), 35.73 (S- CH_2), 29.82 ($CH_2C=O$), 14.25 (CH_3). MS: m/z 434.31; Anal. Calcd. for $C_{25}H_{26}N_2O_3S$: C, 69.56; H, 6.21; N, 6.94. Found: C, 69.34; H, 6.32; N, 6.51.

2-methyl-3-((3-oxo-3-(4-(pyridin-2-yl) piperazin-1-yl) propyl) thio) naphthalene-1, 4-dione (MB-5):

Obtained as yellow solid in 61 % yield; mp 173-175 °C. FTIR (KBr, ν cm^{-1}): 3039.73 (aromatic C-H stretch); 2923.04 (aliphatic C-H stretch); 1737.11 (C=O stretch); 1690.13 (C=O stretch); 1627.77, 1584.63 (C=C ring stretch); 1434.40 (C-N stretch), 1271.80 (C-O stretch); 734.04 cm^{-1} (C-H bend). 1H NMR ($CDCl_3$, 400 MHz): δ 8.13 (dd, 1H, $J_m = 1.16$ Hz, $J_o = 6.00$ Hz ArH), 8.03 (m, 2H, ArH), 7.68 (m, 2H, ArH), 7.51 (m, 1H, ArH), 6.67 (m, 2H, ArH), 3.74 (m, 2H, $-SCH_2$), 3.64 (m, 4H, -

$N(CH_2)_2$), 3.51 (m, 2H, $-CH_2CO$), 3.30 (t, 2H, $J = 6.48$ Hz, $-N-CH_2$), 2.90 (t, 2H, $J = 6.48$, $-N-CH_2$), 2.37 (s, 3H, CH_3). ^{13}C NMR ($CDCl_3$, 100 MHz): δ 184.84 (C=O), 179.46 (C=O), 170.94 (C=O), 158.90 (ArC_q), 148.87 (CH pyridinyl), 140.12 (CH_2 pyridinyl), 139.17 (CH_2 pyridinyl), 137.21 (ArC), 133.02 (ArC_q), 132.17 ($2 \times ArC_q$), 128.91 ($2 \times ArC$), 127.62 (ArC), 113.61 (CH_2 pyridinyl), 107.70 (CH_2 pyridinyl), 47.24 ($2 \times CH_2$ piperazinyl) 44.32 ($2 \times CH_2$ piperazinyl), 35.15 (S- CH_2), 29.95 ($CH_2C=O$), 13.84 (CH_3). MS: m/z 421.97; Anal. Calcd. for $C_{23}H_{23}N_3O_3S$: C, 65.92; H, 5.53; N, 9.23. Found: C, 65.50; H, 5.82; N, 9.14.

2-methyl-3-((3-oxo-3-(4-(o-tolyl) piperazin-1-yl) propyl) thio) naphthalene-1, 4-dione (MB-6):

Obtained (KBr, ν cm^{-1}): 3030.29 (aromatic C-H stretch); 2918.25 (aliphatic C-H stretch); 1732.48 (C=O stretch); 1694.49 (C=O stretch); 1625.11 (C=C ring stretch); 1464.76 (C-N stretch), 1272.33 (C-O stretch); 776.76 cm^{-1} (C-H bend). 1H NMR ($CDCl_3$, 400 MHz): δ 8.22 (dd, 1H, $J_m = 1.36$ Hz, $J_o = 5.84$ Hz ArH), 8.11 (dd, 1H, $J_m = 1.36$ Hz, $J_o = 5.84$ Hz ArH), 7.66 (m, 2H, ArH), 6.91 (m, 2H, ArH), 6.55 (m, 2H, ArH), 3.75 (dt, 4H, $J_m = 3.96$ Hz, $J_o = 16.92$ Hz $-N(CH_2)_2$), 3.53 (t, 2H, $J = 3.96$ Hz $-S-CH_2$), 3.40 (t, 2H, $J = 3.92$ Hz, $-CH_2CO$), 3.23 (t, 2H, $J = 4.48$, $-N-CH_2$), 2.95 (t, 2H, $J = 4.48$ Hz, $-N-CH_2$), 2.72 (s, 3H, CH_3), 2.20 (s, 3H, CH_3). ^{13}C NMR ($CDCl_3$, 100 MHz): δ 188.15 (C=O), 174.84 (C=O), 173.84 (C=O), 150.93 (ArC_q), 139.27 (ArC_q), 133.50 (ArC), 132.47 ($2 \times ArC_q$), 130.54 ($2 \times ArC$), 130.06 (ArC_q), 129.40 (ArC_q), 128.30 (ArC), 127.99 (ArC), 127.10 (ArC), 120.99 (ArC), 117.82 (ArC), 50.27 ($2 \times CH_2$ piperazinyl), 44.14 ($2 \times CH_2$ piperazinyl) 35.73 (S- CH_2), 29.36 ($CH_2C=O$), 17.23 (CH_3), 13.73 (CH_3). MS: m/z 433.12; Anal. Calcd. for $C_{25}H_{26}N_2O_3S$: C, 69.20; H, 6.03; N, 7.07. Found: C, 69.32; H, 6.18; N, 6.98.

2-((3-(4-(2-chlorophenyl) piperazin-1-yl)-3-oxopropyl) thio)-3-methylnaphthalene-1, 4-dione (MB-7):

Obtained as creamy solid in 68 % yield; mp 221-223 °C. FTIR (KBr, ν cm^{-1}): 3057.01 (aromatic C-H stretch); 2916.26 (aliphatic C-H stretch); 1738.63 (C=O stretch); 1690.14 (C=O stretch); 1625.26 (C=C ring stretch); 1485.74 (C-N stretch), 1226.67 (C-O stretch); 747.73 (C-H

bend); 675.74 cm^{-1} (C-Cl Stretch). ^1H NMR (CDCl_3 , 400 MHz): δ 8.08 (m, 2H, ArH), 7.74 (m, 2H, ArH), 7.09 (dd, 1H, ArH), 6.96 (td, 1H, ArH), 6.61 (m, 2H, ArH), 3.82 (t, 2H, $J = 4.08$ Hz, N-CH_2), 3.68 (t, 2H, $J = 4.08$ Hz, N-CH_2), 3.53 (t, 2H, $J = 4.08$ Hz, N-CH_2), 3.44 (m, 4H, -N-CH_2 ; -SCH_2), 3.02 (t, 2H, $J = 5.12$ Hz, $\text{-CH}_2\text{CO}$), 2.28 (s, 3H, CH_3). ^{13}C NMR (CDCl_3 , 100 MHz): δ 187.18 (C=O), 175.73 (C=O), 170.79 (C=O), 148.43 (ArC_q), 139.92 (ArC_q), 137.66 (ArC), 133.84 (ArC_q), 132.35 ($2 \times \text{ArC}_q$), 131.75 ($2 \times \text{ArC}$), 130.51 (ArC), 128.33 (C-Cl), 127.62 (ArC), 127.27 (ArC), 120.56 (ArC), 119.18 (ArC), 50.40 ($2 \times \text{CH}_2$ piperazinyl), 44.27 ($2 \times \text{CH}_2$ piperazinyl), 35.47 (S- CH_2), 29.01 ($\text{CH}_2\text{C=O}$), 16.12 (CH_3). MS: m/z 453.80 ($\text{M}^+ + 1$), 455.80 ($\text{M}^+ + 2$); Anal. Calcd. for $\text{C}_{24}\text{H}_{23}\text{ClN}_2\text{O}_3\text{S}$: C, 63.32; H, 5.20; N, 6.98. Found: C, 63.42; H, 5.13; N, 6.84.

2-((3-(4-(2, 3-dichlorophenyl) piperazin-1-yl)-3-oxopropyl) thio)-3-methylnaphthalene-1, 4-dione (MB-8) : Obtained as yellow solid powder in 73 % yield; mp 241-243 °C. FTIR (KBr, ν cm^{-1}): 3038.75 (aromatic C-H stretch); 2926.93 (aliphatic C-H stretch); 1738.68 (C=O stretch); 1684.51 (C=O stretch); 1627.31, 1500.84 (C=C ring stretch); 1421.31 (C-N stretch), 1251.13 (C-O stretch); 808.65 (C-H bend); 708.43 cm^{-1} (C-Cl Stretch). ^1H NMR (CDCl_3 , 400 MHz): δ 8.02 (m, 2H, ArH), 7.66 (m, 2H, ArH), 6.88 (t, 1H, $J = 5.96$, ArH), 6.63 (dd, 1H, ArH), 6.55 (dd, 1H, ArH), 3.80 (t, 2H, $J = 4.08$ Hz, N-CH_2), 3.74 (t, 2H, $J = 4.12$ Hz, N-CH_2), 3.65 (t, 2H, $J = 4.08$ Hz, N-CH_2), 3.41 (m, 4H, -N-CH_2 ; -SCH_2), 2.98 (t, 2H, $J = 4.32$ Hz, $\text{-CH}_2\text{CO}$), 2.43 (s, 3H, CH_3). ^{13}C NMR (CDCl_3 , 100 MHz): δ 185.12 (C=O), 178.94 (C=O), 171.46 (C=O), 149.83 (ArC_q), 139.39 (ArC_q), 137.93 (ArC), 134.73 (ArC_q), 133.95 (C-Cl), 132.09 ($2 \times \text{ArC}_q$), 130.73 ($2 \times \text{ArC}$), 128.56 (ArC), 128.15 (C-Cl), 127.84 (ArC), 121.12 (ArC), 118.47 (ArC), 50.22 ($2 \times \text{CH}_2$ piperazinyl), 44.97 ($2 \times \text{CH}_2$ piperazinyl), 35.32 (S- CH_2), 29.38 ($\text{CH}_2\text{C=O}$), 12.41 (CH_3). MS: m/z : 488.53 ($\text{M}^+ + 1$); 490.53 ($\text{M}^+ + 2$). Anal. Calcd. for $\text{C}_{24}\text{H}_{22}\text{Cl}_2\text{N}_2\text{O}_3\text{S}$: C, 58.86; H, 4.32; N, 6.00: Found: C, 58.57; H, 4.40; N, 5.92.

2-((3-(4-(4-chlorophenyl) piperazin-1-yl)-3-oxopropyl) thio)-3-methylnaphthalene-1, 4-

dione (MB-9) : Obtained as brownish solid in 66 % yield; mp 197-199 °C. FTIR (KBr, ν cm^{-1}): 3073.30 (aromatic C-H stretch); 2928.41 (aliphatic C-H stretch); 1728.47 (C=O stretch); 1685.30 (C=O stretch); 1629.75, 1592.24 (C=C ring stretch); 1453.39 (C-N stretch), 1244.41 (C-O stretch); 757.93 (C-H bend); 687.20 cm^{-1} (C-Cl Stretch). ^1H NMR (CDCl_3 , 400 MHz): δ 8.06 (m, 2H, ArH), 7.71 (m, 2H, ArH), 7.12 (d, 2H, $J = 6.00$, ArH), 6.61 (d, 2H, $J = 5.96$, ArH), 3.77 (m, 4H, $\text{N}(\text{CH}_2)_2$), 3.62 (m, 2H, -SCH_2), 3.45 (m, 4H, $\text{-N}(\text{CH}_2)_2$), 2.98 (t, 2H, $J = 6.44$ Hz, $\text{-CH}_2\text{CO}$), 2.56 (s, 3H, CH_3). ^{13}C NMR (CDCl_3 , 100 MHz): δ 186.98 (C=O), 173.84 (C=O), 165.38 (C=O), 150.29 (ArC_q), 139.23 (ArC_q), 137.40 (ArC), 133.84 (ArC_q), 132.58 ($2 \times \text{ArC}_q$), 132.58 ($2 \times \text{ArC}$), 130.44 (ArC), 129.98 (ArC), 128.33 (C-Cl), 127.90 (ArC), 117.28 ($2 \times \text{ArC}$), 49.39 ($2 \times \text{CH}_2$ piperazinyl), 44.61 ($2 \times \text{CH}_2$ piperazinyl), 35.65 (S- CH_2), 29.21 ($\text{CH}_2\text{C=O}$), 8.25 (ArC_q). MS: m/z 454.81 ($\text{M}^+ + 1$), 456.81 ($\text{M}^+ + 2$); Anal. Calcd. for $\text{C}_{24}\text{H}_{23}\text{ClN}_2\text{O}_3\text{S}$: C, 63.76; H, 5.12; N, 6.88. Found: C, 63.52; H, 5.22; N, 6.80.

2-((3-(4-(2-fluorophenyl) piperazin-1-yl)-3-oxopropyl) thio)-3-methylnaphthalene-1, 4-dione (MB-10) : Obtained as white solid in 70 % yield; mp 171-173 °C. FTIR (KBr, ν cm^{-1}): 3053.48 (aromatic C-H stretch); 2950.20 (aliphatic C-H stretch); 1740.99 (C=O stretch); 1680.05 (C=O stretch); 1621.85, 1584.62 (C=C ring stretch); 1463.60 (C-N stretch), 1217.26 (C-O stretch); 1120.82 (C-F Stretch); 766.20 cm^{-1} (C-H bend). ^1H NMR (CDCl_3 , 400 MHz): δ 8.17 (m, 2H, ArH), 7.70 (m, 2H, ArH), 6.79 (m, 2H, ArH), 6.56 (m, 2H, ArH), 3.80 (t, 2H, $J = 3.98$, N-CH_2), 3.71 (t, 2H, $J = 3.98$, N-CH_2), 3.57 (t, 2H, $J = 4.00$, -N-CH_2), 3.41 (t, 2H, $J = 3.98$, -NCH_2), 3.35 (t, 2H, $J = \text{-S-CH}_2$), 2.88 (t, 2H, $J = 6.46$ Hz, $\text{-CH}_2\text{CO}$), 2.74 (s, 3H, CH_3). ^{13}C NMR (CDCl_3 , 100 MHz): δ 185.04 (C=O), 179.46 (C=O), 172.40 (C=O), 154.75 (C-F), 142.68 (ArC_q), 139.19 (ArC_q), 137.96 (ArC), 135.27 ($2 \times \text{ArC}_q$), 133.67 (ArC_q), 132.15 ($2 \times \text{ArC}$), 127.86 (ArC), 125.88 (ArC), 119.76 (ArC), 118.31 (ArC), 117.17 (ArC), 50.75 ($2 \times \text{CH}_2$ piperazinyl), 44.35 ($2 \times \text{CH}_2$ piperazinyl), 35.31 (S- CH_2), 29.66 ($\text{CH}_2\text{C=O}$), 17.03 (CH_3). MS: m/z 437.94 ($\text{M}^+ + 1$); 439.94 ($\text{M}^+ + 2$). Anal. Calcd. for $\text{C}_{24}\text{H}_{23}\text{FN}_2\text{O}_3\text{S}$: C,

66.12; H, 5.84; N, 6.10. Found: C, 65.99; H, 5.63; N, 6.24.

2-((3-(4-(4-fluorophenyl) piperazin-1-yl)-3-oxopropyl) thio)-3-methylnaphthalene-1, 4-dione (MB-11) : Obtained as yellow solid in 68 % yield; mp 198-200 °C. FTIR (KBr, ν cm⁻¹): 3066.96 (aromatic C-H stretch); 2938.45 (aliphatic C-H stretch); 1737.96 (C=O stretch); 1695.47 (C=O stretch); 1625.73, 1601.61 (C=C ring stretch); 1476.03 (C-N stretch); 1217.37₁ (C-O stretch); 1087.15 (C-F Stretch); 754.43 cm⁻¹ (C-H bend). ¹H NMR (CDCl₃, 400 MHz): δ 8.14 (m, 2H, ArH), 7.67 (m, 2H, ArH), 6.76 (t, 2H, *J* = 6.10 Hz, ArH), 6.55 (m, 2H, ArH), 3.75 (m, 4H, N(CH₂)₂), 3.53 (t, 2H, *J* = 3.88 Hz, -N-CH₂), 3.41 (t, 2H, *J* = 3.88 Hz, -N-CH₂), 3.26 (t, 2H, *J* = 4.46, -SCH₂), 2.97 (m, 5H, -CH₂CO; CH₃). ¹³C NMR (CDCl₃, 100 MHz): δ 184.59 (C=O), 176.98 (C=O), 172.40 (C=O), 158.25 (d, *J* = 209.04 Hz, C-F), 149.49 (ArC_q), 139.17 (ArC_q), 137.66 (ArC), 133.77 (ArC_q), 132.35 (2 × ArC), 130.93 (2 × ArC), 127.37 (ArC), 118.59 (2 × ArC), 117.68 (2 × ArC), 49.95 (2 × CH₂ piperazinyl), 44.33 (2 × CH₂ piperazinyl) 35.38 (S-CH₂), 29.59 (CH₂C=O), 14.84 (ArC_q). MS: *m/z* 438.75 (M⁺ + 1) 440.75 (M⁺ + 2). Anal. Calcd. for C₂₄H₂₃FN₂O₃S: C, 65.54; H, 5.76; N, 6.91. Found: C, 65.83; H, 5.89; N, 6.36

2-methyl-3-((3-oxo-3-(4-(4-(tri-fluoro methyl) phenyl) piperazin-1yl) propyl) thio) naphthalene-1, 4-dione (MB-12) : Obtained as brownish solid in 69% yield; mp 218-220°C. FTIR (KBr, ν cm⁻¹): 3079.04 (aromatic C-H stretch); 2927.33 (aliphatic C-H stretch); 1721.44 (C=O stretch); 1657.60 (C=O stretch); 1625.03, 1600.35 (C=C ring stretch); 1444.63 (C-N stretch); 1248.82 (C-O stretch); 1125.93 (C-F stretch); 773.40 cm⁻¹ (C-H bend). ¹H NMR (CDCl₃, 400 MHz): δ 8.20 (m, 2H, ArH), 7.72 (m, 2H, ArH), 7.33 (d, 2H, *J* = 5.96, ArH), 6.60 (d, 2H, *J* = 5.96, ArH), 3.78 (m, 4H, N(CH₂)₂), 3.64 (m, 2H, -N-CH₂), 3.47 (m, 2H, -N-CH₂), 3.31 (t, 2H, *J* = 4.46 Hz, -SCH₂), 3.02 (m, 5H, -CH₂CO; CH₃). ¹³C NMR (CDCl₃, 100 MHz): δ 184.24 (C=O), 175.12 (C=O), 173.84 (C=O), 154.24 (ArC_q), 139.25 (ArC_q), 137.49 (ArC), 133.17 (ArC_q), 132.77 (2 × ArC), 130.85 (2 × ArC), 128.00 (ArC), 127.51 (2 × ArC_q), 126.85 (d, *J* = 209.06

Hz, CF₃) 124.46 (ArC_q), 114.17 (2 × ArC), 49.96 (2 × CH₂ piperazinyl), 44.38 (2 × CH₂ piperazinyl) 35.81 (S-CH₂), 29.81 (CH₂C=O), 14.24 (CH₃). MS: *m/z* 488.06 (M⁺ + 1); 490.14 (M⁺ + 2). Anal. Calcd. for C₂₅H₂₃F₃N₂O₃S: C, 61.40; H, 4.25; N, 5.55. Found: C, 61.22; H, 4.45; N, 5.76.

2-((3-(4-(3-fluorophenyl) piperazin-1-yl)-3-oxopropyl) thio)-3-methylnaphthalene-1, 4-dione (MB-13) : Obtained as white solid in 66 % yield; mp 161-163 °C. FTIR (KBr, ν cm⁻¹): 3038.75 (aromatic C-H stretch); 2926.93 (aliphatic C-H stretch); 1738.68 (C=O stretch); 1684.91 (C=O stretch); 1627.31, 1591.91 (C=C ring stretch); 1452.51 (C-N stretch); 1251.13₁ (C-O stretch); 1087.76 (C-F stretch); 708.43 cm⁻¹ (C-H bend). ¹H NMR (CDCl₃, 400 MHz): δ 8.32 (dd, 1H, *J*_m = 1.52 Hz, *J*_o = 5.60 Hz ArH), 8.17 (dd, 1H, *J*_m = 1.52 Hz, *J*_o = 5.60 Hz ArH), 7.72 (m, 2H, ArH), 7.06 (m, 1H, ArH), 6.41 (m, 3H, ArH), 3.88 (m, 2H, -N-CH₂), 3.72 (m, 4H, -N(CH₂)₂), 3.46 (m, 2H, -N-CH₂), 3.36 (t, 2H, *J* = 4.56, -SCH₂), 3.01 (t, 2H, *J* = 4.56 Hz, -CH₂CO), 2.80 (s, 3H, CH₃). ¹³C NMR (CDCl₃, 100 MHz): δ 183.48 (C=O), 179.46 (C=O), 170.94 (C=O), 163.20 ((d, *J* = 209.08 Hz-F), 139.318 (ArC_q), 137.73 (ArC_q), 133.64 (ArC_q), 133.11 (ArC), 132.40 (2 × ArC), 130.29 (2 × ArC), 128.97 (ArC), 127.90 (ArC), 113.76 (ArC), 107.73 (ArC), 103.48 (ArC), 49.80 (2 × CH₂ piperazinyl), 44.30 (2 × CH₂ piperazinyl) 35.28 (S-CH₂), 29.27 (CH₂C=O), 15.56 (CH₃). MS: *m/z* 438.32 (M⁺ + 1); 440.32 (M⁺ + 2). Anal. Calcd. for C₂₄H₂₃FN₂O₃S: C, 65.76; H, 5.35; N, 6.30. Found: C, 65.88; H, 5.47; N, 6.21.

2-((3-(4-(4-methoxyphenyl) piperazin-1-yl)-3-oxopropyl) thio)-3-methylnaphthalene-1, 4-dione (MB-14) : Obtained as white solid in 69% yield; mp 148-150 °C. FTIR (KBr, ν cm⁻¹): 3073.30 (aromatic C-H stretch); 2928.41 (aliphatic C-H stretch); 1728.47 (C=O stretch); 1685.30 (C=O stretch); 1629.75, 1592.24 (C=C ring stretch); 1453.39 (C₁-N stretch); 1244.41 (C-O stretch); 757.93 cm⁻¹ (C-H bend). ¹H NMR (CDCl₃, 400 MHz): δ 8.11 (m, 2H, ArH), 7.73 (m, 2H, ArH), 6.72 (d, 2H, *J* = 6.04 Hz, ArH), 6.66 (d, 2H, *J* = 6.04 Hz, ArH), 3.82 (m, 5H, OCH₃; -N-CH₂), 3.69 (m, 4H, N(CH₂)₂), 3.44 (m, 4H, -N-CH₂; -SCH₂), 2.98 (t, 2H, *J* = 4.14 Hz, -CH₂CO), 2.70 (s, 3H, CH₃).

^{13}C NMR (CDCl_3 , 100 MHz): δ 186.20 (C=O), 176.19 (C=O), 173.84 (C=O), 152.81 (ArC_q), 143.73 (ArC_q), 139.17 (ArC_q), 137.58 (ArC), 133.82 (ArC_q), 132.81 ($2 \times \text{ArC}$), 130.47 ($2 \times \text{ArC}$), 127.90 (ArC), 116.20 ($2 \times \text{ArC}$), 116.19 ($2 \times \text{ArC}$), 56.04 (- OCH_3), 49.51 ($2 \times \text{CH}_2$ piperazinyl), 44.76 ($2 \times \text{CH}_2$ piperazinyl), 35.16 (S- CH_2), 29.16 ($\text{CH}_2\text{C}=\text{O}$), 16.19 (CH_3). MS: m/z 450.41. Anal. Calcd. for $\text{C}_{25}\text{H}_{26}\text{N}_2\text{O}_4\text{S}$: C, 66.31; H, 5.90; N, 6.21. Found: C, 66.87; H, 5.63; N, 6.39.

2-((3-(4-(2-methoxyphenyl) piperazin-1-yl)-3-oxopropyl) thio)-3-methylnaphthalene-1,4-dione (MB-15)

Obtained as Brownish solid in 65 % yield; mp 161-163 °C. FTIR (KBr, ν cm^{-1}) 3053.48 (aromatic C-H stretch); 2950.20 (aliphatic C-H stretch); 1740.99 (C=O stretch); 1680.05 (C=O stretch); 1621.85 (C=C ring stretch); 1415.45₁ (C-N stretch); 1217.26 (C-O stretch); 812.78 cm^{-1} (C-H bend). ^1H NMR (CDCl_3 , 400 MHz): δ 8.07 (m, 2H, ArH), 7.72 (m, 2H, ArH), 6.84 (m, 1H, ArH), 6.77 (m, 1H, ArH), 6.71 (m, 2H, ArH), 3.83 (t, 2H, $J = 3.90$ Hz, - N-CH_2), 3.78 (s, 3H, OCH_3), 3.74 (t, 2H, $J = 3.88$ Hz, - N-CH_2), 3.68 (t, 2H, $J = 3.88$ Hz, - N-CH_2), 3.49 (t, 2H, $J = 3.88$ Hz, - N-CH_2), 3.40 (t, 2H, $J = 6.46$ Hz, - SCH_2), 2.99 (t, 2H, $J = 6.46$ Hz, - CH_2CO), 2.60 (s, 3H, CH_3). ^{13}C NMR (CDCl_3 , 100 MHz): δ 185.84 (C=O), 179.46 (C=O), 172.64 (C=O), 149.31 (ArC_q), 142.64 (ArC_q), 139.50 (ArC_q), 133.37 (ArC), 132.32 ($2 \times \text{ArC}$), 130.30 (ArC_q), 128.29 ($2 \times \text{ArC}$), 122.28 (ArC), 120.27 (ArC), 117.27 ($2 \times \text{ArC}$), 113.15 (ArC), 56.79 (- OCH_3), 50.54 ($2 \times \text{CH}_2$ piperazinyl), 44.55 ($2 \times \text{CH}_2$ piperazinyl), 35.75 (S- CH_2), 29.73 ($\text{CH}_2\text{C}=\text{O}$), 15.84 (CH_3). MS: m/z 450.27. Anal. Calcd. for $\text{C}_{25}\text{H}_{26}\text{N}_2\text{O}_4\text{S}$: C, 66.87; H, 5.43; N, 6.25. Found: C, 66.36; H, 5.49; N, 6.35.

2-methyl-3-((3-(4-(4-nitrophenyl) piperazin-1-yl)-3-oxopropyl) thio) naphthalene-1, 4-dione (MB-16)

Obtained as white crystalline solid in 63 % yield; mp 241-243 °C. FTIR (KBr, ν cm^{-1}) 3062.97 (aromatic C-H stretch); 2909.20 (aliphatic C-H stretch); 1728.33 (C=O stretch); 1703.88 (C=O stretch); 1630.86, 1602.9 (C=C ring stretch); 1450.99 ($\text{C}_1\text{-N}$ stretch); 1266.14 (C-O stretch); 746.78 cm^{-1} (C-H bend). ^1H NMR (CDCl_3 , 400 MHz): δ 8.06 (m, 4H, ArH), 7.72 (m, 2H, ArH),

6.91 (d, 2H, $J = 5.92$ Hz, ArH), 3.83 (m, 2H, - N-CH_2), 3.77 (m, 4H, - $\text{N}(\text{CH}_2)_2$), 3.55 (m, 2H, - N-CH_2), 3.42 (t, 2H, $J = 6.46$ Hz, - SCH_2), 2.98 (t, 2H, $J = 6.50$ Hz, - CH_2CO), 2.63 (s, 3H, CH_3). ^{13}C NMR (CDCl_3 , 100 MHz): δ 185.94 (C=O), 174.84 (C=O), 171.81 (C=O), 158.30 (ArC_q), 139.44 (ArC_q), 137.88 (ArC_q), 133.82 ($2 \times \text{ArC}$), 132.40 ($2 \times \text{ArC}$), 130.40 (ArC), 128.33 (ArC_q), 127.90 (ArC), 126.40 ($2 \times \text{ArC}$), 112.41 ($2 \times \text{ArC}$), 49.44 ($2 \times \text{CH}_2$ piperazinyl), 44.95 ($2 \times \text{CH}_2$ piperazinyl), 35.31 (S- CH_2), 29.77 ($\text{CH}_2\text{C}=\text{O}$), 15.23 (CH_3). MS: m/z 465.60. Anal. Calcd. for $\text{C}_{24}\text{H}_{23}\text{N}_3\text{O}_5\text{S}$: C, 61.80; H, 4.65; N, 9.28. Found: C, 61.88; H, 4.83; N, 9.19.

2-((3-(4-(2, 3-dimethylphenyl) piperazin-1-yl)-3-oxopropyl) thio)-3-methylnaphthalene-1, 4-dione (MB-17)

Obtained as white solid in 70 % yield; mp 231-233 °C. FTIR (KBr, ν cm^{-1}) 3079.32 (aromatic C-H stretch); 2926.70 (aliphatic C-H stretch); 1720.40 (C=O stretch); 1684.73 (C=O stretch); 1592.24 (C=C ring stretch); 1429.05 (C-N ring stretch); 1251.73 (C-O stretch); 707.61 cm^{-1} (C-H bend). ^1H NMR (CDCl_3 , 400 MHz): δ 8.28 (m, 1H, ArH), 8.17 (m, 1H, ArH), 7.83 (m, 2H, ArH), 6.95 (t, 1H, $J = 6.46$ Hz, ArH), 6.57 (dd, 1H, ArH), 6.45 (dd, 1H, ArH), 3.65 (m, 4H, - $\text{N}(\text{CH}_2)_2$), 3.45 (t, 2H, $J = 4.68$, - SCH_2), 3.21 (m, 4H, - $\text{N}(\text{CH}_2)_2$), 2.96 (t, 2H, $J = 4.56$, - CH_2CO), 2.72 (s, 3H, CH_3), 2.38 (s, 3H, CH_3), 2.29 (s, 3H, CH_3). ^{13}C NMR (CDCl_3 , 100 MHz): δ 186.08 (C=O), 176.20 (C=O), 173.29 (C=O), 153.29 (ArC_q), 139.95 (ArC_q), 138.15 (ArC_q), 137.90 (ArC), 132.40 ($2 \times \text{ArC}$), 130.53 ($2 \times \text{ArC}$), 128.82 (ArC_q), 127.84 (ArC), 126.73 (ArC), 126.56 (ArC_q), 122.77 (ArC), 115.96 (ArC), 51.49 ($2 \times \text{CH}_2$ piperazinyl), 44.44 ($2 \times \text{CH}_2$ piperazinyl), 35.13 (S- CH_2), 29.03 ($\text{CH}_2\text{C}=\text{O}$), 19.77 (CH_3), 13.84 (CH_3), 13.12 (CH_3). MS: m/z 447.25. Anal. Calcd. for $\text{C}_{26}\text{H}_{28}\text{N}_2\text{O}_3\text{S}$: C, 69.54; H, 6.67; N, 6.83. Found: C, 69.62; H, 6.82; N, 6.73.

2-((3-(4-(4-bromo-2, 5-dimethoxybenzyl) piperazin-1-yl)-3-oxopropyl) thio)-3-methylnaphthalene-1, 4-dione (MB-18)

Obtained as yellowish solid in 68 % yield; mp 194-196 °C. FTIR (KBr, ν cm^{-1}) 3068.87 (aromatic C-H stretch); 2932.69 (aliphatic C-H stretch); 1725.66 (C=O stretch); 1689.28 (C=O stretch); 1429.27 (C-N stretch); 1247.91 (C-O stretch); 751.90 cm^{-1}

(C-H bend). ¹H NMR (CDCl₃, 400 MHz): δ 8.19 (dd, 1H, $J_m = 1.64$ Hz, $J_o = 5.52$ Hz ArH), 8.10 (dd, 1H, $J_m = 1.68$ Hz, $J_o = 5.48$ Hz ArH), 7.79 (m, 2H, ArH), 7.08 (s, 1H, ArH), 6.81 (s, 1H, ArH), 3.80 (s, 6H, OCH₃), 3.71 (s, 2H, -N-CH₂), 3.53 (t, 2H, $J = 4.16$ Hz, -N-CH₂), 3.43 (t, 2H, $J = 4.24$ Hz, -N-CH₂), 3.30 (t, 2H, $J = 4.16$ Hz, -N-CH₂), 2.98 (t, 2H, $J = 4.16$ Hz, SCH₂), 2.82 (t, 2H, $J = 6.0$ Hz, -CH₂CO), 2.64 (t, 2H, $J = 4.16$ Hz, -CH₂-), 2.23 (s, 3H, CH₃). ¹³C NMR (CDCl₃, 100 MHz): δ 183.10 (C=O), 177.92 (C=O), 170.94 (C=O), 153.10 (ArC_q), 151.68 (ArC_q), 139.39 (ArC_q), 132.32 (2 × ArC), 133.33 (2 × ArC), 128.30 (ArC), 127.29 (2 × ArC), 116.88 (ArC_q), 113.56 (ArC), 113.29 (ArC), 110.19 (C-Br), 58.22 (ArC), 56.78 (OCH₃), 55.07 (OCH₃), 54.61 (2 × CH₂piperaziny), 49.23 (2 × CH₂piperaznyl), 32.45 (S-CH₂), 32.27 (CH₂C=O), 8.59 (CH₃). MS: m/z 572.42 (M⁺ + 1); 574.42 (M⁺ + 2). Anal. Calcd. for C₂₇H₂₉BrN₂O₅S: C, 56.80; H, 5.28; N, 4.64. Found: C, 56.88; H, 5.20; N, 4.72

2-methyl-3-((3-(4-(2-nitrophenyl) piperazin-1-yl)-3-oxopropyl) thio) naphthalene-1, 4-dione (MB-19): Obtained as creamy solid in 67 % yield; mp 263-265 °C. FTIR (KBr, ν cm⁻¹) 3067.95 (aromatic C-H stretch); 2931.94 (aliphatic C-H stretch); 1726.61 (C=O stretch); 1662.41 (C=O stretch); 1428.22 (C-N stretch); 1246.76 (C-O stretch); 812.09 cm⁻¹ (C-H bend). ¹H NMR (CDCl₃, 400 MHz): δ 8.18 (dd, 1H, $J_m = 1.65$ Hz, $J_o = 5.50$ Hz ArH), 8.04 (dd, 1H, $J_m = 1.68$ Hz, $J_o = 5.46$ Hz ArH), 7.87 (m, 1H, ArH), 7.62 (m, 2H, ArH), 7.44 (m, 1H, ArH), 6.97 (m, 1H, ArH), 6.89 (m, 1H, ArH), 3.65 (t, 2H, $J = 4.44$ Hz, -N-CH₂), 3.57 (t, 2H, $J = 4.44$ Hz, -N-CH₂), 3.34 (m, 6H, -N(CH₂)₂-SCH₂), 3.08 (t, 2H, $J = 4.56$ Hz, -CH₂CO), 2.68 (s, 3H, CH₃). ¹³C NMR (CDCl₃, 100 MHz): δ 187.73 (C=O), 177.54 (C=O), 172.40 (C=O), 145.31 (ArC_q), 140.76 (ArC_q), 139.30 (ArC), 135.11 (2 × ArC), 137.62 (ArC_q), 134.94 (ArC), 133.84 (ArC_q), 132.59 (2 × ArC), 128.15 (ArC), 127.48 (ArC), 119.77 (ArC), 118.15 (ArC), 52.04 (2 × CH₂piperaziny), 44.84 (2 × CH₂piperaziny), 35.26 (S-CH₂), 29.36 (CH₂C=O), 12.40 (CH₃). MS: m/z 465.70. Anal. Calcd. for C₂₄H₂₃N₃O₅S: C, 61.37; H, 4.54; N, 9.92. Found: C, 61.65; H, 4.38; N, 9.45.

Cell culture : Cancer cell lines MCF-7, HeLa and HePG2 were purchased from the National Center for Cell Sciences (NCCS) Pune. Dulbecco's modified Eagle medium (DMEM) supplemented with 1% penicillin-streptomycin (Gibco), 10% (v/v) heat-inactivated FBS and 10% fetal bovine serum (Gibco) was used to culture the procured cancer cell lines. Further, this media was maintained at 37 °C in a humidity controlled incubator containing 5% carbon dioxide.

In vitro cytotoxicity (MTT assay) : *In vitro* anticancer activity (cytotoxicity) was investigated by means of MTT assay. The cancer cell lines were spread in 96-well cell culture plate (5 × 10³ cells /well) and were allowed to stand in a humidified atmosphere (5% CO₂) overnight at 37 °C. Various concentrations (10, 20, 30, 40 and 50 μM) of synthesized compounds were added after 24 h of incubation. Further cells were incubated for another 24 h. The phosphate buffer solution was utilized for washing the cells in well, subsequently plate was incubated at 37 °C after adding 20 μL MTT staining solution (0.005 % w/w in phosphate buffer) to each well. For dissolving the formazan crystals, in each well 100 μL of dimethyl sulfoxide (DMSO) was added, and the absorbance of the resulting solution was observed at 570 nm using micro titer plate reader. The IC₅₀ was computed by employing graph Pad Prism Version5.

Tyrosine kinase inhibitory activity : The kinase activity was evaluated with enzyme-linked immunosorbent assay (ELISA). The assays were performed in 96-well micro titer plates that had been coated overnight with 2.0 μg of a polyGlu-Tyr peptide (4:1) (Sigma P-0275) in 0.1 mL of PBS per well. The purified kinases were diluted in kinase assay buffer (100 Mm Hepes pH 7.5, 100 mM NaCl, and 0.1 mM sodium orthovanadate) and added to all test wells at 5 ng of GST fusion protein per 0.05 mL volume buffer. Test compounds were diluted in DMSO and added to test wells (0.025 mL/well). The kinase reaction was initiated by the addition of 0.025 mL of 40 μM ATP/40 mM MnCl₂, and plates were shaken for 10 min before stopping the reactions with the addition of 0.025 mL of 0.5 M EDTA. The final ATP concentration was 10 μM,

which is twice the experimentally determined K_m value for ATP. Negative control wells received $MnCl_2$ alone without ATP. The plates were washed three times with 10 mM Tris pH 7.4, 150 mM NaCl, and 0.05% Tween-20 (TBST). Rabbit polyclonal anti-phosphotyrosine antiserum was added to the wells at a 1:10000 dilution in TBST for 1 h. The plates were then washed three times with TBST. Goat anti-rabbit antiserum conjugated with horseradish peroxidase was then added to all wells (Biosource Cat. No. ALI0404; 1:10000 dilution in TBST) for 1 h. The plates were washed three times with TBST, and the peroxidase reaction was detected with the addition of 2, 2' -azinobis (3- ethylbenzthiazoline-6-sulfonic acid) (ABTS) (Sigma A1888). The Plate was read using a multiwell spectrophotometer at 492 nm. The inhibitory rate (%) was calculated with the formula: $[1 - \text{treated groups}/\text{control groups}] \times 100\%$. IC_{50} values were calculated from the inhibitory curves.

Molecular Docking : Epidermal growth factor receptor (EGFR), (PDB: 2GS6) was obtained from the Protein Data Bank (PDB). Molecular docking was performed with the help of MDS (version 15.2). All the synthesized compounds (**MB1-MB19**) were docked using an irreversible inhibitor of EGFR protein as a covalent docking module. First of all the protein was prepared and refined by excluding water molecules from the complex protein structure followed by the addition of hydrogen atoms as well as deleting the cofactor and ligand. The structure of compounds (2D) was drawn with the help of ChemBioDraw Ultra 12.0, and then these structures were subjected to conversion from 2D to 3D followed by refinement and energy minimization (Merck Molecular Force Field) method. The analytical gradient and lowest energy conformations were selected for further studies.

Statistical analysis

The statistical analysis was run using Sigma Plot (version 11.1) by applying one-way analysis of variance (ANOVA), followed by Tukey's multiple comparison tests. Statistical significance was considered at $p < 0.05$.

RESULTS AND DISCUSSION

Chemistry : The pathway for the synthesis of compounds MB-1-MB-19 has been depicted in Scheme 1. The key intermediate 3-((3-methyl-1, 4-dioxo-1, 4-dihydronaphthalen-2-yl) thio) propanoic acid (**3**) was synthesized according to the reported method³³ summarized in the proceeding text. Compounds MB-1-MB-19 were synthesized by condensation of naphthalene-1,4-dione (**1**) with 4-mercapto propanoic acid (**2**) to form compound 3-((3-methyl-1,4-dioxo-1,4-dihydronaphthalen-2-yl)thio)propanoic acid (**3**) which in turn were converted to final compound MB-1-MB-19 by reaction with thionyl chloride and substituted piperazines.

The structures of the synthesized compounds were established using spectral techniques (FT-IR, ¹HNMR and ¹³CNMR). The presence of the carboxylic acid functionality in all the synthesized compounds was confirmed by the disappearance of -OH band at 3358.31 cm^{-1} in the IR spectra and appearance of a characteristic peak of the carbonyl group between 1673 cm^{-1} to 1739 cm^{-1} . In the proton NMR spectra of all the compounds, the disappearance of characteristic broad singlet of the hydroxyl proton at δ 9.47 ppm. The aromatic protons resonated in the range of δ 8.25 to 6.18 ppm in the proton NMR spectra of all the compounds. Compound MB-6 showed singlet at δ 2.20 of the methyl group. Two singlet at the frequency of δ 2.72 and 2.38 ppm for two methyl groups in compound (MB-17). There was a characteristic peak of the methylene group in all the compounds at a frequency of δ 2.00 ppm. In the ¹³CNMR spectrum, carbonyl carbon of naphthalene ring was observed at δ 186.0 ppm and 175.0 ppm, whereas carbon of aliphatic carbonyl of the target compounds appeared at δ 170.0 ppm. Signals of ¹³CNMR spectrum further confirmed the synthesis of the targeted compounds as all the aromatic carbons appeared in the range of δ 155.00-102.00 ppm however the methylene carbon peak emerged at δ 16.19-8.59 ppm. The physicochemical data of the synthesized compounds and the spectral data have been listed in Table 1 and Table 6.

Pharmacological evaluation

In vitro cytotoxic activity

All the synthesized compounds **MB-1-MB-19** were evaluated *in vitro* for their anticancer activity. The cytotoxic effects of all newly synthesized compounds (1,4-naphthoquinone derivatives) were subjected to assess *in vitro* anticancer potency using various cancer cell lines, such as MCF-7 (breast carcinoma), HepG2 (liver carcinoma) and cervical carcinoma (HeLa) using imatinib as a standard. *In vitro* cytotoxicity results suggested that the cytotoxicity were dose-dependent. Almost all the compounds showed anticancer activity in a dose-dependent manner. Cell viability decreased and cytotoxicity increased with increase in the concentration of the compound.

The synthesized compounds exposed that the cytotoxicity was found to be poor to strong comparatively to the standard drug (Table 2). The compounds (**MB-4, MB-9, MB-13, and MB-18**) exhibited intense anticancer activity on HeLa cell line and all of them are having electron withdrawing group of F, Cl, Br. Especially, **MB-9, MB-18** exhibited stronger activity than Imatinib (standard). The electron withdrawing chlorine group and the methoxy substituents on the benzene ring attached to the piperazine ring increased the cytotoxicity (MB-9, IC_{50} 13.45 ± 0.48), (MB-18, IC_{50} 19.29 ± 0.22) on HeLa cells. Six compounds (MB-9, MB-10, MB-12, MB-17, MB-18, and MB-19) against MCF-7 cell line demonstrated promising antineoplastic action. The trifluoro-phenyl substituent (MB-12, IC_{50} 23.94 ± 0.83) should give better cytotoxicity than the para chloro phenyl substitution (MB-9, IC_{50} 15.63 ± 0.74) on the piperazine ring but it revealed strong electronegative group substitution that hinder the binding of the ligand with the active site. The compounds (MB-2, MB-6, MB-9, MB-12, MB-15, MB-17 and MB-18) exposed extensive cytotoxic with HepG2 cell lines. Moreover, the remaining synthesized compounds devoid of any critical cytotoxic action against tested cancer cell lines. Thus, the compound **MB-9 and MB-18** revealed as a most potent anticancer agent against MCF-7, HepG2 and HeLa cell lines when compared to standard drug imatinib (Figure 3).

In-vitro enzyme assay (EGFR kinases inhibition)

: After *in-vitro* cytotoxicity screening of synthesized compounds against cancer cell lines, compounds were subjected for evaluation of EGFR kinases inhibition with the help of self-made kit of tyrosine kinase using Imatinib as standard drug. Evidently, the majority of compounds indicated pronounced tyrosine kinase inhibition. Table 3 summarized the inhibition IC_{50} values of all the synthesized compounds. Compounds MB-2, MB-6, MB-7 and MB-(10-13) possess more comparable inhibitory effect against EGFR. While compound MB-9 (IC_{50} = 1.80 ± 0.06 μM) and MB-18 (IC_{50} = 2.03 ± 0.07 μM) are the most potent inhibitor approximately one to two times more than standard drug imatinib (IC_{50} = 3.54 ± 0.11 μM) (Figure 4).

Computational studies

Molecular docking : Molecular docking has been performed to determine the binding affinity of the compound. In the present manuscript, docking was done on the epidermal growth factor receptor (EGFR). Docking studies suggested the superior protein-ligand binding of synthesized compounds with key amino acids on the active site. Methionine residues (MET 793), cysteine (CYS797) and tyrosine (TRY253) are the key residues of the protein-ligand binding. These amino acid residues play a key role in the formation of a bridge within EGFR. Moreover, docking examinations of MB-1-MB-19 on EGFR demonstrated a considerable binding communication of the synthesized compound on the peripheral site and catalytic site of the protein. All the compounds have been found to possess a good binding affinity with the EGFR and afforded high dock score from -54.10 to -75.25 (Table 3). Amongst all the docked ligands, compound MB- has shown a highest binding affinity for EGFR with the highest dock score (-75.25). Table 4 described molecular docking score of synthesized compounds. The 2D/3D and binding pocket representation of the ligand-receptor interactions of the most active compounds MB-9 and MB-18 displayed in Figure 2a-c and Figure 3a-c. Docked pose of the fitted ligands was visualized extending deep into the active site

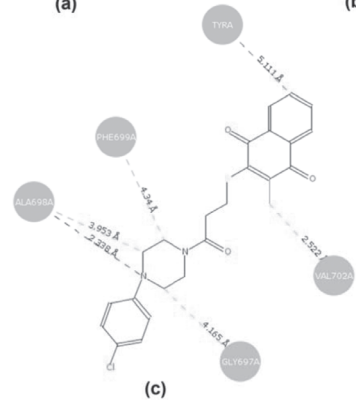
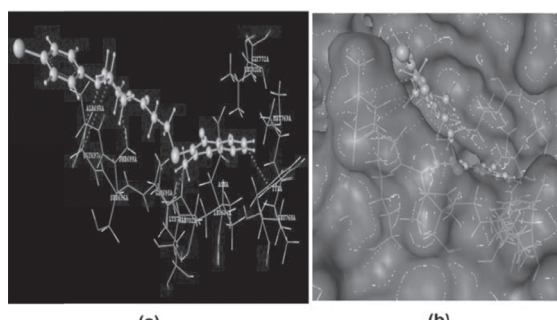
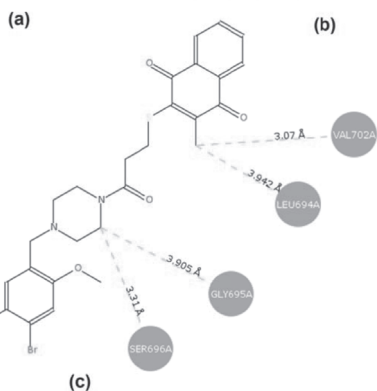
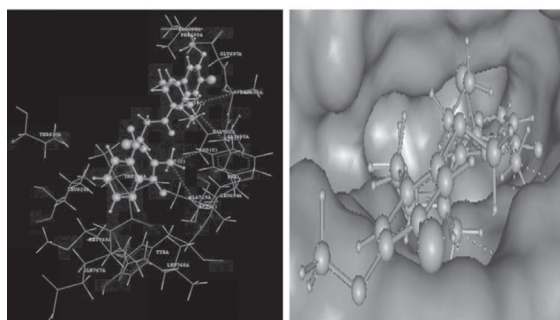


Fig. 2. (a-c) (2a) 3D Hydrogen Bonding Interaction of MB-18 representation showing the binding orientation of the compounds MB-18 into the active side of 2GS6, (2b) 3D Surface and Hydrogen Bonding Interaction of MB-18, (2c) 2D representation showing the binding orientation of the compounds MB-18 into the active site of 2GS6

-----: Hydrophobic Interactions
 -----: Hydrogen Bonding

Fig. 3. (a-c) (3a) 3D Hydrogen Bonding Interaction of MB-9 representation showing the binding orientation of the compounds MB-9 into the active side of 2GS6, (3b) 3D Surface and Hydrogen Bonding Interaction of MB-9, (3c) 2D representation showing the binding orientation of the compounds MB-9 into the active site of 2GS6

-----: Hydrophobic Interactions
 -----: Hydrogen Bonding

pocket and showed several interactions such as Vander Waal's, hydrophobic contacts, hydrogen bonds and π - π stacking interactions with the key residues of the catalytic site as well as the peripheral site. The high dock score of compound MB-9 attributed to its hydrogen bond interactions with amino acid residue ALA698A, to the piperazine nitrogen along with distance 2.338Å. Furthermore, it forms hydrophobic interaction with ALA698A, GLY697A, PHE699A and VAL702A with distanced 3.953 Å, 4.165 Å, 4.34 Å and 2.522 Å.

As well it formed aromatic interaction with tyrosine with 5.111 Å distanced. Compound MB-18 formed hydrophobic interactions with the amino acid residue of VAL702A, LEU694A, GLY695A, and SER696A with distance 3.07 Å, 3.942 Å, 3.905 Å, 3.31 Å respectively. Therefore, compounds 1,4-naphthoquinone derivatives formed considerable interactions with essential amino acid residues and revealed the association of the docking studies with anticancer activity of the compounds.

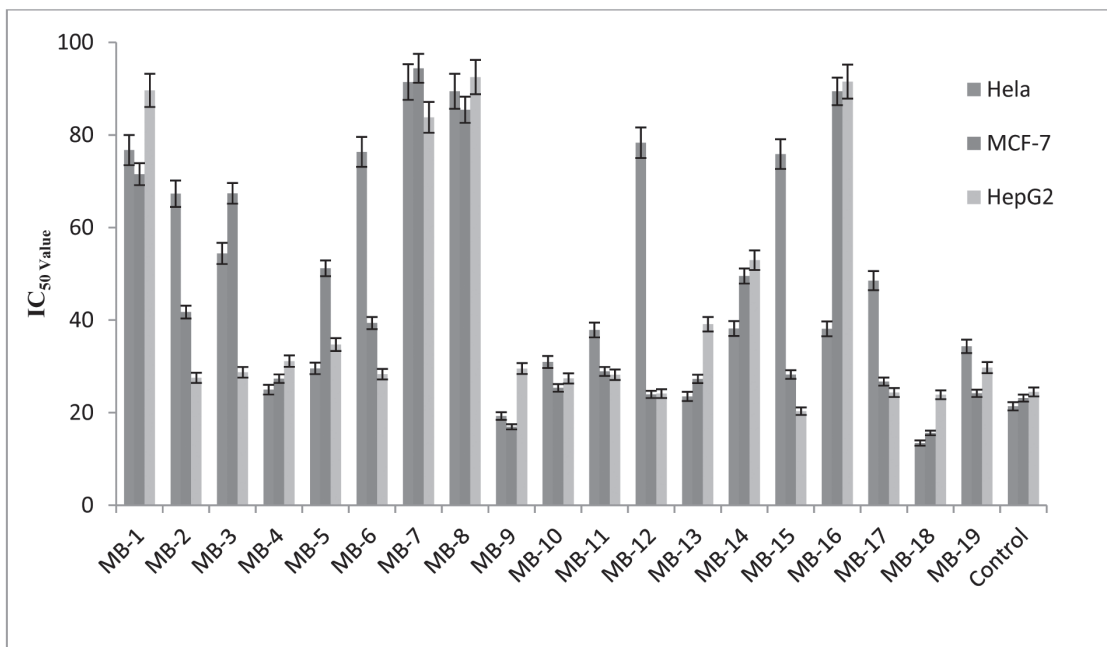


Fig.4: *In-vitro* cell viability of compounds. The differences in the percentage of cell viability of compounds MB-9 and MB-18, are statistically significant $P < 0.05$ ($n=3$).

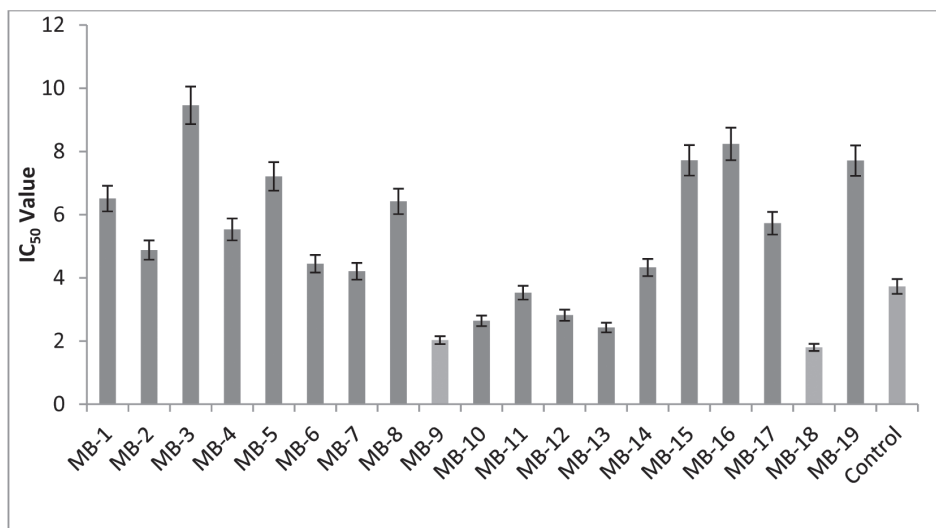


Fig.5: Enzyme inhibitory activity of protein tyrosine kinase of compounds. The percentage of inhibition of compound MB-9 and MB-18 are statistically significant $P < 0.05$ ($n=3$).

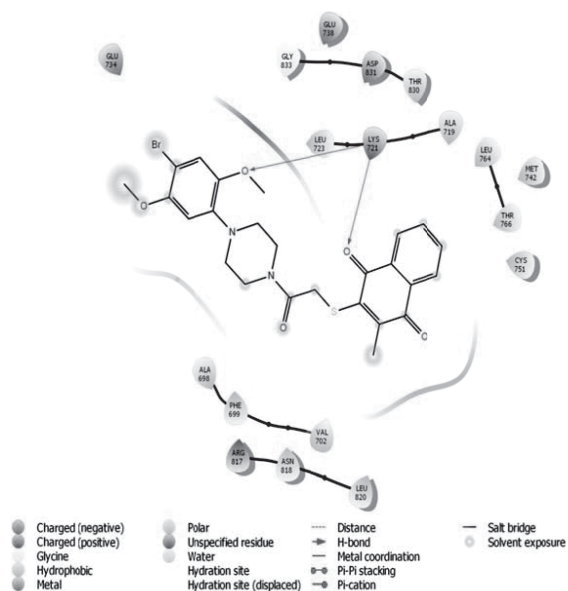


Fig. 6: 2D representation showing the binding orientation of the compounds MB-18 (i) into the active site of 2GS6.

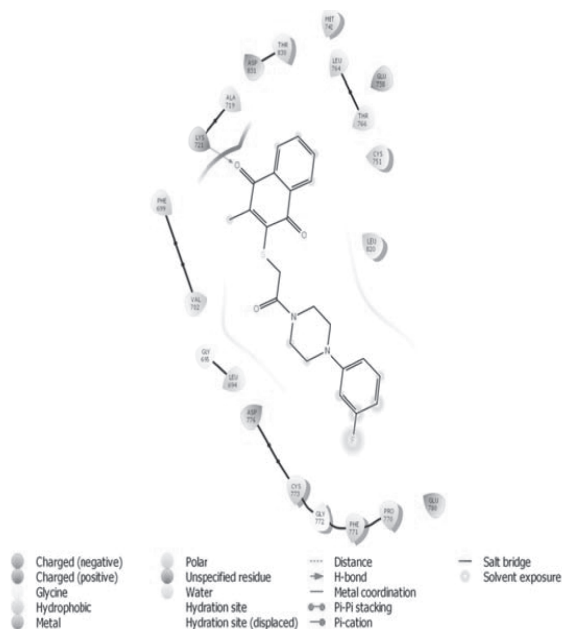


Fig. 7: 2D representation showing the binding orientation of the compounds MB-13 (i) into the active site of 2GS6.

Drug likeliness

Compound MB-9 was evaluated for drug – likeliness characteristics using the QikProp module of Schrodinger software and the result was found to be comparable with standard drug imatinib (Table-5). The predicted QPlogKhsa values affirm their strong binding with plasma protein. The outcome of Lipinski’s rule of five (molwt < 500, QPlogPo/w < 5, donor HB - 0 to 6.0, accept or HB- 2.0 to 20) along with the other predicted parameters (SASA 300 to 1000, QPlogBB -3.0 to 1.2, QPlogPo/w -2.0 to 6.5) reflected that compound MB-9 elicited “drug like” characteristics.

CONCLUSION

In conclusion, we have successfully synthesized a series of piperazine substituted 1,4-naphthoquinone derivatives. The compounds were evaluated for their cytotoxic effect using MCF-7, HeLa, and HepG-2 cancer cell lines. Almost all the synthesized derivatives possess considerable anticancer activity. Compounds MB-9 and MB-18

revealed the utmost powerful anticancer potencies. Furthermore, on the enzyme inhibition assay compounds MB-9 and MB-18 showed the good promising inhibitory activity with $IC_{50} = 1.80 \pm 0.06 \mu\text{M}$ and $IC_{50} = 2.03 \pm 0.07 \mu\text{M}$. Molecular docking study revealed the strong binding capability with the active sites of enzymes. Therefore, these findings suggested that the rational design of piperazine substituted 1,4-naphthoquinone as a hopeful potential anticancer agent for auxiliary expansion in cancer therapy.

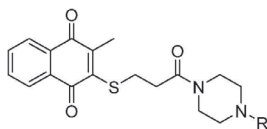
ACKNOWLEDGEMENT

The authors gratefully acknowledge IIT-BHU for the funding of this work. The authors also acknowledge to Panjab University, Chandigarh and NIPER Mohali, Panjab to provide spectral and cell line facilities.

Reference

1. Peerzada, M.N., Khan, P., Ahmad, K., Hassan, M.I. and Azam, A. (2018).

TABLE 1: Chemical structure of various piperazine substituted 1, 4-Naphthoquinone derivatives



Compounds	R	Mol. Weight	Melting point (°C)	Appearance	Log P	M/z	% Yield	Solubility
MB-1	H	344.12	146-148	White	-0.6	344.86	58	Ethanol
MB-2		420.15	200-202	Brown	2.39	419.65	63	Chloroform
MB-3		510.20	195-197	Yellow	3.76	510.55	64	Chloroform
MB-4		434.17	161-163	Brownish	2.05	434.31	71	Methanol
MB-5		421.15	173-175	Yellow	1.77	421.97	61	Chloroform
MB-6		434.17	209-211	White	2.88	433.12	69	Chloroform
MB-7		454.11	221-223	Creamy	2.95	453.80	68	Ethanol
MB-8		488.07	241-243	Yellow	3.15	488.53	73	Ethanol
MB-9		454.11	197-199	Brownish	2.95	454.81	66	Methanol
MB-10		438.14	171-173	White	2.55	437.94	70	Chloroform
MB-11		438.14	198-200	Yellow	2.55	438.75	68	Methanol
MB-12		488.14	218-220	Brownish	3.31	488.06	69	Methanol
MB-13		438.14	161-163	White	2.55	438.32	66	Ethanol
MB-14		450.16	148-150	White	2.27	450.41	69	Chloroform

1, 4-naphthoquinone derivatives as epidermal growth factor receptor inhibitors

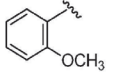
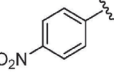
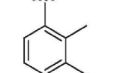
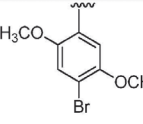
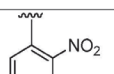
MB-15		450.16	161-163	Brownish	2.27	450.27	65	Ethyl acetate
MB-16		465.14	241-243	White	2.53	465.60	63	Methanol
MB-17		448.18	231-233	White	3.37	447.25	70	Methanol
MB-18		572.10	194-196	Yellowish	2.63	572.42	68	Chloroform
MB-19		465.14	263-265	Creamy	2.53	465.70	67	Chloroform

Table 2: IC₅₀ of the tested compounds against HeLa, MCF-7 and HepG-2 cell lines.

Compounds	HeLa cell IC ₅₀ (μM) \pm SEM	MCF-7 cell IC ₅₀ (μM) \pm SEM	HepG2 cell IC ₅₀ (μM) \pm SEM
MB-1	76.73 \pm 0.32	71.53 \pm 0.26	89.63 \pm 0.87
MB-2	67.32 \pm 0.19	41.74 \pm 0.98	27.53 \pm 1.32
MB-3	54.42 \pm 0.64	67.40 \pm 1.03	28.73 \pm 0.88
MB-4	24.98 \pm 0.62	27.34 \pm 0.23	31.13 \pm 0.39
MB-5	29.56 \pm 0.67	51.21 \pm 0.41	34.71 \pm 1.30
MB-6	76.35 \pm .98	39.37 \pm 0.50	28.32 \pm 0.85
MB-7	91.44 \pm 0.45	94.39 \pm 0.61	83.80 \pm 0.63
MB-8	89.43 \pm 0.67	85.43 \pm 0.32	92.50 \pm 1.41
MB-9	13.45 \pm 0.48	15.63 \pm 0.47	23.87 \pm 0.59
MB-10	30.96 \pm 0.41	25.35 \pm 0.22	27.41 \pm 0.55
MB-11	37.87 \pm 0.80	28.91 \pm 0.94	28.20 \pm 1.02
MB-12	78.33 \pm 0.75	23.94 \pm 0.38	24.12 \pm 0.74
MB-13	23.52 \pm 0.61	27.30 \pm 0.28	39.12 \pm 0.37
MB-14	38.19 \pm 0.52	49.53 \pm 1.31	52.95 \pm 0.61
MB-15	75.86 \pm 0.41	28.24 \pm 0.82	20.32 \pm 0.73
MB-16	38.13 \pm 0.29	89.43 \pm 1.03	91.53 \pm 0.75
MB-17	48.53 \pm 0.67	26.72 \pm 0.81	24.35 \pm 0.74
MB-18	19.29 \pm 0.22	16.96 \pm 0.21	19.53 \pm 0.39
MB-19	34.33 \pm 0.81	24.19 \pm 0.82	29.74 \pm 0.94
Imatinib	21.38 \pm 0.76	23.16 \pm 0.30	24.48 \pm 0.71

IC₅₀: Compounds concentration required to inhibit the cell viability, SEM = standard error mean; each value is the mean of three values.

Table 3 : Enzyme inhibitory activity of compounds against protein tyrosine kinase enzyme.

Compounds	Tyrosine kinase inhibitory activity IC ₅₀ (µM) ± SEM
MB-1	6.51 ± 0.48
MB-2	4.88 ± 0.45
MB-3	9.46 ± 0.26
MB-4	5.53 ± 0.22
MB-5	7.21 ± 0.21
MB-6	4.45 ± 0.23
MB-7	4.21 ± 0.20
MB-8	6.42 ± 0.15
MB-9	1.80 ± 0.06
MB-10	3.64 ± 0.18
MB-11	3.73 ± 0.10
MB-12	3.82 ± 0.14
MB-13	2.43 ± 0.11
MB-14	4.33 ± 0.14
MB-15	7.72 ± 0.13
MB-16	8.24 ± 0.17
MB-17	5.73 ± 0.11
MB-18	2.03 ± 0.07
MB-19	7.71 ± 0.38
Imatinib	3.54 ± 0.11

Table 4 : Docking scores of compounds (MB-1 to MB-19).

Compound No	D-Score
MB-1	- 57.26
MB-2	- 63.22
MB-3	- 54.10
MB-4	- 61.74
MB-5	- 67.07
MB-6	- 61.39
MB-7	- 64.67
MB-8	- 61.69
MB-9	- 70.47
MB-10	- 68.72
MB-11	- 57.42
MB-12	- 58.45
MB-13	- 69.19
MB-14	- 57.50
MB-15	- 56.55
MB-16	- 61.09
MB-17	- 60.25
MB-18	- 75.25
MB-19	- 66.57
Imatinib	- 62.92

IC₅₀: Compound concentration required to inhibit the enzyme activity by 50%, SEM = Standard error mean; each value is the mean of three values.

Synthesis, characterization and biological evaluation of tertiary sulfonamide derivatives of pyridyl-indole based heteroaryl chalcone as potential carbonic anhydrase IX inhibitors and anticancer agents. *Eur J Med Chem*, 155: 13-23.

2. Guichard, N., Guillaume, D., Bonnabry, P. and Fleury-Souverain, S. (2017). Antineoplastic drugs and their analysis: a state of the art review. *Analyst*, 142 (13): 2273-321.

3. Rebucci, M. and Michiels, C. (2013). Molecular aspects of cancer cell resistance to chemotherapy. *Biochem Pharmacol*, 85 (9): 1219-26.

4. Frankish, H. (2003). 15 million new cancer cases per year by 2020, says WHO. *The Lancet*, 361(9365): 1278.

5. Belpomme, D., Irigaray, P., Sasco, A., Newby, J., Howard, V., Clapp, R. and Hardell, L. (2007). The growing incidence of cancer: role of lifestyle and screening detection. *International journal of oncology*, 30 (5): 1037-1049.

6. Gschwind, A., Fischer, O. M. and Ullrich, A. (2004). The discovery of receptor tyrosine

TABLE-5: QikProp analysis of compound MB-9

Parameters	Imatinib	MB-9
MolWt ^a	493.61	454.97
Donor HB ^b	2	0
AcceptorHB ^c	10.5	8.5
SASA ^d	905.42	735.75
QPlogBB ^e	-0.451	-0.614
QPlogPo/w ^f	3.54	3.18
QPPMDCK ^g	25.26	1325.9
QPlogKhsa ^h	0.535	-0.261

^a MolWt - molecular weight of the molecule (130-725).

^b Donor HB - number of hydrogen bonds (0.0 - 6.0).

^c AcceptorHB- number of hydrogen bonds (2.0 - 20.0).

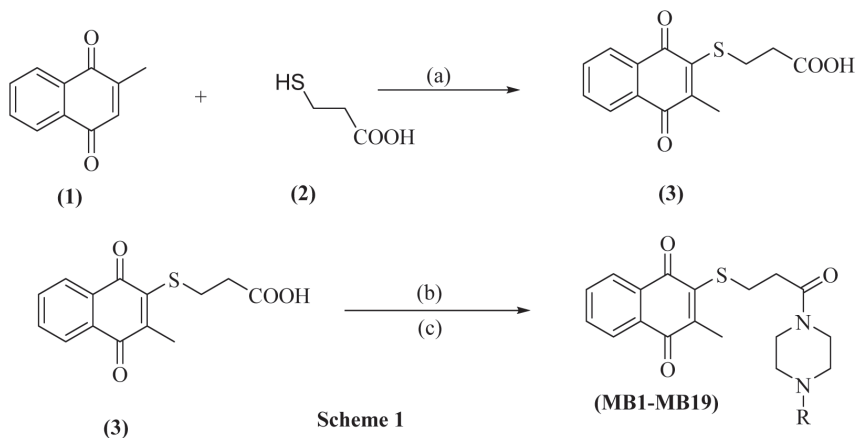
^d SASA- Total solvent accessible surface area in square angstroms using a probe with 1.4Å radius (300-1000).

^e QPlogBB - predicted brain/blood partition coefficient (-3.0 - 1.2).

^f QPlogPo/w - this gives the predicted octanol/water partition coefficient (-2.0 - 6.5).

^g QPPMDCK- predicted MDCK cell permeability in nm/s using the affix scale (< 25 is considered poor and > 500 is considered excellent).

^h QPlogKhsa- prediction of binding to human serum albumin (-1.5 – 1.5).



Scheme 1-Synthesis of target compounds.

Chemical reagents and conditions: (a) absolute ethanol, reflux, 3-5 h. (b) dry DCM, thionyl chloride, r.t, 3-5 h. (c) dry DCM, substituted piperazines, stirring, 9-10 h.

TABLE 6: Spectral data and elemental analysis compounds.

Compounds	IR (KBr) ν_{\max} (cm ⁻¹)	¹ H NMR (CDCl ₃ , 400 MHz) (δ)	¹³ C NMR (CDCl ₃ , 100 MHz) (δ)	Anal. Calcd.
MB-1	3320.12 (N-H stretch); 3068.08 (aromatic C-H stretch); 2927.11 (aliphatic C-H stretch); 1735.77 (C=O stretch); 1689.24 (C=C stretch); 1624.70, 1505.83 (C=C ring stretch); 1415.08 (C-N stretch); 1268.44, 1215.39 (C-O stretch); 734.38 cm ⁻¹ (C-H bend)	8.16 (m, 2H, ArH), 7.72 (m, 2H, ArH), 3.56 (t, 2H, <i>J</i> = 4.12 Hz, -N-CH ₂), 3.33 (m, 4H, -N-CH ₂), -S-CH ₂), 2.88 (m, 6H, NH(CH ₂) ₂), -CH ₂ CO), 2.77 (s, 3H, CH ₃), 1.27 (s, 1H, -NH)	185.73 (C=O), 178.54 (C=O), 171.15 (C=O), 139.11 (ArC _q), 137.48 (2 × ArC _q), 133.84 (ArC _q), 132.95 (2 × ArC _q), 130.94 (ArC), 128.10 (ArC), 46.84 (2 × CH ₂ piperazinyl), 44.92 (2 × CH ₂ piperazinyl), 35.73 (S-CH ₂), 29.56 (CH ₂ C=O), 12.40 (CH ₃)	C ₁₈ H ₂₀ N ₂ O ₃ S: 62.58; H, 5.65; N, 8.21. Found: C, 62.45; H, 5.95; N, 8.71
MB-2	3068.08 (aromatic C-H stretch); 2916.47 (aliphatic C-H stretch); 1738.78 (C=O stretch); 1690.04 (C=O stretch); 1623.42 (C=C ring stretch); 1428.3 (C-N stretch); 1227.74 (C-O stretch); 750.23 cm ⁻¹ (C-H bend)	8.25 (dd, 1H, <i>J_m</i> = 1.44 Hz, <i>J_o</i> = 5.60 Hz, ArH), 8.17 (dd, 1H, <i>J_m</i> = 1.40 Hz, <i>J_o</i> = 5.80 Hz, ArH), 7.74 (m, 2H, ArH), 7.07 (t, 2H, <i>J</i> = 5.88 Hz, ArH), 6.62 (m, 3H, ArH), 3.79 (m, 4H, -N(CH ₂) ₂), 3.66 (m, 2H, N-CH ₂), 3.46 (m, 2H, N-CH ₂), 3.13 (t, 2H, <i>J</i> = 4.36 Hz, -S-CH ₂), 3.00 (t, 2H, <i>J</i> = 4.40 Hz, -CH ₂ CO), 2.76 (s, 3H, CH ₃)	185.73 (C=O), 178.54 (C=O), 171.40 (C=O), 150.96 (ArC _q), 139.68 (ArC _q), 137.51 (2 × ArC), 133.84 (ArC), 132.92 (2 × ArC _q), 130.94 (ArC _q), 129.35 (2 × ArC), 128.15 (ArC), 120.31 (ArC), 116.77 (2 × ArC), 49.17 (2 × CH ₂ piperazinyl), 44.84 (2 × CH ₂ piperazinyl), 35.73 (S-CH ₂), 29.56 (CH ₂ C=O), 15.12 (CH ₃)	C ₂₃ H ₂₄ N ₂ O ₃ S: 68.32; H, 5.46; N, 6.39. Found: C, 68.42; H, 5.36; N, 6.34
MB-3	3384.66 (aromatic C-H stretch); 2943.91 (aliphatic C-H stretch); 1724.39 (C=O stretch); 1695.18 (C=O stretch); 1629.13, 1585.27 (C=C ring stretch); 1412.46 (C-N stretch); 1218.84 (C-O stretch); 733.20 cm ⁻¹ (C-H bend)	8.04 (dd, 1H, <i>J_m</i> = 1.40 Hz, <i>J_o</i> = 5.80 Hz, ArH), 8.00 (dd, 1H, <i>J_m</i> = 1.40 Hz, <i>J_o</i> = 5.80 Hz, ArH), 7.69 (m, 2H, ArH), 7.27 (m, 10H, ArH), 3.52 (t, 2H, <i>J</i> = 4.08 Hz, -N-CH ₂), 3.42 (t, 2H, <i>J</i> = 4.08 Hz, -N-CH ₂), 3.34 (t, 2H, <i>J</i> = 4.16, -S-CH ₂), 2.96 (t, 2H, <i>J</i> = 4.08, -N-CH ₂), 2.90 (t, 2H, <i>J</i> = 4.08, -N-CH ₂), 2.64 (m, 5H, -CH ₂ CO; CH ₃)	184.55 (C=O), 179.34 (C=O), 171.80 (C=O), 140.56 (2 × ArC _q), 139.46 (ArC _q), 137.51 (ArC), 133.84 (ArC _q), 132.40 (2 × ArC), 130.94 (2 × ArC _q), 129.28 (4 × ArC), 128.85 (4 × ArC), 128.39 (ArC), 126.73 (4 × ArC), 77.58 (CH), 50.80 (2 × CH ₂ piperazinyl), 44.55 (2 × CH ₂ piperazinyl), 35.73 (S-CH ₂), 29.56 (CH ₂ C=O), 13.12 (CH ₃)	C ₃₁ H ₃₀ N ₂ O ₃ S: 72.37; H, 5.10; N, 5.21. Found: C, 72.56; H, 5.21; N, 5.27
MB-4	3035.42 (aromatic C-H stretch); 2925.02 (aliphatic C-H stretch); 1735.81 (C=O stretch); 1692.80 (C=O stretch); 1627.99 (C=C ring stretch); 1467.80 (C-N stretch); 1233.26 (C-O stretch); 736.29 cm ⁻¹	8.18 (dd, 1H, <i>J_m</i> = 1.41 Hz, <i>J_o</i> = 5.80 Hz, ArH), 8.05 (dd, 1H, <i>J_m</i> = 1.40 Hz, <i>J_o</i> = 5.82 Hz, ArH), 7.75 (m, 2H, ArH), 7.25 (m, 5H, ArH), 3.62 (m, 4H, -NH(CH ₂) ₂), 3.44 (t, 2H, <i>J</i> = 6.66 Hz, -N-CH ₂ -C), 3.35 (t, 2H, <i>J</i> = 4.24 Hz, -N-CH ₂), 2.88 (m, 4H, -S-CH ₂), -CH ₂ CO), 2.66 (t, 2H, <i>J</i> = 4.24	186.55 (C=O), 178.54 (C=O), 177.95 (C=O), 139.46 (ArC _q), 138.39 (ArC _q), 137.17 (ArC), 133.84 (ArC), 132.38 (2 × ArC), 130.33 (2 × ArC _q), 128.93 (2 × ArC), 127.90 (2 × ArC), 127.90 (ArC), 126.55 (ArC), 63.66 (ArC _q), 51.15 (2 ×	C ₂₅ H ₂₆ N ₂ O ₃ S: 69.56; H, 6.21; N, 6.94. Found: C, 69.34; H, 6.32; N, 6.51

			Hz, N-CH ₂ , 2.48 (s, 3H, CH ₃)	CH ₂ piperazinyl) 44.25 (2 × CH ₂ piperazinyl), 35.73 (S-CH ₂), 29.82 (CH ₂ C=O), 14.25 (CH ₃)	C ₂₃ H ₂₃ N ₃ O ₃ S: 65.92; H, 5.53; N, 9.23. Found: C, 65.50; H, 5.82; N, 9.14
MB-5	3039.73 (aromatic C-H stretch); 2923.04 (aliphatic C-H stretch); 1737.11 (C=O stretch); 1690.13 (C=O stretch); 1627.77, 1584.63 (C=C ring stretch); 1434.40 (C-N stretch), 1271.80 (C-O stretch); 734.04 cm ⁻¹ (C-H bend)	8.13 (dd, 1H, J _m = 1.16 Hz, J _o = 6.00 Hz ArFf), 8.03 (m, 2H, ArFf), 7.68 (m, 2H, ArFf), 7.51 (m, 1H, ArFf), 6.67 (m, 2H, ArFf), 3.74 (m, 2H, -SCH ₂), 3.64 (m, 4H, -N(CH ₂) ₂), 3.51 (m, 2H, -CH ₂ CO), 3.30 (t, 2H, J = 6.48 Hz, -N-CH ₂), 2.90 (t, 2H, J = 6.48, -N-CH ₂), 2.37 (s, 3H, CH ₃)	184.84 (C=O), 179.46 (C=O), 170.94 (C=O), 158.90 (ArC _q), 148.87 (CH ₂ pyridinyl), 140.12 (CH ₂ pyridinyl), 139.17 (CH ₂ pyridinyl), 137.21 (ArC), 133.02 (ArC _q), 132.17 (2 × ArC _q), 128.91 (2 × ArC), 127.62 (ArC), 113.61 (CH ₂ pyridinyl), 107.70 (CH ₂ pyridinyl), 47.24 (2 × CH ₂ piperazinyl) 44.32 (2 × CH ₂ piperazinyl), 35.15 (S-CH ₂), 29.95 (CH ₂ C=O), 13.84 (CH ₃)		
MB-6	3030.29 (aromatic C-H stretch); 2918.25 (aliphatic C-H stretch); 1732.48 (C=O stretch); 1694.49 (C=O stretch); 1625.11 (C=C ring stretch); 1464.76 (C-N stretch); 1272.33 (C-O stretch); 776.76 cm ⁻¹ (C-H bend)	8.22 (dd, 1H, J _m = 1.36 Hz, J _o = 5.84 Hz ArFf), 8.11 (dd, 1H, J _m = 1.36 Hz, J _o = 5.84 Hz ArFf), 7.66 (m, 2H, ArFf), 6.91 (m, 2H, ArFf), 6.55 (m, 2H, ArFf), 3.75 (dt, 4H, J _m = 3.96 Hz, J _o = 16.92 Hz -N(CH ₂) ₂), 3.53 (t, 2H, J = 3.96 Hz -S-CH ₂), 3.40 (t, 2H, J = 3.92 Hz, -CH ₂ CO), 3.23 (t, 2H, J = 4.48, -N-CH ₂), 2.95 (t, 2H, J = 4.48 Hz, -N-CH ₂), 2.72 (s, 3H, CH ₃), 2.20 (s, 3H, CH ₃)	188.15 (C=O), 174.84 (C=O), 173.84 (C=O), 150.93 (ArC _q), 139.27 (ArC _q), 133.50 (ArC), 132.47 (2 × ArC _q), 130.54 (2 × ArC), 130.06 (ArC _q), 129.40 (ArC _q), 128.30 (ArC), 127.99 (ArC), 127.10 (ArC), 120.99 (ArC), 117.82 (ArC), 50.27 (2 × CH ₂ piperazinyl), 44.14 (2 × CH ₂ piperazinyl) 35.73 (S-CH ₂), 29.36 (CH ₂ C=O), 17.23 (CH ₃), 13.73 (CH ₃)	C ₂₅ H ₂₆ N ₂ O ₃ S: 69.20; H, 6.03; N, 7.07. Found: C, 69.32; H, 6.18; N, 6.98	
MB-7	3057.01 (aromatic C-H stretch); 2916.26 (aliphatic C-H stretch); 1738.63 (C=O stretch); 1690.14 (C=O stretch); 1625.26 (C=C ring stretch); 1485.74 (C-N stretch), 1226.67 (C-O stretch); 747.73 (C-H bend); 675.74 cm ⁻¹ (C-Cl Stretch)	8.08 (m, 2H, ArFf), 7.74 (m, 2H, ArFf), 7.09 (dd, 1H, ArFf), 6.96 (td, 1H, ArFf), 6.61 (m, 2H, ArFf), 3.82 (t, 2H, J = 4.08 Hz, N-CH ₂), 3.68 (t, 2H, J = 4.08 Hz, N-CH ₂), 3.53 (t, 2H, J = 4.08 Hz, -N-CH ₂), 3.44 (m, 4H, -N-CH ₂ ; -SCH ₂), 3.02 (t, 2H, J = 5.12 Hz, -CH ₂ CO), 2.28 (s, 3H, CH ₃)	187.18 (C=O), 175.73 (C=O), 170.79 (C=O), 148.43 (ArC _q), 139.92 (ArC _q), 137.66 (ArC), 133.84 (ArC _q), 132.35 (2 × ArC _q), 131.75 (2 × ArC), 130.51 (ArC), 128.33 (C-Cl), 127.62 (ArC), 127.27 (ArC), 120.56 (ArC), 119.18 (ArC), 50.40 (2 × CH ₂ piperazinyl), 44.27 (2 × CH ₂ piperazinyl), 35.47 (S-CH ₂), 29.01 (CH ₂ C=O), 16.12 (CH ₃)	C ₂₄ H ₂₃ Cl N ₂ O ₃ S: C, 63.32; H, 5.20; N, 6.98. Found: C, 63.42; H, 5.13; N, 6.84	
MB-8	3038.75 (aromatic C-H stretch); 2926.93 (aliphatic C-H stretch); 1738.68 (C=O stretch); 1684.51 (C=O stretch); 1627.31, 1500.84 (C=C ring stretch); 1421.31 (C-N stretch), 1251.13 (C-O stretch);	8.02 (m, 2H, ArFf), 7.66 (m, 2H, ArFf), 6.88 (t, 1H, J = 5.96, ArFf), 6.63 (dd, 1H, ArFf), 6.55 (dd, 1H, ArFf), 3.80 (t, 2H, J = 4.08 Hz, N-CH ₂), 3.74 (t, 2H, J = 4.12 Hz, N-CH ₂), 3.65 (t, 2H, J = 4.08 Hz, -N-CH ₂), 3.41 (m, 4H, -N-CH ₂ ; -SCH ₂), 2.98 (t, 2H, J = 4.32 Hz, -CH ₂ CO), 2.43	185.12 (C=O), 178.94 (C=O), 171.46 (C=O), 149.83 (ArC _q), 139.39 (ArC _q), 137.93 (ArC), 134.73 (ArC _q), 133.95 (C-Cl), 132.09 (2 × ArC _q), 130.73 (2 × ArC), 128.56 (ArC), 128.15 (C-Cl), 127.84 (ArC), 121.12 (ArC), 118.47	C ₂₄ H ₂₂ Cl ₂ N ₂ O ₃ S: C, 58.86; H, 4.32; N, 6.00: Found: C, 58.57; H, 4.40; N, 5.92	

		(s, 3H, CH ₃)		(ArC), 50.22 (2 × CH ₂ piperazinyl), 44.97 (2 × CH ₂ piperazinyl), 35.32 (S-CH ₃), 29.38 (CH ₂ C=O), 12.41(CH ₃)	C ₂₄ H ₂₃ Cl N ₂ O ₃ S: C, 63.76; H, 5.12; N, 6.88. Found: C, 63.52; H, 5.22; N, 6.80
MB-9	808.65 (C-H bend); 708.43 cm ⁻¹ (C-Cl Stretch) 3073.30 (aromatic C-H stretch); 2928.41 (aliphatic C-H stretch); 1728.47 (C=O stretch); 1685.30 (C=O stretch); 1629.75, 1592.24 (C=C ring stretch); 1453.39 (C-N stretch), 1244.41 (C-O stretch); 757.93 (C-H bend); 687.20 cm ⁻¹ (C-Cl Stretch)	8.06 (m, 2H, ArH), 7.71 (m, 2H, ArH), 7.12 (d, 2H, J = 6.00, ArH), 6.61 (d, 2H, J = 5.96, ArH), 3.77 (m, 4H, N(CH ₂) ₂), 3.62 (m, 2H, -SCH ₂), 3.45 (m, 4H, -N(CH ₂) ₂), 2.98 (t, 2H, J = 6.44 Hz, -CH ₂ CO), 2.56 (s, 3H, CH ₃)		186.98 (C=O), 173.84 (C=O), 165.38 (C=O), 150.29 (ArC _q), 139.23 (ArC _q), 137.40 (ArC), 133.84 (ArC _q), 132.58 (2 × ArC _q), 132.58 (2 × ArC _q), 130.44 (ArC), 129.98 (ArC), 128.33 (C-Cl), 127.90 (ArC), 117.28 (2 × ArC), 49.39 (2 × CH ₂ piperazinyl), 44.61 (2 × CH ₂ piperazinyl), 35.65 (S-CH ₃), 29.21 (CH ₂ C=O), 8.25 (CH ₃)	
MB-10	3053.48 (aromatic C-H stretch); 2950.20 (aliphatic C-H stretch); 1740.99 (C=O stretch); 1680.05 (C=O stretch); 1621.85, 1584.62 (C=C ring stretch); 1463.60 (C-N stretch), 1217.26 (C-O stretch); 1120.82 (C-F Stretch); 766.20 cm ⁻¹ (C-H bend)	δ 8.17 (m, 2H, ArH), 7.70 (m, 2H, ArH), 6.79 (m, 2H, ArH), 6.56 (m, 2H, ArH), 3.80 (t, 2H, J = 3.98, N-CH ₂), 3.71 (t, 2H, J = 3.98, N-CH ₂), 3.57 (t, 2H, J = 4.00, -N-CH ₂), 3.41 (t, 2H, J = 3.98, -NCH ₂), 3.35 (t, 2H, J = -S-CH ₂), 2.88 (t, 2H, J = 6.46 Hz, -CH ₂ CO), 2.74 (s, 3H, CH ₃)		185.04 (C=O), 179.46 (C=O), 172.40 (C=O), 154.75 (C-F), 142.68 (ArC _q), 139.19 (ArC _q), 137.96 (ArC), 135.27 (2 × ArC _q), 133.67 (ArC _q), 132.15 (2 × ArC _q), 127.86 (ArC), 125.88 (ArC), 119.76 (ArC), 118.31 (ArC), 117.17(ArC), 50.75 (2 × CH ₂ piperazinyl), 44.35 (2 × CH ₂ piperazinyl) 35.31 (S-CH ₂), 29.66 (CH ₂ C=O), 17.03 (CH ₃)	C ₂₄ H ₂₃ FN ₂ O ₃ S (438.14): C, 66.12; H, 5.84; N, 6.10. Found: C, 65.99; H, 5.63; N, 6.24
MB-11	3066.96 (aromatic C-H stretch); 2938.45 (aliphatic C-H stretch); 1737.96 (C=O stretch); 1695.47 (C=O stretch); 1625.73, 1600.61 (C=C ring stretch); 1476.03 (C-N stretch); 1217.37 (C-O stretch); 1087.15 (C-F Stretch); 754.43 cm ⁻¹ (C-H bend)	8.14 (m, 2H, ArH), 7.67 (m, 2H, ArH), 6.76 (t, 2H, J = 6.10 Hz, ArH), 6.55 (m, 2H, ArH), 3.75 (m, 4H, N(CH ₂) ₂), 3.53 (t, 2H, J = 3.88 Hz, -N-CH ₂), 3.41 (t, 2H, J = 3.88 Hz, -N-CH ₂), 3.26 (t, 2H, J = 4.46, -SCH ₂), 2.97 (m, 5H, -CH ₂ CO; CH ₃)		184.59 (C=O), 176.98 (C=O), 172.40 (C=O), 158.25 (d, J = 209.04Hz, C-F), 149.49 (ArC), 139.17 (ArC _q), 137.66 (ArC), 133.77 (ArC _q), 132.35 (2 × ArC _q), 130.93 (2 × ArC), 127.37 (ArC), 118.59 (2 × ArC), 117.68 (2 × ArC), 49.95 (2 × CH ₂ piperazinyl), 44.33 (2 × CH ₂ piperazinyl) 35.38 (S-CH ₂), 29.59 (CH ₂ C=O), 14.84 (CH ₃)	C ₂₄ H ₂₃ FN ₂ O ₃ S: C, 65.54; H, 5.76; N, 6.91. Found: C, 65.83; H, 5.89; N, 6.36
MB-12	3079.04 (aromatic C-H stretch); 2927.33 (aliphatic C-H stretch); 1721.44 (C=O stretch); 1657.60 (C=O stretch); 1625.03, 1600.35 (C=C ring stretch); 1444.63 (C-N	8.20 (m, 2H, ArH), 7.72 (m, 2H, ArH), 7.33 (d, 2H, J = 5.96, ArH), 6.60 (d, 2H, J = 5.96, ArH), 3.78 (m, 4H, N(CH ₂) ₂), 3.64 (m, 2H, -N-CH ₂), 3.47 (m, 2H, -N-CH ₂), 3.31 (t, 2H, J = 4.46 Hz, -SCH ₂), 3.02 (m, 5H, -CH ₂ CO; CH ₃)		184.24 (C=O), 175.12 (C=O), 173.84 (C=O), 154.24 (ArC _q), 139.25 (ArC _q), 137.49 (ArC), 133.17 (ArC _q), 132.77 (2 × ArC), 130.85 (2 × ArC), 128.00 (ArC), 127.51 (2 × ArC _q), 126.85 (d, J = 209.06	C ₂₃ H ₂₃ F ₃ N ₂ O ₃ S: C, 61.40; H, 4.25; N, 5.55. Found: C, 61.22; H,

1, 4-naphthoquinone derivatives as epidermal growth factor receptor inhibitors

	stretch); 1248.82 (C-O stretch); 1125.93 (C-F stretch); 773.40 cm (C-H bend)		H _z (CF ₃)124.46 (ArC _o), 114.17 (2 × ArC), 49.96 (2 × CH ₂ piperazinyl), 44.38 (2 × CH ₂ piperazinyl) 35.81 (S-CH ₂), 29.81 (CH ₂ C=O), 14.24 (CH ₃)	4.45; N, 5.76
MB-13	3038.75 (aromatic C-H stretch); 2926.93 (aliphatic C-H stretch); 1738.68 (C=O stretch); 1684.91 (C=O stretch); 1627.31, 1591.91 (C=C ring stretch); 1452.51 (C-N stretch); 1251.13 (C-O stretch); 1087.76 (C-F stretch); 708.43 cm (C-H bend)	8.32 (dd, 1H, J _m = 1.52 Hz, J _o = 5.60 Hz ArH), 8.17 (dd, 1H, J _m = 1.52 Hz, J _o = 5.60 Hz ArH), 7.72 (m, 2H, ArH), 7.06 (m, 1H, ArH), 6.41 (m, 3H, ArH), 3.88 (m, 2H, -N-CH ₂), 3.72 (m, 4H, - N(CH ₂) ₂), 3.46 (m, 2H, -N-CH ₂), 3.36 (t, 2H, J = 4.56, -SCH ₂), 3.01 (t, 2H, J = 4.56 Hz, - CH ₂ CO), 2.80 (s, 3H, CH ₃)	183.48 (C=O), 179.46 (C=O), 170.94 (C=O), 163.20 (dd, J = 209.08 Hz-F), 139.318 (ArC _o), 137.73 (ArC _o), 133.64 (ArC _o), 133.11 (ArC), 132.40 (2 × ArC), 130.29 (2 × ArC), 128.97 (ArC), 127.90 (ArC), 113.76 (ArC), 107.73 (ArC), 103.48 (ArC), 49.80 (2 × CH ₂ piperazinyl), 44.30 (2 × CH ₂ piperazinyl) 35.28 (S-CH ₂), 29.27 (CH ₂ C=O), 15.56 (CH ₃)	C ₂₄ H ₂₃ N ₃ O ₅ S: C, 65.76; H, 5.35; N, 6.30. Found: C, 65.88; H, 5.47; N, 6.21
MB-14	3073.30 (aromatic C-H stretch); 2928.41 (aliphatic C-H stretch); 1728.47 (C=O stretch); 1685.30 (C=O stretch); 1629.75, 1592.24 (C=C ring stretch); 1453.39 (C-N stretch); 1244.41 (C-O stretch); 757.93 cm (C-H bend)	8.11 (m, 2H, ArH), 7.73 (m, 2H, ArH), 6.72 (d, 2H, J = 6.04 Hz, ArH), 6.66 (d, 2H, J = 6.04 Hz, ArH), 3.82 (m, 5H, OCH ₃ ; -N-CH ₂), 3.69 (m, 4H, N(CH ₂) ₂), 3.44 (m, 4H, -N-CH ₂); - SCH ₂), 2.98 (t, 2H, J = 4.14 Hz, -CH ₂ CO), 2.70 (s, 3H, CH ₃)	186.20 (C=O), 176.19 (C=O), 173.84 (C=O), 152.81 (ArC _o), 143.73 (ArC _o), 139.17 (ArC _o), 137.58 (ArC), 133.82 (ArC _o), 132.81 (2 × ArC), 130.47 (2 × ArC), 127.90 (ArC), 116.20 (2 × ArC), 116.19 (2 × ArC), 56.04 (-OCH ₃), 49.51 (2 × CH ₂ piperazinyl), 44.76 (2 × CH ₂ piperazinyl), 35.16 (S-CH ₂), 29.16 (CH ₂ C=O), 16.19 (CH ₃)	C ₂₅ H ₂₆ N ₂ O ₄ S (450.16): C, 66.31; H, 5.90; N, 6.21. Found: C, 66.87; H, 5.63; N, 6.39
MB-15	3053.48 (aromatic C-H stretch); 2950.20 (aliphatic C-H stretch); 1740.99 (C=O stretch); 1680.05 (C=O stretch); 1621.85 (C=C ring stretch); 1415.45 (C-N stretch); 1217.26 (C-O stretch); 812.78 cm (C-H bend)	δ 8.07 (m, 2H, ArH), 7.72 (m, 2H, ArH), 6.84 (m, 1H, ArH), 6.77 (m, 1H, ArH), 6.71 (m, 2H, ArH), 3.83 (t, 2H, J = 3.90 Hz, -N-CH ₂), 3.78 (s, 3H, OCH ₃), 3.74 (t, 2H, J = 3.88 Hz, -N- CH ₂), 3.68 (t, 2H, J = 3.88 Hz, -N-CH ₂), 3.49 (t, 2H, J = 3.88 Hz, -N-CH ₂), 3.40 (t, 2H, J = 6.46 Hz, -SCH ₂), 2.99 (t, 2H, J = 6.46 Hz, -CH ₂ CO), 2.60 (s, 3H, CH ₃)	185.84 (C=O), 179.46 (C=O), 172.64 (C=O), 149.31 (ArC _o), 142.64 (ArC _o), 139.50 (ArC _o), 133.37 (ArC), 132.32 (2 × ArC), 130.30 (ArC _o), 128.29 (2 × ArC), 122.28 (ArC), 120.27 (ArC), 117.27 (2 × ArC), 113.15 (ArC), 56.79 (- OCH ₃), 50.54 (2 × CH ₂ piperazinyl), 44.55 (2 × CH ₂ piperazinyl) 35.75 (S- CH ₂), 29.73 (CH ₂ C=O), 15.84 (CH ₃)	C ₂₅ H ₂₆ N ₂ O ₄ S: C, 66.87; H, 5.43; N, 6.25. Found: C, 66.36; H, 5.49; N, 6.35
MB-16	3062.97 (aromatic C-H stretch); 2909.20 (aliphatic C-H stretch); 1728.33 (C=O stretch); 1703.88 (C=O stretch); 1630.86, 1602.9 (C=C ring stretch); 1450.99 (C-N stretch); 1266.14 (C-O stretch); 746.78 cm (C-H bend)	δ 8.06 (m, 4H, ArH), 7.72 (m, 2H, ArH), 6.91 (d, 2H, J = 5.92 Hz, ArH), 3.83 (m, 2H, -N- CH ₂), 3.77 (m, 4H, -N(CH ₂) ₂), 3.55 (m, 2H, -N- CH ₂), 3.42 (t, 2H, J = 6.46 Hz, -SCH ₂), 2.98 (t, 2H, J = 6.50 Hz, -CH ₂ CO), 2.63 (s, 3H, CH ₃)	185.94 (C=O), 174.84 (C=O), 171.81 (C=O), 158.30 (ArC _o), 139.44 (ArC _o), 137.88 (ArC _o), 133.82 (2 × ArC), 132.40 (2 × ArC), 130.40 (ArC), 128.33 (ArC _o), 127.90 (ArC), 126.40 (2 × ArC), 112.41 (2 × ArC), 49.44 (2 × CH ₂ piperazinyl), 44.95 (2 × CH ₂ piperazinyl), 35.31 (S- CH ₂), 29.77 (CH ₂ C=O), 15.23 (CH ₃)	C ₂₄ H ₂₃ N ₃ O ₅ S: C, 61.80; H, 4.65; N, 9.28. Found: C, 61.88; H, 4.83; N, 9.19

<p>MB-17</p>	<p>3079.32 (aromatic C-H stretch); 2926.70 (aliphatic C-H stretch); 1720.40 (C=O stretch); 1684.73 (C=O stretch); 1592.24 (C=C ring stretch); 1429.05 (C-N ring stretch); 1251.73 (C-O stretch); ⁻¹ 707.61 cm (C-H bend)</p>	<p>8.28 (m, 1H, ArH), 8.17 (m, 1H, ArH), 7.83 (m, 2H, ArH), 6.95 (t, 1H, J = 6.46 Hz, ArH), 6.57 (dd, 1H, ArH), 6.45 (dd, 1H, ArH), 3.65 (m, 4H, -N(CH₂)₂), 3.45 (t, 2H, J = 4.68, -SCH₂), 3.21 (m, 4H, -N(CH₂)₂), 2.96 (t, 2H, J = 4.56, -CH₂CO), 2.72 (s, 3H, CH₃), 2.38 (s, 3H, CH₃), 2.29 (s, 3H, CH₃)</p>	<p>186.08 (C=O), 176.20 (C=O), 173.29 (C=O), 153.29 (ArC_q), 139.95 (ArC_q), 138.15 (ArC_q), 137.90 (ArC), 132.40 (2 × ArC), 130.53 (2 × ArC), 128.82 (ArC_q), 127.84 (ArC), 126.73 (ArC), 126.56 (ArC_q), 122.77 (ArC), 115.96 (ArC), 51.49 (2 × CH₂piperazinyl), 44.44 (2 × CH₂piperazinyl), 35.13 (S-CH₃), 29.03 (CH₂C=O) 19.77 (CH₃), 13.84 (CH₃), 13.12 (CH₃)</p>	<p>C₂₆H₂₈N₂O₃S (448.18); C, 69.54; H, 6.67; N, 6.83. Found: C, 69.62; H, 6.82; N, 6.73</p>
<p>MB-18</p>	<p>3068.87 (aromatic C-H stretch); 2932.69 (aliphatic C-H stretch); 1725.66 (C=O stretch); 1689.28 (C=O stretch); 1429.27 (C-N stretch); 1247.91 (C-O stretch); ⁻¹ 751.90 cm (C-H bend)</p>	<p>8.19 (dd, 1H, J_m = 1.64 Hz, J_o = 5.52 Hz ArH), 8.10 (dd, 1H, J_m = 1.68 Hz, J_o = 5.48 Hz ArH), 7.79 (m, 2H, ArH), 7.08 (s, 1H, ArH), 6.81 (s, 1H, ArH), 3.80 (s, 6H, OCH₃), 3.71 (s, 2H, -N-CH₂), 3.53 (t, 2H, J = 4.16 Hz, -N-CH₂), 3.43 (t, 2H, J = 4.24 Hz, -N-CH₂), 3.30 (t, 2H, J = 4.16 Hz, -N-CH₂), 2.98 (t, 2H, J = 4.16 Hz, SCH₂), 2.82 (t, 2H, J = 6.0 Hz, -CH₂CO), 2.64 (t, 2H, J = 4.16 Hz, -CH₂), 2.23 (s, 3H, CH₃)</p>	<p>183.10 (C=O), 177.92 (C=O), 170.94 (C=O), 153.10 (ArC_q), 151.68 (ArC_q), 139.39 (ArC_q), 132.32 (2 × ArC), 133.33 (2 × ArC), 128.30 (ArC), 127.29 (2 × ArC), 116.88 (ArC_q), 113.56 (ArC), 113.29 (ArC), 110.19 (C-Br), 58.22 (ArC), 56.78 (OCH₃), 55.07 (OCH₃), 54.61 (2 × CH₂piperazinyl), 49.23 (2 × CH₂piperazinyl) 32.45 (S-CH₂), 32.27 (CH₂C=O), 8.59 (CH₃)</p>	<p>C₂₇H₂₉BrN₂O₃S; C, 56.80; H, 5.28; N, 4.64. Found: C, 56.88; H, 5.20; N, 4.72</p>
<p>MB-19</p>	<p>3067.95 (aromatic C-H stretch); 2931.94 (aliphatic C-H stretch); 1726.61 (C=O stretch); 1662.41 (C=O stretch); 1428.22 (C-N stretch); 1246.76 (C-O stretch); ⁻¹ 812.09 cm (C-H bend)</p>	<p>8.18 (dd, 1H, J_m = 1.65 Hz, J_o = 5.50 Hz ArH), 8.04 (dd, 1H, J_m = 1.68 Hz, J_o = 5.46 Hz ArH), 7.87 (m, 1H, ArH), 7.62 (m, 2H, ArH), 7.44 (m, 1H, ArH), 6.97 (m, 1H, ArH), 6.89 (m, 1H, ArH), 3.65 (t, 2H, J = 4.44 Hz, -N-CH₂), 3.57 (t, 2H, J = 4.44 Hz, -N-CH₂), 3.34 (m, 6H, -N(CH₂)₂-SCH₂), 3.08 (t, 2H, J = 4.56 Hz, -CH₂CO), 2.68 (s, 3H, CH₃)</p>	<p>187.73 (C=O), 177.54 (C=O), 172.40 (C=O), 145.31 (ArC_q), 140.76 (ArC_q), 139.30 (ArC), 135.11 (2 × ArC), 137.62 (ArC_q), 134.94 (ArC), 133.84 (ArC_q), 132.59 (2 × ArC), 128.15 (ArC), 127.48 (ArC), 119.77 (ArC), 118.15 (ArC), 52.04 (2 × CH₂piperazinyl), 44.84 (2 × CH₂piperazinyl), 35.26 (S-CH₂), 29.36 (CH₂C=O), 12.40 (CH₃)</p>	<p>C₂₄H₂₃N₃O₃S; C, 61.37; H, 4.54; N, 9.92. Found: C, 61.65; H, 4.38; N, 9.45</p>

- kinases: targets for cancer therapy. *Nature Reviews Cancer*, 4 (5): 361.
7. Wee, P. and Wang, Z. (2017). Epidermal growth factor receptor cell proliferation signaling pathways. *Cancers*, 9 (5): 52.
 8. Fry, D. W., Kraker, A. J., McMichael, A., Ambroso, L. A., Nelson, J. M., Leopold, W. R., Connors, R. W. and Bridges, A. J. (1994). A specific inhibitor of the epidermal growth factor receptor tyrosine kinase. *Science*, 265 (5175): 1093-1095.
 9. Chinkers, M. and Brugge, J. S. (1984). Characterization of structural domains of the human epidermal growth factor receptor obtained by partial proteolysis. *J Biol Chem*, 259 (18): 11534-11542.
 10. Carpenter, C. D., Ingraham, H. A., Cochet, C., Walton, G. M., Lazar, C. S., Sowadski, J. M., Rosenfeld, M. G. and Gill, G. N. (1991). Structural analysis of the transmembrane domain of the epidermal growth factor receptor. *J Biol Chem*, 266 (9): 5750-5755.
 11. Araujo, R. P., Petricoin, E. F. and Liotta, L. A. (2005). A mathematical model of combination therapy using the EGFR signaling network. *Biosystems*, 80 (1): 57-69.
 12. Wissner, A., Overbeek, E., Reich, M. F., Floyd, M. B., Johnson, B. D., Mamuya, N., Rosfjord, E. C., Discafani, C., Davis, R., Shi, X., Rabindran, S. K., Gruber, B. C., Ye, F., Hallett, W. A., Nilakantan, R., Shen, R., Wang, Y. F., Greenberger, L. M. and Tsou, H. R. (2003). Synthesis and structure-activity relationships of 6,7-disubstituted 4-anilinoquinoline-3-carbonitriles. The design of an orally active, irreversible inhibitor of the tyrosine kinase activity of the epidermal growth factor receptor (EGFR) and the human epidermal growth factor receptor-2 (HER-2). *J Med Chem*, 46 (1): 49-63.
 13. Albuschat, R., Lowe, W., Weber, M., Luger, P. and Jendrossek, V. (2004). 4-Anilinoquinazolines with Lavendustin A subunit as inhibitors of epidermal growth factor receptor tyrosine kinase: syntheses, chemical and pharmacological properties. *Eur J Med Chem*, 39 (12): 1001-1011.
 14. Asano, T., Yoshikawa, T., Usui, T., Yamamoto, H., Yamamoto, Y., Uehara, Y. and Nakamura, H. (2004). Benzamides and benzamidines as specific inhibitors of epidermal growth factor receptor and v-Src protein tyrosine kinases. *Bioorg Med Chem*, 12 (13): 3529-3542.
 15. Norman, P. (2001). OSI-774 OSI Pharmaceuticals. *Curr Opin Investig Drugs*, 2 (2): 298-304.
 16. Smaill, J. B., Palmer, B. D., Rewcastle, G. W., Denny, W. A., Mcnamara, D. J., Dobrusin, E. M., Bridges, A. J., Zhou, H., Showalter, H. D., Winters, R. T., Leopold, W. R., Fry, D. W., Nelson, J. M., Slintak, V., Elliot, W. L., Roberts, B. J., Vincent, P. W. and Patmore, S. J. (1999). Tyrosine kinase inhibitors. 15. 4-(Phenylamino)quinazoline and 4-(phenylamino)pyrido[d]pyrimidine acrylamides as irreversible inhibitors of the ATP binding site of the epidermal growth factor receptor. *J Med Chem*, 42 (10): 1803-1815.
 17. Fry, D. W., Bridges, A. J., Denny, W. A., Doherty, A., Greis, K. D., Hicks, J. L., Hook, K. E., Keller, P. R., Leopold, W. R., Loo, J. A., Mcnamara, D. J., Nelson, J. M., Sherwood, V., Smaill, J. B., Trumpp-Kallmeyer, S. and Dobrusin, E. M. (1998). Specific, irreversible inactivation of the epidermal growth factor receptor and erbB2, by a new class of tyrosine kinase inhibitor. *Proc Natl Acad Sci U S A*, 95 (20): 12022-12027.
 18. Verma, S., Wang, C. H., Govindarajan, S., Kanel, G., Squires, K. and Bonacini, M. (2006). Do type and duration of antiretroviral therapy attenuate liver fibrosis in HIV-hepatitis C virus-coinfected patients? *Clin Infect Dis*, 42 (2): 262-270.

19. Ilina, T. V., Semenova, E. A., Pronyaeva, T. R., Pokrovskii, A. G., Nechepurenko, I. V., Shults, E. E., Andreeva, O. I., Kochetkov, S. N. and Tolstikov, G. A. (2002). Inhibition of HIV-1 reverse transcriptase by aryl-substituted naphtho- and anthraquinones. *Dokl Biochem Biophys*, 382: 56-59.
20. Lawrence, H. R., Kazi, A., Luo, Y., Kendig, R., Ge, Y., Jain, S., Daniel, K., Santiago, D., Guida, W. C. and Sebti, S. M. (2010). Synthesis and biological evaluation of naphthoquinone analogs as a novel class of proteasome inhibitors. *Bioorg Med Chem*, 18 (15): 5576-5592.
21. Lien, J. C., Huang, L. J., Teng, C. M., Wang, J. P. and Kuo, S. C. (2002). Synthesis of 2-alkoxy 1,4-naphthoquinone derivatives as antiplatelet, antiinflammatory, and antiallergic agents. *Chem Pharm Bull (Tokyo)*, 50 (5): 672-674.
22. Salmon-Chemin, L., Buisine, E., Yardley, V., Kohler, S., Debreu, M. A., Landry, V., Sergheraert, C., Croft, S. L., Krauth-Siegel, R. L. and Davioud-Charvet, E. (2001). 2- and 3-substituted 1,4-naphthoquinone derivatives as subversive substrates of trypanothione reductase and lipoamide dehydrogenase from *Trypanosoma cruzi*: synthesis and correlation between redox cycling activities and in vitro cytotoxicity. *J Med Chem*, 44 (4): 548-565.
23. Tandon, V. K., Chhor, R. B., Singh, R. V., Rai, S. and Yadav, D. B. (2004). Design, synthesis and evaluation of novel 1,4-naphthoquinone derivatives as antifungal and anticancer agents. *Bioorg Med Chem Lett*, 14 (5): 1079-1083.
24. Tandon, V. K., Yadav, D. B., Maurya, H. K., Chaturvedi, A. K. and Shukla, P. K. (2006). Design, synthesis, and biological evaluation of 1,2,3-trisubstituted-1,4-dihydrobenzo[g]quinoxaline-5,10-diones and related compounds as antifungal and antibacterial agents. *Bioorg Med Chem*, 14 (17): 6120-6126.
25. Lanfranchi, D. A., Cesar-Rodo, E., Bertrand, B., Huang, H. H., Day, L., Johann, L., Elhabiri, M., Becker, K., Williams, D. L. and Davioud-Charvet, E. (2012). Synthesis and biological evaluation of 1,4-naphthoquinones and quinoline-5,8-diones as antimalarial and schistosomicidal agents. *Org Biomol Chem*, 10 (31): 6375-6387.
26. Prachayasittikul, V., Pingaew, R., Worachartcheewan, A., Nantasenamat, C., Prachayasittikul, S. and Ruchirawat, S. (2014). Synthesis, anticancer activity and QSAR study of 1,4-naphthoquinone derivatives. *Eur J Med Chem*, 84: 247-263.
27. Danson, S. J., Johnson, P., Ward, T. H., Dawson, M., Denny, O., Dickinson, G., Aarons, L., Watson, A., Jowle, D., Cummings, J., Robson, L., Halbert, G., Dive, C. and Ranson, M. (2011). Phase I pharmacokinetic and pharmacodynamic study of the bioreductive drug RH1. *Ann Oncol*, 22 (7): 1653-1660.
28. Workman P. (1994). Enzyme-directed bioreductive drug development revisited: a commentary on recent progress and future prospects with emphasis on quinone anticancer agents and quinone metabolizing enzymes, particularly DT-diaphorase. *Oncology Research Featuring Preclinical and Clinical Cancer Therapeutics*, 6(10-11): 461-75.
29. Emadi, A. and Karp, J. E. (2012). The clinically relevant pharmacogenomic changes in acute myelogenous leukemia. *Pharmacogenomics*, 13 (11): 1257-1269.
30. Xiang, M., Kim, H., Ho, V. T., Walker, S. R., Bar-Natan, M., Anahtar, M., Liu, S., Toniolo, P. A., Kroll, Y., Jones, N., Giaccone, Z. T., Heppler, L. N., Ye, D. Q., Marineau, J. J., Shaw, D., Bradner, J. E., Blonquist, T., Neuberg, D., Hetz, C., Stone, R. M., Soiffer, R. J. and Frank, D. A. (2016). Gene expression-based discovery of atovaquone as a STAT3 inhibitor and anticancer agent. *Blood*, 128 (14): 1845-1853.

31. Emadi, A., Ross, A. E., Cowan, K. M., Fortenberry, Y. M. and Vuica-Ross, M. (2010). A chemical genetic screen for modulators of asymmetrical 2,2'-dimeric naphthoquinones cytotoxicity in yeast. *PLoS One*, 5 (5): e10846.
32. Chakrabarti, G., Moore, Z. R., Luo, X., Ilcheva, M., Ali, A., Padanad, M., Zhou, Y., Xie, Y., Burma, S., Scaglioni, P. P., Cantley, L. C., Deberardinis, R. J., Kimmelman, A. C., Lyssiotis, C. A. and Boothman, D. A. (2015). Targeting glutamine metabolism sensitizes pancreatic cancer to PARP-driven metabolic catastrophe induced by ss-lapachone. *Cancer Metab*, 3: 12.
33. Wellington, K.W., (2015). Understanding cancer and the anticancer activities of naphthoquinones a review. *RSC Adv*. 5(26): 20309-38.
34. Liu, C., Shen, G. N., Luo, Y. H., Piao, X. J., Jiang, X. Y., Meng, L. Q., Wang, Y., Zhang, Y., Wang, J. R., Wang, H., Xu, W. T., Li, J. Q., Liu, Y., Wu, Y. Q., Sun, H. N., Han, Y. H., Jin, M. H., Cui, Y. D., Fang, N. Z. and Jin, C. H. (2018). Novel 1,4-naphthoquinone derivatives induce apoptosis via ROS-mediated p38/MAPK, Akt and STAT3 signaling in human hepatoma Hep3B cells. *Int J Biochem Cell Biol*, 96: 9-19.
35. Abdelmohsen, K., Gerber, P. A., Von Montfort, C., Sies, H. and Klotz, L. O. (2003). Epidermal growth factor receptor is a common mediator of quinone-induced signaling leading to phosphorylation of connexin-43: role of glutathione and tyrosine phosphatases. *J Biol Chem*, 278 (40): 38360-38367.
36. Al-Ghorbani, M., Begum, B., Zabiulla, M.S.V., Khanum, S.A. (2015). Piperazine and morpholine: Synthetic preview and pharmaceutical applications. *J Chem Pharm Res*, 7(5):281-301.
37. Lacivita, E., Leopoldo, M., De Giorgio, P., Berardi, F. and Perrone, R. (2009). Determination of 1-aryl-4-propylpiperazine pKa values: the substituent on aryl modulates basicity. *Bioorg Med Chem*, 17 (3): 1339-1344.
38. Njuguna, N. M., Ongarora, D. S. and Chibale, K. (2012). Artemisinin derivatives: a patent review (2006 - present). *Expert Opin Ther Pat*, 22 (10): 1179-1203.
39. Rathi, A. K., Syed, R., Shin, H. S. and Patel, R. V. (2016). Piperazine derivatives for therapeutic use: a patent review (2010-present). *Expert Opin Ther Pat*, 26 (7): 777-97.

Screening of ACC-deaminase and antifungal metabolites producing fluorescent pseudomonads isolated from rhizosphere soil of groundnut

Nirmala Jyothi Lukkani¹ and Dr. EC. Surendranatha Reddy*

¹ Department of Genetics and Genomics, Yogi Vemana University, Vemanapuram, Kadapa, Andhra Pradesh, India.

* Department of Genetics and Genomics, Yogi Vemana University, Vemanapuram, Kadapa, Andhra Pradesh, India.

Abstract

Plant Growth Promoting Rhizobacteria that can colonize the root systems are an efficient group of beneficial bacteria. Fluorescent pseudomonads belong to this category that can enhance plant growth and disease suppression by different types of mechanisms. Fifty five fluorescent pseudomonads (JS 1....JS 55) identified from soil samples collected from different places of Rayalaseema region located in Andhra Pradesh, screened for ACC- deaminase enzyme activity and antifungal metabolites production. Results showed that it is highly likely that these pseudomonads isolates deaminated endogenous ACC. Furthermore, these isolates remarkably producing antifungal metabolites like siderophores, chitinases and antibiotics. Among these, 5 isolates (JS 7, JS 16, JS 24, JS 31 and JS 44) are efficient producers of ACC-deaminase and antifungal metabolites.

Key words: ACC-deaminase, PGPR and Fluorescent Pseudomonads

Introduction;

Groundnut (*Arachis hypogaea* L.) is an important oil seed crop of India occupying 45 percent of total oil seed production. Intensive groundnut cultivation largely requires use of chemical fertilizer even though they are costly besides short supply. Plant Growth Promoting Rhizobacteria (PGPR) could take part a major role in the development of sustainable agriculture. Reduction in ethylene production leading to well

developed root system, enhanced the levels of phytohormones viz., auxins, cytokinins, and gibberellins are few effects of PGPR in plant growth patterns (Glick, 1995) and plants can be protected from diseases by the synthesis of antibiotic and pathogen-controlling substances like siderophores, cyanides and chelating agents (Kamnev and Lelie, 2000).

ACC- deaminase enzyme enables pseudomonads to decrease ethylene levels in plants by converting ACC into NH₃ and α -ketobutyrate instead of ethylene (Jacobson *et al.*, 1994; Glick *et al.*, 1998; Shah *et al.*, 1998). Many microorganisms secrete metabolites mainly lytic enzymes which can hydrolyze a wide variety of polymeric compounds which interfere with pathogen (Loper, 1999; Nielsen and Sorensen, 1999; Picard *et al.*, 2000). Pseudomonads are ideal biocontrol antagonists because of their potential pathogen-suppressing ability, adaptive metabolism and ability to release a wide range of inhibitory compounds like antibiotics viz., phenazines (Gurusiddaiah *et al.*, 1986) pyrole resembling compounds (Homna and Suzui, 1989) and polyketides (Kraus and Loper, 1995). These compounds play an important role of microbial competition in rhizosphere, show evidence regarding the presence of bacteria and fungi such as broad band spectrum activity. (Mazzola *et al.*, 1992; Smimov and Kiprianova, 1990).

Fluorescent siderophores are secreted during under low-iron conditions and the subsequent ferric siderophore complex is

unavailable to other organisms. At low concentrations of iron, fungal spores does not germinate at normal rate. (Neilands and Leong, 1986; Dowling *et al.*, 1996). Maximum recognized siderophores can be categorizes as hydroxamate- and phenolate-catecholate type structures and shows different affinities for Fe^{+3} . The hydroxamate ions which can form stable complexes that are more substantial around the root system. The mycolytic activity of fungal as well as bacterial antagonists is mainly due to the lytic enzymes like chitinases and α -1-3-glucanase, protease and lipase (Mitchell and Alexander, 1962; Henis and Chet, 1975). These enzymes produced from pseudomonads function as antifungal agents against several plant pathogenic fungi (Ogasawara and Tanaka, 1978; Tanaka and Watanabe, 1995).

In the present studies, ACC-deaminase and antifungal metabolites producing fluorescent pseudomonads were isolated from the rhizosphere soil of groundnut. These pseudomonads could be efficient and successful tool for promotion of plant growth and biocontrol of deleterious fungi.

Materials and Methods

Screening of Pseudomonads for ACC Deaminase activity

Qualitative method : Isolates were screened on DF salt minimal medium (Dworkin and Foster, 1958 Appendix 1) containing 10 ml of minimal salt solution and 990 ml of distilled water supplement with 3 mM ACC as the only N_2 source. Plates are containing only DF salts minimal medium having no ACC as negative control and having $(NH_4)_2SO_4$ (0.2% w/v) as positive control. The plates were kept incubation at 28°C for 72 h. ACC added plates were compared to negative and positive controls for growth isolates. Later based on growth patterns they were selected based on ACC as nitrogen source.

Quantitative estimation of ACC deaminase
ACC-deaminase enzyme activity (quantitative) was determined according to Honma and Shimomura (1978). Bacterial culture broth was centrifuged at 16,000 g for 5 min and the supernatant is

discarded. In 600 ml 0.1M Tris HCl solution at the pellet was suspended, pH 8.5. Thirty micro-litres of toluene were included into the cell suspension and vortexed for 30s. This suspension was immediately tested for ACC deaminase activity. Two hundred μ l of the toluenized cells were placed in a fresh 1.5 ml micro centrifuge tube; 20 μ l of 0.5M ACC was mixed to the suspension vortexes and then incubated at 30°C for 15 min. After the addition of 1 ml of 0.56 N HCl, the mixture is vortexed and centrifuged for 5 min at 16,000X g. One ml of the supernatant was vortexed along with 800 μ l of 0.56 N HCl in a clean glass tube (100 x 13 mm). Later, 300 μ l of the DNPH reagent solution was added to contents of the glass tube, the contents vortexed and which was later kept incubated at 30°C for 30 min. Once adding 2 ml of 2 N NaOH, the absorbance of the mixture was measured at 540 nm.

Standard preparation for measurement of ACC deaminase

Standard preparation : Standard preparation is essential for the amount of α -ketobutyrate released when ACC deaminase, cleaves ACC. The amount of α -ketobutyrate formed in this reaction was determined by composition of the absorbance at 540 nm of a sample to a standard curve of α -ketobutyrate ranging between 0.1 and 1.0 n mol.

Detection of Siderophore Production

Siderophore detection using CAS: Dye solution (100ml): 60.5 mg CAS dye was dissolved in 50 ml of distilled water and assorted with 10 ml of Fe^{+3} solution (1mM of $FeCl_3$ in 10 mM of HCl). Prepared solution was thoroughly added in very slow manner to 72.9 mg hexadecyltrimethyl ammonium (HDTMA) dissolved in 40 ml distilled water. The resulting dark blue dye solution was autoclaved at 15 psi for 15 min.

Estimation of Siderophore Production through

CAS-shuttle assay : The isolates were inoculated on succinate medium and incubated for 24 – 30 h at 28°C with continuous shaking on a rotator shaking incubator at a rate of 120 rpm. After incubation, the inoculated broth was centrifuged at 10,000 rpm in cooling centrifuge at 4°C for 10

minutes and cell free supernatant was assayed with 0.5 ml CAS solution. Reference was prepared by 0.5 ml of uninoculated succinate medium and 0.5 ml of CAS solution and kept incubated for 20 min. The color of solution was determined using the spectrophotometer at absorbance 630 nm. Depending on the percentage of siderophore units, the proportion of CAS changed the color in accordance with the formula.

$$[(Ar - As)/Ar] \times 100,$$

In the above formula 'Ar' is the A630 nm of reference (CAS assay solution+ uninoculated broth) and 'As' is the A630 nm of the sample (CAS assay solution+ supernatant).

Fungal cell wall degrading lytic enzyme assessment by Pseudomonads

Protease production- Casein hydrolysis : The medium for checking protease production was by Luria–Bertani (LB) agar medium with the supplementation of 1% skimmed milk (Smibert and Krieg, 1994). Overnight grown cultures were inoculated on the media plate and incubated for 48 h. at $28 \pm 2^\circ\text{C}$. Protease positive strains were recorded as showing a zone of clearance around the site of colony growth (Seeley and Vandemark, 1970).

Fungal cell wall degrading lytic enzyme assessment by pseudomonads

Chitinase Activity (Qualitative assay) : Endo-chitinase activity (hydrolytic splitting within chitin polymer) by isolates of *Pseudomonas* spp. was screened by plate assay method on 1% colloidal chitin and for this, an agar plate was used. Colloidal chitin was prepared by the method of Roberts *et al.*, (1968). After inoculation, these were incubated at 37°C for 5-7 days. A clear zone (mm dia) produced around the well (7 mm) or culture bit was noted.

Quantitative Assay for chitinase enzyme production : The colorimetric assay of chitinase was followed according to Boller and Mauch (1988). Chitinase activity was assessed by using the substrate chitin in colloidal form as substrate.

Bacterial isolates were incubated into culture broth was prepared and inoculated with bacterial isolates. The culture tubes were incubated for 3 days at 28°C on rotating shaking incubator. The enzyme solution 1 ml was added in 1 ml of substrate solution after completion of centrifugation of culture broth which was made by suspending 1 percent of colloidal chitin in Phosphate buffer (pH 7). The final suspension was kept incubation at 37°C for 45 minutes and the absorbance was measured at 585 nm.

Standard preparation by Di nitro salicylic acid (DNSA) method :

By measuring the evolution of reducing sugar from colloidal chitin, chitinolytic activity of the culture was assayed. The amount of reducing sugar released from chitin was then confirmed by noting absorbance at 585 nm.

α 1, 3 Glucanase Test : β 1, 3-glucanase activity was tested based on the release of free glucose from yeast cell wall (ycw) as a substrate. Glucose equivalents generated during assay were estimated by using 3, 5 dinitrosalicylic acid (DNS) method by taking glucose as standard at 450 nm. The assay mixture contained phosphate buffer, (pH 7.0) with 50 μl of yeast cell wall, 950 μl of distilled water, 1 ml of the culture filtrate and incubated at 37°C for 40 min, 1 ml of 3,5 dinitrosalicylic acid (DNS) reagent was added and the contents of the mixture was heated in a boiling water-bath for 15 min. As a control, 1.0 ml of distilled water was added instead of culture filtrate, incubated and cooled. Readings of the reducing sugars were quantified in both the test and the control solutions with glucose as standard by the colorimetric method at 450 nm.

Antimicrobial metabolite (antibiotics) production

Phenazine synthesis : Phenazine is a dark pigmented antibiotic majorly produced by Pseudomonads. All isolates were tested for phenazine generation ability as described by Thomashow and Weller (1988). Actively growing isolates were streaked on PDA and incubated at 28°C for 4 days. Dark green pigmentation in the

centre of bacterial colonies was observed as crystals which was an indicative of phenazine production.

Detection of fluorescein and pyocyanin: For the detection of fluorescein and pyocyanine, differential media were used. *Pseudomonas* agar F (Himedia, Mumbai) favours the formation of fluorescein whereas *Pseudomonas* agar P (Himedia, Mumbai) stimulates the production of pyocyanin production and reduces the formation of fluorescein (King *et al.*, 1954). All the isolates of fluorescent pseudomonads were tested for production of fluorescein and pyocyanin.

Result

ACC Deaminase synthesis : Two nitrogen sources (ACC and Ammonium Sulphate) were used to grow the rhizobacterial strains. The growth rates of the isolates for ACC substrate in parallel to ammonium sulphate were studied. Findings of ACC utilization test showed that all 16 isolates metabolized ACC (positive for possessing ACC-deaminase activity) but with various degrees of efficacy. On the basis of growth, measured in terms of OD 550, these 16 isolates were categorized into three groups *i.e.*, High (OD 550 > 0.7), Medium (OD 550: 0.5 - 0.69), Low (OD

550 < 0.5). On the whole, the results demonstrate that the isolates of JS-7, JS-16, JS-24, JS-31 and JS-44 were better performers than the others. Rhizobacterial isolates (JS-16, JS-7, JS-25, JS-48) showing highest growth (OD > 0.75) by utilizing ACC as N source were categorized as Group-A. Similarly, seven isolates showing medium growth (OD 0.75 - 0.50), were placed in Group-B while ten isolates exhibiting least growth (OD < 0.50) were placed in Group-C.

Pseudomonas fluorescens isolates showing variable growth (measured O. D) on the media containing ACC and NH₄Cl.

Detection of Siderophore Production

Fluorescent pseudomonads exhibited yellow coloured halo zone in the region of the bacterial colony on dark blue coloured agar plates confirming the production of siderophore. Yellow halo region varied with the strains. In qualitative assay, out of 55 isolates 40 bacterial isolates produced siderophores on the CAS plate method. The indicated that the fluorescent pseudomonads JS-7, JS-23, JS-16 and JS-43 showed strong producer of siderophores when compared to other isolates measured by hallow zone about of 25, 24 and 23 mm diameter around the colonies on dark blue CAS medium respectively.

ACC	Isolates	ACC utilization	NH ₄ Cl Utilization	Without N source
Strong ACC utilizers Group- A (OD > 0.75)	JS-7	+++	+++	-
	JS-16	+++	+++	-
	JS-25	+++	+++	-
Moderate ACC utilizers Group- B (OD 0.75-0.50)	J S-48	++	+++	-
	JS-44	++	++	-
	JS-31	++	++	-
Weak ACC utilizers Group- C (OD <0.50)	JS-29	+	++	-
	JS-41	+	+	-

Siderophore synthesis

Soil pseudomonads produce fluorescent siderophores with both hydroxamate and catecholate groups. Structurally, Hydroxamate type siderophores form more stable than catechol type. In quantitative method, the range of siderophores between 7.5 - 5.8 $\mu\text{g ml}^{-1}$ for catechol type and hydroxamate type it is 7.9-6.2 $\mu\text{g ml}^{-1}$. Predominantly, most of the isolates tested in the present study produced more amount of hydroxamate type than catechol type of siderophores.

Fungal cell wall degrading lytic enzyme assessment by pseudomonads

Chitinase Test (Qualitative assay)

Isolates that show growth on this media are able to degrade chitin and thus are chitinase positive while those which could not grow on this media are chitinase negative. The chitin degrading isolates formed clear zones of 5 - 10 mm in diameter on 7 days of incubation, thus indicating the chitinase activity on Chitin amended agar plates. Isolates like JS-34 and JS-42 have shown moderate growth on chitin media after incubation period of 7 d while rests of the isolates are chitinase negative.

Quantitative Assay

Among all these twelve chitinolytic isolates JS-7, JS-12, JS-16, JS-24, JS-31 and JS-52 were the most potent chitinolytic isolates produce 15-18 mg/ml GlcNAC in quantitative assays. It has been observed that a strong correlation between the chitinolytic potential of different bacterial isolates and *in vitro* lysis of fungal mycelium.

Glucanase Activity

Identification of glucanase producing activity qualitatively is by formation of clear zones on Glucan agar plate. Majorly, four isolates JS-7, JS-16, JS-24 and JS-31 have produced significant amount of glucanase. The isolates JS-7, JS-16 are imperative producers of both chitinase and α -1, 3 glucanase in pure substrates.

Protease production- Casein hydrolysis

A zone of proteolysis was detected on the casein/skimmed milk agar plates. The hydrolysis zone produced on the casein agar could be related to the amount of protease produced by the bacteria. Majority of isolates produced proteases among those JS-46, JS-7, JS-16, JS-24 and JS-31 are significant protease producers.

Antimicrobial metabolite (antibiotics) production

Detection of Fluorescein and Pyocyanin synthesis

All the bacterial isolates that were tested to produced fluorescein and pyocyanin in varied quantities after 48 h of incubation. The isolates JS-16 and JS-7 showed strong production of fluorescein and isolates JS-26, JS-24 and JS-52 exhibited higher germination of pyocyanin in the specific *Pseudomonas* agar medium.

Phenazine Antibiotic production

Colonies were streaked on PDA and incubated at 28°C for a period of four days. Dark green pigmented crystals in the centre of bacterial colonies were formed which confirmed phenazine production. About 18 isolates were positive for this test.

Discussion

Pseudomonads are a group of PGPR that are a part of the rhizosphere. They exert a positive impact on plant health and soil fertility. Pseudomonads have the potential ability to synthesize ACC deaminase to decrease the ethylene levels in the roots of the budding plants, which leads to increase in the root length and growth (Glick, 1995). Enhanced yield was observed when plants were inoculated with rhizobacteria with ACC-deaminase. (Shaharoon *et al.*, 2007; Zahir *et al.*, 2009; Siddikee *et al.*, 2011).

Pseudomonads can easily colonize roots and possess catabolic adaptability. They also produce a variety of enzymes and metabolites. Nielsen *et al.*, (1998) reported that endochitinase produced from fluorescent pseudomonads inhibit

plant pathogenic *R. solani*. Lim *et al.*, (1991) recognized that extracellular chitinase and α -1, 3-glucanase produced by *P. stutzeri* could *Fusarium solani* mycelia thereby preventing fungus from causing crop loss due to root rot. Fridlender *et al.*, (1993) stated that α -1, 3-glucanase producing *P. Cepacia* decreased the incidence of diseases caused by *R. solani* and *S. rolfsii*. Palumbo *et al.*, (2005) reported that α -1, 3-glucanase significantly act as biocontrol activities of *Lysobacter enzymogenes* strain C3. Nandakumar *et al.*, (2001) and Nayar (1996) observe early and high stimulation of chitinase by *P. fluorescens* Pf1 enhanced induction of ISR offered protection against *R. Solani* in rice.

Fluorescent Pseudomonads exhibits multiple numbers of mechanisms which serve as potential biocontrol agents (Ramamoorthy *et al.*, 2001; Vivekananthan *et al.*, 2004). Among those most important metabolites are antibiotics, which inhibit the growth of plant pathogenic organisms. *Pseudomonas* strains with the ability of producing multi-antibiotics might have superior potential for broad-spectrum disease suppression. *Pseudomonas* spp. strain PHZ48 reported to produces both phenazine and pyrrolnitrin (De Souza and Raaijmakers 2003).

Siderophore production helps in better survival and competence of isolates and also acts as biocontrol against plant pathogens (fungal and bacterial) in iron deficient conditions. Kloepper *et al.*, (1981) demonstrated the role of siderophores formed by fluorescent pseudomonads in pathogens control. Siderophores of fluorescents pseudomonads has been associated in the biocontrol of wilt diseases caused by *Fusarium oxysporum* and damping off in cotton affected by *Pythium ultimum* (Loper, 1988). Manwar *et al.*, (2004) evaluated purified siderophores from *Pseudomonas* culture showed significant antifungal activity against the plant deleterious fungi like *Aspergillus niger*.

Conclusion : While it is clear that fluorescent pseudomonads are effective biocontrol agents can release various compounds into their surrounding environment. Such metabolites produced in

natural systems in the presence and absence of plant disease can have prominence for sustainable agriculture and hold great promise in the enhancement of agricultural yields. The use of PGPR is progressively increasing in agriculture and offers an attractive way to replace chemical fertilizers, pesticides, and supplements.

References

1. Boller, T. and Mauch, F. 1988. Colorimetric assay for chitinase. *Methods in Enzymology*, 161: 430-435.
2. De Souza, J., Arnould, C., Deulvot, C., Lamanceau, P., Pearson, V. G., and Raaijmakers, J. M., 2003, Effect of 2, 4 diacetyl phloro glucinol on Pythium: Cellular responses and variation in sensitivity among propagules and species. *Phytopathology* 93: 966-975.
3. Dowling, D.N., Sexton, R., Fenton, A., Delany, I., Fedi, S., McHugh, B., Callanan, M., Moenne Loccoz, Y. and O'Gara F., 1996, Iron regulation in plant-associated *Pseudomonas fluorescens* M114: implications for biological control. In: *Molecular Biology and Pseudomonads*. Eds. Nakazawa, T., Furukawa, K., Haas, D., Silver, S. American Society for Microbiology Press, Washington, DC, pp.502-511.
4. Dworkin, M & Foster, J. W. (1958). "Experiment with some Microorganisms which Utilize Ethane and Hydrogen", *Journal of Bacteriology*, 75: 529-601.
5. Fridlender M., Inbar J., and Chet I. 1993. Biological control of soil borne plant pathogens by a P-1.3 glucanase-producing *Pseudomonas* spp *Plant Physiol.* 96: 928-936.
6. Glick, B.R. 1995. The enhancement of plant growth by free-living bacteria. *Can. J. Microbiol.* 41, 109-117
7. Glick, B.R., Penrose, D.M. and Li, J., 1998, a model for the lowering of plant ethylene concentrations by plant growth-promoting bacteria. *J. Theor. Biol.*, 190: 63-68.

8. Gurusiddaiah, D.M. Weller, A. Sarkar, R.J. Cook Characterization of an antibiotic produced by a strain of *Pseudomonas fluorescens* inhibitory to *Gaeumannomyces graminis* var. *tritici* and *Pythium* spp. *Antimicrobial Agents Chemother*, 29 (1986), pp. 488–495.
9. Henis, Y. and Chet, I. (1975) Microbiological control of plant pathogens. *Adv. Appl. Microbiol.* 19, 85-111.
10. Honma M and Shimomura T (1978) Metabolism of 1- aminocyclopropane-1-carboxylic acid. *Agric. Biol. Chem.* 42:1825-1831.
11. Hornma, Y., and T. Suzui. 1989. Role of antibiotic production in suppression of radish damping-off by seed bacterization with *Pseudomonas cepacia*. *Ann. Phytopathol. Soc. Jpn.* 55:643-652.
12. King, E.O., M.K.E. Ward and D.E. Raney, 1954. Two simple media for the demonstration of pyocyanin and fluorescin. *J. Laboratory and Clinical Medicine*, 44: 301-307.
13. Kloepper J. W. and Schroth M. N. (1981) Relationship of in vitro antibiosis of plant growth-promoting rhizobacteria to plant growth and the displacement of root microflora. *Phytopathology* 71, 1020-1024.
14. Kraus, J., and J. E. Loper. 1995. Characterization of a genomic region required for production of the antibiotic pyoluterin by the biological control agent *Pseudomonas fluorescence* Pf5. *Appl Environ Microbiol.* 61:849-854.
15. Lim H. S., Kim Y. S., and Kim S. D. 1991. *Pseudomonas stutzeri* YPL-1 genetic transformation and antifungal mechanism against *Fusarium solani*, an agent of plant root rot. *Appl. Environ. Microbiol.* 57: 510-516.
16. Loper, J.E., 1988, Role of fluorescent siderophore production in biological control of *Pythiummultimum* by a *Pseudomonas fluorescens* strain. *Phytopathol.* 78: 166-172.
17. Loper, J.E., Henkels, M.D. 1999. Utilization of heterologous siderophore enhances levels of iron available to *Pseudomonas putida* in the rhizosphere. *Applied Environmental Microbiology.* 65, 5357- 5363.
18. Manwar, A.V., Khandelwal, S.R., Chaudhari, B.L., Meyer, J.M. and Chincholkar, S.B., 2004, Siderophore production by a marine *Pseudomonas aeruginosa* and its antagonistic action against phytopathogenic fungi. *Applied Biochem. Biotechnol.* 118: 243-252.
19. Mazzola, M., Cook, R.J., Thomashow, L.S., Weller, D.M. and Pierson, L.S. (1992) Contribution of phenazine antibiotic biosynthesis to the ecological competence of fluorescent pseudomonads in soil habitats. *Appl Environ Microbiol* 58, 2616–2624.
20. Mitchell, R. and Alexander, M. (1962) Lysis of soil fungi by bacteria. *Can. J. Microbiol.* 9, 169-177.
21. Nandakumar R., S. Babu, R. Viswanathan, T. Raguchander and R. Samiyappan, 2001a. Induction of systemic resistance in rice against sheath blight disease by *Pseudomonas fluorescens*. *Soil Biology and Biochemistry* 33, 603–612.
22. Nayar, K., 1996, Development and evaluation of a biopesticide formulation for control of foliar diseases of rice. *Ph.D. Thesis*, Tamil Nadu, Agric. Univ., Coimbatore, p.223.
23. Ramamoorthy V., Viswanathan R., Raguchander T., Prakasan V., Samiyappan R., 2001. Induction of systemic resistance by plant growth promoting rhizobacteria in crop plants against pests and diseases. *Crop Protection* 20: 1-11.
24. Neilands, J.B. and Leong, S.A., 1986, Siderophores in relation to plant growth and disease. *Ann. Rev. Pl. Physiol.*, 37: 187-208.

25. Nielsen, K.F., Hansen, M.Ø., Larsen, T.O., Thrane, U., 1998. Production of trichothecene mycotoxins on water damaged gypsum boards in Danish buildings. *Int. Biodeter. Biodegr.* 42, 1–7.
26. Neilsen, M. N., and J. Sorensen. 1999. Chitinolytic activity of Pseudomonas strains isolated from barley and sugar beet rhizosphere. *FEMS Microbiol. Ecol.* 30:217- 227.
27. Ogasawara N. and Tanaka H. Japanese kokoku patent Sho 53-41025, August 1978.
28. Palumbo, J. D., Yuen, G. Y., Jochum, C. C., Tatum, K., and Kobayashi, D. Y. 2005. Mutagenesis of beta-1, 3-glucanase genes in *Lysobacter enzymogenes* strain C3 results in reduced biological control activity toward *Bipolaris* leaf spot of tall fescue and *Pythium* damping-off of sugar beet. *Phytopathology* 95: 701-707.
29. Picard, C., Di Cello, F., Ventura, M., Fani, R. & Guckert, A. (2000). Frequency and biodiversity of 2,4-diacetylphloroglucinol-producing bacteria isolated from the maize rhizosphere at different stages of plant growth. *Appl Environ Microbiol*, 66, 948-955.
30. Roberts, J., Prager, M. and Bachynsky, N. (1968) New procedures for purification of L-asparaginase with high yield from *E. coli*. *J. Bacteriol.* 95, 2117-2123.
31. Seeley, H. W. and Vandemark, P. J. 1970. *Microbes in action: A laboratory manual of microbiology*, D. P. Tarapo Revale Sons and Company Ltd., Bombay. pp. 86-95.
32. Shah, S., Li, J., Moffatt, B.A. and Glick, B.R. (1998). Isolation and characterization of ACC deaminase genes from two different plant growth promoting rhizobacteria, *Can. J. Microbiol.* 44: 833 – 843.
33. Smibert RM, Krieg NR (1994) Phenotypic characterization. In: *Methods for General and Molecular Biology*, ed. by P.R.G. Gerhardt, E. Murray, W.A. Wood, and N.R. Krieg,. Washington, DC: American Society for Microbiology. pp. 607– 654.
34. Smirnov, V. V. & Kiprianova, E. A. (1990). *Bacteria of the Genus Pseudomonas*. Kiev: Naukova Dumka (in Russian).
35. Tanaka H. and Watanabe T. 1995. Glucanases and Chitinases of *Bacillus circulans* WL-12. *J. Indus. Microbiol.* 114:478-483.
36. Thomashow L.S. and D.M. Weller, 1988. Role of phenazine antibiotic from *Pseudomonas fluorescens* in biological control of *Gaeumannomyces graminis* var. *tritici*. *Journal of Bacteriology* 170, 3499– 3508.
37. Vivekananthan, R., Ravi, M., Ramanathan, A. and Samiyappan, R., 2004, Lytic enzymes induced by *Pseudomonas fluorescens* and other biocontrol organisms mediate defence against the anthracnose pathogen in mango. *World J. Microbiol. Biotechnol.*, 20: 235-244.

***In-Silico* Analysis and Identification of functional Single Nucleotide Polymorphism (SNPs) of the DISC1 gene**

Neema Tufchi^{*}, Kumud Pant, Syed Mohsin Waheed, Devvret
Department of Biotechnology, Graphic Era University, Dehradun, India.
^{*}Corresponding Author : neematufchi@gmail.com

Abstract

SNPs (Single-nucleotide polymorphisms) are essential for understanding the genetic origin of various complex human diseases. The identification of the functional SNPs responsible for the disease is still a challenge so there is an urgent need for identification of functional SNPs. In this work, analysis was made on the genetic variations which can alter both the function and expression of the DISC1 gene using computational approaches. The total of 23 SNPs was found, out of which 12 are missense (non-synonymous or nsSNPs), 8 occurred in 3'UTR region and 3 are synonymous SNPs. The 2 nsSNPs (rs6675281 and rs821616) were found to be damaging by PolyPhen and SIFT servers. I-mutant server showed decrease in the stability of rs6675281 and increase in the stability of rs821616 protein upon mutations. Structural analysis of proteins with mutations was done using SPDBV (Swiss PDB viewer), MUSTER (MULTI—Sources ThreadER) and PyMol tools for the detection of molecular dynamics and energy minimization calculations. This study revealed that L607F and S704C variants could indirectly or directly destabilize the amino acid interactions.

Keywords: SNPs, DISC1, Schizophrenia, PolyPhen, SIFT, MUSTER.

1. Introduction

A single nucleotide polymorphism (SNP) pronounced as “snip” is a change at a single position in a nucleotide sequence and is most commonly responsible for the variation in human

genes. About 500,000 SNPs lies in the exons of the total human genome¹. SNPs are categorized into synonymous and non-synonymous. Synonymous SNPs (sSNPs) do not cause any change in the protein sequence while non-synonymous SNPs (nsSNPs) are known for causing changes in the residues of the amino acid in the protein sequence. 50% of the SNPs were found to be in noncoding regions, 25 % are missense or non-sense and the other 25 % are silent mutations or synonymous SNPs². Moreover, the nsSNPs contributes in the diversity of the encoded proteins which are present in the human genome³. The nsSNPs alters the transcriptional binding factors and DNA⁴ and for maintaining the integrity of cells and tissues⁵. The nsSNPs also affects the signal transduction of proteins especially hormonal, visual and other stimulants⁶. The non-synonymous and synonymous SNPs affect both promoter activity and stability of pre-mRNA. SNPs are thought to be present in several hundred bases and they provides important medicinal information via genome wide association studies (GWAS) of several diseases, and also the genes can be identified which is associated with the efficacy and side-effects of the drugs⁹. Even though a SNP is not able to cause a disorder, but some SNPs are also linked with certain diseases. These associations help scientists to estimate an individual's genetic susceptibility of developing the disease.

Amongst large number of complex diseases, schizophrenia might be closely associated with SNPs mutations. Schizophrenia

may be due to small expression alterations in many genes which is different from many complex diseases. As no particular genes with significant expression alteration can cause schizophrenia thus we can conclude that dysregulation of genes plays an essential role in schizophrenia as compared with altered expression of genes by themselves¹⁰.

Schizophrenia is a human brain disorder and 1% of the population gets affected by this chronic disease. The symptom includes disorganized speech, abnormal behaviour, figments of the imagination, avolition, affective flattening and alogia¹¹. The environmental factors, genetic factors, polygenic components and other factors may influence the vulnerability of schizophrenia with 80% of heritability¹². The prominent site for affecting schizophrenia is the dorsal prefrontal cortex (PFC) which alters the pre- and postsynaptic element¹³. The symptom generally starts in the young adulthood and has a prevalence of about 0.3-0.7%. According to recent data analysis it is estimated that males are more susceptible to get affected by the disease 40% higher than in females. Schizophrenia is one of the leading disability diseases worldwide, but currently there is no treatment available, except the antipsychotic drugs which can only prevent the disease or lower down the symptoms of the disease¹⁴. Although there are over 130 genes responsible for causing the disease, but some of them have been replicated and only few have biological support. One of the candidate genes susceptible for causing schizophrenia is Disrupted in schizophrenia 1 (DISC1). This gene is disrupted on chromosome 1. This gene is also responsible for other bipolar disorders and other psychiatric disorders¹⁵. It is a large protein with molecular weight of 93kDa and is present throughout the adult and fetal brain mostly in hippocampus¹⁶. It changes the intracellular levels of cAMP under high concentration of cAMP production during the interactions with PDE4 enzymes. DISC1 is present in HCN1 channels of layer III dendritic spines in all primates. Thus DISC1 may help to bind PDE4 with the appropriate subcellular

location which acts like a molecular brake to maintain normal cAMP levels. Inversely, loss of the DISC1 function in pre-frontal cortex would hamper the proper functioning of PDE4 function which may lead to dysregulated formation of cAMP in spines¹⁷.

2. Methodology

2.1 Datasets : The data on DISC1 (Disrupted in schizophrenia 1) was collected from National Centre for Biological Information (NCBI) database. The information regarding SNPs of the DISC1 gene was retrieved from the NCBI dbSNP (<https://www.ncbi.nlm.nih.gov/projects/SNP/>). The SNPs information about four genes of DISC1 with accession no. NP_001012975, NP_001012976, NP_001012977, and NP_061132 were retrieved from SNPs3D (<http://www.SNPs3D.org>). SNPs3D is a web server which provides functional effects of nsSNPs (non-synonymous SNPs) on the basis of structure and sequence analysis. SNPs3D has three modules i.e., SNP analysis (for involvement of genes in specific disease), gene-gene network (for finding relationship between candidate genes) and disease candidate gene (for analyzing the impact of non-synonymous SNPs on protein function)¹⁸.

2.2 SIFT : Sequence homology tool (SIFT) is used for evaluating functional impact of coding nsSNPs. SIFT uses an input sequence and performs their multiple sequence alignments for distinguishing between tolerated and damaged substitutions for each position of the input sequence¹⁹. It generates output via different steps (i) sequences are searched for similarities (ii) closely associated sequences with same function are chosen (iii) multiple sequence alignment of protein sequences and (iv) estimating probabilities of all probable substitutions at each position. If the normalized probabilities of substitutions at each position is greater or equal to 0.05 are considered to be tolerated and if the score is less than a 0.05 are considered as deleterious or intolerant. If the tolerance index is higher the functional impact of amino acid substitution is said to be less. This tool uses algorithm for searching the homologous

sequences with the default settings (UniProt-TrEMBL 39.6 database, median conservation of 3.00), 90% of the sequence identical to query sequence should be removed. The totals of 14 DISC1 nsSNPs which were filtered from the dbSNP database were analyzed⁸.

2.3 PolyPhen-2 : Polymorphism Phenotyping version 2 (PolyPhen-2) (<http://genetics.bwh.harvard.edu/pph2/>) is a web server tool so as to predict the affect of an amino acid substitution on the function and structure of any human protein with the use of empirical rules. Input can be any database ID/accession number, protein sequence, amino acid variant, amino acid position details. This tool predicts the PSIC (the position-specific independent count) for each amino acid and estimates the variation in scores. On the basis of combination of all the properties it also estimates the possibilities of the missense mutation being damaged. The amino acid substitution is said to have higher functional impact if the PISC score difference is higher. It uses machine learning classification method to predict a multiple protein sequence alignment²⁰.

2.4 Cis regulatory elements identification

2.4.1 PROSCAN version 1.7 (<https://www-bimas.cit.nih.gov/molbio/proscan/>) : The PROSCAN Version 1.7 is a server developed by Dr. Dan Prestridge. It scans the promoter regions on the basis of homology with eukaryotic Pol II promoter sequences. It also finds the regions in the DNA sequence which can be good regions for testing the functionality of the promoter. This program is quite reliable as it recognizes about 70% of primate promoter sequences showing false positive result for only one in every 14,000 bases²¹.

2.4.2 Promoter 2.0 Prediction Server (<http://www.cbs.dtu.dk/services/Promoter/>) : It is a new approach for the prediction of eukaryotic Pol II promoters in any DNA sequence and it is used for the prediction of transcription factors which interacts with sequences present in the promoter regions. It is based on the common neural networks and genetic algorithms²². This site is

maintained and checked at the Technical University of Denmark by Steen Knudsen.

2.4.3 TSSG : This server (<http://www.softberry.com/>) is used for the detection of transcription start sites and promoter regions of human Pol II from Softberry. It is the generally used program (Prestridge's algorithm) which predicts more accurately mammalian cis element²³.

2.5 Modeling of nsSNP on protein sequences

2.5.1 I-Mutant and FOLD-X : I-Mutant 2.0 is a protein stability predicting tool which is based on support vector machine (SVM) and neural network. It is used for the analysis of protein alterations and stability after the changes through single-site mutations. It takes both protein sequence and structure as input for the prediction of mutation effect on stability of protein. It allows the selection of protein stability changes at different ranges of temperature and pH²⁴. FOLD-X is an algorithm which is used for the evaluation of protein stability. This tool is used for comparing the mutant and wild type models in accordance with Vander Waals force, which affects the energy decomposition to a great extent²⁵.

2.5.2 3-D modeling byMUSTER and energy minimization by Swiss PDB viewer : A Multi-Source ThreadER (MUSTER) is a protein threading program for identification of the template structures using PDB library. It considers six different sources: (i) profiles derived from sequences (ii) prediction of secondary structures (iii) profiles derived from structures (iv) solvent accessibility (v) dihyderal torsional (psi and phi) angles and (vi) hydrophobic scoring matrix. All the features are dependent on each other e.g., the solvent accessibility is correlated with structure profile and secondary structure is related with torsion angle prediction. MUSTER uses MODELLER v 8.2 for calculating the Z-score. If the Z- score is more than 7.5 then the template is considered as good otherwise it is rejected²⁶. For the prediction of threading alignments, Z-score can be calculated as

$$Z - \text{Score} = \frac{\{R'_{\text{Score}} - (R'_{\text{Score}})\}}{\sqrt{(R'_{\text{Score}})^2 - (R'_{\text{Score}})^2}}$$

Where

R'_{Score} = Normalized Score

(R'_{Score}) = Average over all templates

If the cut off value (Z-score) of the alignments is 7.5, then the false negative and false positive rates are 5.3% and 1.2% respectively. Thus the targets can be defined as “Easy” if the Z- score is higher than 7.5 and “Hard” if the Z-score is lower than 7.5.

3. Results

The database dbSNP consists of both non-validated and validated polymorphisms. The primary analysis of SNPs of DISC1 was done using dbSNP database but the SNPs of four genes (NP_001012975, NP_001012976, NP_001012977, and NP_061132) of DISC1 were retrieved from SNPs3d. It consists of a total 23 SNPs, in which 12 are nsSNP missense, 8 are present in the 3' UTR mRNA and 2 were synonymous SNPs as shown in Figure 1. For further investigation we have selected missense or nsSNPs.

3.1 SIFT program for finding deleterious nsSNP

: SIFT is a sequence homology based tool used for the identification of conservation level of a

specific protein in a particular position²⁶. SIFT server also predicts the tolerance index for which protein sequences were submitted. If the tolerance index of protein sequences is less, its functional impact of a substituted amino acid will also be less and vice versa. Among the selected 12 nsSNPs, two was found to be damaging with the tolerance index of 0.01 and 0.06. The results are illustrated in Table 1.

3.2 Analysis of nsSNPs by PolyPhen server:

The previously submitted nsSNPs were also uploaded to PolyPhen server. It calculates PSIC score difference, and if the score is 0.5 and above is considered to be damaging. Three nsSNPs (rs3738401, rs34574703 and rs28930675) were considered as benign which means they are lacking phenotypic effect. Two nsSNPs (rs34622148, rs6675281) are known to be probably damaging and one nsSNP (rs821616) was known to be possibly damaging which exhibits a PSIC score ranging between 0.5 to 1.0.

3.3 Cis regulatory element analysis and Softberry TSSG :

PROSCAN was used for the analysis of cis elements and the predicted cis region was found on forward strand at 419 bp to 832 bp in L607F variant. According to Softberry TSSG server one promoter was predicted at 2953 LDF.

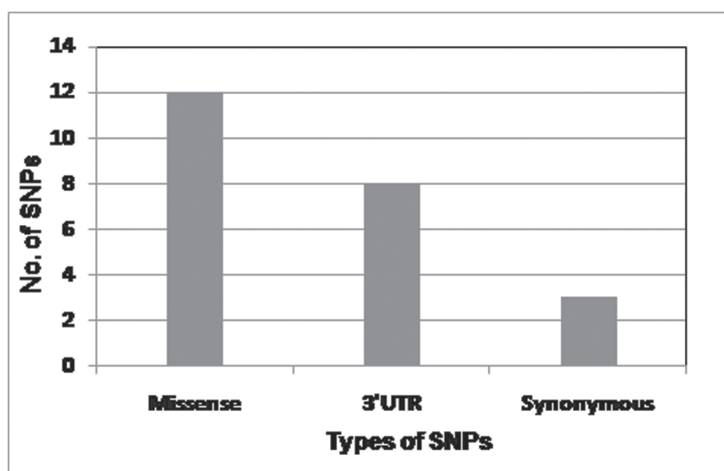


Fig. 1. Distribution of different SNPs

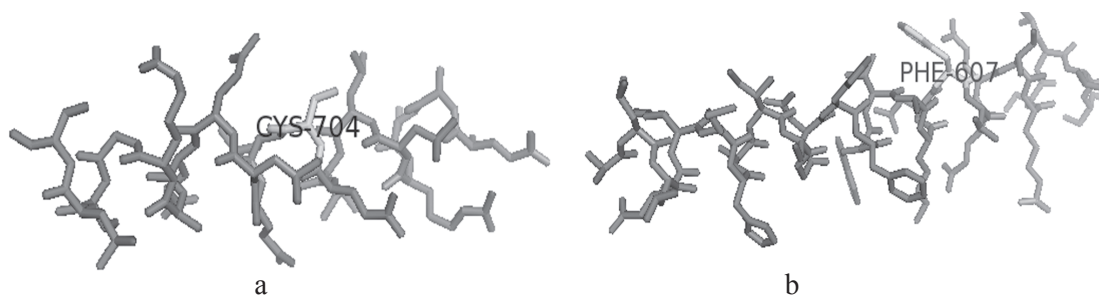


Fig 2: Modelled structures of two amino acid variants (a) L607F (b) S704C

3.4 Promoter 2.0 Prediction Server

3.5 Analysis of mutant structures : The two nsSNPs (rs6675281, rs821616) which were found to be deadly by PolyPhen or SIFT server were then mapped to the reference structure by server I mutant 2.0. After that the energy minimization were done by SPDBV for the native as well as mutant modelled structures.

3.6 Protein structure stability : I-Mutant is a tool used for the analysis of protein stability by taking into account the single-site mutation. This server is also used for calculating free energy by using FOLD-X web server. By understanding the FOLD-X calculations 93% accuracy can be achieved. The mutations (S704C and L607F) of DISC1 gene have been preferred in accordance with PolyPhen. These mutations were uploaded to I-Mutant server for prediction of the stability and RI (reliability index).

The decrease in stability means free energy ($\delta \delta G$) is more than zero and if $\delta \delta G$ is less than zero it means there is an increase in stability.

3.7 Mutant structure modelling

The 3D structure of DISC1 was not available in PDB databank hence was modelled using MUSTER. The two nsSNPs which were found to be highest damaging nature amongst all the nsSNPs were also modelled for further analysis. The mutations in the amino acid variants linked with this nsSNP are S C at the location of S704C and R'S at the position of L607F were also modelled as shown in figure 1. MUSTER was used for the modelling of both native sequence of DISC1

and the other nsSNPs. If the Z-score value is greater than 7.5, then the sequence template is known to be good otherwise bad. The Z-score of all the templates were found as 7.5 or more thus they can be of good type.

4. Discussion

Computational tools were used for the prediction of structural and functional impacts of SNPs in the DISC1 gene. There are total of 23 SNPs, out of which 12 are nsSNP missense, 8 were found to be in the 3' UTR mRNA and 2 were synonymous SNPs. Among 12 missense nsSNPs, 3 were detected as deleterious using PolyPhen and SIFT tool. The results obtained after structural analysis revealed that mutations S704C (rs6675281) and L607F (rs821616) had the maximum impact on the stability of the DISC1 protein. According to our results it can be concluded that the SNPs play an essential role for causing diseases related to DISC1 gene.

Acknowledgement

The authors express the deep sense of gratitude to the Department of Biotechnology of Graphic Era University for all the support, assistance, and constant encouragements to carry out this work.

References

1. Collins, F. S., Brooks, L. D., and Chakravarti, A. (1998). A DNA polymorphism discovery resource for research on human genetic variation. *Genome research*, 8: 1229-1231.

Table 1: List of nsSNPs analyzed by SIFT.

SNP	Amino acid change	Protein ID	Amino Acid	Prediction	Score	Median info
rs34574703	P106T	NP_001012975	P	TOLERATED	1.00	3.48
rs3738401	R264Q	NP_001012975	T	TOLERATED	0.37	3.36
			R	TOLERATED	0.56	
rs34622148	L330F	NP_001012975	Q	TOLERATED	0.37	1.89
			L	TOLERATED	1.00	
rs28930675	T453M	NP_001012975	F	TOLERATED	0.10	1.86
			T	TOLERATED	1.00	
rs6675281	L607F	NP_001012975	M	TOLERATED	0.06	1.85
			L	TOLERATED	1.00	
rs821616	S704C	NP_001012975	F	DAMAGING	0.01	1.85
			S	TOLERATED	0.94	
rs821616	R683S	NP_001158013	C	DAMAGING	0.06	2.25
			R	TOLERATED	0.63	
			S	TOLERATED	0.64	

Table 2: Result of nsSNPs using Promoter 2.0 Prediction Server

S.No.	Position (bp)	Score	Likelihood
1.	2000	0.631	Marginal prediction
2.	2400	0.665	Marginal prediction
3.	3400	1.293	Highly likely prediction
4.	4100	0.661	Marginal prediction
5.	5000	0.596	Marginal prediction
6.	5600	0.634	Marginal prediction
7.	6300	0.583	Marginal prediction

Table 3: Protein stability estimation based on free energy change.

Mutation	Position	WT	New	pH	Temperature	Stability	RI
607: L F	607	L	F	7.0	25	Decrease	9
704: S C	704	S	C	7.0	25	Increase	1

Here, "WT" is the wild type amino acid which is present in native protein; "New" is the change in amino acid.

Table 4: Energy minimization score of protein (native and mutant) structures.

Amino Acid Variants	Energy after minimization (kJ/mol)	Electrostatic constraint
Native Structure	-18503.891	-15756.26
S704C	-15923.394	-15468.24
L607F	-15321.709	-14703.40

Table 5: Z score value of different templates analyzed by MUSTER.

L607F variant					
Rank	Template	Align_length	Coverage Z score	Seq_id	Type
1	5fvmA	826	11.186	0.079	Good
2	5a9qA	821	10.423	0.119	Good
3	5ijoJ	830	10.181	0.087	Good
4	1sjjA	789	10.103	0.085	Good
S704C variant					
1	5fvmA	828	11.194	0.087	Good
2	5a9qA	820	10.338	0.120	Good
3	5ijoJ	830	10.207	0.082	Good
4	5ue8A	771	10.090	0.096	Good

- Shastry, B. S. (2007). SNPs in disease gene mapping, medicinal drug development and evolution. *Journal of human genetics*, 52: 871-880.
- Lander, E. S. (1996). The new genomics: global views of biology. *Science*, 274: 536-539.
- Barroso, I., Gurnell, M., Crowley, V. E. F., Agostini, M., Schwabe, J. W., Soos, M. A., and Chatterjee, V. K. K. (1999). Dominant negative mutations in human PPAR α associated with severe insulin resistance, diabetes mellitus and hypertension. *Nature*, 402: 880.
- Thomas, R., McConnell, R., Whittacker, J., Kirkpatrick, P., Bradley, J., and Sandford, R. (1999). Identification of mutations in the repeated part of the autosomal dominant polycystic kidney disease type 1 gene, PKD1, by long-range PCR. *The American Journal of Human Genetics*, 65: 39-49.
- Dryja, T. P., McGee, T. L., Hahn, L. B., Cowley, G. S., Olsson, J. E., Reichel, E., and Berson, E. L. (1990). Mutations within the rhodopsin gene in patients with autosomal dominant retinitis pigmentosa. *New England Journal of Medicine*, 323: 1302-1307.
- Smith, E. P., Boyd, J., Frank, G. R., Takahashi, H., Cohen, R. M., Specker, B., and Korach, K. S. (1994). Estrogen resistance caused by a mutation in the estrogen-receptor gene in a man. *New England Journal of Medicine*, 331:1056-1061.
- Rajasekaran, R., Sudandiradoss, C., Doss, C. G. P., and Sethumadhavan, R. (2007). Identification and in silico analysis of functional SNPs of the BRCA1 gene. *Genomics*, 90: 447-452.
- Iida, A., Sekine, A., Saito, S., Kitamura, Y., Kitamoto, T., Osawa, S., and Nakamura, Y.

- (2001). Catalog of 320 single nucleotide polymorphisms (SNPs) in 20 quinone oxidoreductase and sulfotransferase genes. *Journal of human genetics*, 46: 225-240.
10. Sun, X., and Zhang, J. (2014). Identification of putative pathogenic SNPs implied in schizophrenia-associated miRNAs. *BMC bioinformatics*, 15: 194.
 11. Sehgal, S. A., Khattak, N. A., and Mir, A. (2013). Structural, phylogenetic and docking studies of D-amino acid oxidase activator (DAOA), a candidate schizophrenia gene. *Theoretical Biology and Medical Modelling*, 10: 3.
 12. Sehgal, S. A., Mannan, S., Kanwal, S., Naveed, I., and Mir, A. (2015). Adaptive evolution and elucidating the potential inhibitor against schizophrenia to target DAOA (G72) isoforms. *Drug design, development and therapy*, 9: 3471.
 13. Mirnics, K., Middleton, F. A., Stanwood, G. D., Lewis, D. A., and Levitt, P. (2001). Disease-specific changes in regulator of G-protein signaling 4 (RGS4) expression in schizophrenia. *Molecular psychiatry*, 6: 293.
 14. Clapcote, S. J., Lipina, T. V., Millar, J. K., Mackie, S., Christie, S., Ogawa, F., and Kaneda, H. (2007). Behavioral phenotypes of *Disc1* missense mutations in mice. *Neuron*, 54: 387-402.
 15. Schurov, I. L., Handford, E. J., Brandon, N. J., and Whiting, P. J. (2004). Expression of disrupted in schizophrenia 1 (DISC1) protein in the adult and developing mouse brain indicates its role in neurodevelopment. *Molecular psychiatry*, 9: 1100.
 16. Wexler, E. M., and Geschwind, D. H. (2011). DISC1: a schizophrenia gene with multiple personalities. *Neuron*, 72: 501-503.
 17. Gamo, N. J., Duque, A., Paspalas, C. D., Kata, A., Fine, R., Boven, L., and Peng, K. (2013). Role of disrupted in schizophrenia 1 (DISC1) in stress-induced prefrontal cognitive dysfunction. *Translational psychiatry*, 3: e328.
 18. Yue, P., Melamud, E., and Moul, J. (2006). SNPs3D: candidate gene and SNP selection for association studies. *BMC bioinformatics*, 7: 166.
 19. Ng, P. C., and Henikoff, S. (2003). SIFT: Predicting amino acid changes that affect protein function. *Nucleic acids research*, 31: 3812-3814.
 20. Adzhubei, I., Jordan, D. M., and Sunyaev, S. R. (2013). Predicting functional effect of human missense mutations using PolyPhen2. *Current protocols in human genetics*, 7: 20.
 21. Prestridge, D. S. (1995). Predicting Pol II promoter sequences using transcription factor binding sites. *Journal of molecular biology*, 249: 923-932.
 22. Knudsen, S. (1999). Promoter2.0: for the recognition of PolII promoter sequences. *Bioinformatics (Oxford, England)*, 15: 356-361.
 23. Solovyev, V. V., Shahmuradov, I. A., and Salamov, A. A. (2010). Identification of promoter regions and regulatory sites. In *Computational biology of transcription factor binding* (pp. 57-83). Humana Press, Totowa, NJ.
 24. Berman, H. M., Westbrook, J., Feng, Z., Gilliland, G., Bhat, T. N., Weissig, H., and Bourne, P. E. (2006). The protein data bank, 1999-. In *International Tables for Crystallography Volume F: Crystallography of biological macromolecules* (pp. 675-684). Springer Netherlands.
 25. Schymkowitz, J., Borg, J., Stricher, F., Nys, R., Rousseau, F., and Serrano, L. (2005). The FoldX web server: an online force field. *Nucleic acids research*, 33: W382-W388.
 26. Ng, P. C., and Henikoff, S. (2003). SIFT: Predicting amino acid changes that affect protein function. *Nucleic acids research*, 31: 3812-3814.

Molecular Characterization of a Biopolymer Producing Bacterium Isolated from Sewage Sample

A. Ranganadha Reddy^a, S. Krupanidhi^a, T.C.Venkateswarulu^{a*}, R. Bharat Kumar^d,
P. Sudhakar^c, K. Vidya Prabhakar^{b*}

^aDepartment of Biotechnology, Vignans' Foundation for Science, Technology & Research, Valdamudi - 522213, India

^b Department of Biotechnology, Vikrama simhapuri University, SPSR Nellore-524003, India

^cDepartment of Biotechnology Acharya Nagarjuna University Guntur - 522510, India

^d Departemnt of Botany, Rayalaseema University, Kurnool - 518002, India

*Correspondence : kodalividyaprabhakar@gmail.com
venki_biotech327@yahoo.com : rangaaluri@gmail.com

ABSTRACT

Plastics and polypropylene polymers are synthesized from nonrenewable resources and persist in environment long after intended use, resulting into problems of global environmental pollution. Hence, the present study focused on production of polyhydroxybutyrate (PHB) microbial polyester by bacterial fermentation. In the present study, 05 PHB producing bacterial species were isolated from sewage waste, Guntur, India. Among all one isolate showed the maximum PHB yield of 4g/L. The high PHB producing bacterium was identified as *Acinetobacter nosocomialis* RR20, based on biochemical and molecular methods. Further, the characterization of PHB produced from this strain was also studied by analytical methods namely, FT-IR, DTA, TGA, ¹H NMR, ¹³C NMR and LC-MS.

Key words: Poly-3-hydroxybutyrate (PHB), *Acinetobacter nosocomialis* RR20, FT-IR, TGA, DTA, NMR, LC-MS.

1. Introduction

Polypropylene based plastics widespread in today's modern life of science and technology due to the favorable thermal and mechanical properties of plastics, such as their stability and durability. Plastics are non biodegradable synthetic polymers, which are made up of repeating monomer units (1). The non-

biodegradable plastics pose serious threat to the surroundings by accumulating in the global environment at a rate of 25 x 10⁶ tons per year (2). Poly-3-hydroxybutyrate (PHB) member of Polyhydroxyalkanoates, emerged recently as an alternative for synthetic plastics as its structural properties are similar to polypropylene (3,4,5) and yet it is completely biodegradable(6,7,8). Polyhydroxyalkanoates (PHAs) in terms of physicochemical properties are similar to petroleum-based plastics; as substitute to petroleum-based plastic, these can be used in packaging, in personal hygiene articles such as diapers, and in preparation of toners for printers and adhesives for coating (9). Polyhydroxyalkanoates (PHA) are bio-polyesters which are synthesized and accumulated in cells as intracellular granules (inclusion bodies) because of nutritional limitation or excess carbon in the growth media by a diverse group of bacteria and they are biodegraded by the bacteria itself (10,11,12). In previous studies many researchers reported the production of PHB from different bacterial species such as *Bacillus* sp., *Pseudomonas* sp., *Methylobacterium* sp., *Ralstonia* sp., *Alcaligenes* sp., through the submerged fermentation (13, 14, 15, 16, 17). However, no reports were found on the production of PHB from *Acetanobacter* species for higher yields, hence we aiming the production of PHB from the newly isolated bacterial strain.

2. Materials and Methods

2.1. Sample collection and isolation of PHB producing isolates

: Sewage sample was collected in sterile bottle from dump yard at outskirts of Guntur, Andhra Pradesh. Pure colonies of bacterial isolates were obtained by serial dilution-pour plate technique on Luria Bertani (LB) agar plates. Bacterial colonies with distinct characteristic features were maintained as pure cultures on nutrient agar slants and stored at 4 °C.

2.2 Screening of PHB producing isolates by Sudan Black B staining

: Poly-3-hydroxy butyrate producers were further confirmed by Sudan black staining method. Sudan black was used in the microscopic observation for a possible accumulation of intracellular PHB by the isolated strain. The thin smear of bacterial culture was prepared on clean grease free slide and air dried thoroughly. The strain was treated with Sudan black B solution (Sudan Black B 3%, 70% ethyl alcohol) for 10-15 minutes. Later the slides were washed with distilled water and counter stained with safranin for 20 seconds and then, slides were again washed with distilled water and dried on tissue paper. The bacterial cultures positive for PHB production were selected by observing the granules in the cytosol of bacterial isolate under fluorescence microscope.

2.3. Morphological and Biochemical Characterization

: The PHB producing bacterial isolate was characterized based on the morphological and physiological properties according to the Bergey's manual (18, 19).

2.4 Amplification of 16S rDNA and Phylogenetic Analysis

: Genomic DNA was isolated from 1mL of bacterial culture (20) and 16S rDNA sequence was amplified by PCR, in a 50 µL reaction mixture. The master mixture contained 5 µL amplification buffer, 5 µL MgCl₂ (1.5 mM), 3 µL of 0.5µM forward primer 27F (21) (5'-AGA GTTTGATCMTGG CTC AG -3'), 3 µL of 0.5µM reverse primer 1492R (22) (5'-TACGGYTACCTTGTTACGACTT -3'), 1 µL dNTPs (500 µM) and 0.25 µL Taq DNA polymerase. The

16S rDNA sequence of bacterial isolate was compared with known sequences in National Center for Biotechnology Information (NCBI) (<http://www.ncbi.nlm.nih.gov>) database using BLAST (23). Multiple sequence alignment was performed using ClustalW(24) and phylogram was constructed using neighbor-joining (NJ) method.

2.5 Cell Dry Weight Measurement

: After 48hrs of incubation at 37 °C bacterial cells were harvested and centrifuged at 10,000 rpm for 15 min at 15°C. The liquid supernatant was discarded and the solid cell pellet was washed with distilled water twice. The bacterial cells were then dried by lyophilization and cell dry weight was determined in g/L (25).

2.6 Extraction and Quantification of PHB

: The bacterial culture 10 mL sample was collected and centrifuged for 15min at 10,000 rpm and lyophilized and then, cell pellet was treated with 4% of sodium hypochlorite at 37 °C for 1 h. The cell pellet was collected by centrifugation, later washed with phosphate buffer saline, water, acetone and ethanol respectively. Finally, the extracted biopolymer was dissolved in hot chloroform and kept for complete evaporation (26). Dry weight of PHB estimated as g/L and the residual biomass estimated as difference between cell dry weight and dry weight of PHB (27). The percentage of intracellular PHB is estimated as the percentage composition of PHB.

2.7 Characterization of PHB

2.7.1 FT-IR analysis : The biopolymer extracted from *A. nosocomialis* RR 20 was subjected to Fourier Transform Infra Red analysis, in order to find out the functional groups that represent the signal peaks of PHB. Extracted Biopolymer was mixed with KBr (analytical grade) and IR spectrum was recorded using a single beam spectrometer (Carry 630 FT-IR spectrometer (Diamond Attenuated Total Reflection method Agilent Technologies USA (using NaCl cell) in the wave number range i.e. 4000 to 400cm⁻¹).

2.7.2 TGA and DTA analysis : Thermal stability of the extracted biopolymer from *A. nosocomialis*

RR 20 was investigated using a Simultaneous Thermal Analyzer, STA 7200(Hitachi HTG, Japan) under nitrogen atmosphere. Approximately 5–10 mg of biopolymer was loaded in to aluminium crucible and heated in the temperature range i.e. from 35 °C to 700 °C with a heating rate of 10 °C min⁻¹. The characteristic decomposition temperature (T_d) and melting temperature was (T_m) determined.

2.7.3 Nuclear Magnetic Resonance Spectroscopy (NMR) : ¹H NMR and ¹³C NMR spectra were recorded for the biopolymer extracted from *A. nosocomialis* RR 20 and standard PHB (sigma) sample using CDCl₃ (deuterated chloroform) as solvent by using Avance III HD Bruker (400 MHz) spectrometer. Tetramethylsilane (TMS) was used as reference compound for analysis. The chemical shifts were reported in parts per million and coupling constants were reported in Hz.

2.7.4 Liquid Chromatography Mass spectrometer (LC-MS): Biopolymer extracted from *A.nosocomialis* RR 20 and standard PHB (sigma) were diluted in Chloroform and injected directly into MS detector to obtain the spectra.

3. Results and Discussion

3.1 Morphological and biochemical characterization of bacterial isolate : In the present study, 15 strains were isolated from sewage waste, Guntur. Among those 05 bacterial isolates accumulated PHBs in their cytosol. PHB accumulation was confirmed by Sudan black B staining method. Organism positive for PHB production appeared blue-violet and negative yellow-brown (28). Based on the morphological and biochemical characteristic features as listed in Table-1, isolated bacterial strain belonged to the genus *Acinetobacter*. Similar findings were reported by earlier researchers (29).

3.2 Amplification of 16S rDNA and Phylogenetic Analysis : The PCR amplified product of bacterial isolate RR20 was shown in the gel image and length of amplicon was found to be 1439 base pairs (Figure-1). The phylogram was constructed based on 16S rDNA using the

MEGA5.0v software. The PHB producing isolate exhibited unique branching pattern from other *Acinetobacter* species and is closely related to *Acinetobacter nosocomialis* strain RUH 2376 with 98% similarity (Figure-2). The bacterial isolate was named as *Acinetobacter nosocomialis* RR20 based on the biochemical and phylogenetic analysis. The 16S rDNA sequence of this strain has been deposited in the GenBank database and the NCBI accepted as new bacterial strain with the accession number KY913802.

3.3 Extraction of PHB : The *A. nosocomialis* RR20 bacterial strain was grown for 2-5 days in a rotary shaker at 37 °C. The PHB was extracted using soxhlet apparatus and is obtained as a pellet after extraction. Earlier previous researchers reported that PHB was produced by a large number of gram positive and gram negative bacterial species (30, 31). Maximum PHB production 2.2 g/L was reported in *Bacillus sphaericus* NCIM 5149(32) and 2.64 g/L in *Acinetobacter junii* BP25 (33). Poly- β -hydroxybutyrate (PHB) producing, Gram negative *Oceanimonas* sp. GK1 was isolated from the soil samples of Gavkhooni Wetland Iran was reported already (34).

3.4 Characterization of PHAs by FTIR Analysis : FT-IR is used as a rapid screening tool for Poly-3Hydroxy Butyrate producing bacteria (35). Biopolymer extracted from *Acinetobacter nosocomialis* RR 20 is subjected to FT-IR analysis. The spectra of the biopolymer extracted from *Acinetobacter nosocomialis* RR 20 and standard

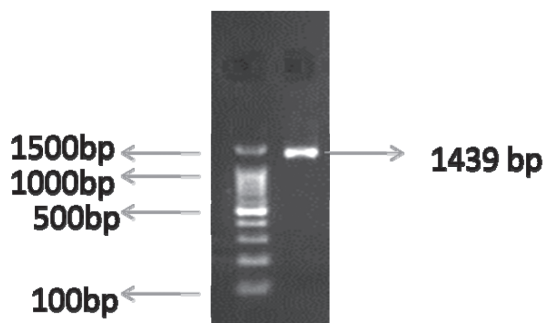


Fig. 1. Polymerase chain reaction with universal primers

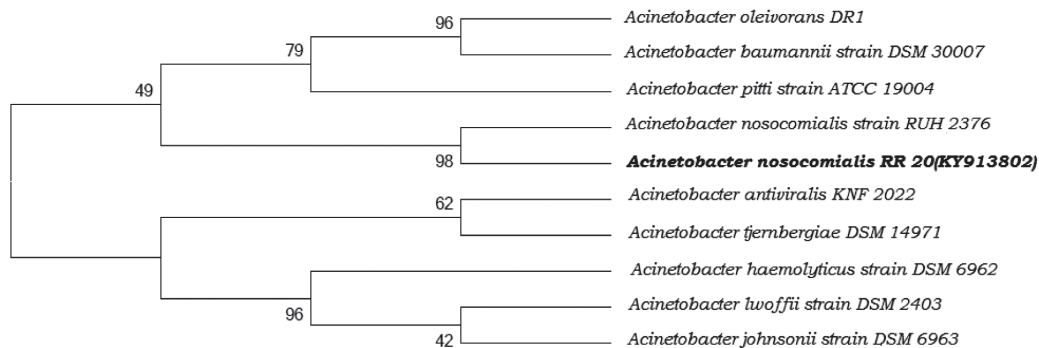


Figure 2. Phylogenetic analysis of *A. nosocomialis* RR20 with other related species using Neighbor joining algorithm.

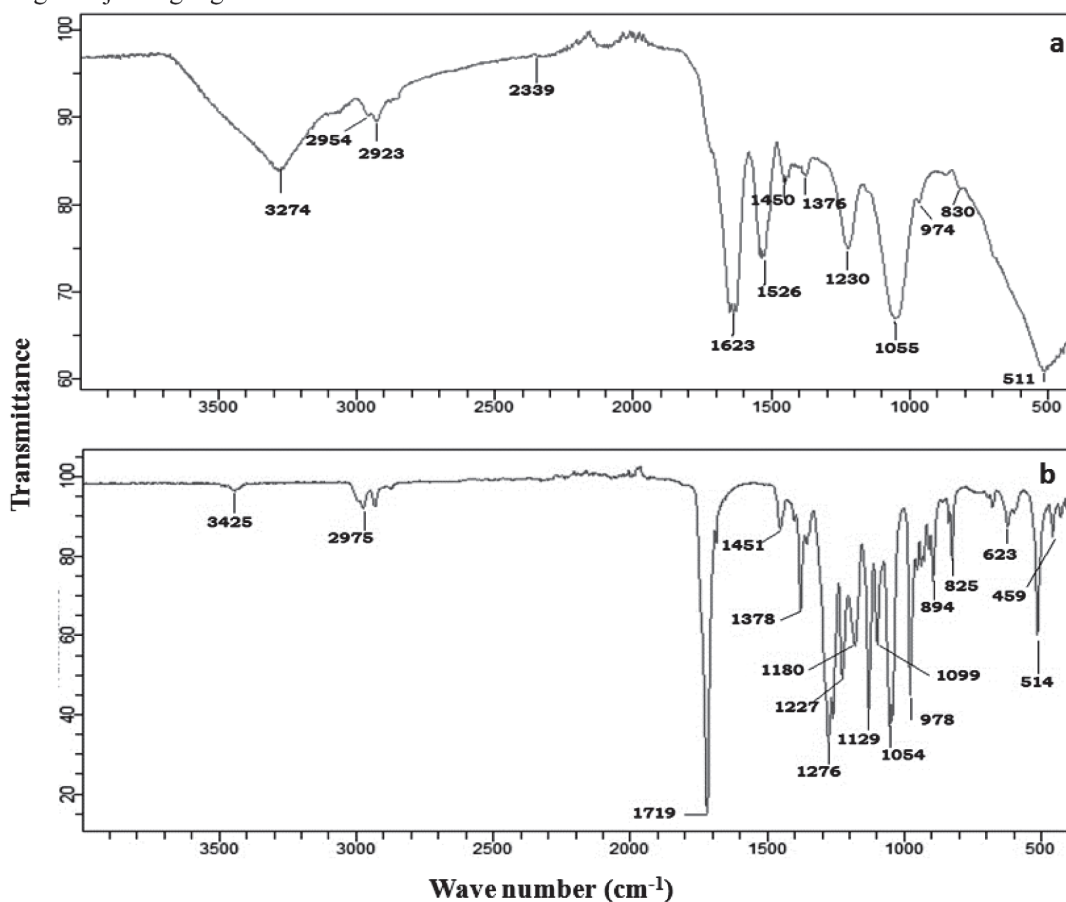


Figure 3. FT-IR Analysis of a) PHB from *A. nosocomialis* RR 20 b) Standard PHB

PHB (Sigma) are illustrated in Figure-3 (a),(b) respectively. The spectrum revealed that the absorption peaks at wave number 3274cm^{-1} corresponds to hydroxyl group (-OH). The Peaks at wave numbers 2923cm^{-1} , 2954cm^{-1} represents methylene group. The peaks at wave numbers 2339cm^{-1} , 1623cm^{-1} , 1526cm^{-1} corresponds to $-\text{Ca}^{12}\text{C}$ -stretch, $-\text{C}=\text{C}$ -stretch and N-O asymmetric stretch respectively. The absorption peaks at wave numbers 1450cm^{-1} , 1376cm^{-1} indicates CH vibrations of methylene ($-\text{CH}_2$) and methyl($-\text{CH}_3$) functional groups. The absorption peaks at wave numbers 1230cm^{-1} , 1055cm^{-1} and $500\text{-}1000\text{cm}^{-1}$ denotes C=O ester group, C-O stretch and OH group. The FT-IR analysis results of biopolymer correlated with the previous reports (36, 37, 38) and the absorption spectrum of standard PHB (Sigma).

3.5 Thermo gravimetric analysis (TGA) : Thermal stability of PHB extracted from *A. nosocomialis* RR20 was obtained in the range of

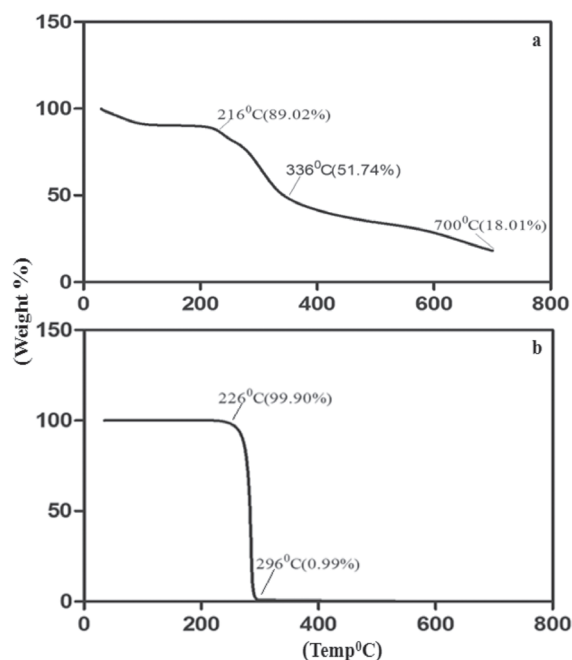


Fig. 4. Thermo gravimetric analysis of polymer (a) *A. nosocomialis* RR20 (b) Standard PHB

30–400 °C using Thermogravimetric analysis (TGA). The weight loss of standard PHB figure-4b started at around 226 °C and its T_{d5} was at 266 °C, completely decomposed at 296 °C. Figure-4a shows that the Thermal decomposition (T_d) of PHB extracted from *A. nosocomialis* RR20 is 216 °C. In addition, 82% was decomposed at 700 °C indicating that the PHB consists of 18% inorganic material which may come from bacterial dry mass.

3.6 Differential thermal analysis : Differential Thermal Analysis (DTA) was used to find out the melting temperature (T_m) of PHB extracted from *A. nosocomialis* RR20 and it was compared with standard PHB. The melting temperature of PHB varies from 160 °C -180 °C as reported by (39,40). Melting temperature (T_m) of PHB extracted from *Acinetobacter nosocomialis* RR20 is 160 °C which was very close to melting temperature (T_m) 169 °C of standard PHB sample as shown in figure-5a,5b. Differential Thermal Analysis (DTA) results of biopolymer correlated with earlier reports of (41, 42).

3.7 NMR Spectroscopy : The ^{13}C NMR spectrum of the biopolymer extracted from *A. nosocomialis*

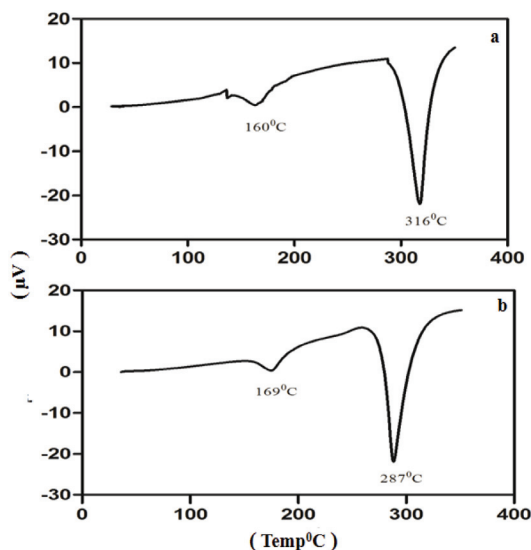


Fig. 5. DTA thermogram of PHB (a) *A. nosocomialis* RR20 (b) Standard PHB

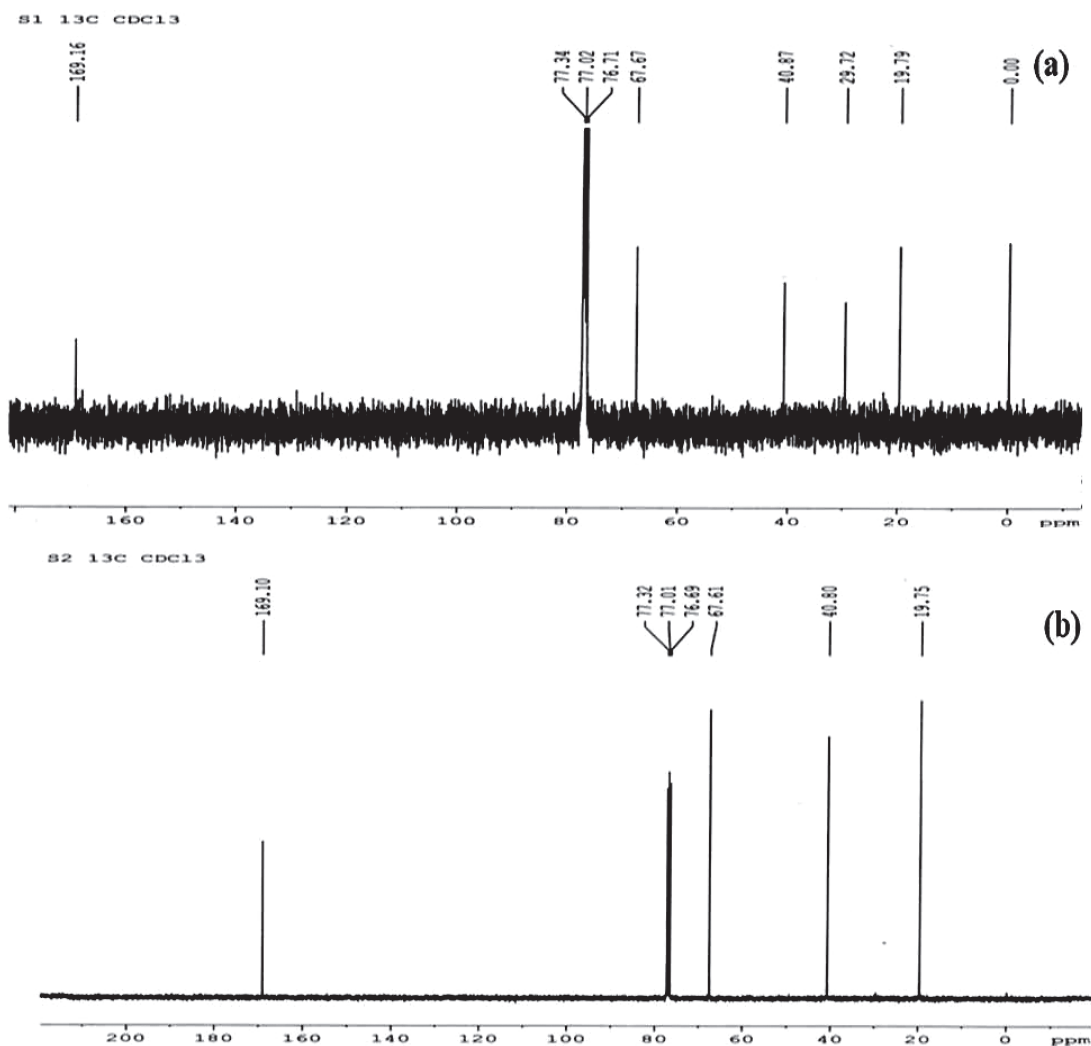


Fig. 6: ¹³C NMR spectrum of polymer (a) *A. nosocomialis* RR 20 (b) Standard PHB

RR 20 figure-6a shows predominant peaks of intensities at 19.79ppm, 40.87ppm, 67.67ppm, 169.16ppm characteristic to the methyl group (CH₃), methylene group (CH₂), methine group(CH) and carbonyl group(C=O). The ¹³C NMR spectrum of standard PHB figure-6b shows four sharp peaks of intensities at 19.75ppm, 40.80ppm, 67.61ppm, 169.10ppm characteristic to the methyl group(CH₃), methylene group(CH₂), methine group(CH) and carbonyl group(C=O). Chemical shift signals of ¹³C NMR spectrum of extracted

PHB from *A. nosocomialis* RR20 correlated with the results of (43) and standard PHB as shown in Table 2.

The ¹H NMR spectrum of the biopolymer extracted from *Acinetobacter nosocomialis* RR20 as shown in Figure-7a revealed the prominent peaks at intensities 1.256 ppm, 2.446 ppm, 5.218 ppm, 7.263ppm represented by methyl group (-CH₃-), methylene group (-CH₂-), methyne group (-CH-) and CDCl₃ group. The ¹H NMR spectrum of the standard PHB (sigma) Figure-7b shows

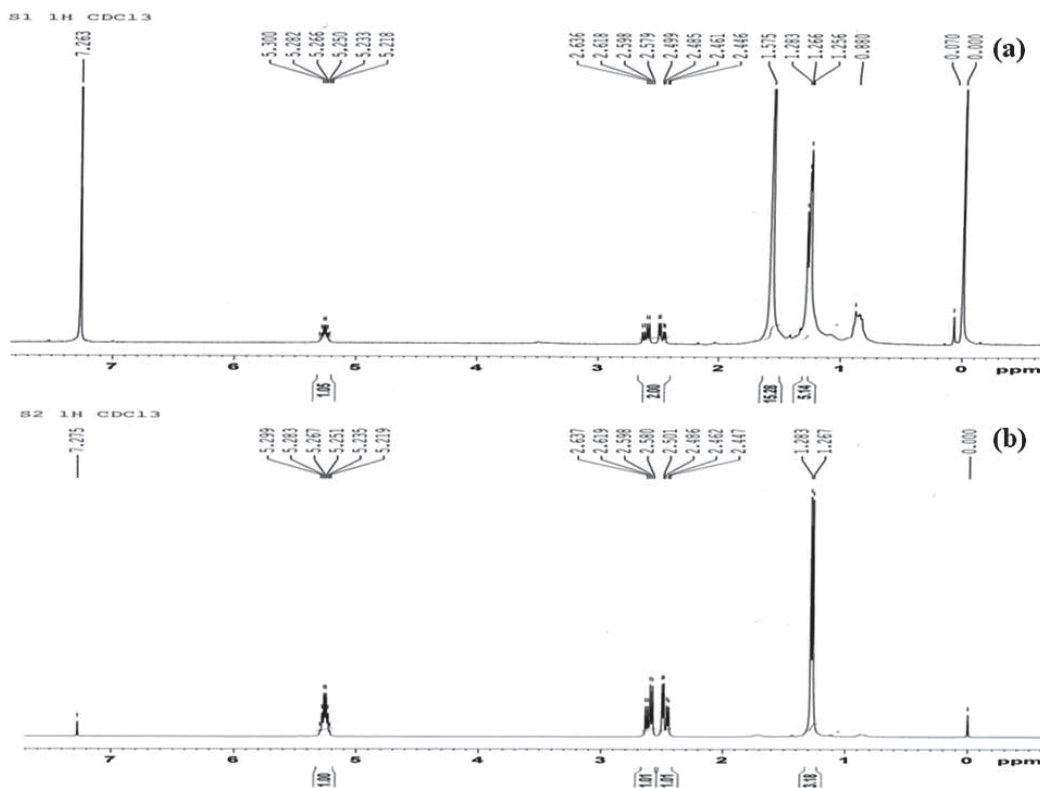


Fig. 7. ¹H NMR spectrum of polymer (a) *A. nosocomialis* RR 20 (b) Standard PHB

Table-1: Biochemical identification of *Acinetobacter nosocomialis* RR20

Test	RR 20
Gram's staining	-
Cell shape	<i>Coccobacillus</i>
Motility	-
Indole	-
Methyl Red	+
VP	-
Citrate	+
Catalase	+
Starch	-
Urea	+
Oxidase	-
Glucose	+
D-galactose	+
Mannitol	-
Sucrose	-

sharp peaks at 1.267 ppm, 2.447 ppm, 5.219 ppm, 7.275 ppm corresponding to methyl group (-CH₃-), methylene group (-CH₂-), methyne group (-CH-) and CDCL₃ group. ¹H NMR spectrum of extracted PHB and standard PHB was identical as shown in Table 3 and similar findings were reported earlier by (44,45).

3.8 Liquid Chromatography-Mass Spectrometry Analysis (LC-MS)

LC-MS analysis of PolyHydroxyAlkanoates showed a biopolymer with molecular mass of m/z 448.5 (Figure-8b). Mass of monomer unit was 86 and that of terminal groups was found to be 104.5. Basic monomer unit is surrounded by 4 monomer units. Hence, the net molecular mass of produced biopolymer was found to be 448.5, due to negative ionization phenomenon of mass spectra proton of both standard PHB and produced biopolymer yielded [M-H]⁻ anions at m/z 447.5 which can be

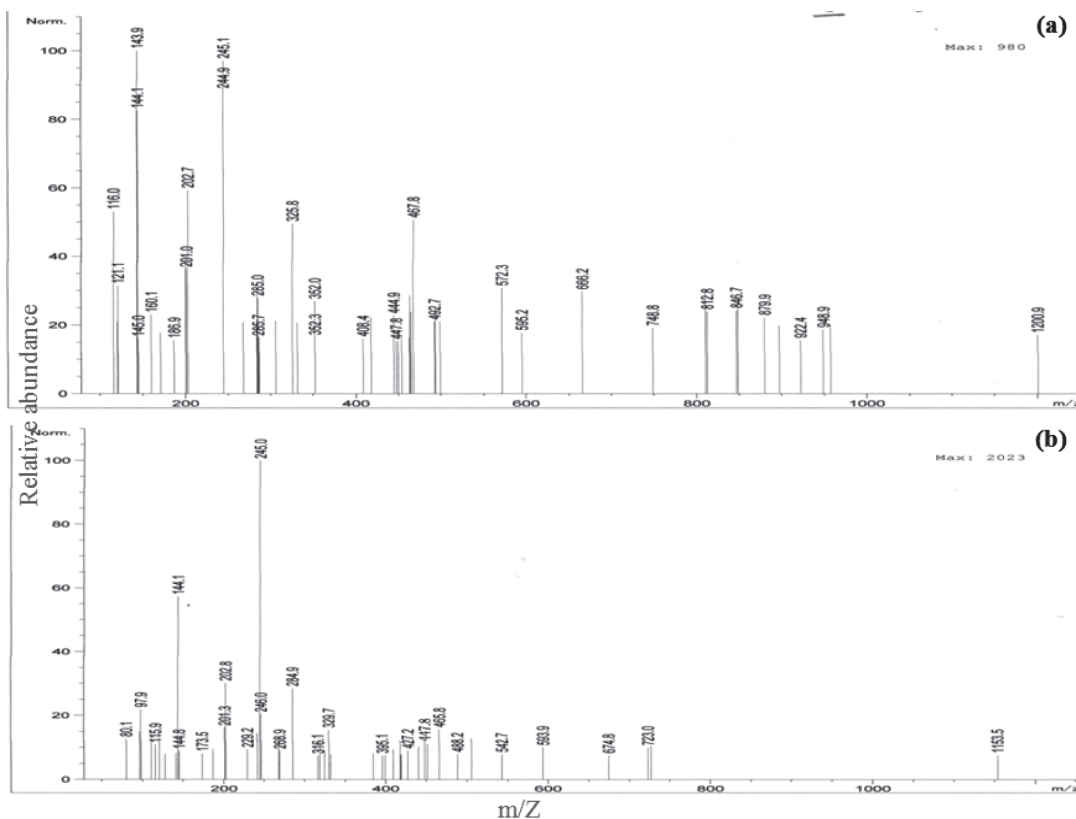


Fig. 8. LC-MS spectrum of polymer (a) *A. nosocomialis* RR 20 (b) Standard PHB

Table 2. ¹³C NMR spectrum comparison of PHB sample and standard PHB

C atom	PHB sample	Standard PHB
CH ₃	19.79	19.75
CH ₂	40.87	40.80
CH	67.67	67.61
C=O	169.16	169.10

Table 3. ¹H NMR spectrum comparison of PHB sample and standard PHB (sigma)

C atom	PHB sample	Standard PHB
CH ₃	1.256	1.267
CH ₂	2.446	2.447
CH	5.218	5.219
CDCL ₃	7.263	7.275

seen from the spectra giving the confirmation of the polymer (Figure-8a) that has four basic repeated units linked in a chain forming the PHB structure (46).

4. Conclusion

The high yielding bacterial strain was identified as *Acinetobacter nosocomialis* RR20. The biopolymer produced by *A. nosocomialis* RR20 was characterized by FT-IR, TGA, DTA, ¹³C NMR, ¹H NMR and LC-MS. These studies revealed that the extracted PHB is a monomer of four carbon compound.

Acknowledgments

The authors are grateful to the Vignan's Foundation for Science, Technology & Research University Guntur India for providing all the laboratory facilities. Dr. KVP acknowledges DBT, Government of India for financial support (project No. BT/PR7952/AAQ/03/642/2013).

References

1. Abdullah, A.A., Arshad, M., Essam, N.S. and Murugan, A.M. (2015). Extraction and Characterization of Polyhydroxybutyrates (PHB) from *Bacillus thuringiensis* KSADL 127 Isolated from Mangrove Environments of Saudi Arabia. *Braz Arch Biol Technol.* 58:781-788.
2. Joa, O., Cavalheiro, M., Almeida, C.M.D.D., Christian, G. and Fonseca, M.M.R. (2009). Poly (3 hydroxybutyrate) production by *Cupriavidus necator* using waste glycerol. *Process Biochem.* 44:509 – 515.
3. Sathiyarayanan, G., Kiran, G.S., Selvin, J. and Saibaba, G. (2013) 'A statistical approach for optimization of polyhydroxybutyrate production by marine *Bacillus subtilis* MSBN17. *Int J Biol Macromolec.* 59:170–177.
4. Sindhu, R., Silviya, N., Binod, P. and Pandey, A. (2013). Pentoseric hydrolysate from acid pretreated rice straw as a carbon source for the production of poly-3-hydroxybutyrate. *Biochem Eng J.* 78:67–72.
5. Arun, A., Arthi, R., Shanmugabalaj, V. and Eyini, M. (2009). Microbial production of poly-b-hydroxybutyrate by marine microbes isolated from various marine environments. *Bioresour Technol.* 100:2320–2323.
6. Yousuf, R.G. and Winterburn, J. B. (2016). Date seed characterisation, substrate extraction and process modelling for the production of polyhydroxybutyrate by *Cupriavidus necator*. *Bioresour Technol.* 222:242–251.
7. Mergaert, J., Anderson, C., Wouters, A., Swings, J. and Kersters, K. (1992). Biodegradation of polyhydroxyalkanoates. *FEMS Microbiol.* 103:317–321.
8. Abhishek, D.T., Suresh, K.S. and Ravipratap, S. (2013). Statistical optimization of physical process variables for bio-plastic (PHB) production by *Alcaligenes* sp. *Biomass Bioenergy.* 55:243-250.
9. Madison, L.L. and Huisman, G.W. (1999). Metabolic engineering of poly (3-hydroxyalkanoates): from DNA to plastic. *Microbiol Mol Bio Rev.* 63:21–53.
10. Venkateswar Reddy, M., Mawatari, Y., Onodera, R., Nakamura, Y., Yajima Y and Chang, Y.C. (2017). Polyhydroxyalkanoates production from synthetic waste using *Pseudomonas pseudoflava*: Polyhydroxyalkanoate synthase enzyme activity analysis from *P. pseudoflava* and *P. palleronii*. *Bioresour Technol.* 234:99-105.
11. Shilpi, K. and Ashok, K.S. (2005). Statistical media optimization studies for growth and PHB production by *Ralstonia eutropha*. *Process Biochem.* 40:2173–2182.
12. Braunegg, G., Bona, R. and Koller, M. (2004). Sustainable Polymer Production. *Polym Plast Technol Eng.* 43:1779-1793.
13. Mohapatra, S., Mohanta, P. R., Sarkar, B., Daware, A., Kumar, C. and Samantaraye, D.P. (2017). Production of Polyhydroxyalkanoates (PHAs) by *Bacillus* Strain Isolated from Waste Water and Its Biochemical Characterization. *Proc Natl Acad Sci, India, Sect B Biol. Sci.* 87:459-466.

14. Otari, S.V. and Ghosh, J.S. (2009). Production and characterization of the polymer polyhydroxy butyrate copolyhydroxy valerate by *Bacillus megaterium* NCIM 2475. *Curr Res J Biol Sci.* 1: 23–26.
15. Yung, H. Y., Christopher, J. B., Charles, F. B., Paolo, B., Laura, B.W., Mohd Ali Hassan, Mohd Yusof, Z.A. and ChoKyun, R.(2010). Anthony JS. Optimization of growth media components for polyhydroxyalkanoate (PHA) production from organic acids by *Ralstonia eutropha*. *Appl Microbiol Biotechnol.* 87:2037–2045.
16. Anderson, A.J. and Dawes, E.A. (1990). Occurrence, metabolism, metabolic role and industrial uses of bacterial polyhydroxyalkanoates. *Microbiol Rev.*54:450–472.
17. Sei, K.H., Yong, K.C., Beom, S.K. and Ho, N.C. (1994). Optimization of Microbial Poly (3-hydroxybutyrate) Recovery Using Dispersions of Sodium Hypochlorite Solution and Chloroform. *Biotechnol Bioeng.* 44:256-261.
18. Krieg, N.R. and Holt, J.G. (1984). *Bergey's Manual of Systematic Bacteriology*, Williams and Wilkins, Baltimore, MD.
19. Holt, J.G., Krieg, N.R., Sneath, P.H.A., Stanley, J.T. and Williams, S.T. (2000). *Bergey's manual of determinative bacteriology*, 9th edn. Lippincot, Williams and Wilkins, Baltimore.
20. Enkicknap, J.J., Kelly, M., Peraud, O. and Hill, R.T. (2006). Characterization of a culturable alphaproteobacterial symbiont common to many marine sponges and evidence for vertical transmission via sponge larvae. *Appl Environ Microbiol.*72:3724–3732.
21. Reysenbach, A.L., Longnecker, K. and Kirshtein, J. (2000) Novel Bacterial and Archaeal Lineages from an In Situ Growth Chamber Deployed at a Mid-Atlantic Ridge Hydrothermal Vent. *Appl Environ Microbiol.* 66:3798–3806.
22. Miyoshi, T., Iwatsuki, T. and Naganuma, T. (2005). Phylogenetic Characterization of 16S rRNA Gene Clones from Deep-Groundwater Microorganisms That Pass through 0.2-Micrometer-Pore-Size Filters. *Appl Environ Microbiol.*71:1084–1088.
23. Altschul, S.F., Gish, W., Miller, W., Myers, E.W. and Lipman, D.J.(1990). Basic local alignment search tool. *J Mol Biol.*215:403-410.
24. Thompson, J. D., Gibson, T. J., Plewniak, F., Jeanmougin, F. and Higgins, D.G. (1997). The CLUSTAL_X windows interface. Flexible strategies for multiple sequence alignment aided by quality analysis tools. *Nucleic Acids Res.* 25:4876–4882.
25. Du, G., Chen, J., Yu, J. and Lun, S. (2001). Continuous production of poly-3-hydroxybutyrate by *Ralstonia eutropha* in a two stage culture system. *J Biotech.*88: 59-65.
26. Arnold, L., Demain, J. and Davis, E. (1999). Polyhydroxyalkanoates. Manual of Microbiology and Biotechnology. Washington, Am Soc Microbiol, USA, 2, pp 616-627.
27. Zakaria, M.R., Ariffin, H., Johar, N.A.M., Aziz, S.A., Nishida, H., Shirai, Y. and Hassan, M.A. (2010). Biosynthesis and characterization of poly (3-hydroxybutyrate-co-3-hydroxybutyrate) copolymer from wild type *Comamonas* sp. EB172. *Polym Degrad Stab.* 95:1382-1386.
28. Sathiyarayanan, G., SeghalKiran, G., Joseph, S. & Saibaba, G. (2013). Optimization of polyhydroxybutyrate production by marine *Bacillus megaterium* MSBN04 under solid state culture. *Int J Biol.* 60:253– 261.
29. Holt, J.G., Krieg, N.R., Sneath, P.H.A., Staley, J.T. and Williams, S.T. (1994). *Bergey's manual of determinative bacteriology*, 9th edn. Williams and Wilkins, Baltimore.
30. Aarthi, N., and Ramana, K.V. (2012). Polyhydroxybutyrate production in *Bacillus mycoides* DFC1 using response surface optimization for physico-chemical process parameters. *3 Biotech,* 2:287-296.

31. Verlinden, R.A.J., Hill, D.J., Kenward, M.A., Williams, C.D. and Radecka, I. (2007). Bacterial synthesis of biodegradable polyhydroxyalkanoates. *J Appl Microbiol* .102:1437-1449.
32. Nisha, V.R., Carlos, R.S. and Ashok P. (2010). A Statistical Approach for Optimization of Polyhydroxybutyrate Production by *Bacillus sphaericus* NCIM 5149 under Submerged Fermentation Using Central Composite Design. *Appl Biochem Biotechnol*.162, 996–1007.
33. Poornacandrika, S., Sabarinathan, D., Anburajan, P. and Preethi, K. (2017). Bioprocess optimization of PHB homopolymer and copolymer P3 (HB-co-HV) by *Acinetobacter junii* BP25 utilizing rice mill effluent as sustainable substrate. *Environ Technol*. DOI:10.1080/09593330.2017.1330902.
34. Ramezani, M., AliAmoozegar, M. & Antonio, V. (2015). Screening and comparative assay of poly-hydroxyalkanoates produced by bacteria isolated from the Gavkhooni Wetland in Iran and evaluation of poly- α -hydroxybutyrate production by halotolerant bacterium *Oceanimonas* sp. GK1. *Ann Microbiol*.65:517–526.
35. Tripathi, A.D. and Srivastava, S.K. (2011). Kinetic Study of Biopolymer (PHB) Synthesis in *Alcaligenes* sp. in Submerged Fermentation Process Using TEM. *J Polym Environ*. 19:732–738.
36. Silverstein, R.M., Bassler, G.C. and Morrill, T.C. (1991). *Spectrometric Identification of Organic Compounds*, fifth ed. John Wiley and Sons, Inc., New York.
37. Hong, K., Sun, S., Tian, W., Chen, G. Q., Huang, W. (1999). A rapid method for detecting bacterial polyhydroxyalkanoates in intact cells by Fourier transform infrared spectroscopy. *Appl Microbiol Biotechnol*. 51:523–526.
38. Silverstein, M.R., Francis, W.X. and David, K.J. (2005). *Spectrometric Identification of Organic Compounds*, seventh ed. John Wiley and Sons, Inc., New York.
39. Khanna, S. and Srivastava, A.K. (2005). Recent advances in microbial polyhydroxyalkanoates. *Process Biochem*.40:607–619.
40. Valappil, S.P., Misra, S.K., Boccaccini, A.R., Keshavarz, T., Bucke, C. and Roy, I. (2007). Large-scale production and efficient recovery of PHB with desirable material properties, from the newly characterized *Bacillus cereus* SPV. *J Biotechnol*.132:251–258.
41. Erceg, M., Kovacic, T. and Klaric, I. (2005). Thermal degradation of poly(3-hydroxybutyrate) plasticized with acetyl tributyl citrate. *Polym Degrad Stab*. 90:313–318.
42. Marjadi, D. and Dharaiya, N. (2014). Recovery and characterization of poly(3-hydroxybutyric acid) synthesized in *Staphylococcus epi-dermidis*. *Afr J Environ Sci Technol*.6:319–329.
43. Doi, Y., Kunioka, M., Nakamura, Y. and Soga, K. (1986). Nuclear magnetic resonance studies on poly(β -hydroxybutyrate) and a copolyester of β -hydroxybutyrate and β -hydroxyvalerate isolated from *Alcaligenes eutrophus* H16. *Macromolecules*. 19:2860-2864.
44. Jan, S., Roblot, C., Courtois, J., Courtois, B., Barbotin, J.N., and Shguin, J.P. (1996). ¹H NMR spectroscopic determination of poly 3-hydroxybutyrate extracted from microbial biomass. *Enzy Microb Technol*.18:195- 201.
45. Bonthron, K.M., Clauss, J., Horowitz, D.M., Hunter, B. K. and Sanders, J.K.M. (1992). The biological and physical chemistry of polyhydroxyalkanoates as seen by NMR spectroscopy. *FEMS Microbiol Rev*.103:269 – 277.
46. Abid, S., Raja, Z.A. and Hussain, T. (2016). Production kinetics of polyhydroxyalkanoates by using *Pseudomonas aeruginosa* gamma ray mutant strain EBN-8 cultured on soybean oil. *3 Biotech*. 6:142.

Image Capturing of Major Plant Pathogens Using Smart Mobile Phone Camera

Kondal Reddy Gaddam¹, Venkateshwarlu Vadapally¹, Santosh Singh², Shyam Haibatpure², Kartik Maheshwari², Varunbhai Priyam Mehta², Madhan Mohan Kolluru^{2*}

¹Ganga Kaveri Seeds Private Limited, Sunanda Farm, Kandlakoya, Medchal-501401, Medchal District, Hyderabad, Telangana, India

²Sayaji Seeds LLP, Behind C L High School, Village Kathwada, Tal Dascroi, Ahmedabad, Gujarat-382430, India.

*For correspondence: ksm.mohan@gmail.com; madanmohan.kolluru@gmail.com

Abstract

Many developing countries, resource poor organizations and universities does not possess sophisticated microscope due to non affordable price or lack of trained personnel to handle the equipment. Therefore, a simple photographing of microorganism has been developed using smart phone camera. The study was conducted to photograph the plant pathogens using inbuilt smart phone cameras. The method has been tested against 18 microorganisms of which, 15 are fungal, three bacteria, pollen grains of paddy and maize for their fertility. The images quality captured with smart phone camera were, being analogous to expensive camera designed for the microscope. Further, live video of yeast cells was also recorded using smart phone camera. We believe that this technology can be an inexpensive, easy and quick to learn for light microscopy in plant pathology for resource poor agriculture R&D institutions, research scholars and academic students for their thesis purpose.

Key words: Microorganisms, Diseases, Plant Pathogens, Smartphone camera and Image capturing.

Introduction

Microscopy is a primary essential technique which is used in both pathology and microbiology laboratories for the diagnostic and research works. Affordable and dependable medical imaging technologies are predominantly lacking, with severe consequences to the health care of a large

part of the world population (1, 2, 3). It is estimated that some three-quarters of the world's population have no access to medical imaging (1). Digital imaging is an important aid in the field of academic, research as well as consultation and assessment of clinical cases. Digital imaging has enhanced this diagnostic role, as sample images are now frequently transferred among technologically-advanced hospitals for further consultation and evaluation (4). Innovative progress in the field of mobile telephones allows us to take images of good quality with the mobile telephones and transmit them directly to other computers or mobile telephones (5). It has been previously demonstrated that a camera-enabled mobile phone can be used to capture images from the eyepiece of a standard microscope (6). The advent of affordable compact box type digital cameras with displays that reflect precisely the image as seen through the camera lens has made possible a simplified method of taking photographs through a microscope (7, 8). Seigel (9) reported the use of his own (Apple: iPhone 5) to capture a sample image of a retinoblastoma tumor.

Breslauer et al (10) developed a high-resolution microscope attachment for camera-enabled mobile phones for capturing digital color images of malaria parasites, sickled red blood cells, from blood using fluorescence and tubercle bacilli in Auramine O stained sputum smear. In India, Godse *et al* (11) reported the use of mobile phone camera microphotography a technique for tele diagnosis of Malaria.

However to our information, till date no reports are available pertaining to the application of smart phone camera for capturing microscopic images and obtaining quality digital photographs of plant pathogens. This technique enables plant pathologists who do not own conventional microscope cameras, to obtain high-quality photomicrographs for use in variety of agricultural and educational applications.

Materials and methods

Sample collection : Disease infected leaf and root samples of *Ricinus communis* (Castor), *Oryza sativa* (Paddy) (Fig. 1A & 1B), *Zea mays* (Maize), *Pennisetum glaucum* (Pearl millet) and *Capsicum annum* L (Hot pepper) crops were collected during 2017 *Kharif* and *Rabi* seasons from Sayaji seeds LLP, Ahmedabad and agriculture fields near Hyderabad. *Macrophomina phaseolina* pathogen isolate was obtained from CIMMYT, Hyderabad, India (Dr. Zerka Rashid, Personal communication). *Streptococcus* and *Diplobacillus* was isolated from soil. While, commercial dried yeast was obtained from commercial stores.

Isolation and maintenance of microbial cultures

: All the microbial isolates were isolated following standard procedures. *Magnaporthe oryzae*, *Rhizoctonia solani*, *Exserohilum turcicum* and *Sarcospora graminicola* were collected from infected leaves by surface sterilization with 0.1 % mercuric chloride followed by 4 to 5 times repeated wash with sterile distilled water respectively. The infected leaf bits were cultured on culture medium and incubated at 27°C for 5 days in dark and 3 days in light for mycelial growth. The established cultures were kept at 4°C for storage and further sub culturing (12, 13, 14). The Bacterial Blight (BB) pathogen was isolated as per the procedure described by earlier research workers (15). The purified isolates were subcultured on modified Wakimotos Media (MWA) for routine use (Fig. 2).

Sheath blight pathogen was isolated following procedure (hyphal tip culture method) using water agar and potato dextrose agar media

(16). *Rhizopus*, *Aspergillus* species, *Curvularia* and *Penicillium* species were isolated from stored paddy seed samples with modifications (17, 18). The infected paddy seed was kept on PDA and Rose Bengal agar and then incubated at 30+1°C in BOD incubator (Equitron, cooling (BOD) incubator classic series) for 3 - 4 days (Fig. 3A & 3D; Fig. 4A & 4D). While, 5 seeds each of maize and castor was directly kept on Rose bengal agar and PDA agar separately in three replications each and incubated at 28°C for 3 to 4 days till optimum fungal growth was observed on the seeds (Fig. 3B & 3E; Fig. 4B & 4E; Fig. 3C & 3F; Fig. 4C & 4F).

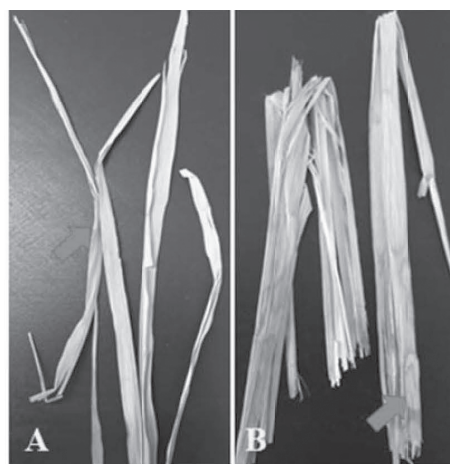


Fig. 1. Disease infected paddy leaf samples A: Bacterial Leaf Blight; B: Sheath Blight



Fig. 2. *Xanthomonas oryzae* pv. *oryzae* bacteria on culture medium

For *Fusarium*, *Streptococcus* and diplobacillus isolations, 1g of soil sample collected from agricultural fields in Hyderabad, India was homogenized in 10ml distilled water. The homogenates were serially diluted and 0.5 ml portions of suitable dilutions were spread in duplicates on nutrient agar medium (19, 20), all plates were incubated for 3 days in a BOD incubator at 30°C. *Colletotrichum capsici*, *Colletotrichum acutatum* and *Alternaria alternata* infected chilli pods were collected from fields situated at Hyderabad in India. The diseased part of the fruits was cut into small pieces (3 - 5mm diameter). The pieces were surface sterilized in 0.1% mercuric chloride solution with 3 - 4 repeated washes and kept on PDA then transferred into BOD incubator at room temperature ($28 \pm 2^\circ\text{C}$). After 2 days, margin of mycelial growth was transferred to another Petri plate in aseptic condition. After 3 to 4 days the culture was revised for the purification of *Colletotrichum capsici* under aseptic condition (21) (Fig. 5).

Microscopic technique :

Lactophenol cotton blue (LPCB) staining for fungal identification : For slide preparation, glass slides (75 - 25 mm, 18 mm diameter cavities, 1.75 mm thickness) and coverslips (22 cm²) were used. The fungal colonies were stained using Lactophenol Cotton Blue (LPCB) method. Where, a LPCB drop was placed on a clean grease-free glass slide and then, a small quantity of the fungal culture was transferred into the drop using sterile needle and teased to facilitate the dispersal of hyphal filaments and then covered with a glass cover slip and examined under low (10x) and high-power (40x) objective for hyphae and conidial morphological features (Fig. 6A, 6B & 6C). While, Pollen fertility was estimated by Iodine Potassium Iodide (IKI) staining technique (22). Where, 10 spikelets were collected from an emerged panicle of rice plant in a vial containing 70% ethanol for pollen fertility test. At laboratory, one drop of 1% Iodine Potassium Iodide (IKI) stain was kept on a glass slide. Total anthers of 3 to 5 spikelets were taken out with the help of forceps and placed on stain of the glass slide. Anthers were gently

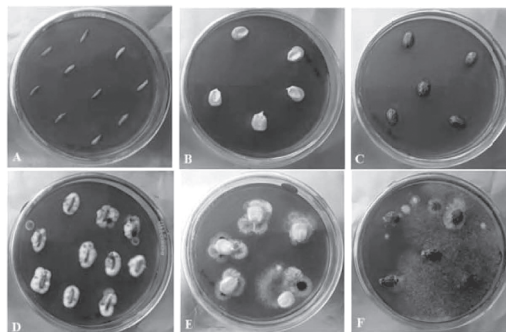


Fig. 3. Seed plated on Rose Bengal agar to detect seed borne pathogens A & D: Paddy; B & E: Maize; C & F: Castor

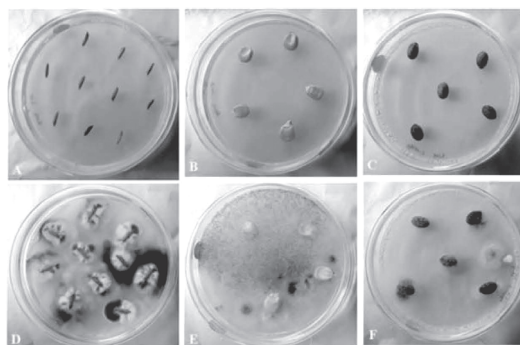


Fig. 4. Seed plated on Potato Dextrose agar to detect seed borne pathogens A & D: Paddy; B & E: Maize; C & F: Castor

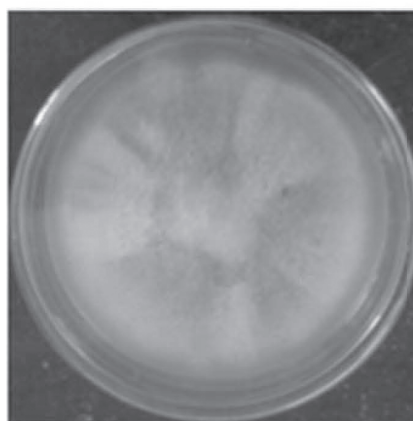


Fig. 5. *Colletotrichum capsici* fungal colony on PDA medium

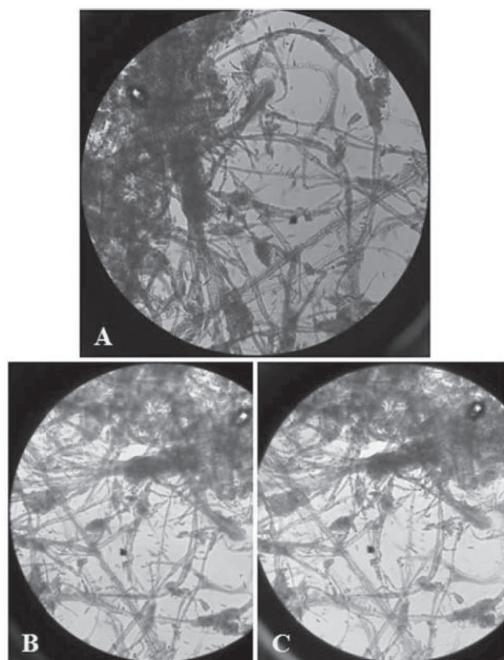


Fig. 6. Image capturing of Lactophenol cotton blue (LPCB) stained fungus A: Samsung Galaxy J7 Prime (Model: SM-G610F); B: HTC 820G plus dual sim; C: Coolpad Mega 2.5D (Model: y83-100)

crushed by using needle to release pollen grains. After removing debris, a cover slip was placed on pollen grains and pollen fertility was observed under a compound microscope.

Gram staining for bacteria : A very thin smear of bacteria was made on a clean, grease-free glass slide and air dried the smear and fixed by flaming the slide. At first, Crystal violet was added to the smear and allowed to stain for 1 min. Later the stain was rinsed under running tap water (taking care that the water flow does not fall directly on the smear) and flooded with Gram's iodine solution to cover the smear and left for 1 minute then again, the smear was rinsed with water in the same way as above. The smear was decolorised with ethanol: acetone (50:50 v/v) for about 15 seconds followed by quick rinse with water and counter stained with safranin for 1 min, and rinse in water. Finally the smear was air dried, and observed under oil immersion (100x) (Fig. 7).

Image capture and analysis : Depending on the specimen, microscopic observations was made using 4X, 10X, 40X and 100X oil immersion Achromat objectives of the Olympus binocular microscope (Model CX21i, Olympus Corporation, Japan) separated by 18.5 mm (0.10N.A.); 10.6 mm (0.25 N.A.); 0.6 mm (0.65 N.A.); 0.13 mm (1.25 N.A.).

Using the microscope, we examined the slide and selected the area of interest by adjusting the light source to get adequate intensity of light. The camera lens was held against the microscope eyepiece. (On doing so a small circle of light would be seen on the camera's LCD screen). The zoom function of the camera was used to increase the size of the circle as required. The autofocus of the camera was self-adjusted and held very still to give a clear image of photograph.

Three different smart mobile phones with built in cameras (Coolpad Mega 2.5D (Model: y83-100) and HTC Desire 820G plus dual sim & Samsung Galaxy J7 Prime (Model: SM-G610) were used for capturing the specimens images/photographs (Fig. 8A, 8B & 8C). The image resolution varied from 8MP to 13 MP with a resolution of 720 X 1280 pixels. This method involves the using the third through fifth fingers of the left hand to steady the hand on the left microscope eyepiece, holding the camera between the thumb and second finger of the left hand and second through fifth fingers of

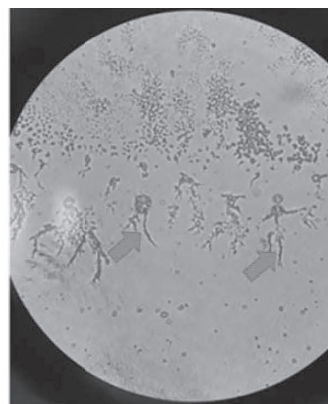


Fig. 7. Gram staining of *streptococcus* bacteria (Magnification: 100X)

the right hand, to leave the right thumb free. Images were captured simply by approaching the lens of the mobile phone camera to the ocular of the microscope carefully centering the observed field until the image would appear perfectly in focus on the screen of the mobile phone. The right thumb is free to focus the camera and capture the image (23, 24) (Fig. 8D).



Fig. 8. Smart phones used in the present investigation A: Samsung Galaxy J7 Prime (Model: SM-G610F); B: HTC 820G plus dual sim; C: Coolpad Mega 2.5D (Model: y83-100); D: Image capturing using smart phone camera

Results

In the present investigation, images of microscopic organisms were photographed using smart phone cameras with different objective lenses (10x, 40x and 100x). A total of 15 fungal, 3 bacterial species, fertile and sterile pollen grains and anthers were photographed. Micro organisms viz., *Xanthomonas oryzae*, diplobacillus, *Streptococcus sps*, *Magnaporthe oryzae*, *Rhiztonia solani*, *Fusarium sps*, *Rhizopus*, *Aspergillus sps*, *Penicillium*, *Exserohilum turcicum*, *Macrophomina phaseolina*, *Alternaria alternata*, *Colletorichum accutatum*, *Colletorichum capsici*, *Sclerospora graminicola*, Yeast, stigma and sterile and fertile pollen grains were also photographed in the present investigation. Excellent images were captured with smart phone camera were, the quality being comparable with that of expensive camera especially designed for the microscope. *Streptococcus* and diplobacillus appeared to be gram positive (Fig. 7; Fig. 9A). While *Xanthomonas oryzae* displayed pink colour

indicating gram negative, rod shape (Fig. 9B). In the present investigation, live video of yeast cells using smart phone camera (data not shown). In yeast budding was observed (Fig. 9C & 9D). In various *Aspergillus species* philiades was observed with globose conidia images was clearly captured (Fig. 11E; 12A to 12H).

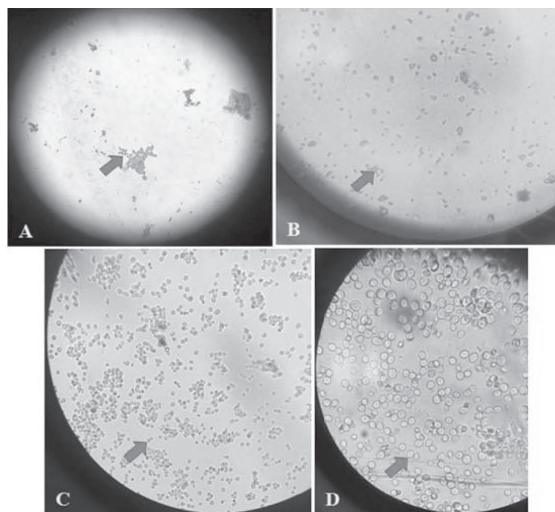


Fig. 9. A: *Diplobacillus sps*; B: *Xanthomonas oryzae* bacteria; C & D: Yeast cells budding (Magnification: 10X & 100X)

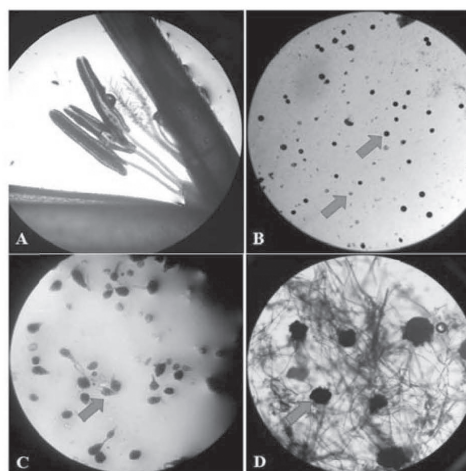


Fig. 10. A: Anthers & stigma; B: Fertile and sterile Pollen grains; C: *Alternaria alternata* conidia; D: *Macrophomina phaseolina* spores

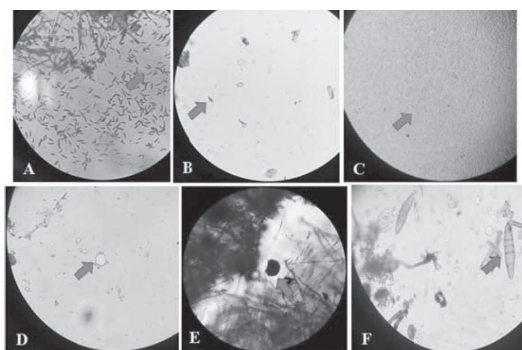


Fig. 11. Images of different fungal conidia captured using m-phone. A: *Fusarium oxysporum*; B: *Magnaporthe grisea*; C: *Colletotrichum acutatum*; D: *Sclerospora graminicola* Oospore; E: *Aspergillus* species and F: *Exserohilum turcicum*

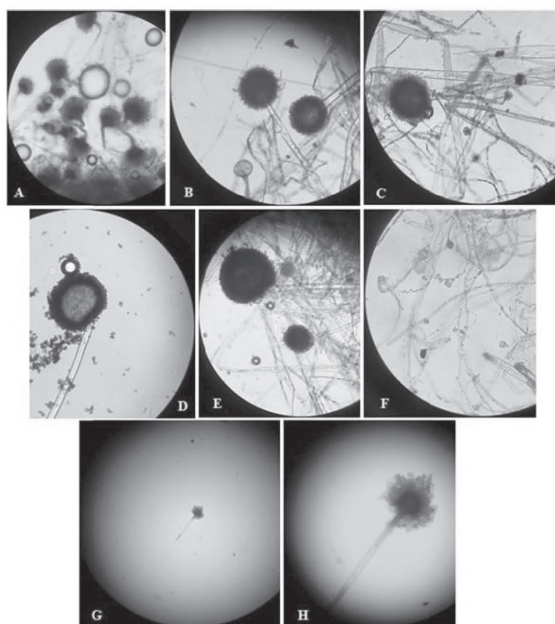


Fig. 12. A to F: Different *Aspergillus* species and G & H: *Aspergillus niger* vesicle and conidia (Magnification: 10 X & 40X).

Apart from stigma and anthers image, a clear image of fertile and sterile pollen was captured using smart phone cameras (Fig. 10A & 10B). *Alternaria alternata* conidia were observed as single, usually 2-6 and were long or short with brown, slightly curved and swollen at apex was

photographed using mobile phone camera (Fig. 10C). *Macrophomina phaseolina* fungal microsclerotia demonstrated aggregates of hyphal cells attached by a melanin material with >100 individual microsclerotia image was captured (Fig. 10D).

The conidia and conidiophores images of various plant pathogens viz., *F. oxysporum*, *Magnaporthe oryzae*, *C. acutatum*, *C. cpsici*, *Curvularia*, *Alternaria alternata*, *S. graminicola* and *Exserohilum turcicum* was clearly photographed (Fig. 11A to 11D & 11F). The mycelium/hyphae of different plant pathogenic fungus like *Magnaporthe oryzae*, *F. oxysporum*, *Penicillium*, *rhizopus*, *C. cpsici*, *Curvularia*, *Rhizoctonia solani*, *Macrophomina phaseolina* (Fig. 13A to 13F) including different *Aspergillus* species images were captured respectively using mobile inbuilt cameras.

Among the smart phones cameras used, image capturing was superior and clear using Samsung Galaxy J7 Prime (Model: SM-G610F) as compared to other two phone cameras used in this study (Fig. 14A, 14B & 14C). We also captured the live image of fungal colony growing on PDA Medium. Using this method, our research team has isolated *Fusarium* fungus (Fig. 15).

Discussion

Microscope-digital cameras are not always promising to use because of its management and difficult to fit it in every microscope. The complexity with Microscope attached camera is that it is not affordable for individual instrument in microbiology or pathology laboratories (25). Earlier, several authors have reported the application of smart phone camera in capturing images of the microscopic organisms or objects in medical and other fields (8, 9, 10, 11, 23, 24, 25, 26, 27, 28, 29, 30). Bellina and Missoni (31) for the first time reported the detailed description of free-hand smartphone microscopic photography without using an adapter. To our knowledge, detailed instructions for obtaining quality smart phone microscopic photographs of plant pathogens have not been published earlier. We assume that we

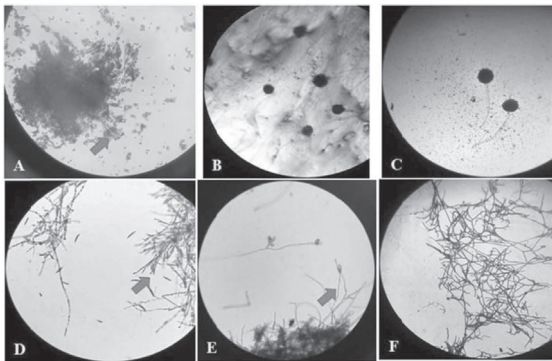


Fig. 13. A: *Penicillium* sps; B: *Rhizopus* sporangium (without staining); C: *Rhizopus* sporangium (with LPCB staining); D: *Colletotrichum capsici* filament and conidia; E: *Curvularia* species with conidia and F: *Rhizoctonia solani* Hyphae

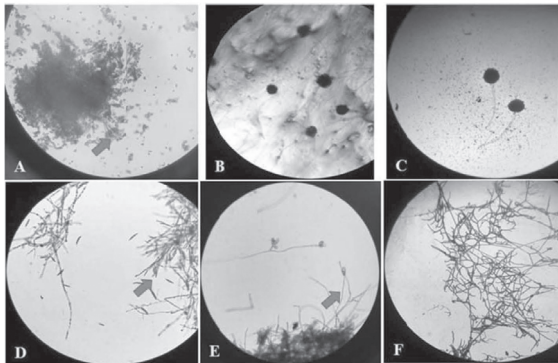


Fig. 14. *Fusarium oxysporium* f. sp. ricini colony captured using different mobile phones A: Samsung Galaxy J7 Prime (Model: SM-G610); B: HTC Desire G plus dual sim; C: Coolpad Mega 2.5D (Model: y83-100)

are the first to report the usage of smart phone cameras and its potential applications in plant pathology suitable for university teaching staff, research workers including post graduate and doctoral students for their research and thesis preparation in the universities, agriculture research institutes, in addition to seed industry.

In a report, cylindrical tube (sleeve) made of routinely used paper around one of the eyepiece of the microscope was used (8). However we confirm that it is a simple, economical and highly practical technique without using any accessories similar to the research conducted by Bellina, Missoni (24, 31). We further demonstrated the capturing of live images of yeast as well as fungus growing on culture medium, similarly live video of motile organisms like trophozoites of *Giardia*, *Entamoeba* as well as larvae of *Strongyloides* was reported by Aher and Kaore (8). We assume that smart phone camera can be used to produce high-quality images suitable for use in presentations, posters, and publications and it is an invaluable tool for plant pathologists, agriculturists, students and trainees, similarly Reshmi and Sneha (25) reported that undergraduate as well as post-graduate students can also use such an easy and affordable techniques which can be reproduced in their dissertations or thesis.

This technique enables agriculture based research institutes and scientists who do not own conventional microscope cameras, to obtain high-quality photomicrographs for use in a variety of

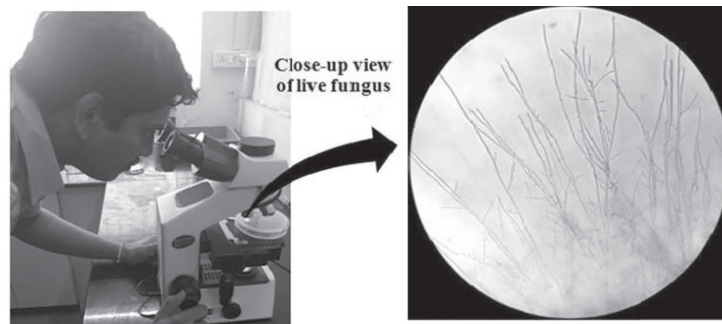


Fig. 15. Image capturing of live fungus growing on Potato dextrose agar medium

agricultural and educational applications; an advantage of mobile phone camera is its affordability, feasibility whose application is lagging in agriculture field as compared to medical sciences (11, 27).

Although, out of three smart phones used, two smart phone cameras viz; Samsung Galaxy J7 Prime and HTC Desire G plus consisting of 13MP rear cameras, we hypothesize that, the clarity of images by Samsung Galaxy J7 Prime smart phone may be due to the camera specifications (f/1.9; 28mm) as compared to HTC Desire G plus (f/2.2; 28mm) respectively which determines the quality of image. While, Coolpad Mega 2.5D (Model: y83-100) smart phone is provided with inbuilt 8MP rear camera due to which we found difference in the quality of image captured using three different smart phones.

Conclusions

We believe that, we are the first to report the application of smart phone cameras and its potential application in plant pathology for image capturing. We consider that this technology can be an inexpensive and powerful tool for light microscopy in agriculture Research. Especially, in plant pathology suitable for universities, research scholars, academic students for their theses works and presentations and agriculture industry. We presume that similar technical advances in smart phone camera application will continue to occur in the future, resulting in replacement of traditional digital microscope cameras and other sophisticated microscopy in resource poor institutions, universities or developing countries with smart phone cameras for digital photomicrograph acquirement.

Acknowledgments

The authors would like to thank M/s. Sayaji Seeds LLP, Ahmedabad, Gujarat, India for funding and providing facilities to carry out the experiment. We also wish to thank Dr. K. Krishnaiah, former Project Director, Directorate of Rice Research, Rajendranagar, Hyderabad, Telangana for his critical review of the manuscript. The authors extended sincere gratitude to Dr. Zerka Rashid,

CIMMYT-Asia, Patancheru, Hyderabad, India for providing *Macrophomina phaseolina* fungal culture.

References

1. WHO report. (2003). Essential health technologies strategy 2004-2007. World Health Organization. http://www.who.int/eh/en/EHT_strategy_2004-2007.pdf.
2. WHO report, Essential Diagnostic Imaging. World Health Organization. <http://www.who.int/eh/en/DiagnosticImaging.pdf>.
3. WHO report, About diagnostic imaging. World Health Organization. http://www.who.int/diagnostic_imaging/about/en/.
4. National Electrical Manufacturers Association (2008) Digital Imaging and Communications in Medicine (DICOM) standard.
5. Ralph, P.B., Jean, L.V., Thomas, L., Christa, P., French, L.E., Aron, J. G., Saurat, J-H. and Salomon D. (2005) Telemedical Wound Care Using a New Generation of Mobile Telephones A Feasibility Study Arch Dermatol.141:254-258.
6. Frean, J. (2007). Microscopic images transmitted by mobile cameraphone. Transactions of the Royal Society of Tropical Medicine and Hygiene, 101: 1053.
7. Roy, R.C. and Dadarya, S. (2012). Use of digital camera in clinical microbiological laboratory: an academic and diagnostic tool. International Journal of Biomedical and Advance Research, 3(5):423-24.
8. Aher, A. and Kaore, N. (2010) Application of camera phone technology in capturing microscopic images. Journal of recent advances in applied sciences. 25: 5-7.
9. Seigel, G.M. (2015). Phoning it in: Smartphone technology in the cancer research lab. Oncocytology, 5: 14-16.
10. Breslauer, D.N., Robi, N.M., Neil, A.S., Wilbur, A.L. and Daniel, A.F. (2009). Mobile

- phone based clinical microscopy for global health applications. PLoS ONE, 4 (7): e6320.
11. Godse, C.S., Patkar, S., Nabar, N.S., Amonkar, A.J., Vaidya, R.A., Raut, A.A. and Vaidya, A.B. (2008). Mobile camera microphotography: A simple but elegant technique for tediagnosis of malaria. JK Science: Journal of Medical Education & Research, 10(3): 155-156.
 12. Madhan, M.K., Madhav, M.S., Srinivas Prasad, M., Rama Devi, S.J.S., Ram Kumar, G. and Viraktamath, B.C. (2012). Analysis of population structure of *Magnaporthe grisea* using genome specific microsatellite markers. Current Trends in Biotechnology and Pharmacy, 6(2): 35-43.
 13. Singh, R., Shiw, M., Mehilal., Ajay, T. and Prasad, D. (2015). Virulence Diversity in *Rhizoctonia Solani* Causing Sheath Blight in Rice Pathogenicitya. Journal of Plant Pathology & Microbiology, 6(8): 296.
 14. Roberto, L.D.R. and Erlei, M.R. (2014). Semi-selective culture medium for *Exserohilum turcicum* isolation from corn seeds. Summa Phytopathologica, 40(2): 163-167.
 15. Yugander, A., Sundaram, R.M., Ladha Lakshmi, D., Hajira, S., Madhav, M.S., Srinivas Prasad, M., Viraktamath, B.C. and Laha, G.S. (2014). Pathogenic and genetic profile of *Xanthomonas oryzae pv. oryzae* isolates from Andhra Pradesh. Indian Journal of Plant Protection, 42(2): 149-155.
 16. Ali, M.A. (2002). Biological variation and chemical control of *Rhizoctonia solani* causing rice sheath blight diseases in Bangladesh. Ph. D. thesis, Univ. London, Imperial College, London. 202.
 17. Uma, V. and Wesely, E.G. (2013). Seed borne fungi of rice from South Tamil Nadu. Journal of Academia Industrial Research, 1(10): 612-614.
 18. Imolehin, E.D. (1983). Rice seed borne fungi and their effect on seed germination. Plant Disease, 67: 1334-1336.
 19. Amin, M., Zeinab, R. and Amanollah, Z.A. (2015). Isolation and identification of *bacillus* species from soil and evaluation of their antibacterial properties. Avicenna Journal of Clinical Microbiology and Infection, 2(1): e23233.
 20. Vishwakarma, R. (2017). Isolation, identification, purification, and characterization of antibiotic-producing bacteria from different soil samples. International Journal of Advance Research, Ideas and Innovations in Technology, 3(5): 196-204.
 21. Saket, K., Vineeta, S. and Ruchi, G. (2015). Cultural and morphological variability in *Colletotrichum capsici* causing anthracnose disease International Journal of Current Microbiology and Applied Sciences, 4(2): 243-250.
 22. Ali, M., Hossain, M.A., Hasan, M.J. and Kabir, M.E. (2014). Identification of maintainer and restorer lines in local aromatic rice (*Oryza sativa*). Bangladesh Journal of Agricultural Research, 39 (1): 1-12.
 23. Morrison, A.S. and Gardner, J.M. (2014). Smart phone microscopic photography a novel tool for physicians and trainees. Archives of Pathology & Laboratory Medicine, 138: 1002.
 24. Bellina, L. and Missoni. (2009). E. Mobile cell-phones (M-phones) in telemicroscopy: increasing connectivity of isolated laboratories. Diagnostic Pathology, 4: 19.
 25. Reshmi, C.R. and Sneha, D. (2012) Use of digital camera in clinical microbiological laboratory: an academic and diagnostic tool International Journal of Biomedical and Advance Research, 03(05): 316-317.

26. Morrison, A.O. and Gardner, J.M. (2015). Microscopic image photography techniques of the past, present, and future. *Archives of Pathology & Laboratory Medicine*, 139: 1558-1564.
27. Zimic, M., Coronela, J., Gilmana, R.H., Lunaa, C.G., Curiosod, W.H. and Moore, D.A.J. (2009). Can the power of mobile phones be used to improve tuberculosis diagnosis in developing countries?. *Transactions of the Royal Society of Tropical Medicine and Hygiene*, 103: 638-640.
28. Granot, Y., Antoni, I. and Boris, R. (2008). A new concept for medical imaging centered on cellular phone technology. *PLoS ONE*, 3(4): e2075.
29. Maude, R.J., Koh, G.C.K.W. and Silamut, K. (2008). Short Report: Taking photographs with a microscope. *American Journal of Tropical Medicine and Hygiene*, 79(3): 471-72.
30. Rost, F.W.D. and Oldfield, R.J. (2000). Limited-budget photomicrography. *Photography with a microscope*. Cambridge: Cambridge University Press.
31. Bellina, L. and Missoni, E. (2011). 'M-learning: mobile phones' appropriateness and potential for the training of laboratory technicians in limited-resource settings. *Health Technology*, 1: 93-97.

Insilico Studies of Ras Protein in Cancer

A. Ranganadha reddy¹, S. Krupanidhi¹, P. Sudhakar²

¹: Department of Biotechnology VFSTR(Deemed to be University) Guntur 522 213

²: Department of Biotechnology Acharya Nagarjuna University Guntur 522 510

Corresponding author:rangaaluri@gmail.com

ABSTRACT

Cancer can be defined as a set of cells that show uncontrollable growth, invasion and also metastasis takes place. Intracellular signaling pathways that have various functions in biological processes are regulated by Ras GTPase proteins and their down-stream effectors. These proteins causes spreading within the cell cycle and also the balance of pro- and anti-apoptotic factors are also affected. Ras controls different functions and also abnormalities and various points in the downstream signaling processes causes carcinogenesis and also the signal mechanisms can be used as therapeutic agents in treating cancer. They play a vital part in the cell development, maintenance and also transformations that are malignant. Changes in the signaling in both upstream and downstream can be caused by activating RAS. RASGRF2 gene is said to encode protein called Ras-specific guanine nucleotide-releasing factor 2. RAS GTPases can be seen in between active GTP-bound state and inactive GDP-bound state. The GDP bound form transforms into active form and this is stimulated by GEFs (Guanine-nucleotide exchange factors) like RASGRFs. RAS protein structure was modeled by using SWISS MODEL and the model was validated by using PROCHECK.

Key words: Cancer, RAS protein, SWISS MODEL, PROCHECK

INTRODUCTION

Cancer is a set or lot of call that shows growth that is uncontrolled, invasion and

metastasis can also be seen. The difference of malignant cancers from benign tumors is because of three different properties they are self limited, invasion or metastasis is not seen [1]. Unlike other cancers leukemia is a type of cancer that does not form tumors. Oncology is defined as a division of medicine that is related to the study, diagnosis, and treatment and preventing cancer [2]. Malformations within the genetic material results in transformations of cell those results in cancer. Carcinogens like smoke from tobacco, chemicals, radiation and other agents that are infectious are said to cause cancer. Errors in replication of DNA or abnormalities that are inherited can also help in promoting cancer and it can be said that it is found in cells right from birth. An intricate interaction between host genome and carcinogens affects the cancer inheritance. Cancer has two types of genes that get affected due to the abnormalities in the gene. Protection against programmed cell death, hyperactive growth and division, loss of respect for normal tissue boundaries and to be able to form in different tissue environments can be activated by cancer promoting oncogenes. In cancer cells tumor suppressor genes are inactivated it causes ability to function like the natural cells like control over the cell cycle, accurate DNA replication, orientation and adhesion within tissues, and interaction with protective cells of the immune system [3].

RAS PROTEIN

Somatic gain of mutation functions are targeted by the Ras genes within the human cancer. Ras–Raf–mitogen-activated and

extracellular-signal regulated kinase (MEK)–extracellular are affected by germline mutations [4]. RASGRF2 encodes a protein called Ras specific guanine nucleotide-releasing factor 2 within the humans. Active GTP bound state and inactive GDP bound state is cycled by RAS GTPases. Conversion of GDP bound form into active form is stimulated by RASGRFs that is an example of Guanine-nucleotide exchange factors (GEFs). The activity of Rac-dependent Extracellular Signal-regulated kinase ½ is regulated by p35/cyclin-dependent kinase 5 phosphorylation of ras guanine nucleotide releasing factor 2 by altering the microtubule-associated protein 1b distribution and RasGRF2 in the neurons. Neuron-specific activators, p35 and p39 do not cause alteration of proline directed kinase Cyclin-dependent kinase 5 (Cdk5). Cdk5 is important for the formation of lamination and cortical structures at the developmental stage. Cdk5 function within the adult nervous system is seen in cell adhesion, signaling of dopamine, release of neurotransmitters and synaptic activity. Additionally it is said that Cdk5 is involved in the cross talk with the other pathways of signal transduction. With the help of two hybrid system the proteins that interact with p35 were identified in order to determine which proteins are involved in cross talk. p35 is related to Ras guanine nucleotide releasing factor 2 (RasGRF2) in colocalization and coimmunoprecipitation studies by using primary cortical neurons and cell lines that are transfected. GTPases Ras and Rac that are small type are regulated by most expressed, calcium activated regulator Ras-GRF2 (GRF2). It is a multidomain protein and contains many recognizable sequence motifs in the following order (NH2 to COOH): pleckstrin homology (PH), coiled-coil, ilimaquinone (IQ), Dbl homology (DH), PH, REM (Ras exchanger motif), PEST/ destruction box, Cdc25. Guanine nucleotide exchange factor (GEF) is present in the domains of DH and Cdc25 and they interact with Ras and Rac. It was found that invitro REM-Cdc25 region is enough for maximum activation of Ras and in vivo caused extracellular signal regulated kinase (ERK) activation and Ras to be independent of

the calcium signals there by predicting that when it is expressed in ectopic manner it contains all the determinants that is necessary that activation, for accessing the Ras signaling[5].

METHODOLOGY

- A) The Fasta sequence of Ras protein (Acc.ID. O14827) **was retrieved from Swiss Prot. BLAST software was used for homology search of Ras protein.**
- B) By using SWISS MODEL server the crystal structure of protein Ras protein was done by using the (PDB ID: 2IJE) as structural template.
- C) Stereo-chemical quality of all the chains in a protein within the given PDB structure can be done by PROCHECK analysis. The regions that have unusual geometry are highlighted and the overall structural estimation is also provided.

BLAST: BLAST is a web based online tool which searches alignments that are of high scores between the target sequence and the homologous sequences that are present in the database by using Smith-Waterman algorithm and following a heuristic approach. BLASTP: In Blastp when a protein query is given the protein sequences that are most similar in the databases are given as output.

SWISS MODEL: It is a fully automated protein structure comparative-modelling server, accessible via the ExPASy web server [6].

PROCHECK: Evaluation of the arrangement of protein structure is very important as it decides the quality of the protein model and for doing this PROCHECK tool was used [7].

RESULTS AND DISCUSSION

Sequence Retrieval

By using UniProtKB/Swiss-Prot database the details of Ras protein (Acc No. O14827) **the information such as helix lengths, N- and C-terminus amino acid lengths etc., was retrieved.** The sequence information is provided below.

Query sequence of Ras protein

>sp|O14827|RGRF2_HUMAN Ras-specific guanine nucleotide-releasing factor 2 OS=Homo sapiens GN=RASGRF2 PE=1 SV=2

```
SAMELAEQITLLDHFVIFRSIPY EEFLGQ  
GWMKL DKNERTPYIMKTSQH FNDMSNLVA  
SQIMNYAD VS SRANAIEKWVAVADICRC  
LHNYNGVL EITSALNRS AIYRLKKTWAK  
VSKQTKA LMD KLQKT VSSEGRFKN LRETLK  
NC      NPPA      VPYLGMYLTDLAFIE  
EGTPNFTEEGLV NFSKM RMISHIIREIRQ  
FQQTSY      RIDHQPKV      AQYLLD  
KDLIIDEDTLIELSLKIEPR
```

BLAST tool helps to search the regions of similarity between nucleotide or protein sequences by using local alignment algorithm. Statistical significance of the matches is calculated by comparing the protein or nucleotide query to the sequences in the database. By using the BLAST tool the target i.e., Ras protein (UniProt ID: O14827) was searched against the protein sequences in the database. It can be seen that maximum identity with target sequences are shown by three different proteins (PDB IDs: 2IJE, 1BKD, 1XD2, 4URU). For further use out of these four sequences 2IJE is selected as template as shown in Fig.1.

Three-Dimensional Structure Prediction by

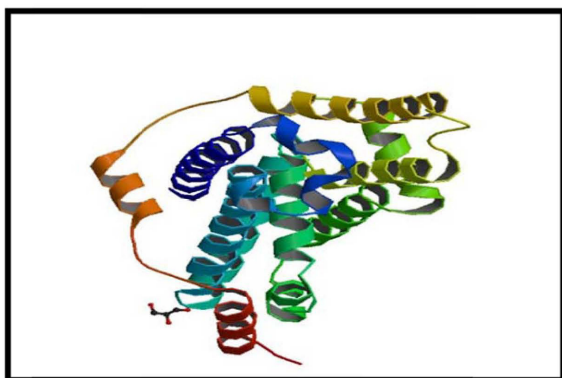


Fig. 1. Crystal Structure of the Cdc25 domain of RasGRF1

SWISS MODEL

2IJE was retrieved through BLAST results and was taken as template, O14827 was taken as query sequence and Protein BLAST was performed, the three dimensional structure of Ras protein (O14827) was predicted by using the tool SWISS MODEL and can be seen in Fig.2. Taking 2IJE.1.A chain as templates that are homologous to query sequence Ras protein, the 3D structure of the Ras protein (O14827) was predicted. A model with RMS deviation is 0.869445 after superimposition of Ras protein structure with

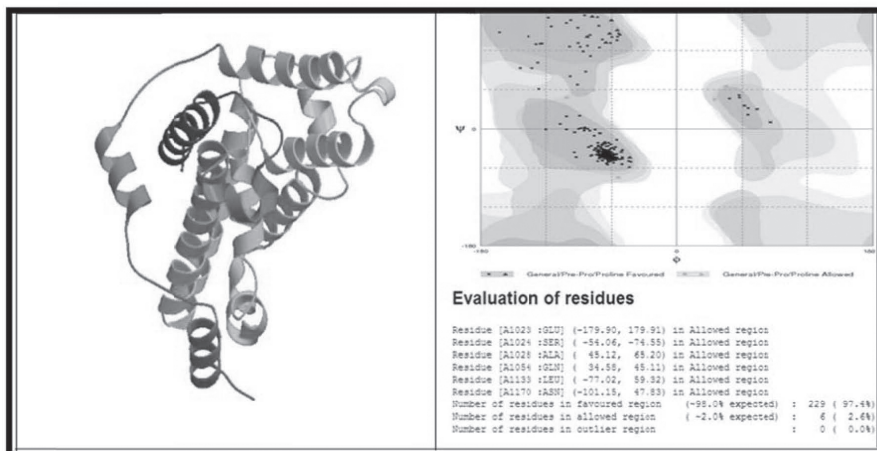


Fig. 2. Crystal Structure of Ras protein (PDB ID: 2IJE) as structural template.

templates 2IJE.1.A was obtained.

Ramachandran Plot

PROCHECK is used for stereochemical assessment of the model. Ramachandran plot was designed by Gopalamudram Narayana Ramachandran and Viswanathan Sasisekharan. It is used to visualize dihedral angles ϕ and ψ of amino acid residues in protein structure and is commonly known as Ramachandran diagram or a Ramachandran map or a $[\psi, \phi]$ plot. It depicts the possible conformations of ψ and ϕ angles for a polypeptide. The model developed by PROCHECK was checked with the Ramachandran plot, Ras protein had 229 amino acid residues (97.4%) in favoured region against (~98.0% expected), 6 amino acid residues (2.6%) in allowed region against (~2.0% expected) and no amino acid residues in outlier region as



shown in Fig.3. which implies that the final model is reliable.

Fig. 3. Homology model of Ras protein and validation of homology model using Ramachandran plot (Procheck)

CONCLUSION

In our study the structure of Ras protein was modeled by taking template as 2IJE in SWISS MODEL and model verification done by PROCHECK.

REFERENCES

1. Community Oncology Alliance, <http://www.communityoncology.org>
2. Siegel R, DeSantis C, Virgo K, Stein K, Mariotto A, Smith T, Cooper D, Gansler T, Lerro C, Fedewa S, Lin C, Leach C, Cannady RS, Cho H, Scoppa S, Hachey M, Kirch R, Jemal A, Ward E. (2012). Cancer treatment and survivorship statistics, 2012. *A Cancer Journal for Clinicians*.62: 220–241
3. IMTECH, <http://www.imtech.res.in>
4. Schubbert S, Shannon K, Bollag G. (2007). Hyperactive Ras in developmental disorders and cancer. *Nature Reviews. Cancer*. 7: 295-308
5. De Hoog CL, Wing-Tze F, Marni DG, Michael FM, Anne Koch C. (2000). Calmodulin-Independent Coordination of Ras and Extracellular Signal-Regulated Kinase Activation by Ras-GRF2. *Molecular and Cellular Biology*.20:2727-2733
6. Benkert P, Biasini M, Schwede T. (2011). Toward the estimation of the absolute quality of individual protein structure models. *Bioinformatics*. 27: 343-350
7. Laskowski Roman A, Malcolm W, MacArthur, David SM, Jnaet MT. (1993). PROCHECK: a program to check the stereochemical quality of protein structures. *Journal of Applied Crystallography*. 26: 283-291.

Application of Medicinal Plants in Management of Endogenous Bioactive Molecules as Potential Biomarkers for Cardiovascular Disease and Disorders

Jitendra Gupta^a, Reena Gupta^a, Varun Kalra^a, Nitin Wahi^b

^aInstitute of Pharmaceutical Research, GLA University¹, Chaumuha-281406, Mathura, Uttar Pradesh, India.

^bDepartment of Biotechnology, GLA University¹, Chaumuha-281406, Mathura, Uttar Pradesh, India.

^{*}Correspondence E-mail - smartjitu79@gmail.com

Abstract

Worldwide, Cardiovascular disease (CVD) endures a prime root cause of death in both advanced and growing countries. It may present as a typical heart attack, an instant death or it may be clinically diagnosed at a contemporary stage and be referred to as a heart attack. CVD involves high blood pressure, coronary heart disease, congestive heart failure, stroke and reports ischemia is definitely the disruption of blood flow to portion of the heart, triggering heart cells to die, typically due to clog of coronary artery. The employ of herbal products has become increasingly popular in recent years. There is a demand of the natural remedy with the aid of worthy medicinal plants for the management of heart disorders. The medication available in the market may not be ample to treat the disease as it is triggered by various factors to control the undesirable effects instigated by the synthetic medicine available. Therefore, finding approaches to decrease the mortality of CVD remains an essential public health aim. This review quotes with medicinal plants having cardiostimulant and cardioprotective activity. The current review stated chemical and pharmacological status of numerous cardioprotective plants consisting of phytoconstituents accountable for cardioprotection, extract employed, dose, pharmacological screening model and mechanism engaged in cardioprotection via endogenous bioactive molecules as potential biomarkers. There exists a need for the natural therapy with the help of

medicinal plants. The advanced scientific concentrated on the natural remedy with the aid of medicinal plants those sustain the employ of the herbal formulation as a powerful cardioprotective. This kind of review certainly facilitates in enlisting the medicinal plants incurring cardioprotective activity.

Key-words: Biomarkers, cardioprotective, cardiostimulant, cardiovascular disease, phytoconstituents.

1. Introduction

Globally a number of disorders of the heart and blood vessels is known as cardiovascular (CV) ailment comprises of heart attack and stroke (1-3). Cardiovascular diseases (CVD) include other disease like hyperlipidemia in chronic kidney disease condition (CKD) has the greatest threat for atherosclerotic directly or indirectly linked to CVD. A significant dysregulation of nitric oxide generation would be counter vasoconstrictive forces and related to severity of heart failure that was within advanced ischemic cardiomyopathy affected individuals in contrast to control subjects (4).

Cardioprotection involves all mechanisms that donate the preservation efficiency to the heart by reducing as well as protecting against myocardial damage. The word cardioprotection is "preservation of the heart, offers all hypothetical implications due to the fact all adaptable and remunerative mechanisms that directly or indirectly play a significant role in myocardial

preservation need to be categorized as cardioprotective (1,5). WHO reviews reveal that around 80% of the world wide inhabitants however depends on vegetation remedies and many herbal supplements possess effective, excellent to clinical application in contemporary times (4-6).

Today ayurvedic herbal remedies typically based on plant gain a respectful status in the growing nations especially where advanced wellness facilities confined. Potent, beneficial and affordable native herbal drugs are gathering popularity among the individuals of both urban and non-urban locations (7-9).

Since forever, in all nationalities medicinal plants have been found a way to obtained medicine virtually. The widely use of herbal treatment and healthcare products as those referred in olden articles acquired from natural sources with medicinal attributes (10). The vast array and opportunity of cardiovascular medicines have enhanced in the previously decades enormously and new herbal medicines are introduced every year. In CVD categories therapeutic drugs comprise of antianginal, anticoagulants, diuretics, antiarrhythmic, hypotension and anticholesterol drugs (1,2).

A variety of medicinal plants have specific preventive effects relating to coronary heart diseases (11,12). Vegetation or Plant remedy with multicomponents has many merits over solitary plant extract/isolated chemical substance and gain more prominent place in the herbal industry because these offer brilliant performance for the manage of many ailments in a synergistic way (13). Mixtures of interacting bioactive compounds made by plants may offer significant combination remedies that concurrently influence several pharmacological objectives and offer therapeutic efficiency outside the solitary substance based drugs. Presently there are a number of medicinal plants showing cardioprotective action. This review emphasize on application of medicinal plants in management of endogenous bioactive molecules as potential biomarkers for cardiovascular diseases and disorders (12).

2. Risk of Endogenous Bioactive Molecules for CV Disease and Disorders :

Intracellular proteins/enzymes produced to blood, subsequent cardiac tissue injury and exhibiting serial concentration alter along with preliminary elevate and succeeding drop in plasma is known as cardiac bioactive molecules/markers. In CV disease/disorders changed the normal value of a number of endogenous bioactive markers for example lactate dehydrogenase (LDH), creatine phosphokinase (CPK), alanine transaminase (ALT) or alkaline phosphatase (ALP), serum glutamate-pyruvate transaminase (SGPT), serum glutamate oxaloacetate transaminase (SGOT) or aspartate transaminase (AST), lipid account especially triglycerides (TGs), low density lipoprotein (LDL), high density lipoprotein (HDL), overall cholesterol, VLDL (very low density lipoprotein), and antioxidant factors particularly glutathione reductase (GR), Glutathione peroxidase (GPx), Superoxide dismutase (SOD), catalase (CAT), glutathione (GSH), myoglobin, MDA (malonal-dialdehyde) and cardiac troponins. Risk of endogenous bioactive molecules for CVD and disorders is demonstrated in [Fig. 1] (14-56).

3. Pharmacological Impact of Cardioprotective Medicinal Plants

A wide variety of phytoconstituents of medicinal plants have been accountable for cardioprotective effect like as cardiac glycosides, carotenoids, polyphenols, flavonoids, fatty acids, triterpenes, terpenoids, alkaloids and saponins etc shown in [Table 1], (4,57-73) that will significantly eliminated the modification of endogenous marker enzymes as biochemical variants LDH, CPK, ALT or SGPT, ALP, AST or SGOT, TGs, LDL, HDL, complete cholesterol, VLDL, and GR, SOD, MDA, CAT, GPx and GSH which usually potential leads to CVD and arrive to close to normal ranges [74]. Cardioprotective activity was assessed employing many pharmacological screening models in rats stimulated by adriamycin evoked cardiomyopathy, isoprenaline stimulated myocardial necrosis and cyclophosphamide activated oxidative myocardial injury; in albino rats stimulated by doxorubicin

activated cardiotoxicity and ischemia-reperfusion-induced myocardial infarction (MI) and cigarette smoke subjected rat etc (14-56,72,73).

The positive results are presumed to be ascribed because of existence of specified antioxidants which often restrict free radical generation and thus respond like cardio protective. For that reason, a wide range of medicinal plants posses cardioprotective agents have been increased enormously in the past few decades, and new cardioprotective herbs are being contributed yearly. So in CVD different categories of various therapeutic cardioprotective agents incorporate such as antihypertensive, antianginal,

diuretics, anticoagulants, anticholesterol and antiarrhythmic, antispasmodic, cardi tonic and sedative (1,75). It assists to take care of CVD by dilating peripheral and coronary blood vessels, and enhances the availability of blood to the heart and extenuating sign in early phase of heart failure. An detail of account of medicinal plants having pharmacological cardioprotective effect with botanical name, family, observation and mechanism involved in cardio protection indicated in [Table 2] (7,14-56,72,73).

4. Conclusion

The renewed attention lookup for innovative drugs from natural resources, specifically from

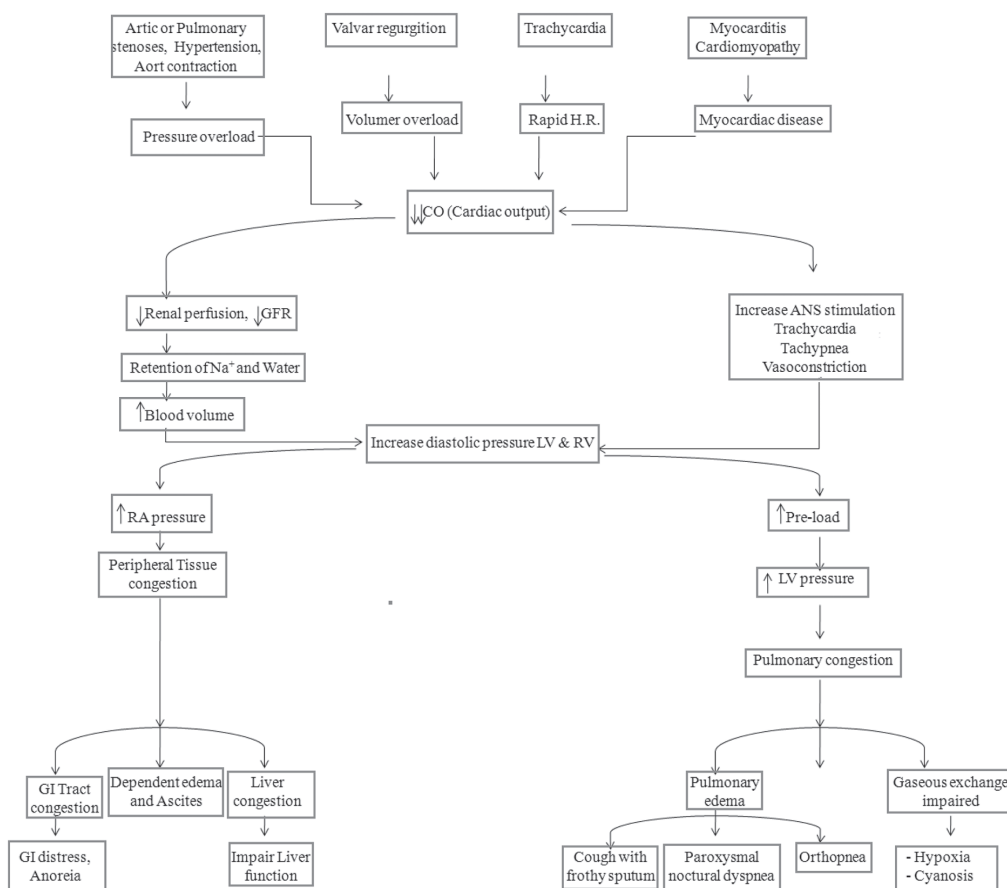


Fig. 1. Risk of Endogenous Bioactive Molecules for CVD and Disorders. ANS: Autonomous Nervous Systems; RA: Right Atrium; RV: Right Ventricle; LV: Left Ventricle; GI: Gastro Intestinal; GFR: Glomerular Filtration Rate; H.R.: Heart Rate.

plant sources with regard to the treatment of cardiovascular ailments, has attained world-wide interest during many decades. Advancement of these kinds of native herbal remedies together with potential cardioprotective results might be a boon for developing nations around the world. The present overview shows the significance of medicinal plants in protecting against CVD and tends to make an effort in order to compile certain cardio protective plants. Medicinal plants and their products may assist in decreasing the associated risk of CVD or disorders. Secondary metabolites like carotenoids, cardiac glycosides, alkaloids, flavonoids, polyphenolic substances, saponins, terpenoids, triterpenes and fatty acids which exist in medicinal plants have been taken into consideration as the accountable remedies for potent cardioprotective action (4).

Right now accessible synthetic cardio-protective drugs possess not only been related to a variety of side effects but are also quite expensive

(76). The easy availability, relatively fewer side effects and minimal price of medicinal plants come up with perhaps even more desirable therapeutic agents (77).

Consequently as a result, a key potential is available in natural resources pertaining to recognizing and choosing effective, economical and safer approaches with regard to cardioprotection [12]. These medicinal plants need to have investigated clinically and carefully to stipulate their role in curing and management of CVD and to be able to promote potential future pharmaceutical progression of therapeutically worthwhile herbal medicines. During the same time period, legalized monitoring of herbal remedies application with low safety margins, undesirable cardiovascular responses and drug affairs need to have implemented (78).

Conflict of Interest :

The author(s) confirm that this article content has no conflict of interest.

Table 1. A brief description of medicinal plant have cardioprotective phytoconstituents(4,75-71).

Family	Plant Botanical Name	Cardioprotective Phytoconstituents
Scrophulariaceae	<i>Digitalis purpurea</i>	Cardiac glycosides [57,58]
Liliaceae	<i>Allium sativum</i>	Sulphur compounds, Allicin[59]
Moraceae	<i>Antiaris toxicaria</i>	Cardiac glycosides [60]
Verbenaceae	<i>Gmelina arborea</i>	n-Hexadecanoic acid, Palmitic 9,12-Octadeca-trienoic acid (Z,Z,Z), Linoleic acid and Oleic acid [61,62]
Tiliaceae	<i>Grewia hirsuta</i>	Ciscarveol, Bisabolene, Elemol, Careen, Cadinol [63]
Theaceae	<i>Green tea</i>	Flavandiols, Catechins, Flavonols [64]
Ranunculaceae	<i>Nigella sativa</i>	Thymoquinone, Carvacrol, β-pinene [65]
Cucurbitaceae	<i>Momordica dioica</i>	Iodine, Vitamin C [66]
Solanaceae	<i>Lycium barbarium</i>	Glucose, p-coumaric acid, Betaine and Daucostero [67]
Verbenaceae	<i>Premna serratifolia</i>	Alkaloids, Gangliosides and Steroidal glycosides [68]
Punicaceae	<i>Punica granatum</i>	Gallic acid, Punicalagin, Ellagic acid and Punicalin [69]
Boraginaceae	<i>Onosma bracteatum</i>	Resins, Tannins, Alkaloids and Glycosides ^[4]
Cruciferae	<i>Raphanus sativus</i>	Caffeic acid [70]
Moraceae	<i>Antiaris toxicaria</i>	Cardiac glycosides [71]
Areacaceae	<i>Elaeis guineensis</i>	Omega-3- fatty acid, Fatty acids [4]

Table 2. Application of medicinal plants in management of CV disease and disorders (20-56).

Plant (Hindi name)	Family	<i>In-vitro/in-vivo</i> model	Extract and Dose administered (mg/kg)	Mechanism involved and observation
<i>Garcinia indica</i> (Kokam)	Clusiaceae	Oxidative myocardial necrosis induced by Isoproterenol in rats	Aqueous extract; 250, 500	Aqueous extract of <i>G. indica</i> showed significant cardioprotective effect against oxidative myocardial necrosis induced by isoproterenol in rats and confirmed histopathology out comes[20]
<i>Daucus carota</i> (Gaajar)	Umbelifer ae	Myocardiac infraction induced by isoproterenol in albino rats	Aqueous; 250,500	Aqueous extract <i>D. carota</i> restored altered level of LDH, ALT, lipid peroxidase, AST in serum to near normal level as well as cardiac total protein lipid peroxidase and LDH[21]
<i>Buchanania axillaries</i> (Piyala)	Anacardia ceae	Cardiotoxicity induced by Doxorubicin in albino rats	Ethanolic; 250,500	Ethanolic extract of <i>B.axillaries</i> significantly restored and reach near to normal level of the alteration of endogenous marker enzymes such as LDH, CPK, SGOT, alkaline phosphatase, SGPT, CPK; antioxidants like GPx, GR SOD, GSH, MDA, CAT; and lipid profile like TGs, VLDL, Total cholesterol, HDL, LDL in Doxorubicin (DOX) induced cardiotoxicity model in albino rats[22]
<i>Bacopa monnieri</i> (Brahmi)	Scrophula riaceae	Isoproterenol induced myocardial injury (MI) in albino rats	Hydroialcohol; 50,100,150,200	<i>B. monmeira</i> hydroalcoholic extract restored the level of endogenous antioxidants (like GSHPx, CAT, SOD and reduced GSH), CK-MB and LDH isoenzyme activities and decline in MDA[23]

<i>Cichorium intybus</i> (Kasni)	Compositae	Ageing myocardium of albino rats	Aqueous; 500	Cichorium aqueous extract was determined to better the age induced necrosis and then protect the heart against oxidative damage and also significantly reduce serum enzymes[24]
<i>Cassia fistula</i> (Amaltas)	Caesalpiniaceae	Cardiotoxicity induced by Doxorubicin in wistar rats	Methanolic; 400	Methanolic extract of <i>C. fistula</i> significantly reduce serum enzymes (creatine kinase MB isoenzyme, SGPT, LDH and SGOT) level in doxorubicin evoked cardiotoxicity in rat[25]
<i>Crataegus oxyacantha</i> (Hawthorn)	Rosaceae	Isoproterenol induced myocardial infraction (MI) in albino rats	Tincture; 0.5 mL/100g	<i>C. oxyacantha</i> tincture prevented one of the isoproterenol-activated declines in antioxidant enzymes in one of the heart and augmented the level of ADP-stimulated oxygen uptake and then respiratory coupling ratio. It also secured from isoproterenol evoked pathological alteration in rat heart[26]
<i>Colebrookea oppositifolia</i> (Binda)	Lamiaceae	Cardiotoxicity induced by Doxorubicin in albino rats	Methanolic; 250, 500	In anti-oxidant enzymes and lipid peroxidation study, methanolic extract of <i>C. oppositifolia</i> significantly increased the level of CAT, SOD GSH; and reduced the level of MDA[27]
<i>Cocos nucifera</i> (Nariyal)	Palmae	Isoproterenol induced myocardial infraction (MI) in albino rats	Aqueous; 100 g/body weight	<i>C. nucifera</i> aqueous extract significantly reduce serum enzymes such as SGPT, LDH, CPK and SGOT and mere myocardial injury in isoproterenol induced rats fed tender coconut water[28]

<i>Commiphora mukul</i> (Guggul)	Burseraceae	Isoproterenol induced myocardial injury(MI) in rats (in vivo), effect of Guggul sterone on lipid peroxidation and Oxygen free generation (in-vivo)	Gum resin; 50	Guggul extract contain guggulsterone isomers showed oxidative degradation of lipids found in LDL <i>in-vivo</i> as well as, rat liver microsomes evoked by means of metal ions <i>in-vitro</i> [29]
<i>Vitis vinifera</i> (Grapes)	Verbenaceae	Myocardiac infraction induced by isoproterenol in albino rats	Grape seed proanthocyanidins; 50,100,150	Grape seed proanthocyanidins pretreatment certainly changed the status of all the parameters analyzed and preserved normal mitochondrial action as correlated with isoproterenol-evoked MI in rats[30]
<i>Mangifera indica</i> (Aam)	Anacardiaceae	Myocardiac infraction induced by isoproterenol in albino rats	Magniferin; 100 mg/g	<i>M. indica</i> extract contain magniferin administration preserved the heart from isoproterenol evoked cardiac injury and reduced the formation of lipid peroxide and restored the myocardial enzymes to near the normal status[31]
<i>Imula racemosa</i> (Pokharmul)	Compositae	Myocardial inschemic reperfusion necrosis	Hydroalcoholic; 100 mg/g	Hydroalcoholic extract <i>I. racemosa</i> of substantially restored one of the myocardial antioxidant level evidenced by means of elevated SOD, CAT, and declined glutathione and interrupted the leakage of CK-MB myocardiospecific enzymes and MDA[32]
<i>Hydrocotyle asiatica</i> (Mandukparni)	Umbelliferae	Iscemia-reperfusion induced myocardial in rat	Alcoholic; 100-1000	Alcoholic extract of <i>H. asiatica</i> showed significant decrease the status of lipid peroxide as well as left ventricle necrosis because of direct free radical scavenging activity or indirectly augment the level of endogenous antioxidants[33]

<i>Terminalia chebula</i> (Harad)	Combretaceae	Cardiac (lysosomal) membrane necrosis induced by isoproterenol in rats	Ethanollic; 250	Alcoholic extract of <i>T. chebula</i> pretreatment significantly restored the action of heart lysosomal enzymes in isoproterenol evoked cardiac injury in rat[34]
<i>Ficus hispida</i> (Kathgular)	Moraceae	Myocardial infraction induced by cyclophosphamide injury in a rats model	Methanolic; 400	Methanolic extract scavenged the free radicals and then protect from cardiotoxicity which was demonstrated by restoration of biochemical variables to near the normal level[35]
<i>Embelica ribes</i> (Vaividang)	Myrsinaceae	Myocardial infraction induced by isoproterenol in albino rats	Aqueous; 100	<i>E. ribes</i> aqueous extract, treatment restored altered heart homogenates and serum biomarker enzyme to normal level and also boost the antioxidant defence mechanism system in contrast to isoproterenol-evoked myocardial necrosis[36]
<i>Dracocephalum moldavica</i> (Tukhmeferunjimishk)	Labiatae	Ischemia/reperfusion induced arrhythmia and infraction size in the isolated rat heart	Methanol-water (Total extract); 25-200µg/ml	Methanol-water (Total extract) extract of <i>D. moldavica</i> showed a significant decline in the quantity of total ventricular ectopic beats, no. of ventricular tachycardia and its duration during ischemic and reperfusion time periods in the isolated rat heart[37]
<i>Azadirachta indica</i> (Neem)	Meliaceae	Isoproterenol induced myocardial infraction (MI) in rats	Leaf extract; 200, 500, 1000	Leaf extract of <i>A. indica</i> and vitamin E restores many biochemical, haemodynamic, likewise, histopathological criteria in affected rats[38]

<i>Curcuma longa</i> (Turmeric)	Zingiberaceae	Hemodynamic, biochemical and histopathological alteration induced by isoproterenol in rats	Hydroalcoholic extract; 100	Hydroalcoholic extract <i>C. longa</i> extract triggers myocardial adaptation by enhancing endogenous antioxidants and control the dysfunction of rat hearts and restored oxygen demand oxidative stress due to ISO induced myocardial necrosis[39]
<i>Cucumis trigonus</i> (Jagalindrāyan)	Cucurbitaceae	Myocardial infraction induced by isoproterenol in albino rats	Ethanollic; 75, 150	Ethanollic extract of <i>C. trigonus</i> exhibited reduce level of enzyme in serum likewise, restored ECG alterations to the near normal range after oral administration and histopathological outcome further confirmed the results[40]
<i>Crocus sativus</i> (Kesar)	Iridaceae	Cardiotoxicity induced by isoproterenol in rats	Aqueous; 5, 10, 20	Aqueous extract of <i>C. sativus</i> contain crocin attuned the actions of myocardial creatine CK-MB isoenzyme, LDH and cause elevate in antioxidant enzymes CAT, SOD and decreased GSH[41]
<i>Zingiber officinale</i> (Adrak)	Zingiberaceae	Oxidative myocardial necrosis induced by isoproterenol in rats	Ethanollic; 200	Ethanollic extract of <i>Z. officinale</i> revealed significantly decrease of endogenous ALT, AST, LDH and CK marker of serum and showed cardiac protection[42]
<i>Terminalia arjuna</i> (Arjun)	Combretaceae	Myocardial ischemic reperfusion injury induced by isoproterenol in rats	Alcoholic; 3, 4, 6.75, 9.75	In the rat heart, alcoholic extract of <i>T. arjuna</i> elevate the level of antioxidant molecules and protect the heart from isoproterenol elicit myocardial ischemic reperfusion injury[43]
<i>Premna serratifolia</i> (Arani)	Verbenaceae	Myocardial infraction induced by isoproterenol in rats	Ethanollic; 1mg/g	Ethanollic extract of <i>P. serratifolia</i> showed significant cardioprotective action due to the occurrence of phytoconstituents such as flavonoids, alkaloids, iridoid glycosides and phenolic compounds[44]

<i>Sida cordifolia</i> (Bala)	Malvaceae	Myocardiac infraction induced by isoproterenol in rats	Hydroalcoholic; 100, 500	Hydroalcoholic extract significantly restored actions of LDH, cardiac CK-MB isoenzyme and decreased GSH, elevate antioxidant molecules such as SOD, CAT Moreover, histopathological analysis support the biochemical outcomes[45]
<i>Sesbania grandiflora</i> (Hathya)	Papilionaceae	cigarette smoke exposed rats	Aqueous; 1000	Aqueous suspension of Hathya significantly control the antioxidant level and maintained the status of micronutrients in cigarette smoke exposed rats[46]
<i>Semecarpus anacardium</i> (Bhilawa)	Anacardiaceae	Myocardiac injury induced by isoproterenol in rats	Hydroalcoholic; 150	Hydroalcoholic extract of Bhilawa significantly increased the activities of CAT and SOD and decrease the serum level of LDH and CK –MB[47]
<i>Piper betle</i> (Pan)	Piperaceae	Cardiotoxicity induced by isoproterenol in rats	Leaf extract; 75, 150, 300	Leaf extract of <i>P. betle</i> significant elevate myocardial antioxidants molecules such as GSH, SOD, GPx, CAT, reduced the leakage of cardiac CK-MB isoenzyme and LDH likewise decreased lipid peroxidation[48]
<i>Picrorrhiza kurroa</i> (Katuka)	Scrofulariaceae	Cardiomyopathy induced by Adriamycin in rats	Ethanollic; 50	Alcoholic extract <i>P. kurroa</i> indicated significant reduction in level of serum enzymes and exhibited cardioprotective action[49]
<i>Trichopus zeylanicus</i> (Jeevani)	Trichopodaceae	Myocardiac infraction induced by isoproterenol in rats	Ethanollic; 500	<i>T. zeylanicus</i> ethanollic extract treated rats reveals the significant reduction in the level of cardiac biomarkers like LDH, ALT, AST, and CK in isoproterenol induced myocardial ischemia model[50]
<i>Nardostachy s jatamansi</i>	Valerianaceae	Cardiotoxicity induced by	Hydroalcoholic; ic;	Alcoholic extract <i>N. jatamansi</i> indicated significant reduction in level of serum enzyme after oral

(Jatamasi)		isoproterenol	85	administration and exhibited cardioprotective action[51]
<i>Tribulus terrestris</i> (Gokharu)	Zygophyllaceae	Myocardiac infraction induced by isoproterenol in rats	Hydroalcoholic; 250	Hydroalcoholic extract of <i>T. terrestris</i> decline the drainage of LDH, CK-MB enzymes against myocardium necrosis. Existence of antioxidant constituents like flavanoids in the extract might be liable for its cardioprotection[52]
<i>Withania somnifera</i> (Ashwagandha)	Solanaceae	Cardiotoxicity induced by Doxorubicin in rats	Ethanollic; 300	Alcoholic extract Ashwagandha showed significant reduction in level of serum enzyme and exhibited cardioprotective action[53]
<i>Syzygium cumini</i> (Jaamun)	Myrtaceae	Myocardiac infraction induced by isoproterenol in rats	Seed; 500	<i>S. cumini</i> seed extract pretreated rats retained to normal level of biomarkers enzymes like LDH, ALT, AST, and CPK) and serum uric acid level in isoproterenol-induced Myocardial Infarction (MI) model[54]
<i>Ocimum sanctum</i> (Tulsi)	Labiatae	Myocardiac infraction induced by isoproterenol in albino rats	Hydroalcoholic; 25, 50, 75, 100, 200, 400	Hydroalcoholic extract of <i>O. sanctum</i> reduced significantly restored various biochemical markers like LDH, GSH, and SOD levels likewise prevented the lipid peroxidation[55]
<i>Pithecellobium dulce</i> (Jungali Jalebi)	Fabaceae	Oxidative myocardial necrosis induced by Isoproterenol in rats	Aqueous and ethanolic extract; 200	Administration of aqueous and ethanolic extract showed significant cardioprotective effect against oxidative myocardial necrosis induced by isoproterenol in rats[56]

Acknowledgements

The author(s) thanks to GLA University for providing necessary facility to accomplish the work.

References:

1. Unnikrishnan, V., Nishteswar, K. (2015) Cardio protective activities of herbal formulation of bhavamishra-a review. *Int. Ayur. Med. J.*,3(3): 850-861.
2. World Health Organization Cardiovascular Disease Fact sheet Updated May 2017 Accessed at: <http://www.who.int/mediacentre/factsheets/fs317/en/> (Accessed Jan 5, 2018)
3. Srivastav, R.K., Siddiqui, H.H., Mahmood, T., Ahsan F. (2013) Evaluation of cardioprotective effect of silk cocoon (Abresham) on isoprenaline-induced myocardial infarction in rats. *Avic. J. Phytomed.*,3(3):216–223.
4. Arya, V., Gupta, V.K. (2011) Chemistry and pharmacology of plant cardioprotectives: A review. *Int. J. Pharm. Sci Res.*,2(5):1156-1167.
5. Kübler, W., Haass, M. (1996) Cardioprotection: definition, classification, and fundamental. *Heart.* 75(4):330–333.
6. Mahmood, Z.A., Mohammad, S., Mahmood, S.B.Z., Karim. (2010) Herbal treatment for cardiovascular disease the evidence based therapy. *Pak. J. Pharm. Sci.*,23(1):119-124.
7. Aryan, K., Gupta, V.K. (2011) Review on some cardioprotective plants from ayurveda *Int. J. Res. Ayur. Pharm.*,2(1):80-83.
8. Meena, A.K. (2009) Plants-herbal wealth as a potential source of ayurvedic drugs. *Asian J. Trad. Med.*,4(4):152-170.
9. Palvolic, M. (2000) Beta blockers in cardioprotection after acute myocardial infarction. *The Sci. J. Med. Bio.*,7(1):11-14.
10. Dasilva, E.J. (1999) Medicinal plants: A re-emerging health aid. *Elec. J. Biotech.*, 2(2):56-70.
11. Ahsan, F., Siddiqui, H.H., Mahmood, T., Srivastav, R.K., Nayeem, A. (2014) Evaluation of cardioprotective effect of *Coleus forskohlii* against isoprenaline induced myocardial infarction in rats. *Ind. J. Pharma. Bio. Res.*,2(1):17–25.
12. Zafar, F., Jahan, N., Ur-Rahman, K., Khan, A., Akram, W. (2015) Cardioprotective potential of polyphenolic rich green combination in catecholamine induced myocardial necrosis in rabbits. *Evi. Bas. Comp. Alter. Med.*,2015:1-9.
13. Wang, X.L. (2015) Potential herb-drug interaction in the prevention of cardiovascular diseases during integrated traditional and western medicine treatment. *Chin. J. Integra. Med.*,21(1):3–9.
14. Das, S., Der, P., Raychaudhuri, U., Maulik, N., Das, D.K. (2006) The effect of *Euryale ferox* (Makhana), an herb of aquatic origin, on myocardial ischemic reperfusion injury. *Mole. Cel. Biochem.*,289:55-63.
15. Nandave, M., Ojha, S.K., Joshi, S., Kumari, S., Arya, D.S. (2009) *Moringa oleifera* leaf extract prevents isoproterenol-induced myocardial damage in rats: evidence for an antioxidant, antiperoxidative, and cardioprotective intervention. *J. Med. Food.*,12(1):47-55.
16. Nivethetha, M., Jayasri, J., Brindha, P. (2009) Effects of *Muntingia calabura* L on isoproterenol-induced myocardial infarction. *Sing. Med. J.*,50(3):300-302.
17. Rao, P.R., Viswanath, R.K. (2007) Cardioprotective activity of silymarin in ischemia reperfusion-induced myocardial infarction in albino rats. *Exp. Clin. Cardiol.*,12(4):179-187.
18. Ahmed, K.K.M., Rana, A.C., Dixit, V.K. (2004) Effect of *Calotropis procera* latex on isoproterenol induced myocardial infarction in albino rats. *Phytomed. Int. J. Phytother. Phytopharmacol.*,11(4):327-330.

19. Gupta, J., Mohan, G., Prabakaran, L. (2015) Formulation, characterization and in-vivo antiischemic activity of ranolazine loaded ethyl cellulose microspheres in albino wistar rats. *Int. J. Drug. Dev. Res.*,7(1):211-222.
20. Karunakar, H., Dhruv, P., Kreethi, V. (2015) Evaluation of cardioprotective activity of aqueous extract of *Garcinia indica* linn fruit extract. *As. J. Pharm. Clin. Res.* 2015;8(2):107-112.
21. Muralidharan, P., Balamurugan, G., Kumar, P. (2008) Inotropic and cardioprotective effects of *Daucus carota* Linn on isoproterenol-induced myocardial infarction. *Bangl. J. Pharmacol.*,(2):74-79.
22. Sakthive, K., Palani, S., Kalash, R.S., Devi, K., Kumar, B.S. (2010) Phytoconstituents analysis by GC-MS, cardioprotective and antioxidant activity of *Buchanania axillaris* against doxorubicin-induced cardio toxicity in albino rats. *Int. J. Pharma. Stu. Res.*,1(1):34-48.
23. Nandave, M., Ojha, S.K., Joshi, S., Kumari, S., Arya, D. (2007) Cardioprotective effect of *Bacopa monnieri* against isoproterenol induced myocardial necrosis in rats. *Int. J. Pharmacol.*,3:385-392.
24. Nayeemunnisa., Rani, M.K. (2003) Cardioprotective effects of *Cichorium intybus* in ageing myocardium of albino rats. *Curr. Sci.*,84(7):941-943.
25. Khatib, N.A., Wadulkar, R.D., Joshi, R.K., Majagi, S.I. (2010) Evaluation of methanolic extract of *Cassia fistula* for Cardioprotective activity. *Int. J. Res. Ayur. Pharm.*,1(2):565-571.
26. Jayalakshmi, R., Niranjali, D.S. (2004) Cardioprotective effect of tincture of *Crataegus* on isoproterenol-induced myocardial infarction in rats. *J. Pharm. Pharmacol.*,56:921-926.
27. Haloi, S., Patel, A.K., Sarkar, N., Haldar, P.K., Kar, P.K. (2010) In-vivo cardioprotective activity of *Colebrookea oppositifolia*. *Int. J. Pharm. Sci. Bio.*,1(4):245-249.
28. Anurag, P., Rajamohan, T. (2003) Cardioprotective effect of tender coconut water in experimental myocardial infarction. *P. F. Hum. Nut.*,58(3):1-12
29. Chander, R., Rizvi, F., Khanna, A.K., Pratap, R. (2003) Cardioprotective activity of synthetic guggulsterone (E and Z - isomers) in isoproterenol induced myocardial ischemia in rats: A comparative study. *Ind. J. Clin. Biochem.*,18(2):71-79.
30. Karthikeyan, K., Bai, B.R.S., Devaraj, S.N. (2009) Efficacy of grape seed proanthocyanidins on cardioprotection during isoproterenol-induced myocardial injury in rats. *J. Cardiovasc. Pharmacol.*, 53(2):109-115.
31. Prabhu, S., Jainu, M., Sabitha, K.E., Devi, C.S.S. (2006) Cardioprotective Effect of Mangiferin on Isoproterenol induced myocardial infarction in rats. *Ind. J. Exp. Bio.*,4:209-215.
32. Ojha, S., Nandave, M., Kumari, S., Arya, D.S. (2010) Cardioprotection by *Inula racemosa* in experimental model of ischemic reperfusion injury. *Ind. J. Exp. Bio.*,48:918-924.
33. Pragada, R.R., Veeravalli, K.K., Chowdary, K.P.R., Routhu, K.V. (2004) Cardioprotective activity of *Hydrocotyle asiatica* L in ischemia-reperfusion induced myocardial infarction in rats. *J. Ethnopharmacol.*, 93 (1):105-108.
34. Suchalatha, S., Shyamala, D.C.S. (2005) Protective effect of *Terminalia chebula* against lysosomal enzyme alterations in isoproterenol induced cardiac damage in rats. *Exp. Clin. Cardiol.*,10(2):91-95.
35. Shanmugarajan, T.S., Arunsundar, M., Somasundaram, I., Krishnakumar, E., Sivaraman, D., Ravichandiran, V. (2008) Cardioprotective effect of *Ficus hispida* on

- Cyclophosphamide provoked oxidative myocardial injury in a rat model. *Int. J. Pharmacol.*,4(2):78-87.
36. Bhandari, U., Ansari, M.N., Islam, F. (2008) Cardioprotective effect of aqueous extract of *Embelica ribes* fruits against Isoproterenol induced myocardial infarction in albino rats. *Ind. J. Exp. Bio.*,46:35-40.
37. Najafi, M., Ghasemian, E., Fathiazad, F., Garjani, A. (2009) Effects of total extract of *Dracocephalum moldavica* on ischemia/reperfusion induced arrhythmias and infarct size in the isolated rat heart. *Ira. J. Bas. Med. Sci.*,11(4):229-235.
38. Peer, P.A., Trivedi, P.C., Nigade, P.B., Ghaisas, M.M., Deshpande, A.D. (2008) Cardioprotective effect of *Azadirachta indica* A Juss on isoprenaline induced myocardial infarction in rats. *Int. J. Card.*,23-126.
39. Mohanty, I.R., Arya, D.S., Gupta, S.K. (2009) Dietary *Curcuma longa* protects myocardium against isoproterenol induced hemodynamic, biochemical and histopathological alternations in rats. *Int. J. Appl. Res. Natur. Prod.*,1(4):19-28.
40. Thippeswamy, B.S., Thakker, S.P., Tubachi, S., Kalyani, G.A., Netra, M.K., Patil, U., Desai, S., Gavimath, C.C., et al. (2009) Cardioprotective effect of *Cucumis trigonus* Roxb on isoproterenol-induced myocardial infarction in rat. *Am. J. Pharmacol. Toxicol.*,4(2):29-37.
41. Goyal, S.N., Arora, S., Sharma, A.K., Joshi, S., Ray, R., Bhatia, J., Kumari, S., Arya, D.S. (2010) Preventive effect of crocin of *Crocus sativus* on hemodynamic, biochemical, histopathological and ultrastructural alterations in isoproterenol-induced cardiotoxicity in rats. *Int. J. Phytother. Phytomedicine.*,17(3-4):227-232.
42. Ansari, M.N., Bhandari, U., Pillai, K.K. (2006) Ethanolic *Zingiber officinale* extract pretreatment elevates Isoproterenol induced oxidative myocardial necrosis in rats. *Ind. J. Exp. Bio.*,44:892-897.
43. Karthikeyan, K., Saralabai, B.R., Gauthaman, K., Sathish, K.S., Devaraj, S.N. (2003) Cardioprotective effect of the alcoholic extract of *Terminalia arjuna* bark in an in vivo model of myocardial ischemic reperfusion injury. *Li. Sci.*,73(21):2727-2739.
44. Rajendran, R., Basha, N.S. (2008) Cardioprotective effect of ethanol extract of stem-bark and stem-wood of *Premna serratifolia* Lin. *Res. J. Pharm. Tech.*,1(4):487-491.
45. Kubavat, J.B., Asdaq, S.M.B. (2009) Role of *Sida cordifolia* L leaves on biochemical and antioxidant profile during myocardial injury. *J. Ethnopharmacol.*,124(1):162-165.
46. Ramesh, T., Mahesh, R., Sureka, C., Begum, V.H. (2008) Cardioprotective effects of *Sesbania grandiflora* in Cigarette smoke-exposed rats. *J. Cardiovasc. Pharmacol.*, 52 (4):338-343.
47. Asdaq, S.M.B., Chakraborty, M. (2010) Myocardial potency of *Semecarpus anacardiumnut* extract against isoproterenol induced myocardial damage in rats. *Int. J. Pharm. Sci. Rev. Res.*, 2(2):10-13.
48. Arya, D.S., Arora, S., Malik, S., Nepal, S., Kumari, S., Ojha, S. (2010) Effect of Piper betle on cardiac function, marker enzymes, and oxidative stress in isoproterenol-induced cardiotoxicity in rats. *Toxicol. Mecha. Meth.*,20(9):564-71.
49. Rajaprabhu, D., Rajesh, R., Kumar, R.J., Buddhan, S., Ganesan, G., Anandan. (2007) Protective effect of *Picrorhiza kurroa* on antioxidant defense status in adriamycin-induced cardiomyopathy in rats. *J. Med. Plant. Res.*,1(4):80-85.
50. Velavan, S., Selvarani, S., Adhithan, A. (2009) Cardioprotective effect of *Trichopus zeylanicus* against myocardial ischemia

- induced by isoproterenol in rats. *Bangl. J. Pharmacol.*,4(2):88-91.
51. Krishnamoorthy, G., Shabi, M.M., Ravindhran, D., Uthrapathy, S., Rajamanickam, V.G., Dubey, G.P. (2009) *Nardostachys jatamansi*: Cardioprotective and hypolipidemic. *Herb. J. Pharm. Res.*,2 (4) :574-578.
52. Ojha, S.K., Nandave, M., Arora, S., Narang, R., Dinda, A.K., Arya, D.S. (2008) Chronic administration of *Tribulus terrestris* improves cardiac function and attenuates myocardial infarction in rats. *Int. J. Pharmacol.*,4(1):1-10.
53. Hamza, A., Amin, A., Daoud, S. (2008) The protective effect of a purified extract of *Withania somnifera* against doxorubicin-induced cardiac toxicity in rats. *Cel. Bio. Toxicol.*,24(1):63-73.
54. Mastan, S.K., Chaitanya, G., Latha, L.B., Srikanth, A., Sumalatha, G., Kumar, K.E. (2009) Cardioprotective effect of methanolic extract of *Syzygium cumini* seeds on isoproterenol-induced myocardial infarction in rats. *De. Pharm. Let.*,1(1):143-149.
55. Sharma, M., Kishore, K., Gupta, S.K., Joshi, S., Arya, D.S. (2001) Cardioprotective potential of *Ocimum sanctum* in isoproterenol induced myocardial infarction in rats. *Mole. Cell. Biochem.*,225(1-2):75-83.
56. Pakutharivu, T., Anitha, A., Usha, V., Sharmila, S., Chitra, S. (2015) Cardioprotective Activity of *Pithecellobium dulce* Fruit Peel on isoproterenol-induced myocardial infarction in rats. *Int. J. Pharm. Sci.*,30(1):133-136.
57. Kumar, A., Krishna, G., Hullatti, P., Tanmoy., Akshara. (2017) Indian Plants with Cardioprotective Activity-A Review. *Sys. Rev. Pharm.*,8(1):8-12.
58. Ziberna, L., Lunder, M., Moze, S., Vanzo, A., Drevensek, G. (2009) Cardioprotective effects of bilberry extract on ischemia-reperfusion-induced injury in isolated rat heart. *BMC Pharmacol.*,9(2):A55.
59. Isensee, H., Rietz, B., Jacob, R. (1993) Cardioprotective actions of garlic (*Allium sativum*). *Arzneimittelforschung* 1993;43 (2) :94-98
60. Shi, L.S., Liao, Y.R., Su, M.J., Lee, A.S., Kuo, P.C., Damu, A.G., Kuo, S.C., Sun, H.D., Lee, K.H., Wu, S.T. (2010) Cardiac Glycosides from *Antiaris toxicaria* with potent cardiotoxic activity. *J. Nat. Prod.*,73(7):1214-1222.
61. Harika, K., Mondi, S., Laxmibai, D.J., Chidraavar, V.R., Rao, V.U.M. (2014) A comprehensive review on cardioprotective medicinal plants. *Int. J. Inv. Pharm. Sci.*,2(4):793-799.
62. Vijay, T., Dhana, R.D.K., Sarumathy, K., Palani, S., Sakthivel, K. (2011) Cardioprotective, antioxidant activities and Phytochemical analysis by GC-MS of *Gmelina arborea* (GA) in Doxorubicin induced myocardial necrosis in Albino rats. *J. Appl. Pharma. Sci.*,1(5):198-104.
63. Dhana, R.M.S., Sarumathy, K., Palanie, S., Sakthivel, K. (2011) Phytochemical studies by GC-MS and cardioprotective effect of *Grewia hirsuta* (GH) on doxorubicin induced cardiotoxicity in albino rats. *Int. J. Univ. Pharm. L. Sci.*,1;1-18.
64. Ahmad, A., Deb, B., Haque, S., Khan, G., Shahzad, N. (2011) Role of green tea extract against doxorubicin-induced cardiotoxicity in rats. *Int. J. Res. Pharm. Sci.*,1(1):44-56.
65. Mahmoud, N., Nagi, M.M.A. (2000) Protective effect of Thymoquinone against doxorubicin-induced cardiotoxicity in rats: a possible mechanism of protection. *J. Pharmacol. Res.*,41(3): 284-289.
66. Shamala, S., Krishna, K.L. (2013) Cardioprotective activity of fruit extracts of *Momordica dioca* Roxb on doxorubicin

- induced toxicity on rats. *Sci. Int.*,1(12):392-400.
67. Yan-Fei, X., Guo-Liang, Z., Zu-Yue, D., Yun-Xiang, C., Yue-Guo, Wu., Pan-Sheng, Xu., Xuan, Y.X. (2007) Protective effect of *Lycium barbarum* on Doxorubicin-induced cardio toxicity. *J. Phytother. Res.*,21(11):1020–1024.
68. Rajendran, R., Basha, N.S. (2008) Cardioprotective effect of ethanol extract of stem-bark and stem-wood of *Premna serratifolia* Lin. *Res. J. Pharm. Tech.*,1(4):487-491.
69. Fard, M.H., Ghule, A.K.E., Bodhankar, L.S., Dikshit, A. (2011) Cardioprotective effect of whole fruit extract of pomegranate on doxorubicin-induced toxicity in rat. *Pharma. Bio.*,49(4):377-382.
70. Zaman, R.U. (2004) Study of Cardioprotective activity of *Raphanus sativus* in rabbits. *Pak. J. Biol. Sci.*,7(5):843-847.
71. Shi, L.S., Liao, Y.R., Su, M.J., Lee, A.S., Kuo, P.C., Damu, A.G., Kuo, S.C., Sun, H.D., Lee, K.H., Wu, S.T. (2010) Glycosides from *Antiaris toxicaria* with Potent Cardiotoxic Activity. *J. Nat. Prod.*73(7):1214–1222.
72. Karunakar, H., Dhruv, P., Kreethi, V. (2015) Evaluation of cardioprotective activity of aqueous extract of *Garcinia indica* linn fruit extract. *As. J. Pharm. Clin. Res.*,8(2):107-112.
73. Pakutharivu, T., Anitha, A., Usha, V., Sharmila, S., Chitra, S. (2015) Cardioprotective Activity of *Pithecellobium Dulce* Fruit Peel on isoproterenol-induced myocardial infarction in rats. *Int. J. Pharm. Sci.*,30(1):133-136.
74. Susila, R., Jeeva, G.R., Balagurusamy, K., Mubarak, H.A. (2013) Review of Siddha Cardiology and Cardioprotective Herbs. *Int. J. Herb. Med.*,1(4):71-75.
75. World Heart Federation: Cardiovascular disease: types and symptoms January 2018, Accessed at : [http://www.world-heartfederation.org/fileadmin/user_upload/documents/ Fact_sheets /2011/Cardiovascular %20 disease_ %20 types% 20 and %20 symptoms](http://www.world-heartfederation.org/fileadmin/user_upload/documents/Fact_sheets/2011/Cardiovascular%20disease_%20types%20and%20symptoms) (Accessed Jan 7, 2018)
76. Kchaou, W., Abbes, F., Atti, H., Besbes, S. (2014) In-vitro antioxidant activities of three selected dates from Tunisia (*Phoenix dactylifera* L). *J. Chem.*,2014:1-8.
77. Liu, J., Peter, K., Shi, D., Zhang, L., Dong, G., Zhang, D., Breiteneder, H., Bauer, J., Jakowitsch, J., Ma, Y. (2014) Anti-inflammatory effects of the chinese herbal formula sini tang in myocardial infarction rats. *Evid. Bas. Compl. Alter. Med.*,2014:1-10.
78. Mohanty, I.R., Gupta, S.K., Mohanty, N., Joseph, D., Deshmukh, Y. (2012) The Beneficial Effects of Herbs in Cardiovascular Diseases. *Glob. J. Med. Res.*,12(4):39-58.

NEWS ITEM

Researchers from NCBI unearths the role of micro RNAs in colour regulation of leaves and fruits :

A team from the National Centre for Biological Sciences (NCBS), Bengaluru, has found that the rich colour in fruits and leaves of plants are indirectly controlled by specific micro RNAs — miR828 and miR858. Grape plants bear fruits having colours that can be deep purple or green. This colour is due to compounds called anthocyanins and flavonols, both of which are present in grape fruits. When the grape plant has a high amount of anthocyanin as compared to flavonol, the fruits are deep purple. When the reverse is true, the grapes are not brightly coloured. The relative abundance of anthocyanin and flavonol is controlled by genes known as the MYB transcription factors. Also referred to as activators, when present in large amounts, they result in dark purple grape, as in the Bangalore Blue variety, and absence correlates with lack of bright colour but high incidence of flavonols as in the Dilkush grape variety. Researchers knew microRNAs can regulate MYBs, but they did not know why such a regulation takes place. They were mostly working with Arabidopsis model where one might not see coloured fruits. The team found that the microRNAs miR828 and miR858 were also found in abundance when the grapes had dark colour. Hence they figured out that there must be an intermediary repressor which was what the miRNA targeted. The paper published in the Journal of Experimental Botany. Micro RNAs are regulators of gene expression, acting like switches. They decide which protein should be made and how much in a given cell or tissue or an organism. They are tiny, having some 20 to 22 digits of RNA. The miRNA inhibit target RNAs by cutting them into two bits in plants. The miRNAs partner with a protein called Argonaute to do this regulation. Anthocyanins and flavonols remove reactive oxygen species that damage DNA, RNA and proteins. Reactive oxygen species are involved in most human diseases.

Vaccine for Ebola shields Congo people :

Preliminary data from vaccination in Congo suggest the vaccine has 97.5% efficacy in preventing Ebola. The 2014–2015 Ebola epidemic mainly in the three western African countries of Guinea, Liberia and Sierra Leone has been the most deadly one since the virus became known in 1976. It caused disease in 28,616 people and killed 11,310 others. But what

stands out as a remarkable scientific and public health achievement has been the conduct of a large clinical trial in Guinea to test the efficacy of an Ebola vaccine in the midst of the epidemic. The phase-3 clinical trial involving thousands of volunteers tested the efficacy of Merck's vaccine (VSV-EBOV) to protect vaccinated individuals from getting infected with Ebola virus. During the trial, the vaccine was administered to 2,119 individuals who had come in contact with a person infected with or died due to Ebola virus and 2,041 people who had come in contact with the primary contacts (known as contacts of contacts). In July 2015, an interim analysis revealed that the vaccine had 100% efficacy. The final results of the trial, too, showed the same result. The duration of protection is not known, though a few studies suggest protection up to one year.

IIT Madras researchers developed microwave aided model in detection of cancer :

Uday Khankhoje's team at IIT Madras is interested in developing a way of detecting breast cancer using microwaves – or radio frequency (RF) waves, as they are called. While several groups have worked on this in Europe and the US, and even made working hardware for this purpose, Dr Khankhoje's group uses the very popular method of deep learning for this. The method not only addresses a mathematical challenge, it also increases the range of the permittivity observed, where permittivity, the square of the refractive index of a material, is the characteristic that distinguishes cancer tissue from normal tissue. Further, this offers a portable, low-cost and safe alternative to X-ray and MRI scans already available for detecting cancer tissue. In their method, what Dr. Khankhoje's team would do is to surround the patient with RF transmitters and receivers and collect the waves that bounce off the tissues. Analysing the waves reflected by the tissue, they would reconstruct the type of tissue, or the permittivities of the tissues, that scattered the waves. The innovation used by this group in solving the inverse scattering problem is deep learning, which is a popular technique involving neural networks. Their article has been published in the journal IEEE Transactions on Computational Imaging.

Anthropocene epoch is on cards : On May 21, a 34-member panel of the Anthropocene Working Group (AWG) voted 29-4 in favour of designating a new

geological epoch — the Anthropocene. The vote signals the end of the Holocene Epoch, which began 11,700 years ago. According to Nature, the panel plans to submit a formal proposal for the new epoch by 2021 to the International Commission on Stratigraphy, which oversees the official geologic time chart. That nearly 90% voted in favour of a naming the new epoch to reflect how the Earth has been shaped by human activity, is not surprising, as an informal vote had already been conducted three years ago in Cape Town at the 2016 International Geological Congress. The term 'Anthropocene' was coined in 2000 by Nobel Laureate Paul Crutzen and Eugene Stoermer to denote the present geological time interval in which human activity has profoundly altered many conditions and processes on Earth. According to the AWG, the phenomena associated with the Anthropocene include an order-of-magnitude increase in erosion and sediment transport associated with urbanisation and agriculture, marked and abrupt anthropogenic perturbations of the cycles of elements such as carbon, environmental changes generated by these perturbations, including global warming, sea-level rise, and ocean acidification, rapid changes in the biosphere and finally proliferation and global dispersion of many new 'minerals' and 'rocks' including concrete, fly ash and plastics, and the myriad 'technofossils' produced from these and other materials.

Researchers from TIFR used gold nano particles for desalination of sea water, bypassing intense energy consumption : Using gold nanoparticles that absorb sunlight over the entire visible region and even the near infrared light, researchers at the Tata Institute of Fundamental Research (TIFR), Mumbai, have been able to desalinate seawater to produce drinking water. Unlike the conventional reverse osmosis that is energy intensive, the gold nanoparticles require no external energy to produce potable water from seawater. Using 2.5 mg of gold nanoparticles, the team led by Vivek Polshettiwar from TIFR's Department of Chemical Sciences was able to use sunlight to heat the water to 85 degree C and generate steam to produce drinking water from seawater. Since the temperature reached is high, about 10% of seawater becomes steam (and hence drinking water) in about 30 minutes. Alternatively, the gold nanoparticles can be used to convert carbon dioxide into methane. This happens when the light absorbed by the gold nanoparticles excites the electrons, and the excited electrons when transferred

into carbon dioxide converts it into methane in the presence of hydrogen. The hydrogen comes from the water that is used as a reaction solvent. At present, the conversion of carbon dioxide to methane is low — about 1.5 micromole per gram. It is desirable to increase the conversion one-fold to millimole range. We are finding ways to improve the conversion rate, says Prof. Polshettiwar. The results of the study were published in the journal Chemical Science.

Study reported that a novel engineering technique – Artificial snow would enshield erosion of massive Antarctic glacier: Study envisages using 12,000 wind turbines to pump seawater 1,500 metres up to the surface, where it would be frozen into snow to try to weigh the sheet down enough to stop it collapsing any further. Governments could stop the West Antarctic Ice Sheet from sliding into the ocean and submerging coastal cities by launching a last-ditch engineering project to blanket its surface with artificial snow, according to a study released on Wednesday. Scientists believe that global warming has already caused so much melting at the south pole that the giant ice sheet is now on course to disintegrate, which would trigger an eventual global sea level rise of at least three metres (10 feet) over centuries. The authors of the new study envisaged using 12,000 wind turbines to pump seawater 1,500 metres (4,900 feet) up to the surface, where it would be frozen into "snow" to try to weigh the sheet down enough to stop it collapsing any further. We have already awoken the giant at the southern pole, said Anders Levermann, a professor at Germany's Potsdam Institute for Climate Impact Research, referring to the ice sheet. With the droughts, floods, storms and wildfires associated with climate change intensifying globally, some scientists have begun to seriously contemplate interventions that would have been dismissed as wildly impractical even a few years ago. The sea level rise from Western Antarctica will eventually submerge Hamburg, Shanghai, New York and Hong Kong, said Mr. Levermann, a physicist and oceanographer who is also affiliated with Columbia University in the United States. You can't negotiate with physics: that's the dilemma here. Mr. Levermann and his co-authors used computer models to calculate that the West Antarctic Ice Sheet could be stabilized by depositing a minimum of 7,400 gigatonnes of artificial snow over 10 years around the Pine Island and Thwaites glacier.

**The 13th Annual Convention of ABAP &
International Conference on
ENVIRONMENTAL SUSTAINABILITY,
HUMAN HEALTH AND DEVELOPMENT
20 - 22nd December, 2019**

First Circular

Jointly Organized by
Association of Biotechnology and Pharmacy



VIGNAN'S
Foundation for Science, Technology & Research
UNIVERSITY
(Estd u/s 3 of UGC Act of 1956)

**Venue: A-Block, Sangamam Seminar Hall
VFSTR, Vadlamudi-522213 A. P., India**

Registered with Registrar of News Papers for India
Regn. No. APENG/2008/28877

Association of Biotechnology and Pharmacy

(Regn. No. 28OF 2007)

Executive Council

Hon. President

Prof. B. Suresh

Hon. Secretary

Prof. K. Chinnaswamy

President Elect

Prof. T. V. Narayana

Bangalore

General Secretary

Prof. K.R.S. Sambasiva Rao

Guntur

Vice-Presidents

Prof. M. Vijayalakshmi

Guntur

Treasurer

Prof. P. Sudhakar

Prof. T. K. Ravi

Coimbatore

Advisory Board

Prof. C. K. Kokate, Belgaum

Prof. B. K. Gupta, Kolkata

Prof. Y. Madhusudhana Rao, Warangal

Prof. M. D. Karwekar, Bangalore

Prof. K. P. R. Chowdary, Vizag

Dr. V. S.V. Rao Vadlamudi, Hyderabad

Executive Members

Prof. V. Ravichandran, Chennai

Prof. Gabhe, Mumbai

Prof. Unnikrishna Phanicker, Trivandrum

Prof. R. Nagaraju, Tirupathi

Prof. S. Jaipal Reddy, Hyderabad

Prof. C. S. V. Ramachandra Rao, Vijayawada

Dr. C. Gopala Krishna, Guntur

Dr. K. Ammani, Guntur

Dr. J. Ramesh Babu, Guntur

Prof. G. Vidyasagar, Kutch

Prof. T. Somasekhar, Bangalore

Prof. S. Vidyadhara, Guntur

Prof. K. S. R. G. Prasad, Tirupathi

Prof. G. Devala Rao, Vijayawada

Prof. B. Jayakar, Salem

Prof. S. C. Marihal, Goa

M. B. R. Prasad, Vijayawada

Dr. M. Subba Rao, Nuzividu

Prof. Y. Rajendra Prasad, Vizag

Prof. P. M. Gaikwad, Ahmednagar

Printed, Published and owned by Association of Bio-Technology and Pharmacy # 6-69-64 : 6/19, Brodipet, Guntur - 522 002, Andhra Pradesh, India. Printed at : Don Bosco Tech. School Press, Ring Road, Guntur - 522 007, A.P., India Published at : Association of Bio-Technology and Pharmacy # 6-69-64 : 6/19, Brodipet, Guntur - 522 002, Andhra Pradesh, India. Editors : Prof. K.R.S. Sambasiva Rao, Prof. Karnam S. Murthy